

**Apatite Fission Track Analysis of the Great Northern Peninsula
of Newfoundland: Evidence for Late Paleozoic Burial**

By Mark Hendriks

submitted in partial fulfillment of the requirements
for the degree of MASTER OF SCIENCE at Dalhousie
University, Halifax, Nova Scotia April, 1991

© Copyright by Mark Hendriks, 1991

DALHOUSIE UNIVERSITY
DEPARTMENT OF GEOLOGY

The undersigned hereby certify that they have read and recommend to the Faculty of Graduate Studies for acceptance a thesis entitled "Apatite Fission Track Analysis of the Great Northern Peninsula, Western Newfoundland: Evidence for Late Paleozoic Burial" by Mark Hendriks in partial fulfillment of the requirements for the degree of Master of Science.

Dated 1 March /91

Supervisor: _____

Readers: _____

DALHOUSIE UNIVERSITY

Date 31 March 1991

Author Mark Hendriks

Title Apatite Fission Track Analysis of the Great

Northern Peninsula of Newfoundland: Evidence

for Late Paleozoic Burial

Department or School Geology

Degree: M.sc. Convocation Spring Year 1991

Permission is herewith granted to Dalhousie University to circulate and to have copied for non-commercial purposes, at its discretion, the above title upon the request of individuals or institutions.

Signature

Author

THE AUTHOR RESERVES OTHER PUBLICATION RIGHTS, AND NEITHER THE THESIS NOR EXTENSIVE EXTRACTS FROM IT MAY BE PRINTED OR OTHERWISE REPRODUCED WITHOUT THE AUTHOR'S WRITTEN PERMISSION.

THE AUTHOR ATTESTS THAT PERMISSION HAS BEEN OBTAINED FOR THE USE OF ANY COPYRIGHTED MATERIAL APPEARING IN THIS THESIS (OTHER THAN BRIEF EXCERPTS REQUIRING ONLY PROPER ACKNOWLEDGMENT IN SCHOLARLY WRITING) AND THAT ALL SUCH USE IS CLEARLY ACKNOWLEDGED.

Table of Contents

	P.
Table of Contents	iv
List of Figures	viii
List of Tables	xi
List of Abbreviations and Symbols	xii
Abstract	xiii
Acknowledgements	xiv
Introduction: Purpose and Scope of the Study	1
Chapter 1. Geological Development of the Great Northern Peninsula	2
1.1 Introduction	2
1.2 Precambrian History	6
1.3 Paleozoic History	8
1.4 Mesozoic-Present History	15
1.5 Geological Development of the Study Area	16
1.5.1 Introduction	16
1.5.2 Southern Transect	18
1.5.3 Central Transect	20
1.5.4 Northern Transect	22
1.5.5 Deer Lake Basin	25
Chapter 2. Apatite Fission Track Analysis: Methodology	28
2.1 Introduction	28

2.2	The Apatite Fission Track Age: A Radiometric Clock	30
2.3	Apatite Fission Track Ages in Exhumation Studies	37
2.4	Apatite Fission Track Lengths	39
2.5	Sample Preparation and Procedures for Apatite Fission Track Length Measurement	42
2.5.1	Mineral Separation	42
2.5.2	Sample Irradiation	44
2.5.3	Fission Track Age and Length Distribution Measurement Procedures	45
Chapter 3.	Apatite Fission Track Analysis: Results	47
3.1	Introduction	47
3.2	Southern Transect	47
3.2.1	Sample Location	47
3.2.2	Fission Track Age Analysis	51
3.2.3	Fission Track Length Distribution Analysis	55
3.3	Central Transect	67
3.3.1	Sample Location	67
3.3.2	Fission Track Age Analysis	70
3.3.3	Fission Track Length Distribution Analysis	73
3.4	Northern Transect	73
3.4.1	Sample Location	73
3.4.2	Fission Track Age Analysis	75
3.4.3	Fission Track Length Distribution Analysis	77
3.5	Deer Lake Basin and Greater Northwestern Newfoundland	77

3.5.1	Sample Location	77
3.5.2	Fission Track Analysis	79
3.5.3	Fission Track Length Distribution Analysis	81
3.6	Inferred Thermal History from Analysis of Track Length vs. Age and Track Length Standard Deviation	82
3.7	Discussion of Experimental Results	89
Chapter 4.	Apatite Fission Track Apparent Age and Track Length Modelling: Temperature-Time Histories	92
4.1	Introduction	93
4.2	Specifics of the Model	93
4.2.1	Forward Modelling (track length distribution as $f(T,t)$)	93
4.2.2	Inverse Modelling (T-t history estimation from apatite age and track length distribution fitting)	95
4.2.3	Modelling Parameters and Assumptions	96
4.3	Modelling Results	100
4.3.1	Southern Transect	100
4.3.2	Central Transect	121
4.3.3	Northern Transect	122
4.3.4	Deer Lake Basin and Greater Northwestern Newfoundland	123
4.4	Discussion of Modelling Results	124
Chapter 5.	Discussion of Results	127
5.1	Introduction	127

5.2	End-Member Hypotheses: Interpretation of Apatite Fission Track Data from the Great Northern Peninsula	127
5.2.1	Exhumation and Erosion of the Long Range Inlier	127
5.2.2	Burial, Exhumation and Erosion of Cover Rock	130
5.3	Hypothesis Constraints from Apatite Fission Track Data and Great Northern Peninsula Geology	138
5.3.1	Hypothesis Constraints from Apatite Fission Track Data: Comparison of Apatite Fission Track Data with Model Predictions	138
5.3.2	Hypothesis Constraints from Geological Relationships in the Great Northern Peninsula	143
5.3.2.1	Southern and Central Transects	143
5.3.2.2	Northern Transect	147
5.3.2.3	Western Platform and Devil's Room Pluton	148
5.3.2.4	Deer Lake Basin	151
5.4	Conclusion	154
Chapter 6. Concluding Remarks		157
Appendix 1: Data for Zeta Determinations		162
Appendix 2: Track Length Distribution Skewness Values		179
Appendix 3: Length-Corrected Apatite Fission Track Ages		180
Appendix 4: Parameters for Inverse T-t Models		182
References		215

List of Figures

	p.
Figure 1.1 Tectono-stratigraphic zones of the Northern Appalachians	5
Figure 1.2 Lower crustal blocks of Newfoundland	5
Figure 1.3 General geology of the Great Northern Peninsula	7
Figure 1.4 General geology of the Long Range Inlier	9
Figure 1.5 Stratigraphy of northwestern Newfoundland	11
Figure 1.6 General geology of the St. Anthony Complex	13
Figure 1.7 Geology of the Southern Transect, Great Northern Peninsula	17
Figure 1.8 Geology of the Central Transect, Great Northern Peninsula	19
Figure 1.9 Geology of the Northern Transect, Great Northern Peninsula	21
Figure 1.10 Geology of the Deer Lake Basin, western Newfoundland	23
Figure 1.11 Stratigraphy of the Deer Lake Basin, western Newfoundland	24
Figure 2.1 Ion spike model for fission track formation	29
Figure 2.2 CN-1 vs. CN-2 glass correlation factor	33
Figure 2.3 Apatite fission track age and mean length vs. isotherm relaxation	38
Figure 2.4 Arrhenius plots for apatite fission track annealing	40
Figure 2.5 Apatite grain mount	46
Figure 3.1 Southern Transect apatite fission track sample locations	48
Figure 3.2 Southern Transect 1 apatite apparent age vs. elevation	52
Figure 3.3 Southern Transect 2 apatite apparent age vs. elevation	54
Figure 3.4 a-m Southern Transect apatite fission track length distributions	56-59
Figure 3.4 n-u Central Transect and Devil's Room Pluton apatite fission track length distributions	60-61
Figure 3.4 v-x Northern Transect apatite fission track length distributions	62
Figure 3.4 y-ee Deer Lake Basin, Hare Bay and Humber Arm Allochthons, Daniel's Harbour, and ST1 east sample track length distributions	63-64
Figure 3.5 Time-temperature paths vs. track length distribution	68
Figure 3.6 Central Transect apatite fission track sample locations	69
Figure 3.7 Central Transect apatite apparent age vs. elevation	72

Figure 3.8 Northern Transect apatite fission track sample locations	76
Figure 3.9 Northern Transect apatite apparent age vs. elevation	78
Figure 3.10 a,b Deer Lake Basin and miscellaneous western Newfoundland apatite fission track sample locations	77
Figure 3.11 Deer Lake Basin and miscellaneous western Newfoundland apatite apparent age vs. elevation	80
Figure 3.12 a,b Mean track length vs. apatite apparent fission track age	83
Figure 3.13 a,b Track length standard deviation vs. mean track length	84
Figure 3.14 Mean track length vs. elevation	87
Figure 3.15 Great Northern Peninsula apatite apparent age vs. elevation	88
Figure 4.1 Modelled T-t paths vs. track length distributions	94
Figure 4.2 Relationship between reduced track density and track length	97
Figure 4.3 Effects of modelling parameters on shape of the T-t path	101
Figure 4.4 a,b Modelled T-t paths and track length distributions (FT89-225,226)	103
Figure 4.4 c,d Modelled T-t paths and track length distributions (FT89-201,196)	104
Figure 4.4 e,f Modelled T-t paths and track length distributions (FT89-203,205)	105
Figure 4.4 g,h Modelled T-t paths and track length distributions (FT89-224,194)	106
Figure 4.4 i,j Modelled T-t paths and track length distributions (FT89-227,193)	107
Figure 4.4 k,l Modelled T-t paths and track length distributions (FT89-191,197)	108
Figure 4.4 m,n Modelled T-t paths and track length distributions (FT89-198)	109
Figure 4.4 n,o Modelled T-t paths and track length distributions (FT89-212,211)	110
Figure 4.4 p,q Modelled T-t paths and track length distributions (FT89-210,207)	111
Figure 4.4 r,s Modelled T-t paths and track length distributions (FT89-209,206)	112
Figure 4.4 t,u Modelled T-t paths and track length distributions (FT89-208 ,LGRA-01)	113
Figure 4.4 v,w Modelled T-t paths and track length distributions (FT89-221,232)	114
Figure 4.4 x,y Modelled T-t paths and track length distributions (FT89-233 ,FT90-050)	115
Figure 4.4 z,aa Modelled T-t paths and track length distributions (FT90-034,035)	116
Figure 4.4 bb,cc Modelled T-t paths and track length distributions (FT89-235,213)	117
Figure 4.4 dd,ee Modelled T-t paths and track length distributions (FT89-222,223)	118

Figure 5.1	End-member cooling/exhumation models	128
Figure 5.2a	Cartoon schematic of the Long Range Inlier basement erosion model	129
Figure 5.2b	Cartoon schematic of the Appalachian Burial and Erosion model	131
Figure 5.3	Trends between mean track length, apatite fission track age, and standard deviation for mixed ages	137
Figure 5.4	General geology and mineral occurrences in the southeastern Great Northern Peninsula	144
Figure 5.5	Cartoon schematic showing possible Carboniferous cover distribution during the post-Appalachian history of the Great Northern Peninsula	153

List of Tables

	p.
Table 2.1 Zeta values determined for the study	35
Table 3.1 Great Northern Peninsula sample elevation, lithology and location	49
Table 3.2 Southern Transect apparent apatite fission track ages	50
Table 3.3 Great Northern Peninsula track length distribution statistics	56
Table 3.4 Central Transect, Northern Transect, Deer Lake Basin and miscellaneous western Newfoundland apparent apatite fission track ages	70
Table 4.1 Model-corrected apatite fission track ages	99
Table 5.1a Age vs. elevation and track length distribution shape for end-member models	132
Table 5.1b Mean track length vs. apatite fission track age and standard deviation vs. mean track length for end-member models	133
Table 5.1c T-t inverse model characteristics for end-member models	134

List of Abbreviations and Symbols

GNP Great Northern Peninsula
ST Southern Transect
CT Central Transect
NT Northern Transect
DLB Deer Lake Basin
BVB Baie Verte/Brompton Line
CAI Conodont Alteration Index
DR Durango
FC Fish Canyon Tuff
RN Renfrew
m meter
km kilometer
kg kilogram
mr millirad
hr hour
t time or age
T temperature
Ma million years
Ga billion years
sd/Std.Dev. standard deviation
m/Mn.Lgth. mean etched track length
m.a. measured age
m.d.a. model age
c.a. corrected age
el elevation
n/N number of tracks
a.s.l. above sea level
m.s.l. mean sea level
I atomic ratio $^{238}\text{U}/^{235}\text{U}$
 Φ thermal-neutron fluence during radiation
 σ 1 sigma error or ^{235}U thermal-neutron fluence cross-section
g counting geometry factor
 λ_d ^{238}U total decay constant
 λ_f ^{235}U spontaneous fission decay constant
 ρ_s/Rhos spontaneous fission track density in grain
 ρ_i/Rhoi induced fission track density in detector

Abstract

Using the apatite fission track thermochronologic method, thirty-one crystalline and sedimentary rock samples were analyzed from the Great Northern Peninsula, western Newfoundland in order to determine the low temperature history (below ~ 120 °C) of this region. A significant amount of track annealing in all the samples means that the apatite fission track ages cannot be interpreted to date a specific event of relatively short duration. Rather, apatite fission track ages, track length distributions, model temperature-time paths and geological relationships are consistent with a substantial amount of burial of much of the Great Northern Peninsula during the Late Paleozoic, enough to completely reset apatite fission track ages of low elevation samples in the Carboniferous Deer Lake Basin. Maximum resetting temperatures were attained sometime during the Early Carboniferous-Early Triassic. Subsequent Great Northern Peninsula thermal history is characterized by slow, fairly continuous cooling consistent with exhumation/denudation of several kilometers of cover rock. Trends in the data may indicate the existence of a partial resetting gradient over the sampled elevation interval which would place some constraint on the thickness of burial. Anomalous data from the Devil's Room Pluton and western platform may be recording localized Jurassic thermal activity in the Peninsula.

Acknowledgements

I thank God for providing the people in my life who ultimately made this piece of work a reality; my parents, for their loving faith and support during the many long phone conversations over the last two years, David and Mary, for their wonderful love and friendship and for believing in me when I did not; Adrian and Elaine, for their friendship and all those Sunday morning pancakes, the people of All Nations, my office mates, mostly for their diversion from studying but also for their stimulating discussions, and my very good friends (they know who they are) who kept me going. My thanks go out to Sandy and Ray for coping with my ignorance and for helping me out of many jams. I am indebted to my thesis committee first of all for making this study a possibility, but also for their many hours spent in channeling my thoughts and providing insight where mine ended. Their careful scrutiny of primary drafts was no doubt laborious and is gratefully acknowledged.

Introduction

The aim of this study is to use apatite fission track thermochronology and recently developed inverse modelling techniques to constrain low temperature thermal histories (less than 120 °C) for a number of specific areas within the Great Northern Peninsula of Newfoundland (Figure 1.1). This knowledge, together with geological relationships in the Great Northern Peninsula, will be used to address the types of questions raised below and constrain the possible answers.

Except for work on conodont alteration indices carried out in Paleozoic sediments (Nowlan and Barnes, 1987), investigations into the low temperature history of the Great Northern Peninsula in general, and one of its main geological features, the Long Range Inlier (Figures 1.3, 1.4), are non-existent. Hypotheses seeking to explain the present erosional surfaces in western Newfoundland, such as the present surface of the Long Range, have never been tested. Nor has the burial history of the Great Northern Peninsula during Appalachian orogenesis been fully addressed by techniques used to date. Radiometric dating applied to rocks from western Newfoundland, particularly from the Long Range Inlier, has been almost exclusively devoted to high closure temperature methods (greater than 300 °C) and therefore is unable to address fully questions such as:

1. To what extent and for how long was the Great Northern Peninsula buried beneath cover related to the main pulses (Taconian and Acadian) of the Appalachian Orogeny?
2. To what extent did the Alleghanian Appalachian Orogeny affect the rocks presently at the surface in the Great Northern Peninsula?
3. What role has erosion played in the post-Appalachian geological history of the Great Northern Peninsula?
4. When and for how long has the Long Range Inlier been exposed?
5. Have any low temperature thermal events (less than 120 °C) affected the Great Northern Peninsula since Appalachian orogenesis?

Since apatite fission track thermochronologic methods are uniquely suited to record temperatures below ~ 120 °C, their application to the rocks of the Great Northern Peninsula should shed some light on the questions raised above.

The Great Northern Peninsula of western Newfoundland lies at the eastern extremity of the exposed Canadian Shield. The main physiographic features of the peninsula include the Newfoundland Coastal and Central Lowlands, and the Newfoundland Highland (Bostock, 1970). The western Coastal Lowland (Figure 1.3) is underlain by low lying sedimentary rocks stretching the length of the western Great Northern Peninsula. It is bordered on the west by the Gulf of St. Lawrence and on the east by crystalline rocks of the Highland (Long Range Inlier). The Highland rises abruptly from the coastal plain to 600-800 m above sea level (a.s.l.) and continues eastward for 60-70 km, slowly diminishing in height to 300-400 m a.s.l. in the north and 400-600 m a.s.l. in the south. Twenhofel and McClintock (1940) referred to this eastward-sloping plateau as the Long Range Peneplain and postulated it to be the result of interaction of repeated vertical tectonic movements and fluvial action since Permian time, with slight modification by more recent glacial activity. They suggested that the most likely period of formation was during the Tertiary or Late Cretaceous based on the excellent preservation of the peneplain and lack of any Late Mesozoic or Early Tertiary sediments. Along its eastern edge the Highland either plunges steeply into the Atlantic Ocean or is bordered by sedimentary rocks of Carboniferous or Cambrian-Ordovician age. To the north the crystalline Highland disappears under Cambrian-Ordovician sedimentary cover and elevations gradually fall off to sea level. A prominent scarp marks the western edge of the Hare Bay Allochthon (see Figures 1.3, 1.6). Its various structural slices form the rolling terrain typical of the Central Lowland region northeast of the Highland (Williams and Smyth, 1983).

Chapter 1. Geological Development of the Great Northern Peninsula

1.1 Introduction

The island of Newfoundland is situated at the northern extremity of the Appalachian mountain belt, an orogenic system extending from southern Alabama through the Canadian Atlantic provinces, a distance of some 3500 km. The continuation

of this system is found across the Atlantic Ocean in the northern British Isles and Scandinavia where it is known as the Caledonides (Belt, 1969; Haworth and Jacobi, 1983). Juxtaposition of belts of ophiolite, calc-alkaline volcanics, and metasedimentary rocks has led to the identification of distinct geologic zones within the Appalachian Orogen, similar in concept to the suspect terranes established for the western Cordillera of North America (Williams, 1978; Williams and Hatcher, 1983).

Differences in Middle Ordovician and older rocks have led to a five fold zonation in the northern Appalachians. From west to east these zones are the Humber, Dunnage, Gander, Avalon, and Meguma, the first four of which are defined in the island of Newfoundland (Williams, 1979, Figure 1.1). The Humber zone records the development and destruction of the Eocambrian continental margin of eastern North America. Fragments of the Iapetus Ocean with island arc sequences and melanges underlain by oceanic crust define the Dunnage Zone. A possible ancient eastern continental margin of Iapetus is represented by the Gander Zone. The Precambrian development of the Avalon Zone was related either to rifting and initiation of Iapetus or subduction prior to its opening. During the Early Paleozoic this region evolved into a stable marine shelf. The Meguma Zone of Nova Scotia represents either a vestige of the ancient continental embankment of northwest Africa or a marine graben fill developed in the Avalon Zone (Williams, 1979). These zones are separated by major structural discontinuities, which in some cases have been interpreted as penetrating the entire crust (Stockmal et al., 1987).

Deep seismic offshore reflection data distinguish three lower crustal blocks underlying these zones (Figure 1.2). The Grenville Block underlies the Humber and part of the Dunnage Zones, abutting the Central Block at mid-crustal to mantle depths in central Newfoundland. A steeply dipping junction penetrating the entire crust marks the eastern boundary of the Central Block with the Avalon Block. The Avalon Block underlies eastern Newfoundland (Marillier et al., 1989).

The Great Northern Peninsula (GNP) of western Newfoundland is wholly located within the Humber Zone (Figure 1.3). The western boundary of this zone is defined by the limit of Appalachian deformation, and its eastern boundary by the Baie Verte/Brompton Line (Figure 1.1, BVB), a steep structural zone characterized by numerous ophiolites (St.Julien et al., 1976; Williams and St.Julien, 1982). Major features of this ancient continental margin are well represented in the GNP and include the following: 1. The eastern limit of Precambrian crystalline inliers related to the Grenville Block (Long Range Inlier, Figure 1.3, 1.4). 2. An eastward thickening wedge of clastic sediments lying unconformably (or structurally emplaced) over Grenville Block basement (Labrador Group, Figure 1.5). 3. Mafic extrusions and intrusions related in time and space to the clastic prism (Long Range Dyke Swarm and related basalt flows, Figure 1.4). 4. An eastward-thickening carbonate package that lies conformably over the clastic sediments (Port au Port, St.George, and Table Head Groups, Figure 1.5). (Williams and Stevens, 1974).

The present geological configuration of the Great Northern Peninsula was established largely during the Paleozoic. The Taconian (Ordovician) and Acadian (Silurian-Devonian) orogenies caused western Newfoundland to evolve from a Late Precambrian passive margin into a major compressional mountain belt by the Middle Paleozoic (Williams and Stevens, 1974; Williams and Hatcher, 1983; Stockmal et al., 1987). Late Paleozoic Alleghanian tectonism was apparently limited to a narrow transpressional zone resulting mainly from strike slip motion (Belt, 1968; Williams and Hatcher, 1983; Hyde, 1984; Hyde et al., 1988). Dyke intrusions and possible Jurassic rocks in central Newfoundland (Jansa and Pe-Piper, 1985; Pe-Piper and Jansa, 1987) record Mesozoic geological development. Cenozoic rocks are absent from the island of Newfoundland perhaps suggesting large scale erosion of the land surface.

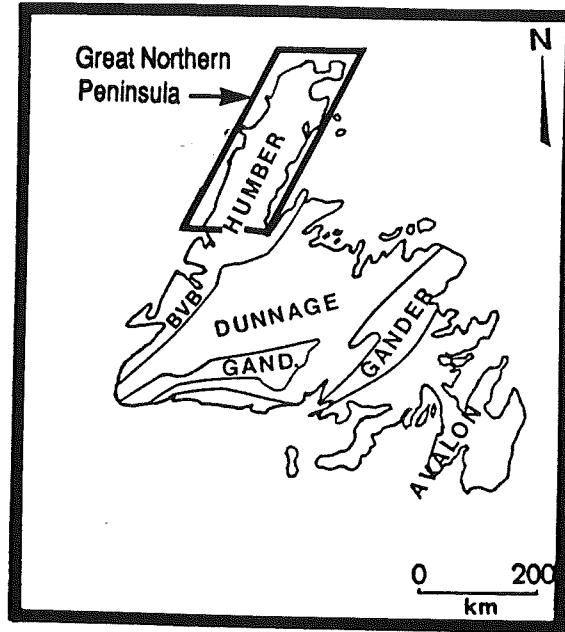


Figure 1.1
Tectono-stratigraphic zones of the northern Appalachians (adapted from Williams, 1979).

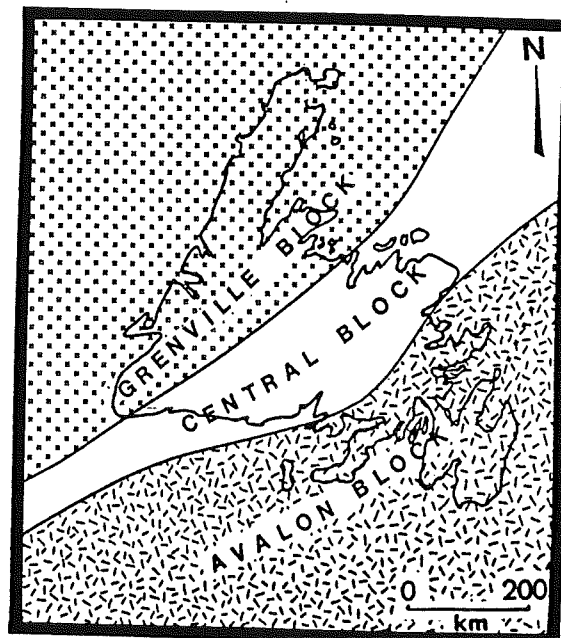


Figure 1.2
The Grenville, Central and Avalon lower crustal blocks of Newfoundland (adapted from Marillier et al., 1989).

1.2 Precambrian History

The Precambrian history of the Great Northern Peninsula is recorded in the Long Range Inlier, the largest Grenvillian crystalline basement inlier in the Appalachian orogenic system (Owen and Erdmer, 1988; Figure 1.3, 1.4). The topography in the western edge of this crystalline basement inlier rises some 600-800 m above autochthonous and allochthonous Cambro-Ordovician sediments of the western platform and is marked by the Long Range Thrust fault (Figure 1.3). Unconformable contacts with similar Cambrian-Ordovician rocks delineate its southern and northern (also parts of its western and eastern) limits. The eastern Long Range either slopes directly into the Atlantic Ocean or is unconformably overlain by Carboniferous or Cambrian-Ordovician sediments.

The inlier comprises mainly tonalitic-granitic orthogneiss intruded by Grenvillian granite-granodiorite (Owen and Erdmer, 1989; 1988; Figure 1.4). Slivers of metamorphosed supracrustal rocks including quartzite, marble, and pelite are scattered throughout the Long Range. Several Precambrian mafic plutons and the Devonian Devil's Room Granite intrude the southeastern Long Range Inlier (Owen and Erdmer, 1989; Figure 1.4). The Late Proterozoic Long Range Dyke Swarm intruded all rock units except the Devil's Room Granite, and served as feeder dykes for the basaltic tholeiite flows that locally cap the northern Long Range (Clifford, 1965; Strong and Williams, 1972; Owen and Erdmer, 1989; Figure 1.4).

The Long Range gneiss complex rocks attained granulite grade metamorphism between 1.5 and 1.02 Ga, prior to Grenvillian igneous intrusion (1130 Ma, Rb-Sr whole rock, Pringle, 1971; 1020-970 Ma, U-Pb zircon Baadsgaard et al., in prep.). Amphibolite facies metamorphism affected both the gneiss and Grenvillian granites at ca. 970 Ma (Pb-Pb titanite, Baadsgaard et al., in prep.). High level, Late Proterozoic Long Range Swarm dykes and basalt flows of the Lighthouse Cove Formation record the opening of the proto-Atlantic Iapetus Ocean (605 Ma, $^{40}\text{Ar}/^{39}\text{Ar}$ whole rock, Stukas and

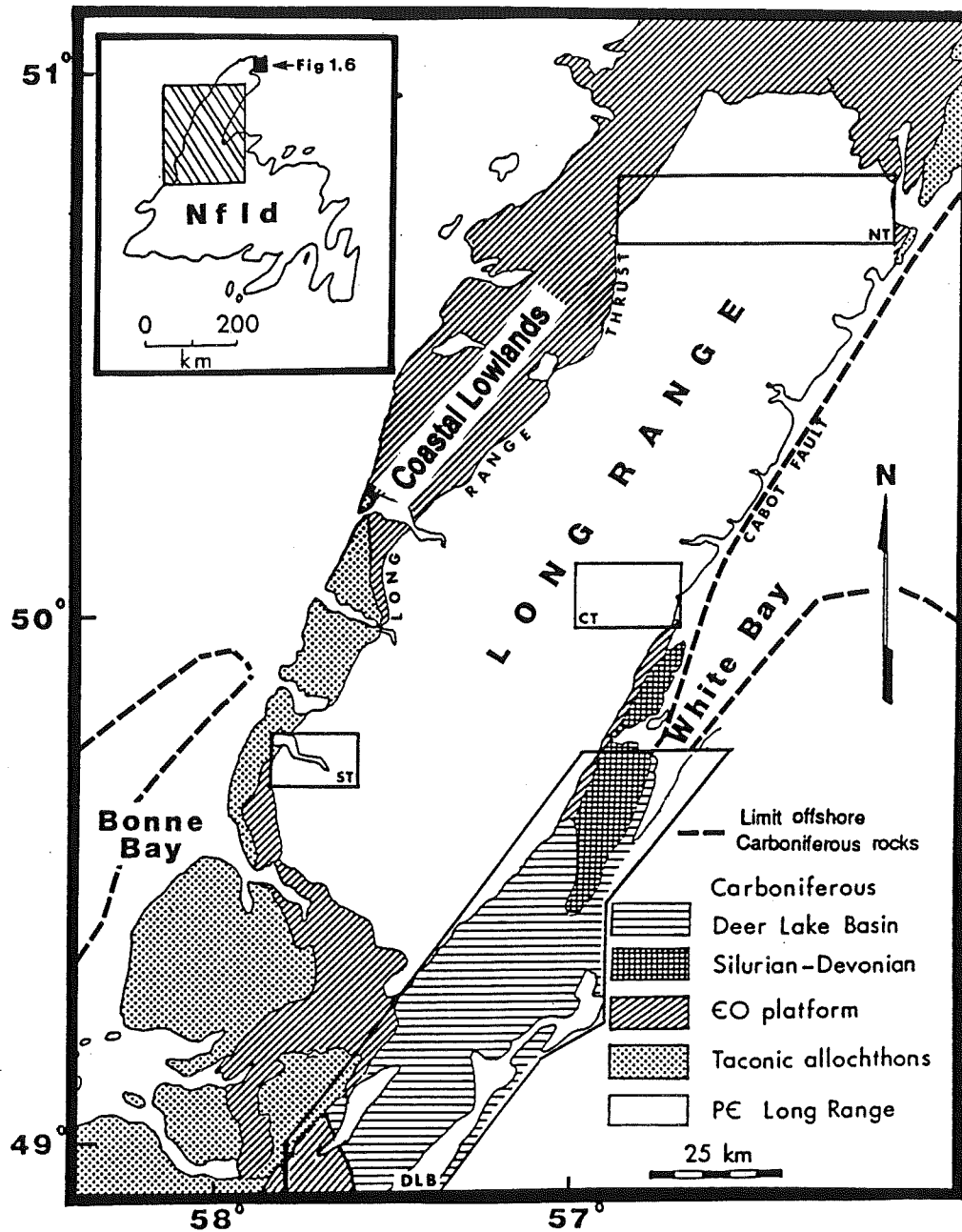


Figure 1.3
General geology of the Great Northern Peninsula of northwestern Newfoundland. Outlined study areas are the Southern (ST), Central (CT) and Northern Transects (NT) and the Deer Lake Basin (DLB). Inset shows location of the St. Anthony Complex of the Hare Bay Allochton (Fig 1.6).

Reynolds, 1974) and indicate uplift of rocks at the present Long Range surface from mid-crustal depths during Mid to Late Proterozoic (Owen and Erdmer, 1989). Uniform lithology and thickness of subsequent onlapping continental margin sediments onto the inlier indicate no nearby source area and suggest low relief of the inlier during Late Precambrian-Cambrian times (Williams, 1969). Proterozoic $^{40}\text{Ar}/^{39}\text{Ar}$ dates from hornblende and biotite suggest no major cooling/uplift of the western Long Range has occurred since Proterozoic times (Hendriks et al., 1989), although greenschist to lower amphibolite facies minerals (chlorite, epidote, hornblende) overprint the Long Range Dyke Swarm and their host rocks in the eastern part of the inlier (Erdmer, 1984).

Grenvillian plutons of the Long Range are well defined by aeromagnetic signatures, and in the case of the Lake Michel Intrusive Suite (Figure 1.4) may be traced across the Long Range Thrust below the Cambrian-Ordovician cover rocks, implying minimal displacement across the thrust in these parts of the inlier (Owen and Erdmer, 1989). This is supported by structural observations which limit lateral movement on the Long Range Thrust to no more than several kilometers (Cawood and Williams, 1986). Other workers have suggested more significant displacement (tens of kilometers) of the inlier and its southern carbonate cover based on structural observations in the Port au Port Peninsula further south (Waldron and Stockmal, 1989). Some of this displacement may have been accommodated on a sole thrust in the basement or underneath the western platform (Grenier and Cawood, 1988).

1.3 Paleozoic History

By the beginning of the Paleozoic the Humber Zone of Newfoundland coincided with a fully fledged passive continental margin obtaining its sediments from exposed Grenville basement to the west. The arrival of easterly derived flysch signalled a new source area to the east which had replaced the proto-Atlantic Ocean, and marked a rapid subsidence of the margin (Stevens, 1970). The ensuing Middle Ordovician Taconian

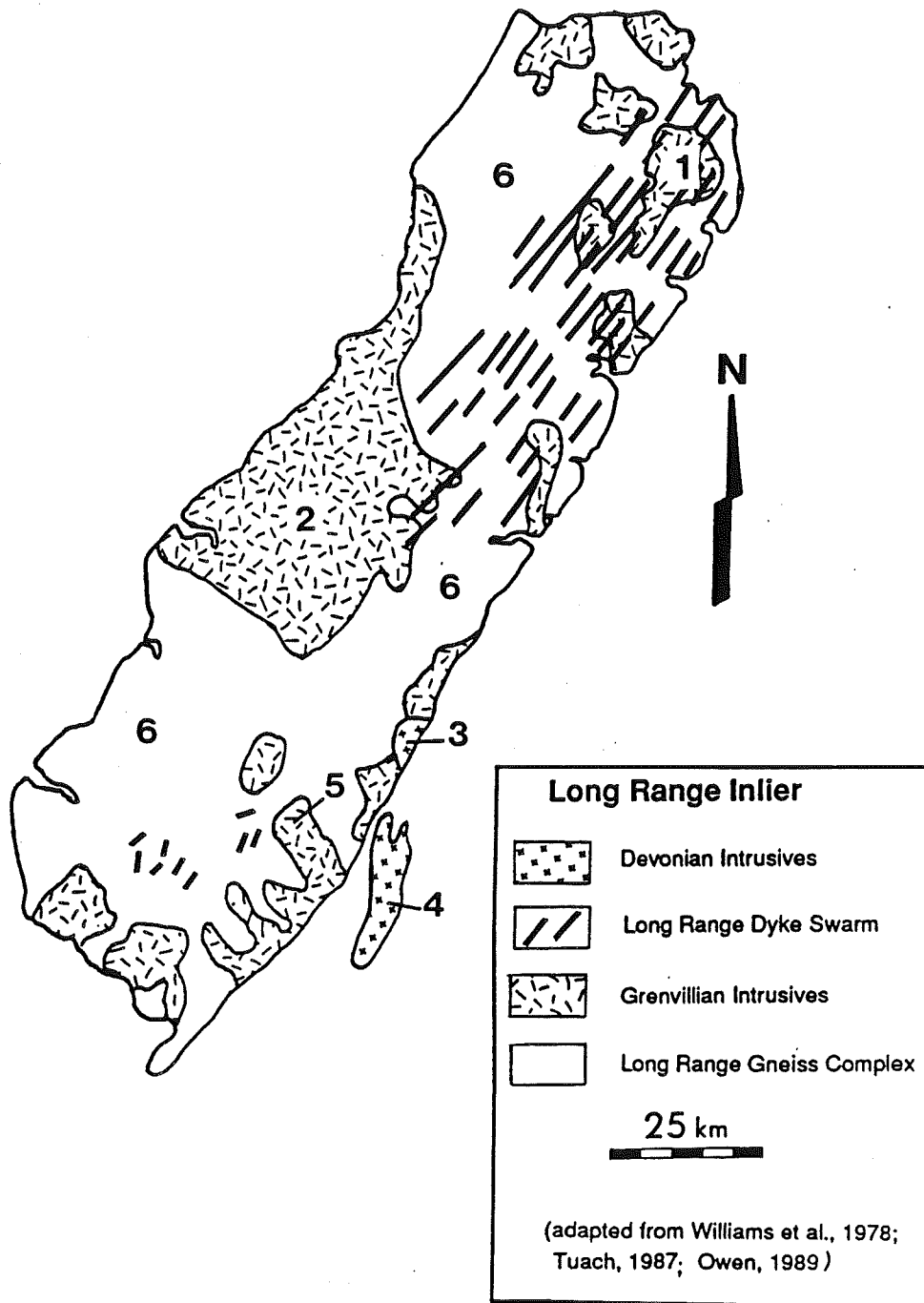


Figure 1.4

General geology of the Long Range Inlier of the Great Northern Peninsula. (1) Hooping Harbour Pluton (2) Lake Michel Intrusive Suite (3) Devil's Room Pluton (4) Gull Lake Intrusive Suite (5) Taylor Brook Gabbro Complex (6) Long Range Gneiss Complex. (adapted from Williams et al., 1978; Tuach, 1987; Owen, 1989)

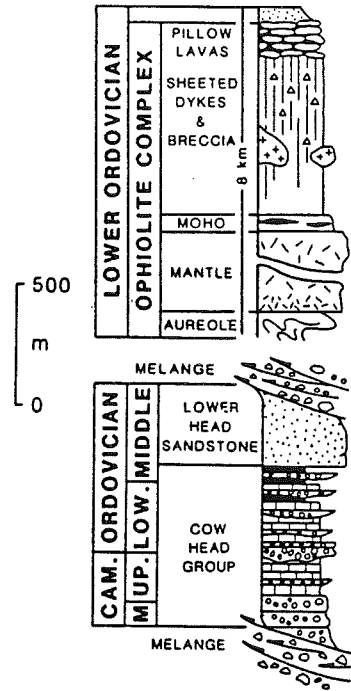
Orogeny caused destruction of the margin in an eastward dipping subduction zone and subsequent west directed thin-skinned thrusting onto the Humber Zone of sedimentary and ophiolite slices (Rodgers and Neale, 1963; Stevens, 1970; Williams, 1975; Stockmal, et al., 1987; Erdmer and Owen, 1989), now exposed as the Humber Arm, Southern White Bay and Hare Bay Allochthons (Cawood and Williams, 1988). For a detailed description and overview of the Cambrian-Ordovician autochthonous and Taconian allochthonous rocks of the Great Northern Peninsula see James and Stevens (1986).

Relatively, autochthonous platform rocks are broadly divided into a basal clastic unit and an overlying carbonate unit which both thicken and get older eastward. Arkosic sandstone and minor conglomerate of the Labrador Group rest on Precambrian basement along the northern perimeter of the Long Range Inlier as well as sporadically along its western and eastern borders (James and Stevens, 1986; Figure 1.3, 1.5). Metamorphic equivalents of originally poorly sorted conglomerate, graywacke, siltstone, shale, sandstone and limestone are found to the east in the Fleur de Lys Supergroup and East Pond Metamorphic Suite (Williams and Stevens, 1974; Hibbard, 1983; Jamieson, 1990).

The Mid-Cambrian to Mid-Ordovician Port au Port Group and St. George Group carbonates (Figure 1.5) were deposited in a shallow marine environment, but a 5 Ma hiatus during the Early Ordovician allowed karst and Mississippi Valley type ore deposits to develop locally (Beales, et al., 1974; Cumming, 1983; Lane, 1984; Strong and Saunders, 1986; Swinden et al., 1988). Time of ore development, though poorly constrained, seems to be limited to the Paleozoic (Swinden et al., 1988). The St. George Group is followed unconformably by interbedded shallow and deeper marine sediments and limestone breccia of the Table Head Group which records the last deposition of rocks related to the carbonate prism before the first flysch deposits arrive from the east (Stevens, 1970; Klappa et al., 1980; James and Stevens, 1986; Knight and James, 1987).

The Humber Arm and Hare Bay Allochthons comprise rocks of widely varying

ALLOCHTHONOUS
ROCKS
HUMBER ARM
ALLOCHTHON



AUTOCHTHONOUS
ROCKS

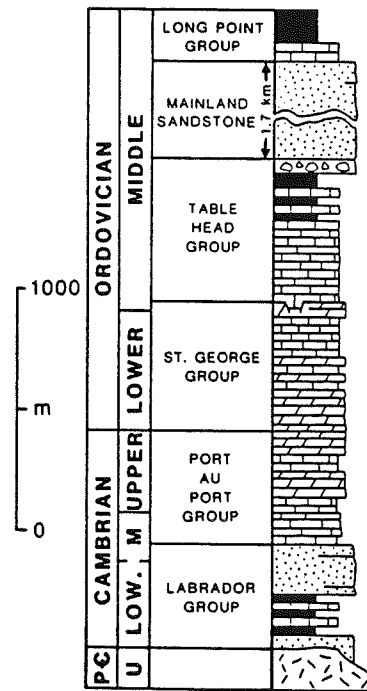


Figure 1.5
Simplified stratigraphy of the autochthonous and allochthonous rocks of northwestern Newfoundland. Ophiolite complex overlies Curling Group (coeval with Cow Head Group and Lower Head Sandstone) in the southern Humber Arm Allochthon. (from James and Stevens, 1986)

lithologies which were thrust westward onto the continental margin during the Taconian Orogeny (Figure 1.3, 1.5). The lowest structural slices of the allochthons are deeper water sediments coeval with the structurally underlying autochthonous rocks. Along the southwestern Long Range, the Humber Arm Allochthon is separated from autochthonous rocks by flysch (Goose Tickle Group) and shaly melange (Williams et al., 1985; James and Stevens, 1986; Figure 1.5). Lack of metamorphism and relatively low conodont alteration index values (CAI = 1.5-2.0) suggest that the lower structural slices west of the inlier have never been deeply buried beneath the higher slices that are part of the allochthons to the south and north of the Long Range (James and Stevens, 1986; Nowlan and Barnes, 1987). These higher level igneous and metamorphic sections comprise ultramafic rocks, gabbros, sheeted dikes, pillow lavas and clastic sedimentary rocks and are separated by shaly melange zones (Cawood and Williams, 1988).

The highest structural slice in the Hare Bay Allochthon (St. Anthony Complex) is separated from underlying sedimentary rocks by the Middle Ordovician Hare Bay Fault (Jamieson and Talkington, 1980; Figure 1.6). The metamorphic gradient of the St. Anthony Complex is 'inverted' as a result of progressive assembly of the ophiolite thrust stack, and ranges from greenschist facies in the structurally lowest Ireland Point Volcanics to upper amphibolite facies near the Green Ridge Amphibolite contact with the overlying White Hills Peridotite (Jamieson, 1981). This peridotite-metamorphic aureole contact is characterized by a narrow peridotite mylonite zone which locally contains mylonitized alkaline rocks (jacupirangite and syenite) along its northeastern boundary (Jamieson and Talkington, 1980).

Traditionally, the Appalachian Orogeny has been divided into two main pulses in the northern Appalachians; the Taconian (Middle Ordovician) and Acadian (Devonian) Orogenies. However, recent work in Middle Paleozoic rocks throughout the Canadian Appalachians (Jamieson et al., 1986; Chandler et al., 1987; Whalen, 1987; Dunning et al., 1990) has shown that Silurian magmatism affects all the Appalachian tectono-stratigraphic zones and may indicate a much more continuous phase of orogenic activity

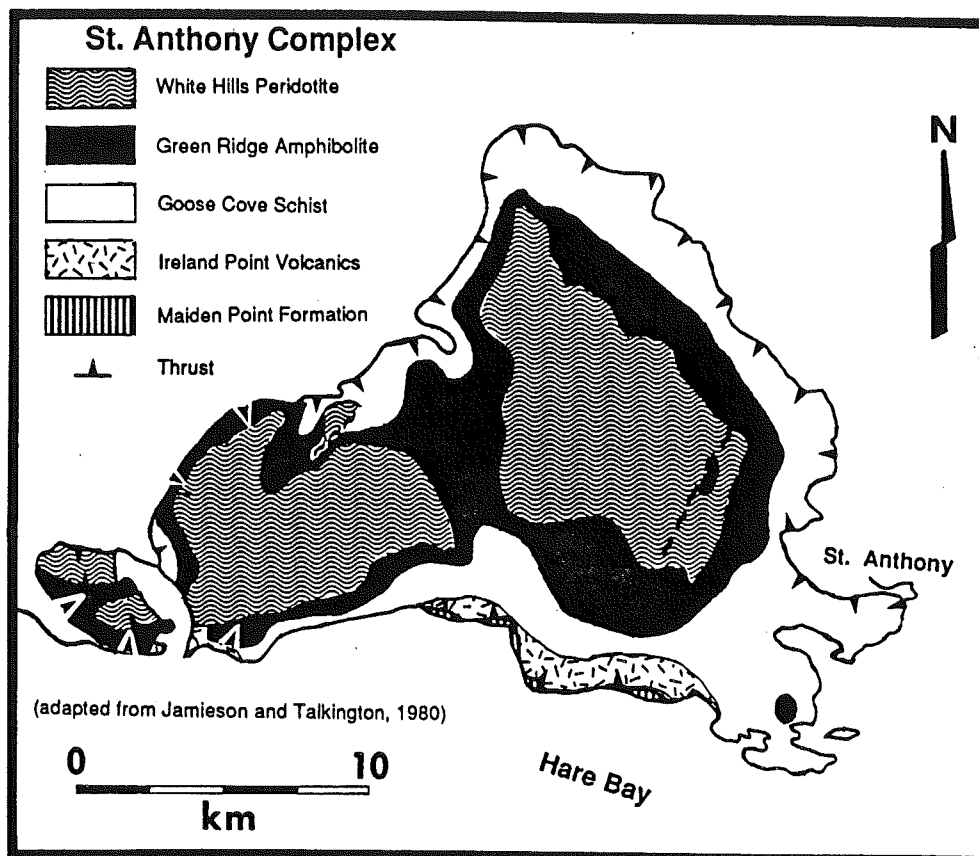


Figure 1.6

General geology of the St. Anthony Complex of the Hare Bay Allochthon, Great Northern Peninsula. (adapted from Jamieson and Talkington, 1980). Location shown on Figure 1.3.

from the Middle Ordovician to Middle Devonian than was previously thought (Bevier and Whalen, 1990). Bimodal volcanic suites and granites intrude Ordovician oceanic and arc-type rocks east of White Bay (Topsails area; Whalen, 1987). Silurian-Devonian lithologies west of White Bay (Figure 1.3) indicate a much different geologic setting from the early Paleozoic passive margin. Thick conglomerates followed by volcanics and redbeds of continental affinity were deposited in local successor basins which were surrounded by tectonically active highlands (Williams, 1969; Williams, 1979).

The Silurian-Devonian Acadian Orogeny are characterized by deep sole thrusts and splays into basement and reworking of the Taconian allochthons (Cawood and Williams, 1988). The Long Range Thrust along the western Long Range Inlier is probably an Acadian feature and is interpreted as a steeply emerging splay above a sole thrust which continues westward below the platform rocks (Grenier and Cawood, 1988; Stockmal and Waldron, 1990; Figure 1.3).

Acadian intrusion within the Humber Zone is limited to the Devil's Room Granite which gives an Early Devonian crystallization age (390+27,-7 U-Pb zircon, Erdmer, 1988) and cuts a greenschist fabric that affects the length of the eastern Long Range (Owen and Erdmer, 1988). The Gull Lake Intrusive suite, about 50 km south and east of the Devil's Room Granite, has a similar age (Figure 1.4; Owen and Erdmer, 1988). Though not associated with a structural fabric, an eastern Long Range Acadian greenschist grade thermal event is suggested by ca. 400 Ma U-Pb titanite ages from Grenvillian plutons in southern LRI (Erdmer, 1986), and a degassing event at 380 Ma ($^{39}\text{Ar}/^{40}\text{Ar}$ K-feldspar, Stukas and Reynolds, 1974) which may be related to the Acadian intrusion. K-Ar dating has yielded Devonian ages for mafic dykes that intrude rocks along the eastern Great Northern Peninsula (408 Ma K/Ar biotite, Wanless et al., 1968; 353 Ma K/Ar phlogopite, Wanless et al., 1973).

Alleghanian orogenic effects in the northern Appalachians were restricted mainly to strike-slip faulting along the narrow Cabot Fault Zone which runs from the

southwestern tip of Newfoundland northeast to White Bay and then north along the flank of the Great Northern Peninsula (Betz, 1943; Hyde, 1984). Great stratigraphic thicknesses of locally derived terrestrial sediments occupy several graben-like basins in this zone. Exact timing and movement history of this Late Paleozoic fault zone is not clear. Extensive sinistral Devonian-Carboniferous displacement within the Appalachians has been suggested based on non-coincidence of paleopoles (Kent and Opdyke, 1978; Kent, 1982; Scotese et.al, 1984; for structural evidence of strike-slip faulting see Hanmer, 1981; Wilton, 1983). Workers in the Newfoundland Carboniferous strata favour relatively minor (< 100 km) dextral motion during the Late Paleozoic (Belt, 1968; Ludman, 1981; Knight, 1983; Hyde, 1984; O'Brien et al., 1986), and more recent paleomagnetic work by Irving and Strong (1984) limits any lateral movement along the Cabot Fault zone to less than a few hundred kilometers.

Offshore, Carboniferous rocks surround the Humber Zone. A wide zone of Early Carboniferous sediments extends north from the Deer Lake Basin into offshore areas east of the Great Northern Peninsula (Haworth et al., 1976; Figure 1.3 see segment labelled White Bay). Early Carboniferous sediments extend northward along the western coast (Haworth and Sanford, 1976; Figure 1.3). South of Newfoundland, Upper Carboniferous offshore rocks locally exceed 9000 m in thickness (Howie and Barss, 1974).

1.4 Mesozoic-Present

Southern and eastern Newfoundland offshore areas were tectonically active during the opening of the present Atlantic Ocean (Haworth and Keen, 1979; Srivastava and Tapscott, 1986; Tankard and Welsink, 1988). Earliest plate motions involve a break-up of North America and northwest Africa during the Mid-Jurassic (Keen and Hyndman, 1979) when the southern Grand Banks served as a transform margin (Todd et al., 1988). A Mid-Cretaceous unconformity over the Grand Banks marks the rifting of eastern North America from Iberia and western Europe (Keen et al., 1977; Masson and Miles, 1984).

Continent-continent transform motion continued along the Charlie Fracture Zone until the Paleocene. Subsidence and sedimentation have characterized the continental margin of Newfoundland ever since. Except for a number of mafic dykes (possibly Mesozoic?) in Ordovician lithologies and in gold bearing stockworks east of the Long Range Inlier (Tuach, 1987b) there seems to be no geological evidence for Mesozoic continental break-up in the Great Northern Peninsula.

Complete glaciation of the Humber Zone occurred during the Wisconsin Ice Age. Roches moutonees, hanging valleys, fjords and glacial erratics provide evidence for glacial action in the Long Range, while lowland areas are the site of glacial deposits and strandline uplift (MacClintock and Twenhofel, 1940; Grant, 1970).

Thus, the Great Northern Peninsula has experienced at least three episodes of compression (Grenvillian, Taconian and Acadian) and at least three episodes of extension (Late Proterozoic, Carboniferous and Mesozoic) with significant Carboniferous transcurrent faulting and more recent glaciation. Geological constraints suggest that the present distribution of rocks in the Great Northern Peninsula is no earlier than Acadian, however the topographic prominence of the Long Range Inlier and straightness of structural boundaries suggests younger events, poorly represented in the rock record, may have influenced today's map pattern.

1.5 Geological Setting of Study Area

1.5.1 Introduction

Four suitable target areas were chosen for this project. General selection criteria included accessibility to areas of highest relief (perimeter of the Long Range Inlier), and availability of apatite, particularly in the case of the Cambrian-Ordovician sedimentary

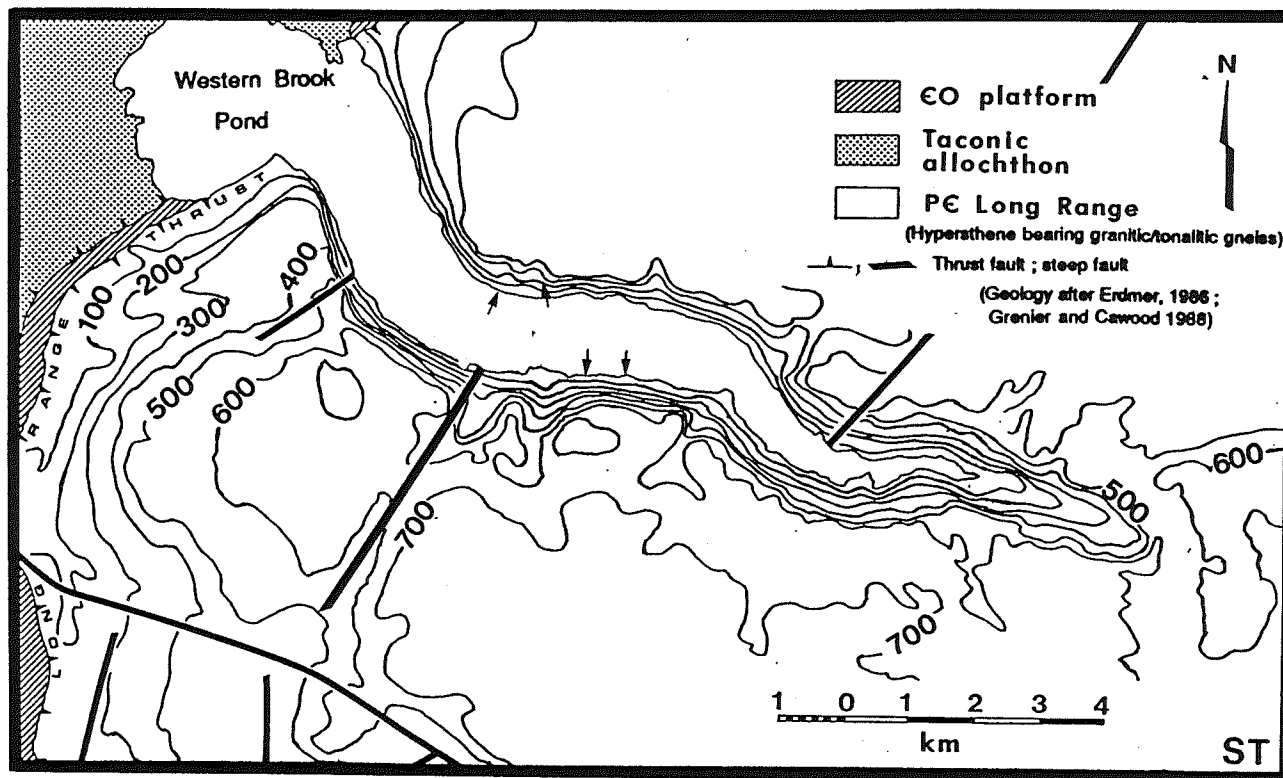


Figure 1.7
 General geology of the Southern Transect, Great Northern Peninsula. Contours in meters above sea level. Arrows indicate approximate location of Long Range Swarm Dykes. (Geology after Erdmer, 1986; Cawood and Grenier, 1988). Location shown on Figure 1.3.

rocks, in order to provide a vertically and laterally constrained sample collection of the Great Northern Peninsula. Three of the study areas are located in the Long Range itself, and one in an overlapping basin (Figure 1.3). 1. The Southern Transect (ST) is located in the southwestern Long Range around Western Brook Pond of Gros Morne National Park. 2. The east-central Long Range is the location for the Central Transect (CT). 3. The Northern Transect (NT) stretches the east-west width of the Long Range Inlier's northern extremity, therefore covering a much larger area than either the Southern or Central Transects. 4. The last study area is the Deer Lake Basin (DLB) which lies unconformably over the southeast Long Range margin. In addition, selected sites in the Cambrian-Ordovician rocks surrounding the Long Range were chosen to relate their low temperature cooling histories to the rest of the rocks in the Great Northern Peninsula.

1.5.2 Southern Transect

The Southern Transect incorporates all three tectonic elements of the Humber Zone; Long Range Inlier crystalline basement, Cambrian-Ordovician autochthonous rocks, and Taconian allochthonous rocks (Figure 1.7). The inlier comprises mainly 1250 Ma granulite facies granitic to tonalitic gneiss (Erdmer, 1986). High level diabase dykes up to 7 m wide pierce the gneiss complex and are well exposed along the 600 m high cliffs of Western Brook Pond. The dykes are only moderately altered relative to their Long Range Swarm counterparts farther east (Bostock and Cumming, 1973) which may reflect the difference in intensity of the Appalachian orogenies between the western and eastern Long Range. Taconian allochthonous rocks are exposed in the northwest area of Figure 1.7. Cambrian-Ordovician platform rocks are wedged as a faulted sliver between the other two tectonic elements (Grenier and Cawood, 1988).

The map area is within the 'southern zone' of Cawood and Grenier (1988) where deformation along the Long Range Thrust front is concentrated in a narrow zone between the Long Range Thrust and the Parson's Pond Thrust splay. Lateral transport along the

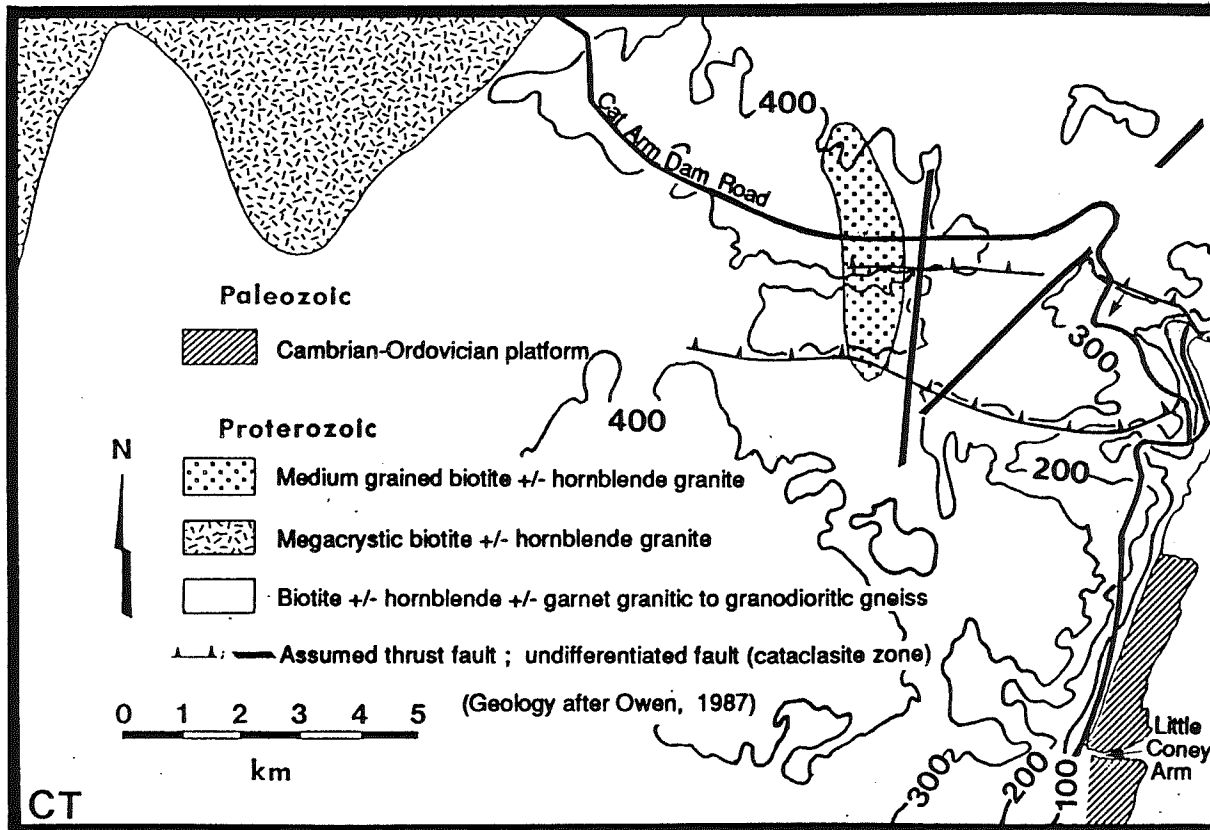


Figure 1.8
 General geology of the Central Transect, Great Northern Peninsula. Contours in meters above sea level. Arrow indicate approximate position of Long Range Swarm Dyke. (Geology after Owen, 1987). Location shown on Figure 1.3.

Long Range Thrust is limited to only a few kilometers (Cawood and Williams, 1986; Cawood et al., 1987). The thrust could have been active any time between post-Middle Ordovician to Early Carboniferous (Acadian?) since it cuts the Taconian allochthon, and Carboniferous cover unconformably overlies a probable southern extension of the thrust system in the Port au Port area (J. Waldron, pers. com., 1990). Two sets of high-level, northeast- and northwest-trending steep faults and shear zones displace the Long Range Thrust south of the Southern Transect (Erdmer, 1986). These faults also cut Precambrian structures in the map area. Their map pattern and concentration around the maximum overlap of basement over sediments, as well as the postulated existence of a sole thrust suggest that the entire inlier may have acted as a thin sheet of competent rock within or above more ductile rocks during Appalachian orogenesis (Erdmer, 1986).

1.5.3 Central Transect

Cambrian-Ordovician platform rocks unconformably overlie the Long Range Inlier in the southeastern Central Transect (Figure 1.8). The rocks dip steeply to the east and display a penetrative schistosity and lower greenschist facies metamorphism (Tuach, 1987b). Across the Great Coney Arm (5-10 km southeast of map area) mainly intrusive mafic and felsic rocks form the Coney Head Complex. These Taconian deformed rocks are known as the Southern White Bay Allochthon and are time equivalent to the Humber Arm and Hare Bay Allochthon rocks (Smyth and Schillereff, 1982; Tuach, 1987b; see Taconic allochthons Figure 1.3).

Amphibolite facies granitic to granodioritic rocks of the 1250 Ma Long Range gneiss complex underlie the Central Transect. Intruding the complex are medium grained and megacrystic Grenvillian plutons (1042 Ma, U-Pb zircon, Baadsgaard et al., in prep.). Long Range Dyke Swarm diabase dykes run northeast across all fabrics. Much younger, similarly oriented mafic dykes intrude Cambrian-Ordovician rocks along the eastern perimeter of the inlier (Smyth and Schillereff, 1982; Tuach, 1987b). One such dyke

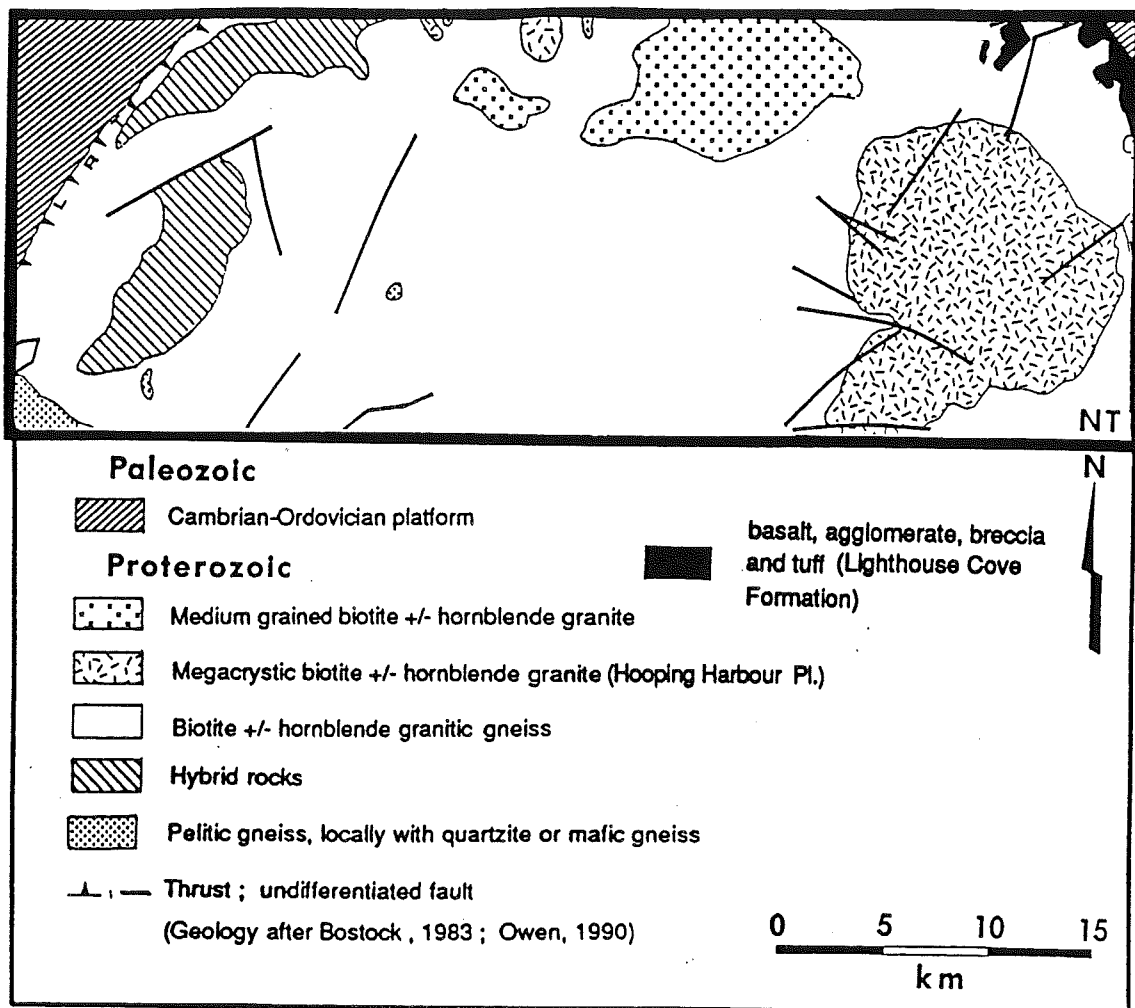


Figure 1.9
General geology of the Northern Transect, Great Northern Peninsula. (Geology after Bostock, 1983; Owen, 1990). Location shown on Figure 1.3.

intrudes Taconian phyllites in the southeastern Central Transect and therefore must be post-Taconian. It is assigned a Late Devonian age (post-Acadian) since it is displaced by a shallow, west-directed Early Carboniferous (?) thrust (Owen and Erdmer, 1988). High level thrusts and cataclasite zones cut the gneiss complex and a Grenvillian pluton, and may also truncate a Long Range dyke. Timing of movement is either Late Grenvillian or Paleozoic (Owen and Erdmer, 1988).

The Middle Ordovician Taconian Orogeny brought the Southern White Bay Allochthon over continental margin rocks producing a low grade fabric within all pre-Middle Ordovician rocks along the eastern Great Northern Peninsula (Smyth and Schillereff, 1982; Owen and Erdmer, 1986). Acadian deformation affects younger Silurian rocks and is characterized by westward thrusting and local mylonite zones accompanied by granitic intrusions and a pervasive greenschist overprint of the eastern Long Range Inlier (Tuach, 1987b; Owen and Erdmer, 1986). Though Carboniferous rocks are relatively unmetamorphosed, Alleghanian deformation produced folding of Lower Carboniferous rocks in the Deer Lake Basin and brecciation as well as fluorite and chlorite formation in older rock units along the eastern perimeter of the Long Range (Tuach, 1987a; Owen and Erdmer, 1988). The Carboniferous Cabot Fault runs parallel to the Central Transect coastline just east of the map area.

1.5.4 Northern Transect

Gneissic rocks of the Northern Transect resemble amphibolite facies quartzofeldspathic gneiss of the Central Transect (Figure 1.9). Widely scattered locations of amphibolite and calcareous gneiss with hypersthene indicate that at least locally the Long Range reached granulite grade during the Proterozoic (Bostock, 1983). Intruding the gneiss complex are the Grenvillian Hooping Harbour megacrystic granite in the eastern Northern Transect and various (Grenvillian?) hybrid rocks (leucocratic to melanocratic gneiss interbanded with granite) in the west (Bostock, 1983). Long Range Swarm dykes

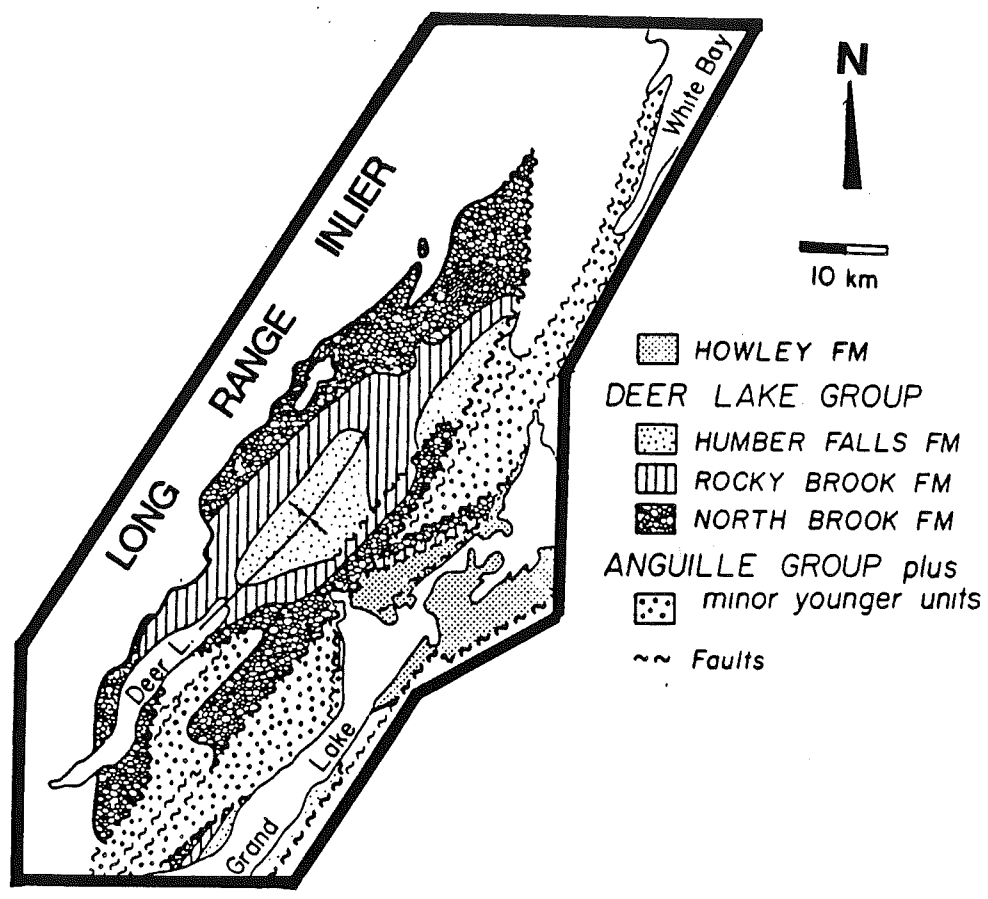


Figure 1.10
General geology of the Deer Lake Basin, western Newfoundland. For relationship to other transects see Figure 1.3. (from Hyde, 1984)

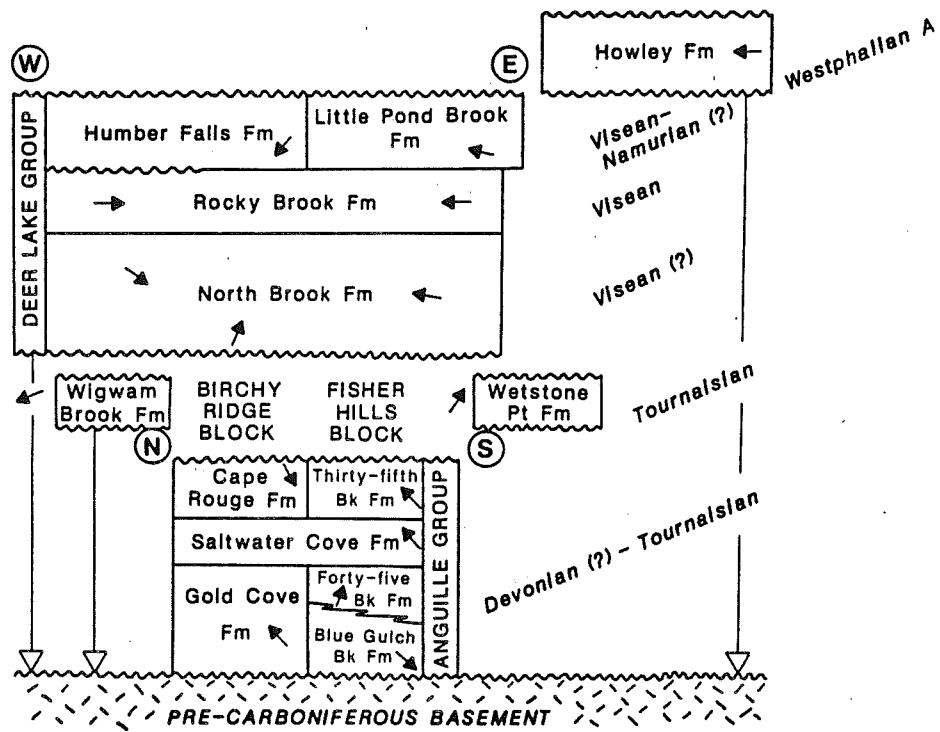


Figure 1.11
 Simplified stratigraphy of the Deer Lake Basin, western Newfoundland. Deer Lake Group and Howley Formation rest directly on pre-Carboniferous basement (open arrows). Wavy pattern denotes unconformities and filled arrows indicate paleoflow direction. (from Hyde et al., 1988)

form prominent lineaments in the eastern Northern Transect and served as feeder dykes to tholeiitic basalt flows of the Lighthouse Cove Formation that locally overlie the gneisses. The 605 Ma age for the dykes fits in well with the stratigraphy, but a mean K-Ar whole rock age of 418 Ma for the flows (Wanless et al., 1965, 1974) has been suggested to reflect cooling due to exhumation of the inlier at the end of the Taconian Orogeny (Bostock, 1983).

The 'northern zone' of the Long Range Thrust Front, in the western Northern Transect, accommodates Acadian deformation over a relatively wide area between the Long Range Thrust and the Ten Mile Lake Thrust (Grenier and Cawood, 1987). The amount of basement uplift relative to present sea level is less than in the Southern Transect. Faults within Long Range basement include cataclasite or breccia zones and mylonites (Bostock, 1983). Some of the faulting probably accompanied Late Precambrian uplift of the inlier but other faults are Paleozoic or younger since they cut Cambrian-Ordovician rocks along the northern Long Range. The Carboniferous Cabot Fault zone runs just east of the map area and is associated with Carboniferous sediments of the Cape Rouge and Conche areas northeast of the Northern Transect (Bostock, 1983).

An early pre-Long Range Dyke Swarm greenschist facies metamorphism may have accompanied Grenvillian granitic intrusion. A later, post-Long Range Swarm greenschist overprint is limited to the eastern half of the map area and extends into platform rocks south and east of the Northern Transect. The grade of this second overprint increases (more epidote in dykes) eastward (Bostock, 1983).

1.5.5 Deer Lake Basin

The Deer Lake Basin forms a relatively small northern section of an extensive zone of Devonian-Carboniferous (mostly sedimentary) rocks known throughout eastern Canada as the Maritimes Basin (Poole, 1972, Figure 1.10). Postulated origins of the

Deer Lake Basin include shearing and extensional tectonics (Belt, 1968) and strike-slip faulting (Webb, 1969; Haworth, 1975).

Three fining upward megasequences, each on the order of one thousand metres thick, characterize the fill of the Deer Lake Basin (Hyde, 1984; figure 1.11). Intensely folded and faulted sandstone, siltstone, and mudstone of the Tournaisian Anguille Group were deformed by transpression into piercement structures during Tournaisian-Viséan time (Popper, 1970; Hyde, 1988). Similar Anguille Group sediments are exposed in the Conche and Cape Rouge areas suggesting a basin length of about 275 km (Williams and Smyth, 1983). Furthermore, a very broad expanse of Mississippian (Tournaisian?) rocks underlies the northeastern coast of Newfoundland (Haworth, 1976). The Deer Lake Basin may thus represent only a small portion of a much larger Early Carboniferous depositional area (Hyde, 1984). Anguille Group paleocurrent indicators generally suggest flow from the southeast (Hyde, 1984).

During the Viséan, mainly dip-slip faulting along the east side of the Deer Lake Basin instigated filling of the basin from the west and east with clastic rock and limestone which constitute the second megasequence (North Brook and Rocky Brook Formations) named the Deer Lake Group. At this time the Deer Lake Basin was considerably wider and shorter so that the North Brook Formation lies with inferred angular unconformity on Anguille Group and on Long Range basement further west. Pebbles of Long Range affinity are found as clasts in the North Brook Formation fanglomerates suggesting positive relief immediately west of the basin. Present day exposure of these sediments is very close to the Early Carboniferous basin extent (Hyde, 1983, 1984).

The final megasequence includes the Viséan-Namurian Humber Falls Formation and conglomerate and coal of the Westphalian A Howley Formation. These formations are in part coeval so that the Howley sediments form an adjacent sub-basin directly overlying pre-Carboniferous basement in the eastern Deer Lake Basin, while the Humber Falls Formation rests on the Deer Lake Group in the west. Paleo-flow directions suggest

a Siluro-Devonian volcanic/plutonic source area north and east of the Deer Lake Basin (Hyde, 1984).

Geological and geophysical evidence suggests the Deer Lake Basin is a strike-slip basin (Hyde et al., 1988). Strike-slip basins are noted for short-lived, elevated heat flow and later regional thermal subsidence beyond the master faults (Bradley, 1982; Pitman and Andrews, 1985). This latter feature may have played a role in the Viséan-Westphalian widening of the Deer Lake Basin (Hyde et al., 1988).

Various methods have been used to determine thermal maturation of the basin. All support higher thermal maturation levels for the older Anguille Group (~200 °C) than for the Deer Lake Group and Howley Formation (~100 °C) (Gall and Hiscott, 1986; Hyde et al., 1988). This may be the result of deeper burial, elevated heat flow, or both (Hyde, 1988) in the Anguille Group.

Chapter 2. Apatite Fission Track Analysis: Methodology

2.1 Introduction

Fission tracks are submicroscopic damage zones in a crystal lattice resulting from the fission of the nuclei of radioactive atoms. This process occurs naturally in a number of radioactive elements but only the fission track accumulation from the ^{238}U atom is considered for most practical purposes. The most widely accepted explanation for fission track formation is the ion spike model (Fleischer et al., 1965). Following a fission event, two positively charged fission fragments are mutually repelled, stripping electrons from the surrounding lattice. Repulsion of a trail of secondary positively charged ions embeds these particles into the surrounding lattice forming a fission track (Figure 2.1). Typical fission tracks in apatite are a few tens of angstroms in diameter and $\sim 16\text{-}17\ \mu\text{m}$ long (Gleadow and Lovering, 1975).

Fission tracks were first observed using scanning electron microscopes (Silk and Barnes, 1959). Price and Walker (1962) discovered that fission tracks may be enlarged by chemical etching so that they can be viewed by an optical microscope. Since then, apatite fission track dating has been applied as a geochronological tool to many regions of the world. The usefulness of this method stems from the low closure temperature of apatite fission tracks ($105 \pm 25\ ^\circ\text{C}$, Harrison and McDougall, 1980; $60\text{-}125\ ^\circ\text{C}$, Gleadow et al., 1983) over geological time. In addition, the apatite fission track length distribution possesses detailed information on the low temperature (less than $125\ ^\circ\text{C}$) thermal history experienced by the host rock (eg. Green et al., 1989). Recently age and track length data together have been used to derive quantitative low temperature thermal histories of samples (Donelick, 1988; Willett et al., 1990). These qualities have made the apatite fission track method particularly valuable in the study of basin development and maturation (Gleadow et al., 1983; Issler et al., in press), ore and secondary mineral emplacement (Naeser, 1984; Maksiyev and Zentilli, 1989), and regional exhumation (Gleadow and Fitzgerald, 1987; Fitzgerald and Gleadow, 1988).

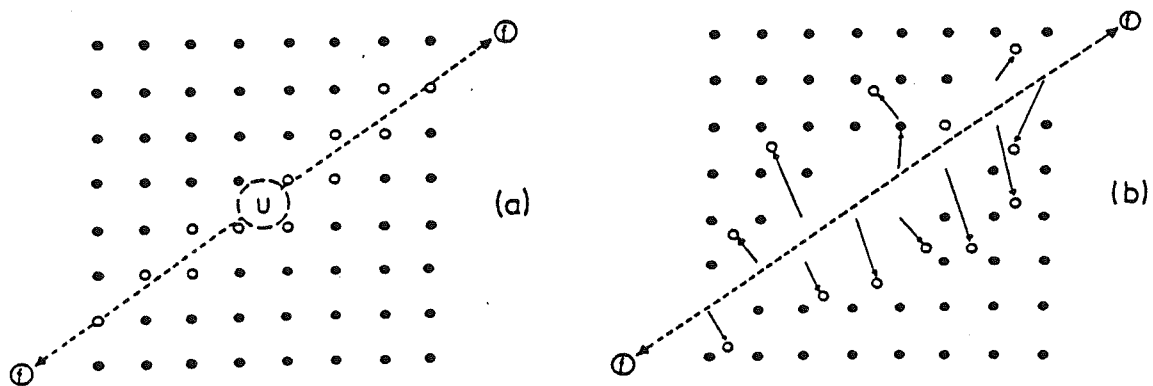


Figure 2.1

ion spike model for formation of fission tracks. a.) Two positively charged fission fragments are mutually repelled, stripping electrons from the lattice. b.) Secondary positively charged ions are then embedded into the surrounding lattice forming a fission track. (from Fleischer et al., 1965)

2.2 The Apatite Fission Track Age: A Radiometric Clock

Apatite fission track dating depends on the amount of parent isotope (^{238}U) and the rate at which the parent is converted to daughter product which, in turn creates a fission track. Measurement of ^{238}U (parent) and the number of spontaneous fission tracks (daughter) is analogous to other radiometric dating techniques involving the measurement of radiogenic and stable isotopes (ie. U/Pb, Rb/Sr, and $^{40}\text{Ar}/^{39}\text{Ar}$ methods). Price and Walker (1963) proposed a fission track dating technique based on the assumption that the number of fission tracks accumulated over time in a given material depends only on the initial concentration of ^{238}U and its decay rate by spontaneous fission. The present ^{238}U is determined by irradiating a sample with a thermal-neutron flux which induces fissioning of ^{235}U in the sample. Since the ratio $^{238}\text{U}/^{235}\text{U}$ is constant in nature (137.88, Steiger and Jaeger, 1977) a count of the induced ^{235}U fission tracks is used to measure indirectly the amount of ^{238}U present in a sample. The fundamental fission track equation is (Price and Walker, 1963):

$$t = \frac{1}{\lambda_d} \ln \left(1 + I \Phi \sigma g \frac{\rho_s \lambda_d}{\rho_i \lambda_f} \right) \quad (1)$$

where

t = the apparent fission track age of the mineral (Ma)

I = the atomic ratio $^{238}\text{U}/^{235}\text{U}$ (137.88; Steiger and Jaeger, 1977)

Φ = the thermal-neutron fluence during irradiation

σ = the ^{235}U thermal-neutron fluence cross-section ($5.802 \times 10^{-26} \text{ cm}^2$)

$g =$ the counting geometry factor (0.5 for External Detector Method)

$\lambda_d =$ the ^{238}U total decay constant ($1.55125 \times 10^{-10} \text{ a}^{-1}$, Steiger and Jaeger, 1977)

$\lambda_f =$ the ^{238}U spontaneous fission decay constant ($\sim 6\text{-}8 \times 10^{-17} \text{ a}^{-1}$, Friedländer et al., 1981)

$\rho_s =$ spontaneous fission track density in grain (tracks/unit area)

$\rho_i =$ induced fission track density in detector (tracks/unit area)

From the above equation it is clear that the main quantities that need to be measured to determine a sample's fission track age are its spontaneous and induced fission track densities. Since fission tracks cannot be seen by the naked eye they must be chemically etched and then observed through a high powered microscope. The track density quantities are obtained by counting the number of etched tracks per unit area intersecting an internal surface of an apatite grain (spontaneous track density (ρ_s)) and the number of etched tracks per unit area in a low U detector placed over the grain (induced track density (ρ_i)), which records the number of tracks resulting from the one way passage of induced ^{235}U fission tracks from the apatite grain. The resulting ratio (ρ_s/ρ_i) is proportional to the age of the sample. The age (t) determined from this density ratio is termed the apparent apatite fission track age because it only considers track density, which leads to an apparent number of tracks per unit volume.

Apatite fission tracks are meta-stable features that progressively fade (anneal) with temperature and time (Green et al., 1985). If track lengths are corrected for their anisotropic behaviour in apatite, line segment theory tells us that there should be a one to one correspondence between density and length of tracks (Green, 1988). Therefore a reduction in track length will be accompanied by a reduction in apparent age. The apparent apatite fission track age does not take into account tracks lost to annealing. The

corrected apparent age (t_{ca}) accounts for the full number of fission tracks present in the volume by considering the mean etchable track length of a sample (m) shortened by annealing and the original mean etchable track length (m_0 , $\sim 16.5 \mu\text{m}$) such that $t_{ca} = (m/m_0)t$. The mean etchable track length of a sample was determined in this study by measuring only etched lengths of tracks that were both confined to the grain and parallel to the internal surface used for track density measurements. If all tracks ever formed in the sample are preserved (ie. no reduction in track number), then t_{ca} is the absolute age of the sample (Donelick, 1987).

A variety of approaches including the population, subtraction, re-etch, re-polish and external detector methods have been developed to determine fission track ages (Hurford and Green, 1982). All involve indirect evaluation of the apatite uranium concentration by inducing tracks from ^{235}U during thermal neutron irradiation. The external detector method (used in this study) is the only method which avoids the assumption of homogeneous uranium concentration in a sample since corresponding areas are counted in the grain and in a low uranium detector. This is especially important for Great Northern Peninsula samples since some apatites displayed inhomogeneous uranium concentration over the core (low U concentration) to the rim (high U concentration) of the grain. The basis for the 0.5 geometry factor (g) in the above equation comes from counting induced tracks resulting from one way passage from the grain into the detector (2π geometry) and from two way passage of spontaneous tracks across an internal surface of the grain (4π geometry). The 0.5 geometry factor is the correct value for apatite sections where the etching efficiency is high, as in prismatic sections. Only prismatic sections were counted in this study.

The most difficult quantities to be measured in the apparent fission track age equation are the fission decay constant (λ_f), the rate of ^{238}U decay due to fissioning, and the neutron fluence (Φ), the thermal-neutron dosage experienced during irradiation of the sample. However, the need for explicit determination of these quantities for solving the apparent fission track age equation is circumvented using the zeta calibration method.

CN1 vs CN2

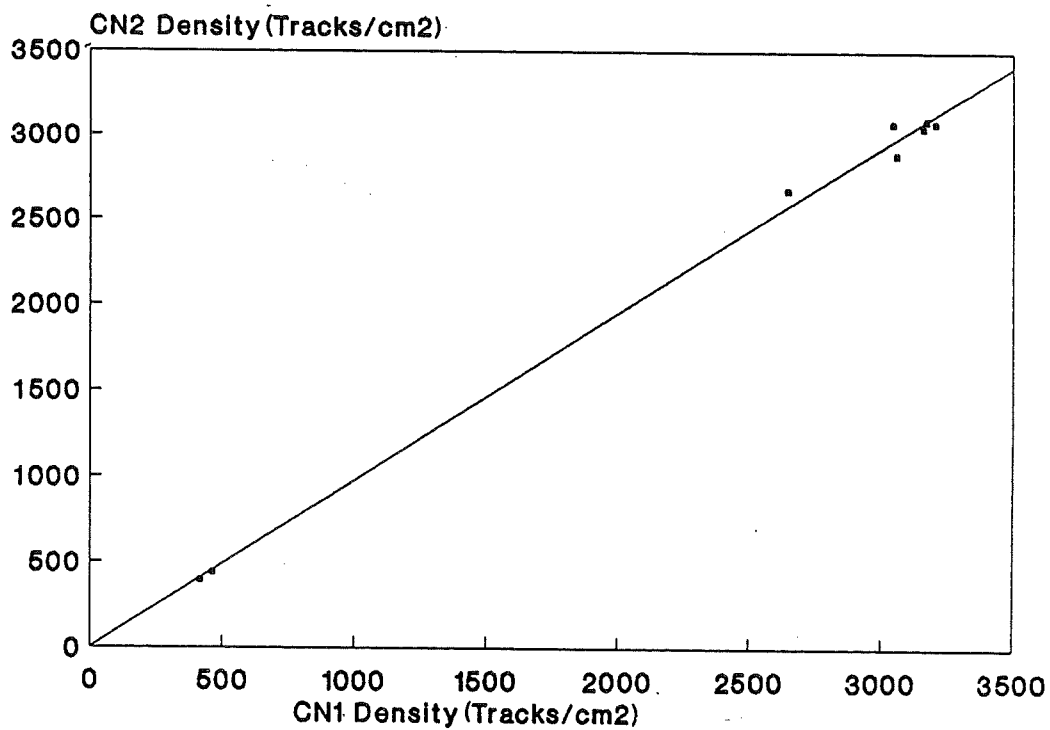


Figure 2.2

Track density correlation plot for paired (same irradiation package) CN-1 vs. CN-2 dosimeter glasses. CN-1 vs. CN-2 correlation factor = 0.970. (from Li et al., 1990)

First proposed by Fleischer (1975; see also Hurford and Green, 1983), the basis for the zeta calibration factor is that for a given thermal-neutron dosimeter (in this study Corning CN-1 and Bureau of Standards SRM614 glasses), the ratio of thermal-neutron fluence and the number of induced fission tracks (ρ_d) crossing the external surface of the dosimeter is constant (Faure, 1986). The glass dosimeter is then calibrated to an independently dated apatite age standard by determining the age standard apatite fission track ρ_s/ρ_i ratio. On this basis, we define the zeta (ζ) calibration factor as a collection of the constants (except λ_d) in the age equation and it can be evaluated by irradiation of dosimeter glasses with apatite age standards so that:

$$\zeta = \frac{1}{g \lambda_d \rho_d} \left(\frac{\rho_i}{\rho_s} \right)_{STD} \exp(\lambda_d t_{STD} - 1) \quad (2)$$

where

$(\rho_i/\rho_s)_{STD}$ = induced to spontaneous fission track density of apatite age standard

t_{STD} = absolute age of apatite age standard

ρ_d = induced track density of a given dosimeter glass

Dosimeter glasses, Corning CN-1 and Bureau of Standards SRM614 were used in this study. Glass track densities were averaged to give a single glass track density value for each irradiation capsule because within analytical error there was no difference in glass track density between the top and bottom of each capsule. A density correlation factor was used to compute CN-1 glass track densities from CN-2 glass densities when CN-1 glasses were not available. This factor is based on experimental work by Li et al., (1990) where paired CN-1 and CN-2 glass densities from the same package were correlated to give a CN-1 vs. CN-2 correlation of 0.970 (for McMaster University nuclear reactor, Figure 2.2).

Zeta values for this study were determined with age standards Fish Canyon Tuff

Glass Dosimeter	Standard	Chi2	Zeta ^a
CN-1	DR	PASS	111.1 +/- 10.0
CN-1	DR	PASS	110.6 +/- 10.0
CN-1	DR	PASS	127.7 +/- 11.3
CN-1	DR	PASS	94.7 +/- 8.6
CN-1	DR	PASS	106.2 +/- 9.1
CN-1	DR	PASS	98.9 +/- 8.6
CN-1	DR	PASS	105.4 +/- 10.4
CN-1	DR	PASS	106.1 +/- 9.9
CN-1	FC	PASS	107.6 +/- 9.3
CN-1	FC	PASS	113.0 +/- 10.0
CN-1	FC	PASS	99.7 +/- 7.8
CN-1	FC	PASS	94.7 +/- 7.6
CN-1	FC	PASS	82.9 +/- 9.2
CN-1	RN	PASS	142.4 +/- 6.7
SRM614	DR	PASS	11774. +/- 678.
SRM614	DR	PASS	12351. +/- 346.

^a one standard deviation

Table 2.1
Zeta values determined during the study (1988-1990) for dosimeter glasses CN-1 and SRM614. Standards used were Durango (DR), Fish Canyon Tuff (FC) and Rentfrew (RN).

($t_{\text{STD}} = 27.8 \pm 0.2 \text{ Ma}$, $^{40}\text{Ar}/^{39}\text{Ar}$; Hurford and Hammerschmidt, 1985), Durango ($t_{\text{STD}} = 31.4 \pm 0.5 \text{ Ma}$, $^{40}\text{Ar}/^{39}\text{Ar}$; McDowell and Keizer, 1977) and Renfrew ($t_{\text{STD}} = 199 \pm 5 \text{ Ma}$, apatite fission track; Donelick, unpublished data) and are given in Table 2.1. The errors in both zeta values and apatite fission track apparent ages are based on the randomness of the fissioning process (Green, 1981). For the zeta values, the random error associated with this process is determined by summing the square roots of the numbers of tracks counted in the glass dosimeter and the apatite age standard. Apparent fission track ages from unknown samples include the random error associated with counting tracks in the unknown sample. The Chi-squared test checks for extra-Poissonian error. It determines whether and how well the data is representative of a single Poissonian population or if the variability in the data requires another explanation (Galbraith, 1982). If extra-Poissonian error was found in the zetas or in ages of unknown samples the mean track ratio rather than the pooled ratio was used to determine the error. All zetas pass the Chi-squared test and therefore each age standard density count may be represented by a single Poissonian population (cut-off $Q < 0.05$). In theory, zeta values are constant for a given dosimeter, neutron energy spectrum during irradiation, and counting technique. Standard practice is to use a running zeta (ie. updating zeta throughout study with new zeta determinations) to calculate unknown ages in order minimize any subjective counting error in the measurement of zeta values. The running zeta used in this study was updated with additional age standards and glasses after each irradiation. The unknown ages of FT90-034, -035, -050 (Table 3.4) were determined at a later date in the study, therefore the zeta used for their age determination was calculated separately and is based on the three age standards. The particular zeta used for each analyzed age is given in Tables 3.2 and 3.4 along with the ages. See Appendix 1 for zeta data.

Once a zeta factor has been established, only the unknown sample ratio of spontaneous to induced fission track remains to be measured to evaluate unknown ages. The age is determined by substitution of (2) into the age equation (1):

$$t = \frac{1}{\lambda_d} \ln \left(1 + \zeta \lambda_d \frac{\rho_s}{\rho_i} \rho_d g \right) \quad (3)$$

which is the apparent age equation used in this study. All ages presented in this study are apparent fission track ages with errors reported at the 2σ level.

2.3 Apatite Fission Track Ages in Exhumation Studies

Apatite fission track dating has been applied to cooling/exhumation chronology in many areas of the world (Schaer et al., 1975; Harrison et al., 1979; Naeser, 1983; Parrish, 1983; Gleadow and Fitzgerald, 1987; Fitzgerald and Gleadow, 1988; Zentilli and Maksiyev, 1989; Maksiyev, 1990). Both time of cooling below ~ 100 °C and, in areas with considerable topographic relief, exhumation rates are theoretically determinable with apatite fission track methods (Wagner et al., 1977; Harrison, et al., 1979).

Apatite ages have generally been observed to increase with elevation (Dodge and Naeser, 1968; Wagner and Reimer, 1972). This pattern is interpreted to be mainly the result of upward movement of a rock column through the critical isotherm (closure of apatite with respect to fission tracks). Higher elevation rocks, which have cooled below their closure temperature sooner, have more time to accumulate fission tracks and thus give older ages than rocks at lower elevations. The age gradient formed over the rock column is defined as the apparent uplift rate of the rock column (Parrish, 1983). Interpreting this rate as the true uplift rate (relative to sea level) of the rock column is dangerous since, in fact, the age gradient only represents the rate at which the critical isotherm moves downward with respect to the rock column (Parrish, 1983). In order for the apparent uplift rate to equal the true uplift rate a number of conditions must be met (Parrish, 1983): 1. The geothermal gradient must have remained uniform over the time

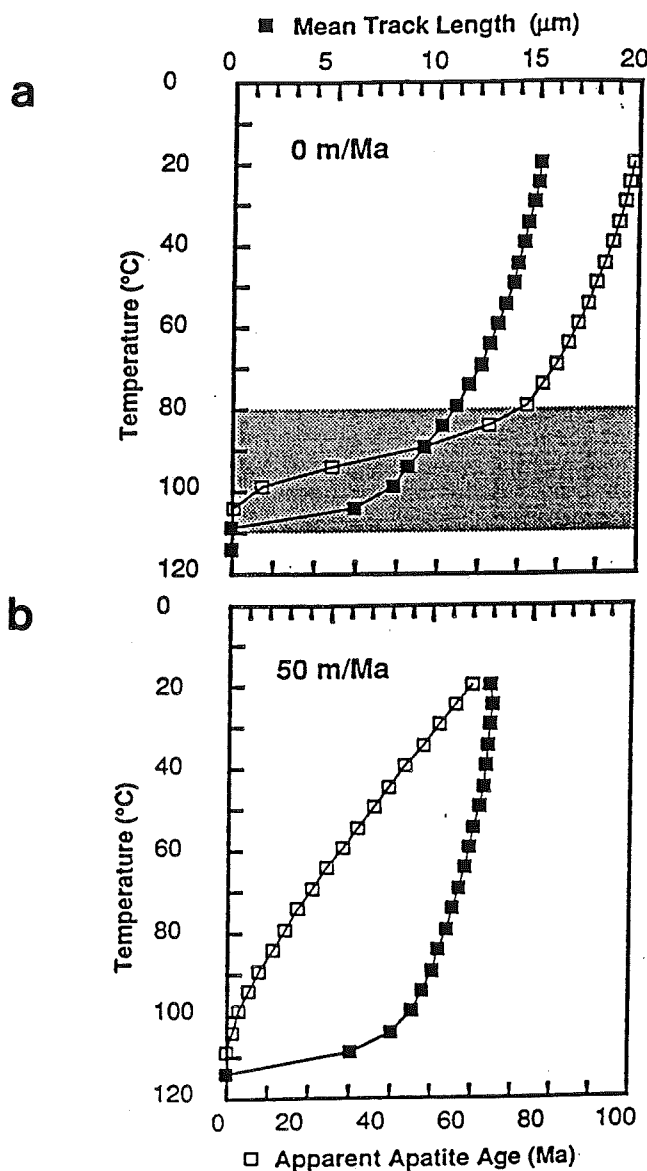


Figure 2.3

Apatite apparent fission track age and mean track length vs. temperature for various isotherm relaxation rates (Laslett et al., 1987; Green et al., 1988). a.) Model isotherms are held constant with respect to the surface for 100 Ma producing a 13 m/Ma age gradient in the partial annealing zone (shaded region). The steeper age gradient developed at low temperatures (above the partial annealing zone) is analogous to fission track age patterns in boreholes and indicates that in fact annealing occurs over all temperatures greater than ~ 20 °C. b.) Model isotherms are relaxed at 50 m/Ma for 100 Ma. The induced age gradient in the partial annealing zone is no longer evident. Note the longer mean length of the surface sample in the static case; its tracks are only slightly annealed relative to the uplifted surface sample which spent some time in the partial annealing zone. Assumed geothermal gradient of 25 °C/km. Model based on annealing characteristics of Durango apatite. (from Fitzgerald and Gleadow, 1988)

period represented by the difference in the apatite fission track ages. 2. Steady state tectonic conditions must apply over that same time period (ie. uplift equal erosion).

Investigation of apatite annealing characteristics has revealed that a single closure temperature for fission tracks in apatite is too simplistic. Closure happens over a range of temperatures (75-125 °C; Naeser, 1979; Gleadow and Duddy, 1981; Gleadow et al., 1983; Green et al., 1986; 60-125 °C;) depending on the cooling rate (Dodson, 1973). The concept of a partial annealing zone has been used to facilitate interpretation of apatite fission track ages by defining a range of temperatures (~70-125 °C) over which apatite fission tracks annealed (faded) and below which tracks were considered stable (Wagner, 1972; Gleadow et al., 1983). Although partial annealing is now known to occur over temperatures 20-125 °C (Green et al., 1985, 1986) the 'partial annealing zone' concept is still useful and in this study is used to distinguish temperatures of relatively greater annealing (~70-125 °C) from minor annealing temperatures (below ~70 °C). This concept introduces the possibility of slow, induced apparent uplift rates in a vertical suite of rocks which has resided at partial annealing temperatures for an extended time period (Figure 2.3) as has been documented in the Transantarctic Mountains of Antarctica (Fitzgerald and Gleadow, 1988). Given the complex interrelationships of all these conditions the ideal situation is rarely met and caution must be exercised in interpretation of apparent uplift rates.

2.4 Apatite Fission Track Annealing

Annealing of tracks occurs over all temperatures greater than 20 °C (Green et al., 1985, 1986; 1989; Donelick, pers. comm. 1990), although the rate of annealing varies with temperature. At low temperatures (less than ~70° C) fading is very slow, but annealing rates progressively increase with temperature to the base of the partial annealing zone (~125 °C) where it is essentially an instantaneous process (Fitzgerald and Gleadow 1988). Given this variability in annealing rate with temperature and the

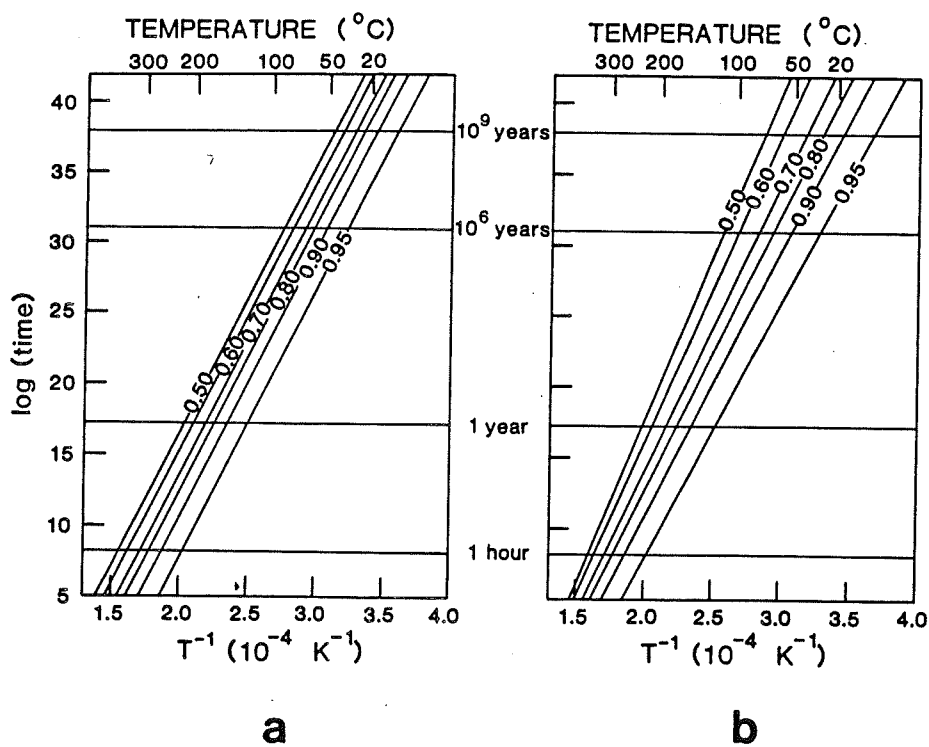


Figure 2.4

Arrhenius plots ($\log(t)$ vs. $1/T$) extrapolating laboratory apatite fission track annealing results to geological timescales. Plots indicate lines of equal annealing (eg. 0.95 line denotes range of time and temperatures over which to expect 5 % annealing or 95 % retention of tracks). a.) Parallel annealing lines produced for a constant activation energy of fission track annealing. b.) Slightly fanning annealing lines resulting from different activation energies for apatite fission track annealing. Although both models fit annealing data of Green et al., (1986), based on goodness of fit (b) is the preferred apatite track annealing model. Note that differences between the two models are magnified with increasing extrapolation. (from Laslett et al., 1987)

fact that fission tracks are produced continuously through time, the confined track length distribution (frequency of confined track lengths vs. track length intervals) will reflect the temperature variation through time experienced by a sample. This means that for a given distribution of track lengths the shortest tracks are the oldest tracks and younger tracks are longest because they have experienced relatively less of the overall thermal history recorded in the distribution. Other thermal history indicators, such as vitrinite reflectance (Epstein et al., 1977) and conodont colouration indices (Castano and Sparks, 1974; Waples, 1980) give the integrated temperature history experienced by a sample but nothing about its variability through time.

Current understanding of apatite annealing characteristics is based on laboratory data which are extended to geological timescales by way of an Arrhenius plot (Naeser and Faul, 1969; Hammerschmidt et al., 1984; Green et al., 1985; Green et al., 1986; Duddy et al., 1988). The annealing kinetics of apatite fission tracks and the resulting nature of the Arrhenius plot distribution have important implications for extracting quantitative information from track length distributions. Because debate exists over the exact fission track annealing kinetics of apatite, a variety of Arrhenius plot distributions have been in use (for a review of this see Laslett et al., 1987). Based on goodness-of-fit modelling, an annealing kinetics model represented by a set of slightly fanning annealing lines in an Arrhenius plot has been suggested as the preferred kinetic model (Laslett et al., 1987; Figure 2.4b). The fanning is viewed as a consequence of different fission track annealing activation energies for the various chemical species present and for different crystallographic orientations in apatite (Laslett et al., 1987). Other kinetic models are represented by parallel annealing lines (constant activation energy, Figure 2.4a) and widely fanning annealing lines in an Arrhenius plot (see Laslett et al., 1987).

2.5 Sample Preparation and Procedures for Apatite Fission Track Age and Track Length Measurement

2.5.1 Mineral Separation

Depending on lithology, 0.5 to 2 kg of each sample was crushed to sand size particles using steel jawcrushers and a pulverizer and then passed through a 300 μm mesh nylon sieve into a large aluminum tray. The sieved fraction was washed with a jet of water to remove adhering clay-sized particles. After the sample grains had sunk in the muddy water, it was decanted and the spraying process repeated until the decanted water was clear. The sample was then bathed in acetone and allowed to dry overnight.

When dry, extremely magnetic minerals (ie. magnetite) were separated by first passing the sample over the magnetic field of the Frantz isodynamic magnetic separator at low amperage before running it through the separator. The sample was then passed through the magnetic separator at low amperage (current = 0.5 amps) to separate the more magnetic minerals such as chlorite and biotite from the fraction containing apatite. In this way most of the more magnetic fraction was removed from the non-magnetic apatite-bearing fraction in order to reduce sample volume and hence the amount of heavy-liquid needed for density separation.

Standard heavy liquid density separation techniques were used to obtain heavy mineral fractions from each sample. The non-magnetic fraction was poured into large glass funnels containing tetrabromoethane (specific gravity = 2.96) and separated into light and heavy fractions. After both fractions were copiously washed with methanol and allowed to dry in the fumehood, the heavy fraction was passed through methylene-iodide (specific gravity = 3.3) and allowed to separate into light and heavy fractions. Methylene-iodide fractions were repeatedly washed with acetone and allowed to dry.

The light Methylene-iodide fraction was hand-picked for apatite grains at 40X

magnification using a Zeiss binocular microscope and a moistened 00 brush. Apatite was recognized by its prominent hexagonal crystal shape, resinous luster, and relatively low index of refraction. In certain cases, where recognition was made more difficult by rounding of the crystal shape, apatite's solubility in weak HCl (grains dissolve in approximately 10 minutes) was used as an aid in identification.

The procedures employed in the preparation of apatite grain mounts for fission track analysis were suggested by Dr. Randall R. Parrish (short-course on the fission track method, Dalhousie University, November, 1984).

Evenly spaced circles were traced on a 20 X 25 X 0.5 cm³ teflon sheet using a marking pen and dime. Cardboard strips were placed close enough on either side of the circle so that a slide placed on them would form a bridge over the circle. 150 to 200 apatite grains were distributed evenly into each labelled circle and covered with 5 or 6 drops of a gently stirred epoxy (Araldite) and hardener mix. A glass slide was immediately placed on the epoxy which was allowed to spread radially out beyond the edge of the marked circle and then to dry for 24 hours.

Apatite grain mounts were ground and polished using a polishing machine with interchangeable polishing wheels. 600 grit silicon-carbide sandpaper was used for initial grinding on a mounted wheel. The mount was slowly revolved in the opposite direction of the 200 r.p.m. spinning wheel until the marking pen circles were barely perceptible. The mount was polished using wheels prepared with 15-, 9-, and 1- μ m diamond compound. Each wheel was used until scratches of the previous grit were invisible under 400 X magnification reflected light. Before changing each wheel the mount was thoroughly washed with soapy water to rid the sample of any left-over diamond compound. The final polish was obtained by running the mount under light pressure over a 0.03 μ m alumina water slurry several turns in each direction. When the polishing was completed the mount was again thoroughly washed with soapy water and rinsed.

To reveal fossil fission tracks, mounts were etched for 40 seconds at a constant 21 °C in 7% HNO₃. After they were etched each grain mount (and glass dosimeter) was removed from the slide and covered with a piece of low-uranium muscovite sheet attached with Scotch-tape. These were placed in an aluminum irradiation capsule in recorded positions, interspersed with 3-4 age standards and capped at the bottom and top by standard dosimeter glasses.

2.5.2 Sample Irradiation

Six capsule packages (MM018, MM033, MM034, MM038, MM039, MM041) were irradiated for fission track analysis at site 9D in the McMaster University Nuclear Reactor in Hamilton, Ontario. Capsule MM018 was irradiated for 550 seconds, while the rest of the packages were irradiated for 900 seconds. The returned irradiated capsules were stored for up to six weeks under lead to allow radioactivity levels to diminish to a workable 2 mr/hr at a one cm distance.

After irradiation sample, age standard and CN-1 glass dosimeter detectors were etched for 14 minutes in 48% HF while SRM614 glass dosimeter detectors were etched in a similar solution for 40 minutes. Detectors were then rinsed thoroughly with distilled water and dried at very low heat for a few minutes on a hotplate to drive off any remaining HF.

Irradiated and etched samples and detectors were mounted across a mirror plane on a glass slide (Figure 2.5). Samples and standards were attached to the slide by a few drops of melted wax and the detectors were held, face-side up, by a few pieces of Scotch-tape.

2.5.3 Fission Track Age and Length Distribution Measurement Procedures

Fission tracks were counted with dry objectives at 1250 X magnification using a Leitz Laborlux D microscope equipped with a computerized stage, 100-watt light source, and an Olympus 5 X 5 mm grid in the right eyepiece. Throughout the study tracks intersecting the surface along the top and right margins of the grid were included and along the bottom and left margins of the grid were excluded. Only prismatic sections of apatite (parallel to c-axis) were chosen and wherever possible tracks were only counted in the middle area of each grain. To avoid counting bias, most samples were analyzed without prior knowledge of sample number and spontaneous tracks in all grains were counted first after which all induced tracks were counted.

Track lengths were measured using a Leitz drawing tube and a Houston Instruments HIPAD digitizing pad, equipped with a LED cursor and a 9-volt battery. Before each measuring session a personal calibration was conducted by measuring a known grid distance in the right graticule twenty times and normalizing the average measured distance by the true distance. Whenever experimental conditions were interrupted or changed (LED focus, graticule focus etc.) the calibration procedure was repeated before track measuring was resumed. Where possible a minimum of 100 track length measurements were made for each sample to achieve statistical 'significance'. Standard track length calculations (mean, standard deviation, skewness) were made for each sample using a computer program developed by Donelick (1987).

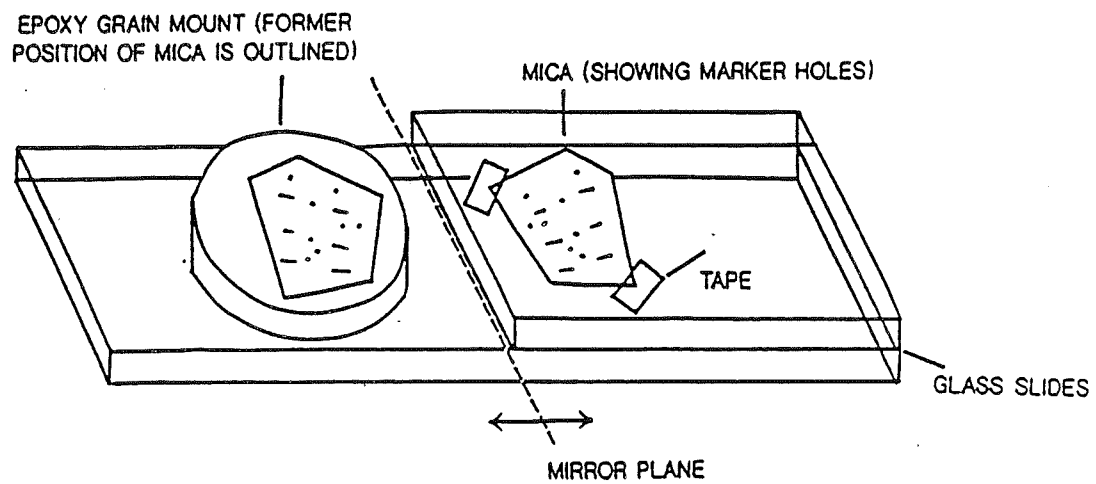


Figure 2.5
Cartoon schematic showing an epoxy grain mount and corresponding external detector (2X magnification).
after Grist (1990)

Chapter 3. Apatite Fission Track Analysis: Results

3.1 Introduction

The apatite fission track method was used to date 31 samples over the full topographic range of the Long Range Inlier and surrounding areas in order to construct apatite apparent age vertical profiles for the Great Northern Peninsula. The majority of the samples were collected by foot or truck, although Northern Transect (NT) samples and highest elevation samples in the Southern Transect (ST) were collected by helicopter. Samples were collected at 50 meter elevation intervals in both the ST and Central Transect (CT) and analyzed at roughly 100 m vertical intervals in these areas. Elevations are known to ± 10 meters based on a control altimeter calibrated to a known elevation or repeated altimeter calibration to sea level. Supplemental samples came from drill core cuttings provided by Newfoundland Department of Mines and Energy in Pasadena (FT89-213) and from the collections of Rebecca Jamieson (Dalhousie University, Halifax, N.S.; FT90-050) and Victor Owen (St. Mary's University, Halifax, N.S.; LGRA-01).

3.2 Southern Transect

3.2.1 Sample Location

A total of thirteen samples forming two vertical transects (ST1 and ST2) were analyzed from the granitic gneiss of the Southern Transect (Figure 3.1). ST1 samples cover the elevation range 75-524 meters above sea level over a four kilometer horizontal distance (Figure 3.1). The lower section of ST1 follows a Pleistocene (?) valley at the eastern end of Western Brook Pond while higher elevation samples were collected over ~ 100 m of relief at the plateau level of the LRI. Additional samples (FT89-222, -223; Table 3.1) were collected east of this transect at highest elevation across the Long Range to provide lateral age control across this part of the inlier. The samples are listed under

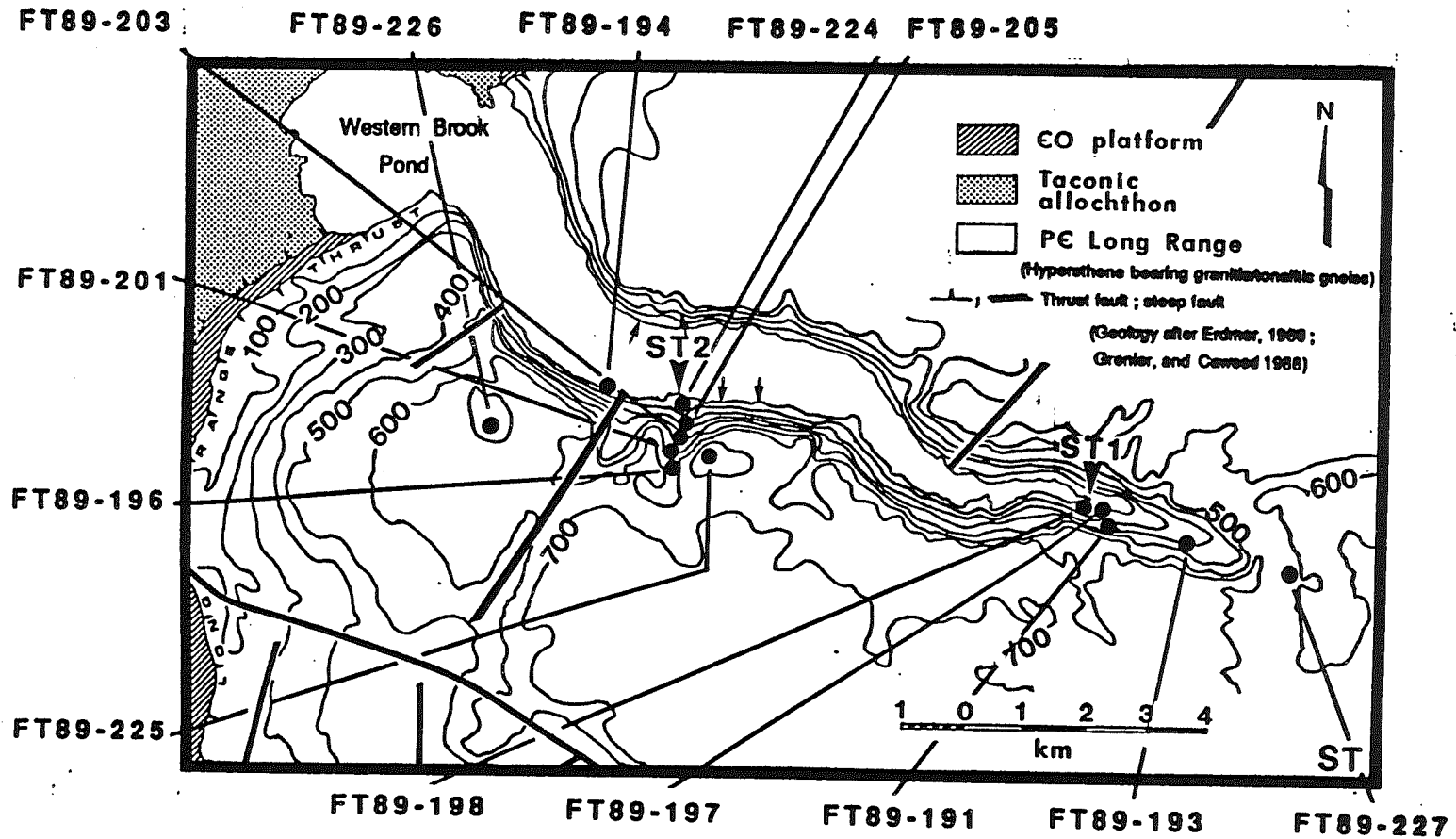


Figure 3.1
 Southern Transect sample location map showing Southern Transect 1 (ST1) and Southern Transect 2 (ST2). Arrows indicate approximate Long Range Swarm dyke locations. Elevation contours above mean sea level are in meters. Transect location shown on Figure 1.3.

<u>Sample</u>	<u>Elevation</u>	<u>Lithology</u>	<u>Location</u>
Southern Transect 1			
FT89-222	615	granitic gneiss	East of ST1, 1:50K topo 12H/11 UTMG *: 67.4 east, 6.3 north
FT89-223	615	dioritic gneiss	East of ST1, 1:50K topo 12H/11 UTMG: 75.5 east, 6.8 north
FT89-227	551	granitic gneiss	Eastern end Western Brook Pond
FT89-193	313	granitic gneiss	Eastern end Western Brook Pond
FT89-191	201	granitic gneiss	Eastern end Western Brook Pond
FT89-197	142	granitic gneiss	Eastern end Western Brook Pond
FT89-198	75	granitic gneiss	Eastern end Western Brook Pond
Southern Transect 2			
FT89-226	750	granitic gneiss	Southern flank of Western Brook Pond
FT89-225	730	granitic gneiss	Southern flank of Western Brook Pond
FT89-201	551	granitic gneiss	Southern flank of Western Brook Pond
FT89-196	455	granitic gneiss	Southern flank of Western Brook Pond
FT89-203	360	granitic gneiss	Southern flank of Western Brook Pond
FT89-205	225	granitic gneiss	Southern flank of Western Brook Pond
FT89-224	75	granitic gneiss	Southern flank of Western Brook Pond
FT89-194	23	granitic gneiss	Southern flank of Western Brook Pond
Central Transect			
FT89-212	480	granite	Cat Arm Dam Road
FT89-211	340	granitic gneiss	Cat Arm Dam Road
FT89-210	211	granitic gneiss	Cat Arm Dam Road
FT89-207	202	granitic gneiss	Cat Arm Dam Road
FT89-209	107	granitic gneiss	Cat Arm Dam Road
FT89-206	105	granitic gneiss	Cat Arm Dam Road
FT89-208	-2	granitic gneiss	Cat Arm Hydroelectric Plant
Northern Transect			
FT89-221	500	granitic gneiss	Western Northern Transect
FT89-232	475	granitic gneiss	Central Northern Transect
FT89-233	335	granite	Eastern Northern Transect (Hooping Harbour Pl.)
Deer Lake Basin and Miscellaneous GNP			
FT90-034	100	granitic gneiss clasts	NBF ^a , Deer Lake Basin, 1:50K topo 12H/6, UTMG: 75.7 east, 72.0 north
FT90-035	257	granite clast	NBF, Deer Lake Basin, 1:50K topo 12H/11, UTMG: 97.9 east, 91.9 north
FT90-050	100	jacupirangite	WHP ^b , Hare Bay All., 1:50K topo 2M/5, UTMG: 89.9 east, 98.5 north
FT89-213	-15	calcareous sandstone	NPF ^c , U.S. Borax drill core BDH2, Daniel's Harbour
FT89-235	0	sandstone	LHF ^d , Lobster Cove Head, 1:50K topo 12H/12, UTMG: 30.9 east, 97.6 north
LGRA-01	50	granite	DRP ^e , Sop's Arm, 1:50K topo 12H/15, UTMG: 5.8 east, 13.8 north

* Universal Transverse Mercator Grid

a North Brook Formation

b White Hills Peridotite

c Norris Point Formation (Mainland Sandstone)

d Lower Head Formation

e Devil's Room Pluton

Table 3.1

Great Northern Peninsula sample elevation, lithology and location by study area.

Sample	Rhos ^a (tr/cm ²)	Ns	Rhoi ^a (tr/cm ²)	Ni	Glass	Rhod ^a (tr/cm ²)	Nd	# Grains	Q	Chi2 ^b	Fission Track Age ^{cd} (Ma)	Zeta
Southern Transect 1												
FT89-222	3.88	895	2.31	698	‡CN-1	4.834	7374	23	0.724	PASS	256 ± 33.8	99.7 ± 8.2
FT89-223	0.888	439	0.622	318	‡CN-1	4.834	7374	23	0.984	PASS	279 ± 47.8	99.7 ± 8.2
FT89-227	1.68	648	1.18	441	‡CN-1	4.834	7374	24	0.681	PASS	285 ± 42.5	119.7 ± 6.6
FT89-193	2.71	596	1.79	394	CN-1	3.285	2859	21	0.965	PASS	253 ± 39.6	104.8 ± 8.2
FT89-191	0.398	226	0.227	157	CN-1	2.998	5499	19	0.971	PASS	253 ± 55.2	119.7 ± 6.6
	0.465	212	0.258	114	CN-1	3.285	2859	20	0.999	PASS	318 ± 77.8	104.8 ± 8.2
FT89-197	0.717	417	0.587	295	CN-1	2.998	5499	20	0.952	PASS	248 ± 41.8	119.7 ± 6.6
FT89-198	0.886	223	0.883	282	CN-1	2.998	5499	9	0.793	PASS	194 ± 39.8	119.7 ± 6.6
Southern Transect 2												
FT89-226	0.683	191	0.398	189	‡CN-1	4.834	7374	19	0.927	PASS	343 ± 87.4	99.7 ± 8.2
FT89-225	1.75	668	1.11	419	‡CN-1	4.834	7374	25	0.929	PASS	389 ± 46.8	99.7 ± 8.2
FT89-281	0.582	228	0.397	158	CN-1	2.998	5499	18	0.888	PASS	257 ± 57.8	119.7 ± 6.6
FT89-196	0.548	383	0.376	288	CN-1	2.998	5499	18	0.616	PASS	255 ± 49.8	119.7 ± 6.6
FT89-283	1.17	594	0.881	488	CN-1	2.998	5499	22	0.824	PASS	256 ± 37.2	119.7 ± 6.6
FT89-285	1.48	728	1.16	568	CN-1	2.998	5499	24	0.768	PASS	223 ± 29.2	119.7 ± 6.6
	1.38	588	0.984	332	CN-1	2.998	5499	27	0.794	PASS	268 ± 41.8	119.7 ± 6.6
FT89-224	1.41	416	1.13	334	‡CN-1	4.834	7374	21	0.642	PASS	246 ± 41.8	99.7 ± 8.2
FT89-194	0.852	361	0.621	263	CN-1	2.998	5499	23	0.996	PASS	241 ± 42.4	119.7 ± 6.6

‡ CN-1 dosimeter glass values from correlation factor

a Rho(s,i,d) x E-06

b test PASS for Q > 0.850; FAIL for Q < 0.850

c two standard deviations

d average age of sample: (FT89-191) 282 ± 66.1 Ma, (FT89-285) 245 ± 35.2 Ma

Table 3.2

Great Northern Peninsula apparent apatite fission track ages for Southern Transect 1 and Southern Transect 2. Rhos, Rhoi, and Rhod = spontaneous, induced, and glass track densities (tracks/cm²); Ns, Ni, and Nd = spontaneous, induced, and glass track count, # Grains = number of grains counted per sample; Q = Chi2 correlation coefficient. Average age for multiple sample counts are found under footnote (d).

but not part of ST1 (Table 3.2). Except for FT89-223 which came from dioritic gneiss, all samples were amphibolite to granulite grade granitic gneiss. ST2 samples were collected east of a steep fault that cuts the Precambrian gneiss, and form an extremely steep vertical section that follows a stream up the southern flank of Western Brook Pond (Figure 3.1). Samples west of the fault are also part of ST2 and complete the ST2 elevational range 23-750 meters above sea level. Other steep faults trend northwest and northeast and displace gneiss in the ST map area. The Long Range Thrust brings the Precambrian Long Range above Cambrian-Ordovician platform rocks in the western part of the map area. Long Range Swarm (inferred) diabase dykes up to 7 m wide (Bostock and Cumming, 1973) intrude the gneiss several hundred meters east of ST2 as well as the northern flank of Western Brook Pond directly across from ST2.

3.2.2 Fission Track Age Analysis

A combination of numerous micro-fractures and etched dislocation features that resembled fission tracks in apatite grains made fission tracks in most ST1 samples difficult to count. These grain characteristics are common in the Long Range Inlier samples so that clear grains containing only unequivocal fission tracks were difficult to find. Long Range samples averaged between 20-25 counted spontaneous tracks per grain. Of this number an estimated 10-20% of the 'tracks' were dislocation features and may have been unknowingly included in the spontaneous count. Where possible, grains with relatively high numbers of spontaneous tracks were counted in order to minimize the possible counting error. Detector contact was good in almost all the analyzed samples (crisp grain replicas with little or no track scatter) and induced tracks reliable. Some samples had induced track scattering around the edges of the replicas but only the middle of grains and replicas (area of best detector contact) were counted minimizing any induced track counting error. All samples had around 20 or more apatite grains except for FT89-198, the lowest elevation sample, which had only 9 countable grains. Single grain ages for each sample can be described by a single Poissonian distribution since all

Southern Transect 1

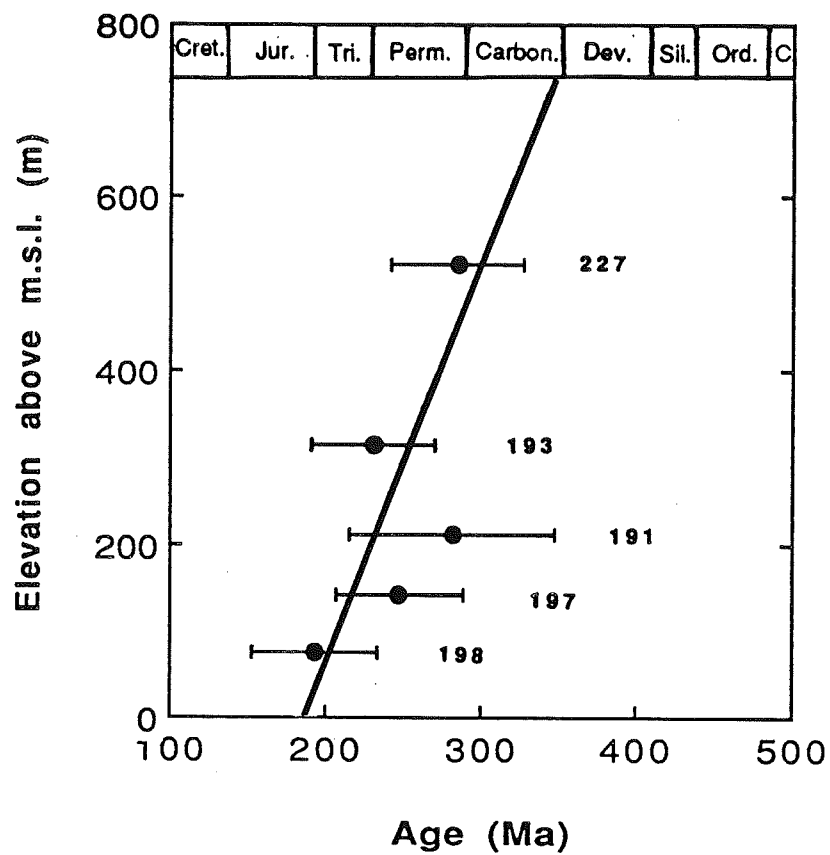


Figure 3.2

Apatite apparent fission track age vs Elevation (meters above mean sea level) for Southern Transect 1. Errors are given as $\pm 2\sigma$. Sample number is given with each age.

samples in ST1 pass the Chi-squared test (Green, 1981; Galbraith, 1982; cut-off Q less than 0.05). Quoted sample ages in Table 3.2 are thus based on a pooled N_s/N_i (number of spontaneous tracks/number of induced tracks) ratio, where N_s and N_i represent all the spontaneous and induced tracks, respectively, in the sample. Samples FT89-222, -223, and -227 were analyzed with CN-1 glass dosimeter values based on a density correlation factor between glasses CN-1 and CN-2 (see section 2.2 for details). Zeta calibration values were constantly renewed for different irradiation packages over the course of six months of counting, resulting in a 20% range of zeta values used for ST1 samples.

Apatite fission track ages in ST1 range from 310 ± 78.0 to 194 ± 39.8 Ma (Late Carboniferous to Late Triassic; 2σ error) (Table 3.2). A second analysis of sample FT89-191 (separate slides) gave ages reproducible within 2σ . The averaged (Early Permian) age for FT89-191 is used in all calculations (Table 3.2, footnote d). Except for the extreme elevation samples FT89-198 and FT89-227, all other samples, including those east of ST1, give ages that overlap within 2σ . These overlapping ages could be statistically represented by a single mean age of 252 ± 45.8 Ma (2σ error).

A common and useful method of presenting the fission track ages is to plot apatite fission track age vs. elevation which shows that despite the 2σ overlap in ST1 ages there is a positive correlation between age and elevation (Figure 3.2). A weighted linear regression of the data by the least squares method of York (1969) fits a straight line through the data with a slope of 7.5 ± 3.3 m/Ma (sum $s=1.98$, $N=5$). The possible implications of such a relationship will be discussed in chapter 5. Sum s is a measure of the goodness-of-fit of the line through the data. The ideal straight line, which goes through all the observed points, would have a sum s value of $N-2$, where N is the number of data points. A sum s value $\gg N-2$ indicates a high degree of scatter in the data which cannot be accounted for by the best fit straight line.

Apatite grain characteristics of ST2 samples were similar to ST1 samples and therefore fission tracks were not easily countable. Spontaneous track counts averaged

Southern Transect 2

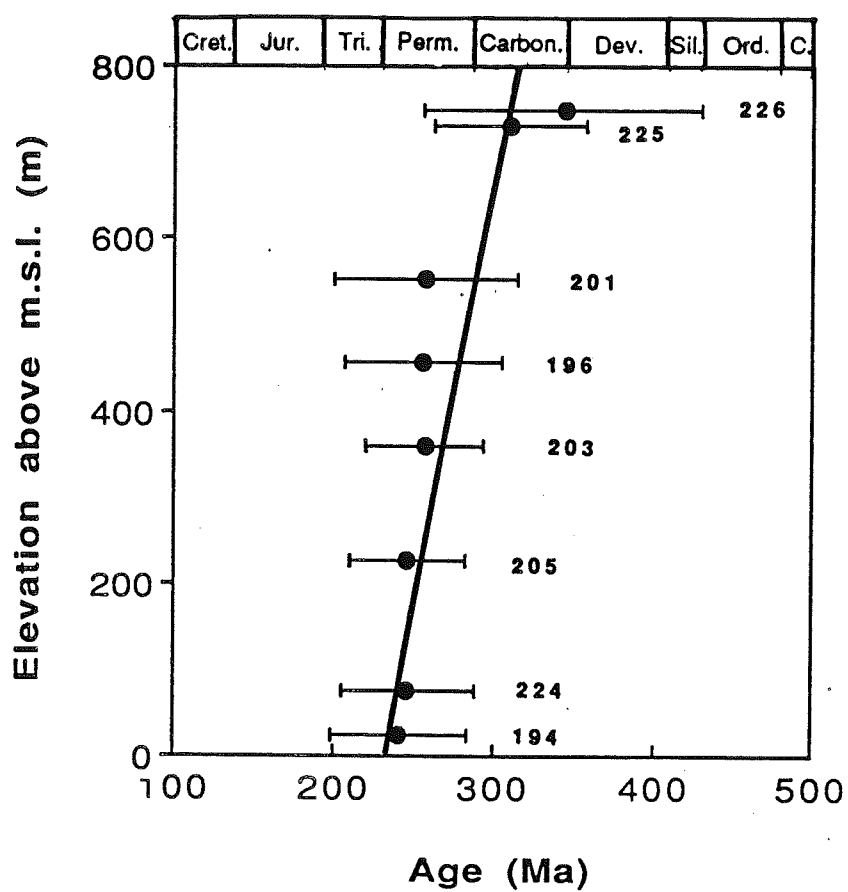


Figure 3.3

Apatite apparent fission track age vs. Elevation (meters above mean sea level) for Southern Transect 2. Errors are given as $\pm 2\sigma$. Sample number is given with each age.

around 20-25 tracks per grain. Detector contact was generally good (crisp replica with little or no track scatter) giving dependable induced track counts. A second analysis of sample FT89-205 (separate slides) gave ages reproducible within 2σ . The average Late Permian age for this sample is used in all calculations (Table 3.1, footnote d). Sample grain counts range from 18-27 grains. All quoted ages are based on pooled Ns/Ni ratios since they all passed the Chi-squared test. Samples FT89-226, -225 and -224 were analyzed using a CN-1 vs. CN-2 glass dosimeter density correlation factor (see section 2.2). ST2 apatite fission track ages range from 343 ± 87.4 to 223 ± 29.2 Ma (Early Carboniferous to Early Triassic; 2σ error), although all ages overlap within 2σ . Therefore, all apatite fission track ages in ST2 could be statistically represented by a single mean age of 269 ± 35.5 Ma. A vertical section of the sample ages is presented in an age vs. elevation plot (Figure 3.3). A weighted linear regression fits a 10.6 ± 2.3 m/Ma slope through the data (sum $s=0.8$, $N=8$). The combined slope of ST1 and ST2 using linear regression is 9.7 ± 2.0 m/Ma (sum $s=2.9$, $N=13$). The implications of this relationship are discussed in chapter 5.

3.2.3 Fission Track Length Distribution Analysis

Percent measured track frequency is plotted against confined track length (bin width = $1\mu\text{m}$) to give track length distribution histograms for ST1 and ST2 (Figure 3.4 a-m). Each figure displays the sample number as well as the mean length (m), standard deviation (sd), number of confined lengths measured (n), elevation of the sample (el) and its apparent fission track age (ma).

Track length distributions are preferably based on 100 or more measurements (Donelick, pers com., 1989). All Southern Transect samples had at least 100 confined tracks except for FT89-223 and FT89-191 whose distributions consist of 34 and 40 track lengths respectively. Mean etched lengths ranged from 12.35 to $13.44\mu\text{m}$ and errors are given at 2 standard errors (Table 3.3). Except for the extreme values, most mean

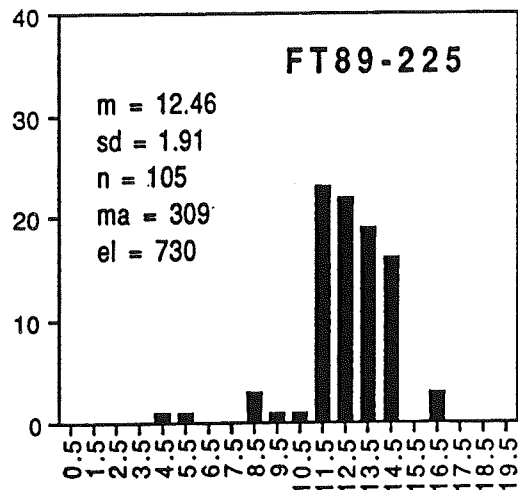
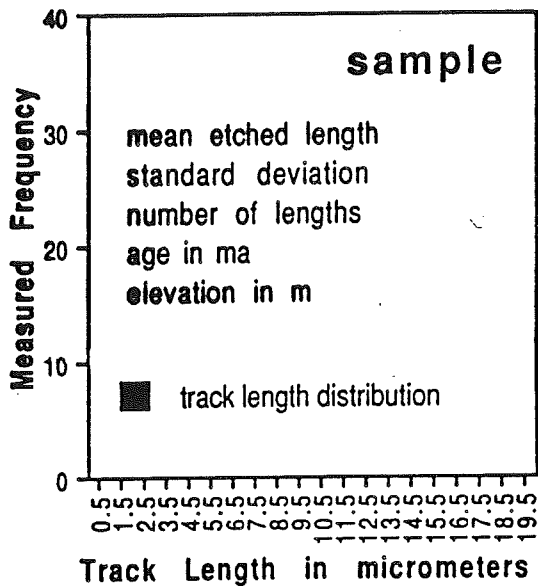
Sample	# Confined Lengths	Mean Etched Length ^a	Standard Deviation
Southern Transect 1			
FT89-222	102	12.84 ± 0.32	1.59
FT89-223	34	12.35 ± 0.96	2.78
FT89-227	104	12.35 ± 0.40	2.00
FT89-193	117	13.85 ± 0.36	1.98
FT89-191	40	12.44 ± 0.72	2.27
FT89-197	111	13.24 ± 0.38	1.55
FT89-198	98	12.91 ± 0.38	1.78
Southern Transect 2			
FT89-226	100	12.42 ± 0.34	1.70
FT89-225	105	12.46 ± 0.38	1.91
FT89-201	109	12.78 ± 0.34	2.01
FT89-196	98	12.71 ± 0.38	1.83
FT89-203	125	13.44 ± 0.32	1.83
FT89-205	109	12.64 ± 0.34	1.78
FT89-224	103	12.38 ± 0.51	2.58
FT89-194	105	12.56 ± 0.34	1.70
FT90-036	105	12.58 ± 0.40	2.00
Central Transect			
FT89-212	104	11.89 ± 0.50	2.56
FT89-211	97	12.48 ± 0.42	2.02
FT89-210	109	12.78 ± 0.38	2.01
FT89-207	107	12.65 ± 0.38	1.95
FT89-209	111	12.62 ± 0.38	2.00
FT89-206	100	12.88 ± 0.50	2.15
FT89-208	117	12.66 ± 0.44	2.32
Northern Transect			
FT89-221	95	13.07 ± 0.40	1.98
FT89-232	110	13.34 ± 0.34	1.73
FT89-233	100	12.78 ± 0.42	2.12
Deer Lake Basin and Miscellaneous GNP			
FT90-034	110	13.14 ± 0.36	1.85
FT90-035	110	12.99 ± 0.40	2.13
FT90-050	100	13.53 ± 0.48	2.40
FT89-213	26	13.01 ± 0.62	1.54
FT90-235	31	12.88 ± 0.42	1.16
LGRA-01	101	13.27 ± 0.28	1.37

^a two standard errors

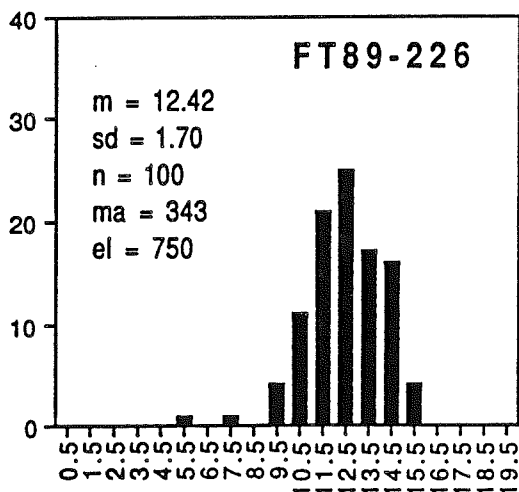
Table 3.3
Great Northern Peninsula sample track length distribution statistics by study area.

Figure 3.4 a-ee

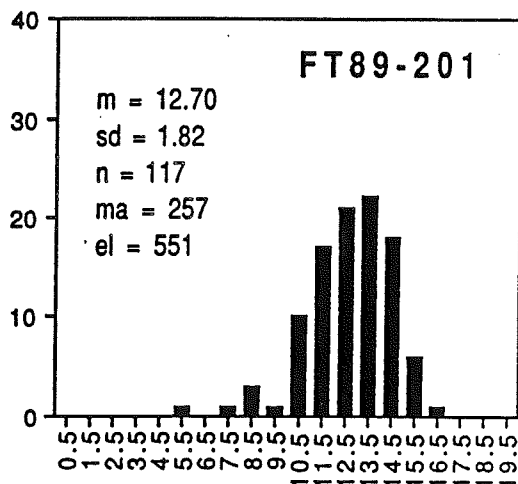
Apatite fission track length distributions for the Great Northern Peninsula. Each distribution displays the sample number, its mean track length (m), standard deviation (sd) and number of confined track lengths measured (n) as well as the sample age in Ma (ma) and elevation in meters (el). Histograms show a 0.5 μm gap between adjacent bins; the gap does not imply absent data but should be regarded as filled.



a

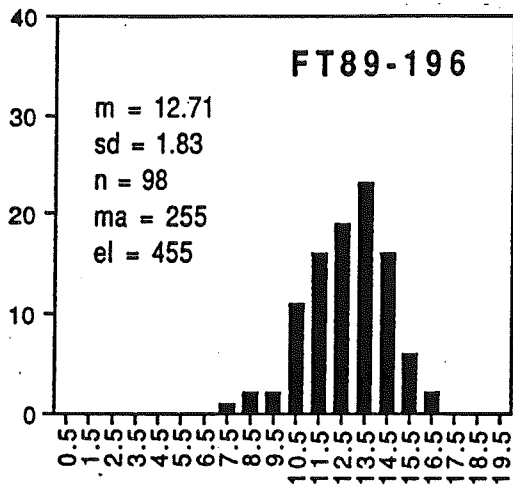


b

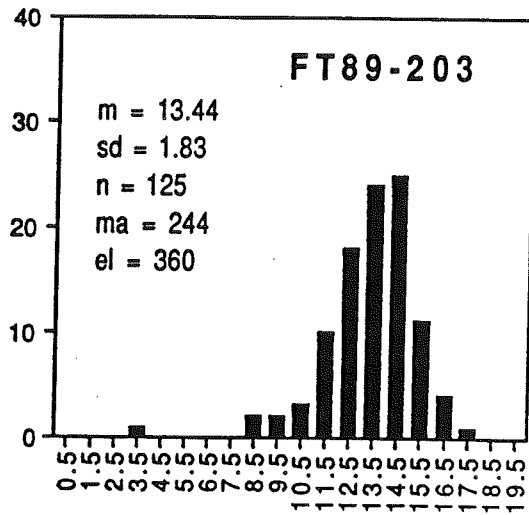


c

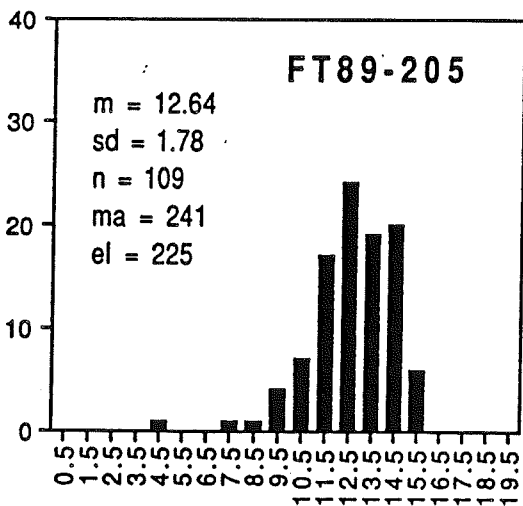
Figure 3.4 a-m
 Apatite fission track length distributions for the Southern Transect (ST1 and ST2).



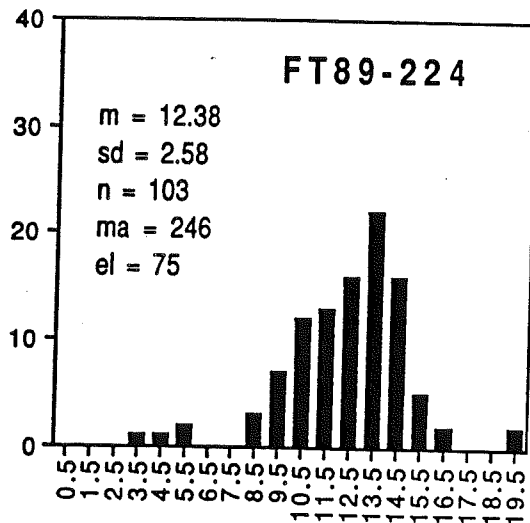
d



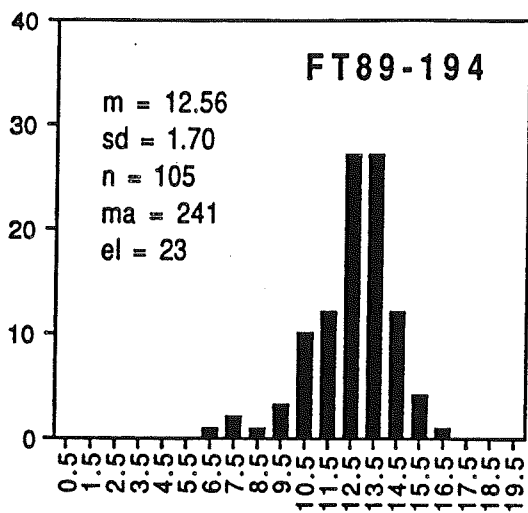
e



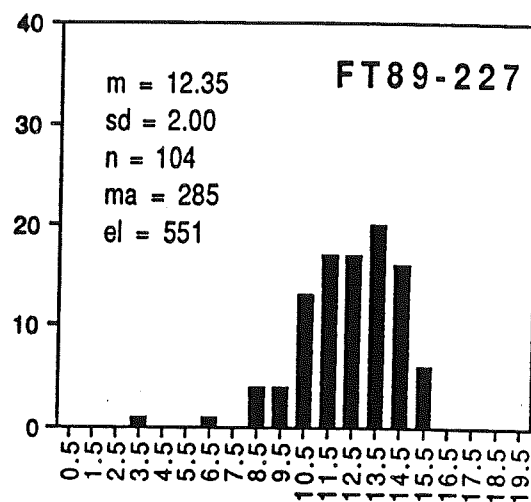
f



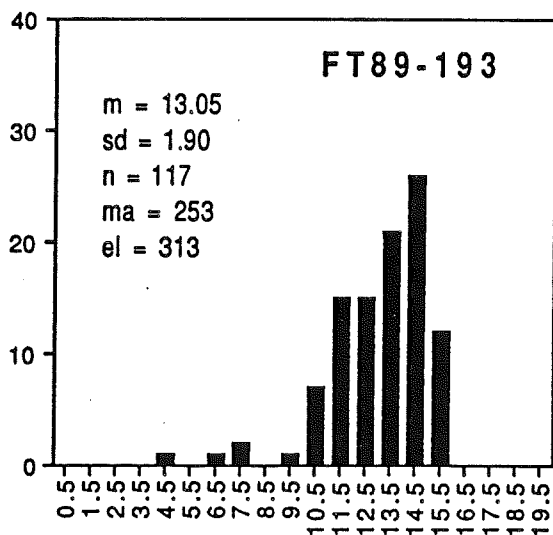
g



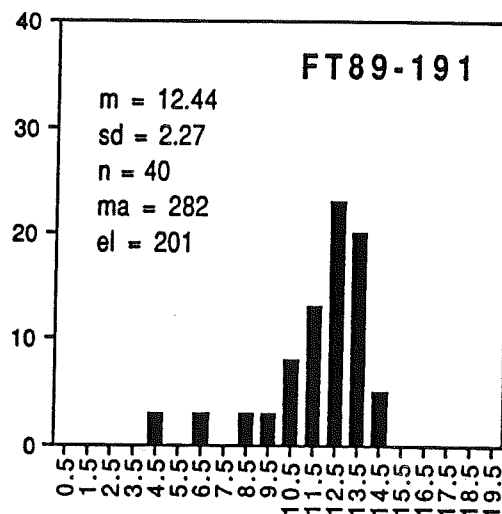
h



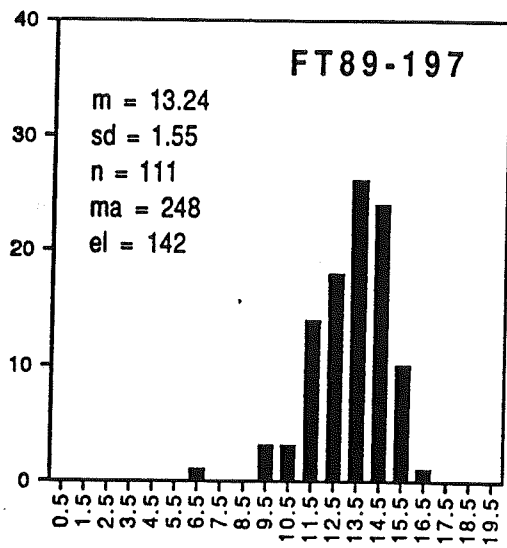
i



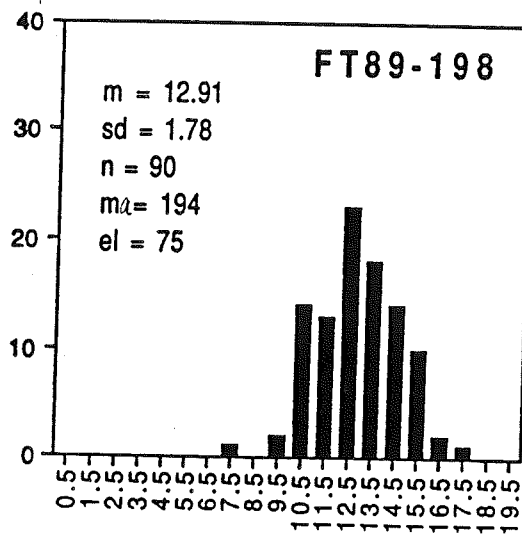
j



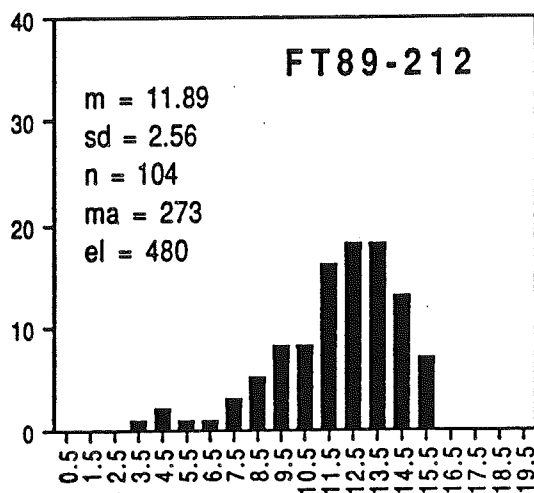
k



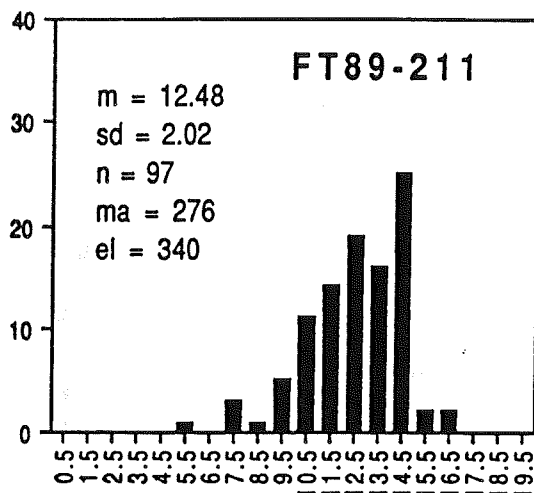
l



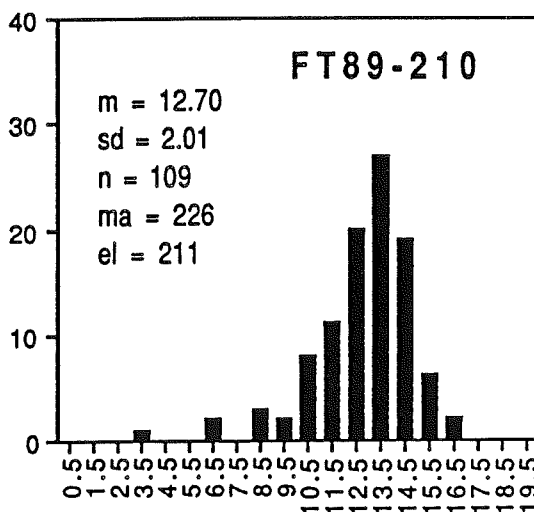
m



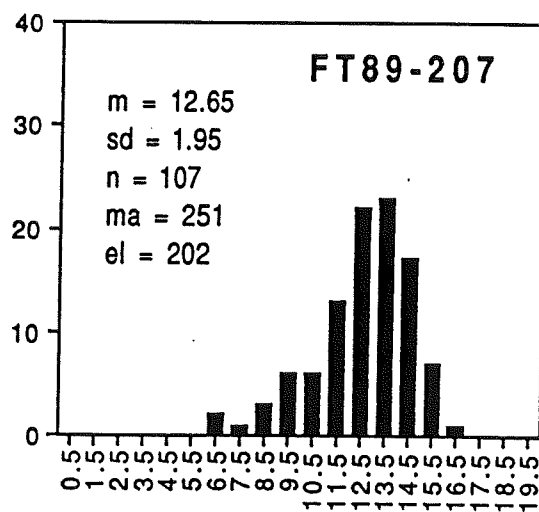
n



o



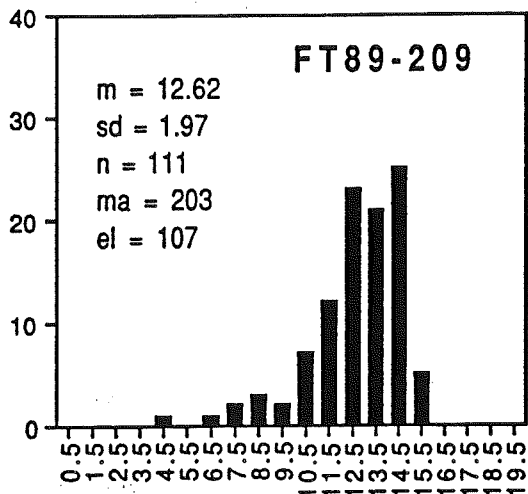
p



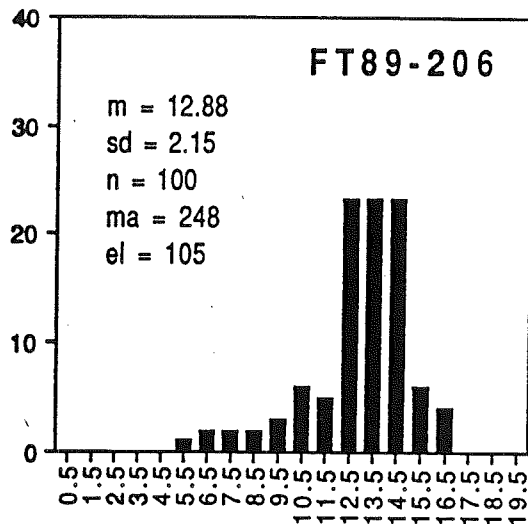
q

Figure 3.4 n-u

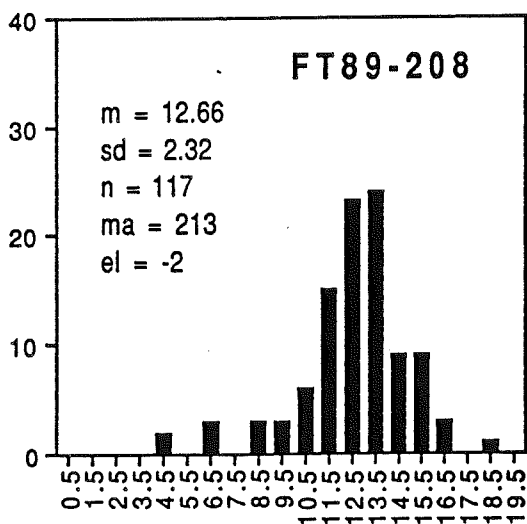
Apatite fission track length distributions for the Central Transect and Devil's Room Pluton (LGRA-01).



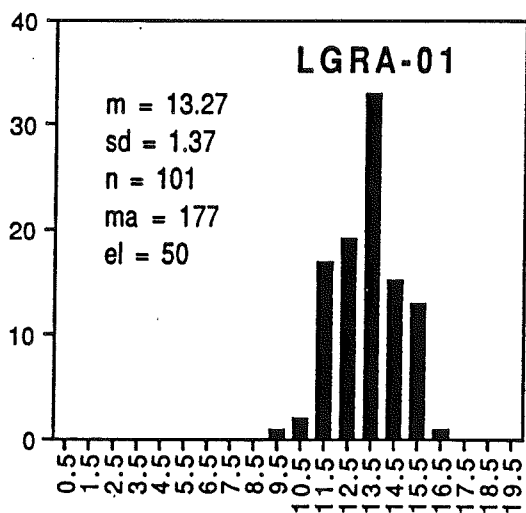
r



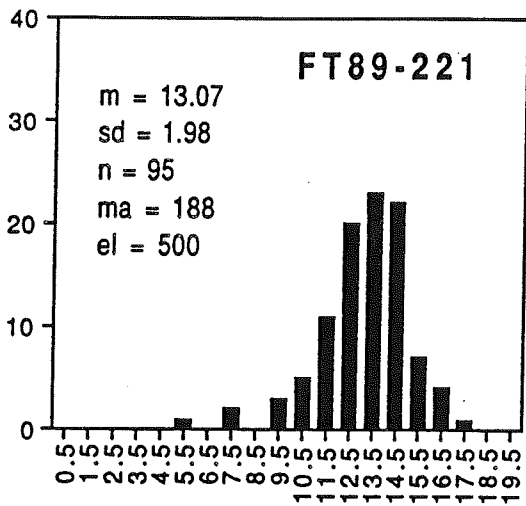
s



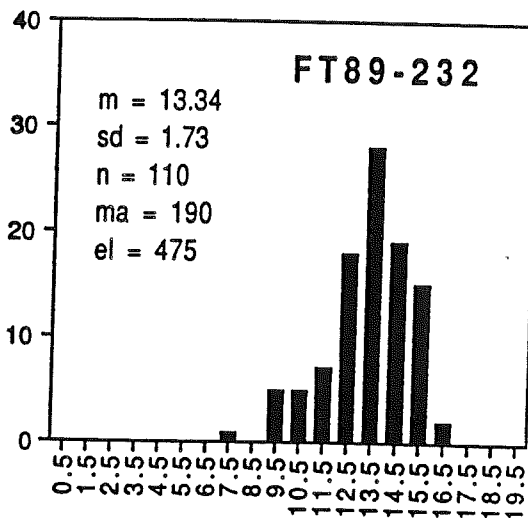
t



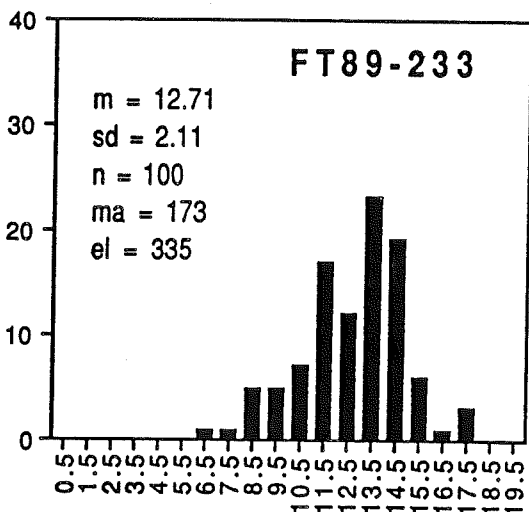
u



V

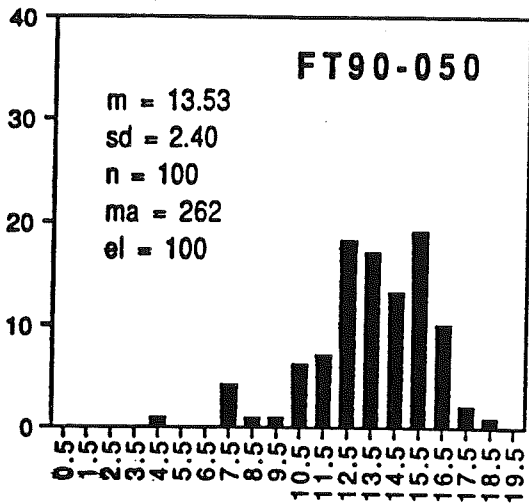


W

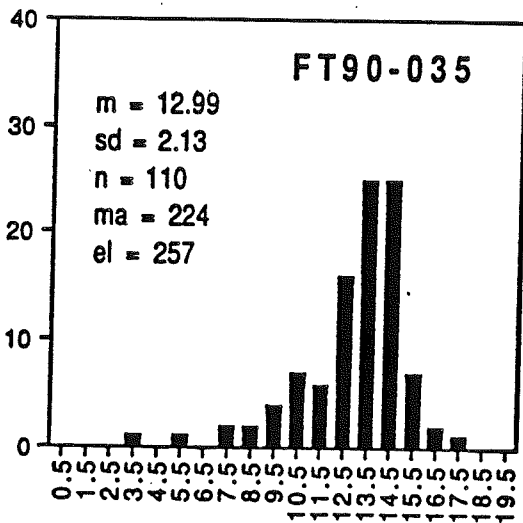


X

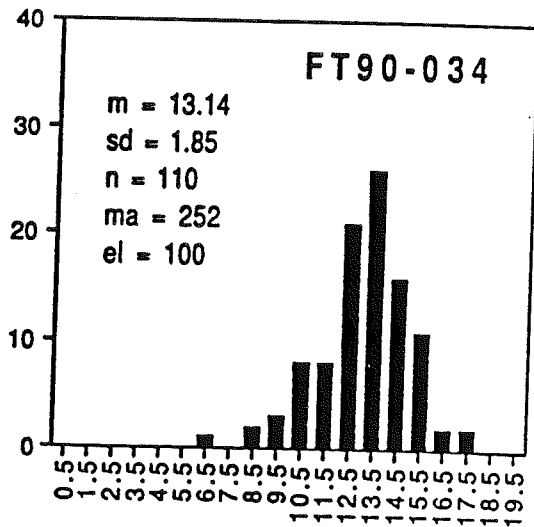
Figure 3.4 v-x
 Apatite fission track length distributions for the Northern Transect.



y

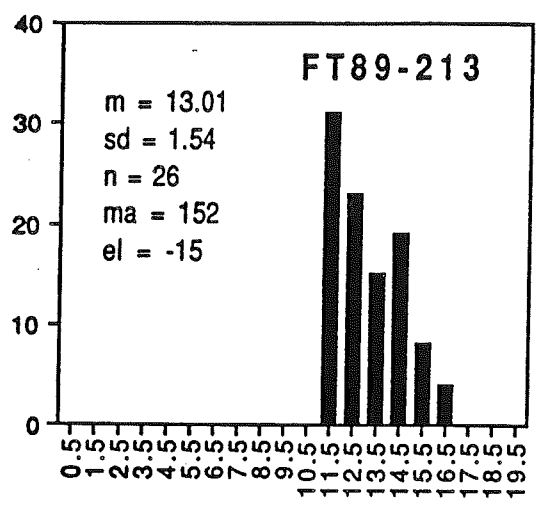


z

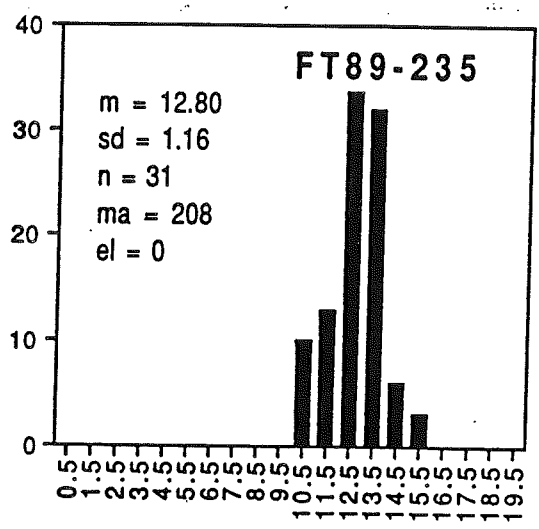


aa

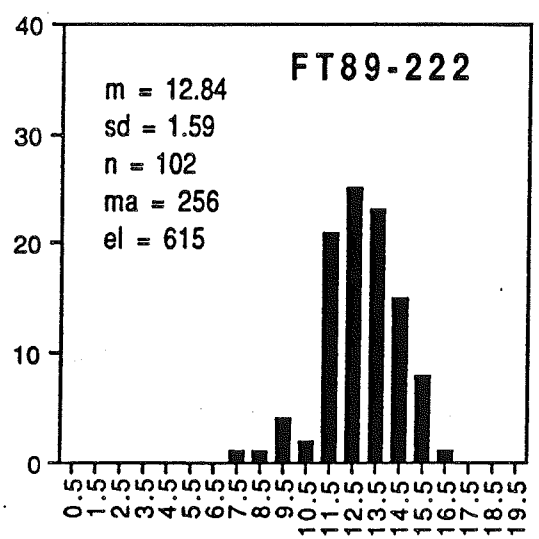
Figure y-ee
 Apatite fission track length distributions for the Deer Lake Basin (-034,-035), Hare Bay Allochthon (-050), Humber Arm Allochthon (-235, Lobster Cove), Western Platform (-213, Daniel's Harbour) and samples east of ST1 (-222, -223).



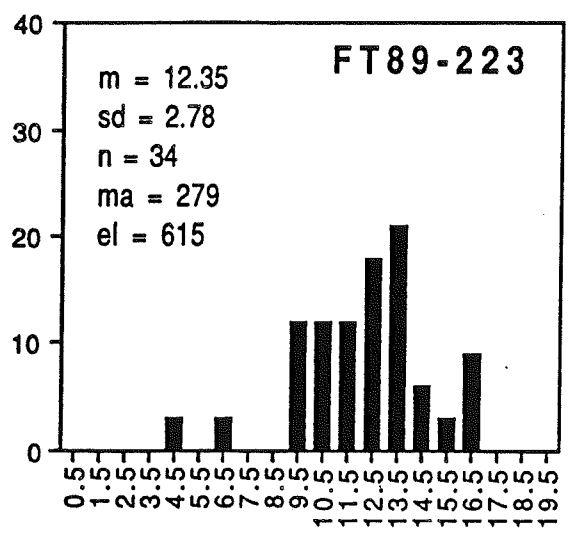
bb



cc



dd



ee

etched lengths overlap within 2 standard errors. Standard deviations range from 1.55 to 2.78 μm , although most fall below 2.00 μm . Standard deviations are inversely proportional to mean etched length, a relationship that will be discussed more fully in section 3.6.

A reduction in the mean track length of a sample is generally concomitant with a reduction in the fission track age of the sample (Green et al., 1986). The relatively young age of FT89-198 is not reflected in its track length distribution; its mean etched length and standard deviation values are within the range defined by other Long Range Inlier samples.

All distributions are negatively skewed (see Appendix 2 for skewness values). Generally, skewness is regarded as significant when it is greater than $6/N$ where N is the number of data points (ie. confined track lengths) (Press et. al., 1986). Most samples in ST1 and ST2 have skewness several times greater than this value reflecting the substantial component of short tracks (less than 8 μm) in many of the samples. The majority of the unimodal distributions record smooth rather than sudden transitions between short and longer track components. Gleadow et al. (1983) describe various hypothetical cooling histories and their relationship to the apatite fission track length distribution. They conclude that negatively skewed, unimodal distributions indicate slow, continuous cooling of the samples since their last passage through the apatite 'closure' temperature range (Figure 3.5b).

3.3 Central Transect

3.3.1 Sample Locations

The Central Transect samples form a transect in the east-central Long Range Inlier which follows the Cat Arm Dam Road north to the Cat Arm hydroelectric plant

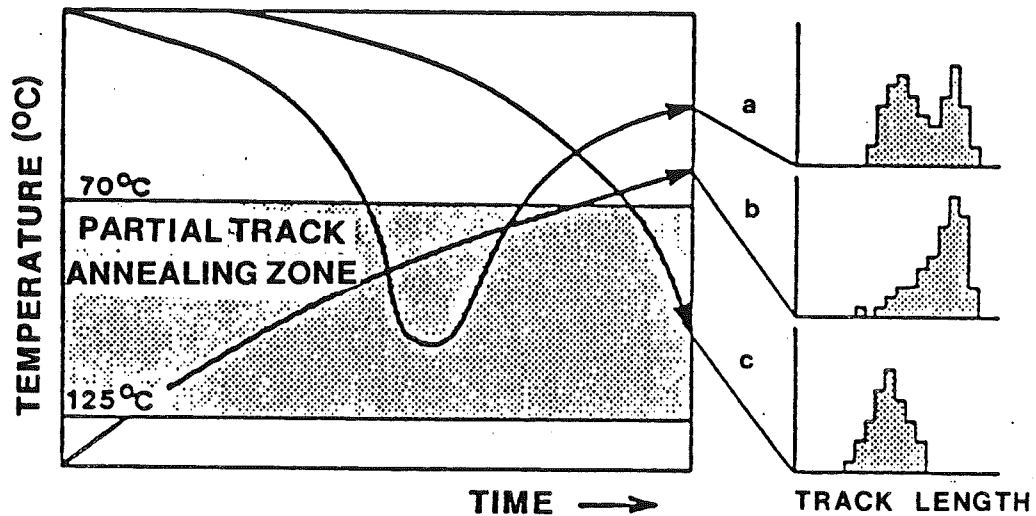


Figure 3.5

Various hypothetical time-temperature paths and their relationship to the apatite fission track length distribution. Typical track length distributions resulting from a.) a past thermal event (bimodal track distribution) b.) slow cooling (negatively skewed, unimodal distribution) and c.) a recent thermal event (unimodal, highly annealed distribution). The majority of Great Northern Peninsula samples have distributions similar to (b) indicative of slow, continuous cooling. (from Gleadow et al., 1983).

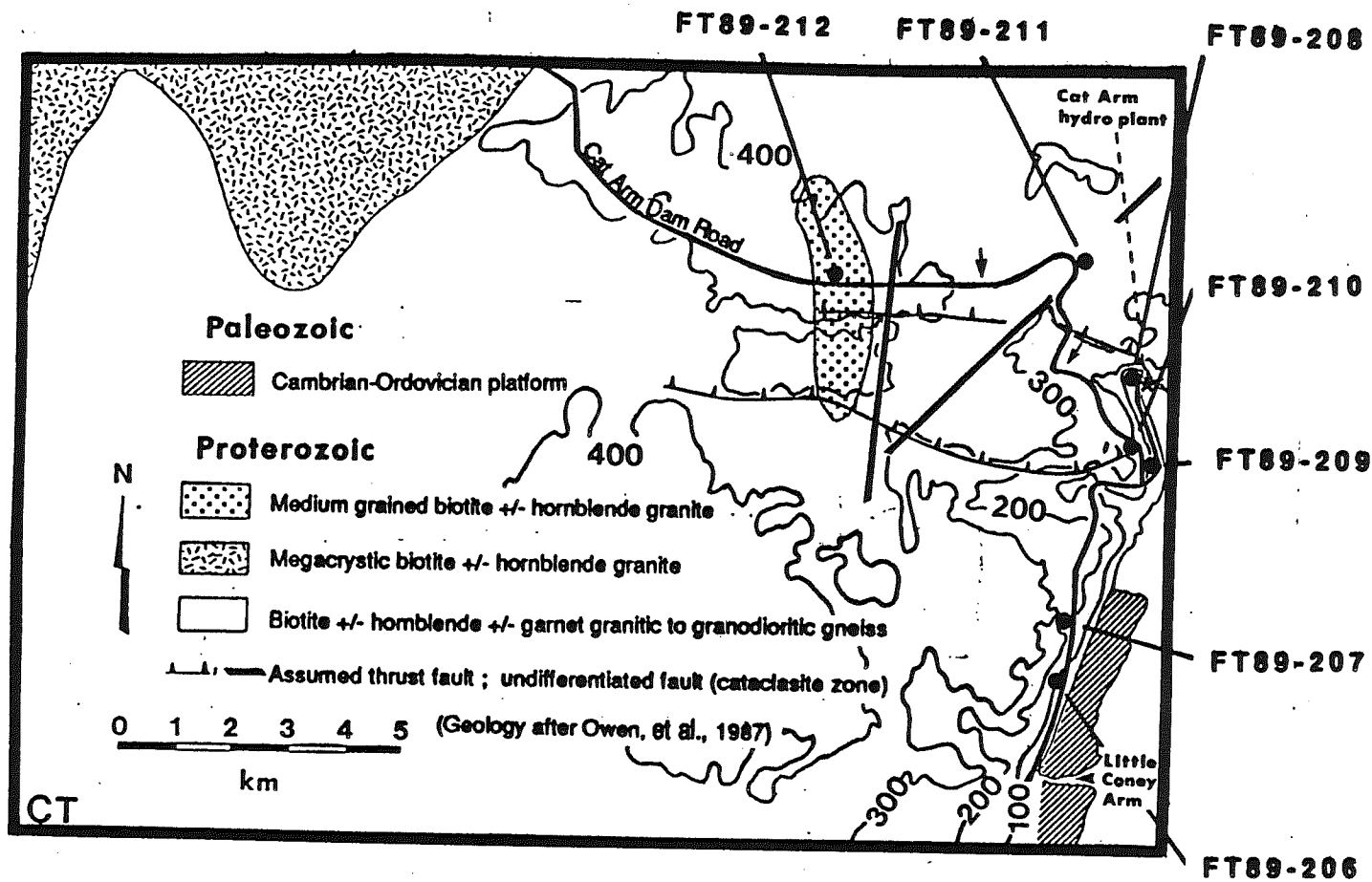


Figure 3.6
 Central Transect sample location map. Arrow indicates approximate Long Range Swarm dyke location. Elevation contours above mean sea level are in meters. Transect location shown on Figure 1.3.

and then west towards the Cat Arm Dam (Figure 3.6). A total of 7 samples were analyzed over the elevation range -2 to 480 meters above sea level covering a lateral distance of about 15 kilometers. Six of the samples were collected from the Precambrian granite gneiss of the inlier and one from an unnamed Grenvillian pluton which intrudes the gneiss (Figure 3.6, Table 3.1). The Cat Arm Dam Road crosses several thrust faults and cataclasite zones (Owen, 1987) within the Central Transect. The thrusts cut the gneiss, the Grenvillian pluton and perhaps a Long Range Swarm dyke (Owen and Erdmer, 1988) producing as much as 30 meters of relief. A probable Long Range Swarm dyke is indicated by the arrow in Figure 3.6 (Owen and Erdmer, 1988).

3.3.2 Fission Track Age Analysis

Central Transect apatite grains had similar characteristics to Southern Transect grains making track counting difficult. All samples passed the Chi-squared test and therefore may be treated as single Poissonian populations. Double analyses of FT89-212, -209 and -210 (separate slides) give ages reproducible to within 2σ (Table 3.4). Averaged ages and errors for these samples are used in all calculations (Table 3.4, footnote d).

Ages in the Central Transect range from 283 ± 38.0 to 197 ± 35.0 Ma (Mid-Permian to Late Triassic; 2σ error). Except for the highest elevation Carboniferous-aged samples of the Southern Transect, this range is generally similar to the Southern Transect age range. Minor age differences (at 1σ) between similar elevation samples in the Central Transect are noticeable. For example, sample FT89-209 (near Cat Arm hydroelectric plant) has an age based on a double analysis which is several tens of Ma younger than similar elevation sample FT89-206 further south near Little Coney Arm (Fig 3.6). Since the ages all overlap within 2σ they could be statistically represented by a mean age of 241 ± 34.6 Ma.

Sample	Rhos ^a (tr/cm ²)	Ns	Rhoi ^a (tr/cm ²)	Ni	Glass	Rhod ^a (tr/cm ²)	Nd	# Brains	Q	Chi2 ^b	Fission Track Age ^{cde} (Ma)	Zeta
Central Transect												
FT89-212	1.12	778	0.693	482	CN-1	2.990	5499	21	0.491	PASS	283 +/- 38.0	119.7 +/- 6.6
	1.44	468	0.954	310	CN-1	2.990	5499	16	0.985	PASS	264 +/- 42.4	119.7 +/- 6.6
FT89-211	1.18	553	0.746	351	CN-1	2.990	5499	21	0.297	PASS	276 +/- 42.2	119.7 +/- 6.6
FT89-210	2.32	1136	1.82	890	CN-1	2.990	5499	17	0.965	PASS	225 +/- 25.2	119.7 +/- 6.6
	2.66	229	2.87	170	CN-1	2.990	5499	7	0.818	PASS	226 +/- 47.6	119.7 +/- 6.6
FT89-207	1.21	1092	0.846	766	CN-1	2.990	5499	27	0.616	PASS	251 +/- 29.0	119.7 +/- 6.6
FT89-209	0.704	495	0.593	417	CN-1	2.990	5499	18	0.996	PASS	209 +/- 31.2	119.7 +/- 6.6
	1.09	312	0.975	279	CN-1	2.990	5499	15	0.830	PASS	197 +/- 35.0	119.7 +/- 6.6
FT89-206	0.617	539	0.437	382	CN-1	2.990	5499	23	0.995	PASS	248 +/- 37.2	119.7 +/- 6.6
FT89-208	3.73	1102	3.09	913	CN-1	2.990	5499	21	0.062	PASS	213 +/- 23.8	119.7 +/- 6.6
Northern Transect												
FT89-221	0.851	290	0.984	308	†CN-1	4.034	7374	18	0.421	PASS	187 +/- 34.4	99.7 +/- 8.2
	0.588	273	0.606	285	†CN-1	4.034	7374	21	0.026	FAIL	223 +/- 60.8	99.7 +/- 8.2
FT89-232	0.108	791	0.112	823	†CN-1	4.034	7374	22	0.299	PASS	190 +/- 25.0	99.7 +/- 8.2
FT89-233	0.712	306	0.821	353	†CN-1	4.034	7374	27	0.817	PASS	173 +/- 30.3	99.7 +/- 8.2
Deer Lake Basin and Miscellaneous GNP												
FT90-034	2.17	643	1.56	463	CN-1	3.710	4488	22	0.113	PASS	252 +/- 42.6	99.6 +/- 11.4
FT90-035	1.03	377	0.833	306	CN-1	3.710	4488	19	0.944	PASS	224 +/- 43.2	99.6 +/- 11.4
FT90-050	1.12	236	0.772	163	CN-1	3.710	4488	15	0.912	PASS	262 +/- 61.2	99.6 +/- 11.4
FT89-213	0.576	127	0.676	149	†CN-1	4.034	7374	13	0.516	PASS	169 +/- 43.4	99.7 +/- 8.2
	0.699	188	0.926	249	CN-1	2.990	5499	12	0.211	PASS	134 +/- 27.4	119.7 +/- 6.6
FT89-235	1.79	286	1.71	272	†CN-1	4.034	7374	14	0.325	PASS	208 +/- 39.4	99.7 +/- 8.2
LBRA-01	1.62	1330	1.10	903	SRM614	2.190	1400	21	0.943	PASS	187 +/- 28.0	11774 +/- 670.
	1.58	1171	1.27	942	SRM614	2.190	1400	19	-	PASS	166 +/- 19.4 ^f	12351 +/- 346.

† CN-1 glass dosimeter values from correlation factors

a $Rho(s, i, d) \times E-06$

b test PASS for $Q > 0.050$; FAIL for $Q < 0.050$

c two standard deviations

d average age of sample: (FT89-212) 273 +/- 40.2 Ma, (FT89-210) 225.5 +/- 36.4 Ma, (FT89-209) 203 +/- 33.2 Ma, (FT89-213) 151.5 +/- 35.4 Ma, (LBRA-01) 177 +/- 24.2 Ma

e combined age of sample: (FT89-221) 188 +/- 27.4 Ma

f J. Mooers analyst

Table 3.4

Great Northern Peninsula apparent apatite fission track ages for the Central Transect, Northern Transect, Deer Lake Basin and greater northwestern Newfoundland. See Table 3.2 for explanation of columns. Average and combined ages for multiple sample counts found under footnotes (d) and (e).

Central Transect

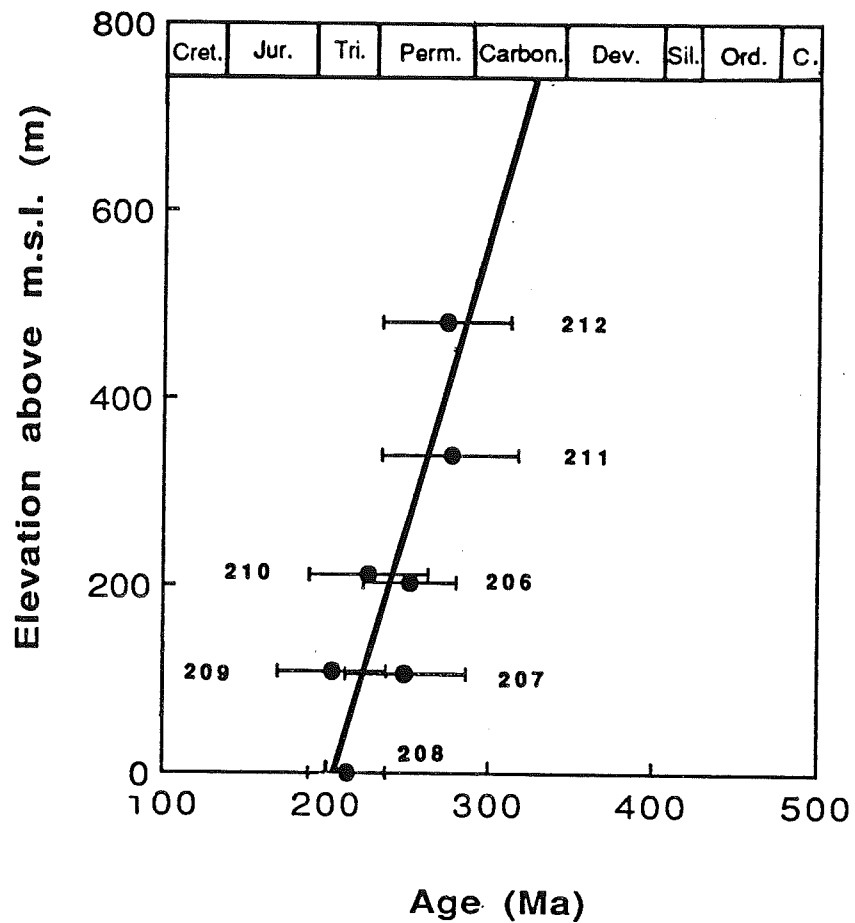


Figure 3.7

Apatite apparent fission track age vs. Elevation (meters above mean sea level) for the Central Transect. Errors are given as $\pm 2\sigma$. Sample number is given with each age.

An age vs. elevation plot for Central Transect samples (Figure 3.7) shows a positive correlation between age and elevation (slope = 7.0 ± 1.8 m/Ma, $s = 1.4$, $N = 7$). The implications of this relationship are discussed in chapter 5.

3.3.3 Fission Track Length Distribution Analysis

Central Transect track length distributions are presented in Figures 3.4 n-t. One hundred or more confined track lengths were measured for all samples (Table 3.3). Sample mean etched lengths range from 11.89 to 12.88 μm and standard deviations from 1.95 to 2.56 μm . Standard deviations generally correlate inversely with mean etched length. Comparison of distributions for FT89-209 and with -206 indicates that their age difference is minor since mean etched lengths and standard deviations of these similar elevation samples are almost identical.

All Central Transect length distributions are negatively skewed reflecting a component of short track preservation. The transition between short (less than 8 μm) and long tracks is not a sudden but a smooth increase in track frequency with track length. The smoothness of the distributions suggests slow, continuous sample cooling since they last experienced apatite fission track annealing temperatures.

3.4 Northern Transect

3.4.1 Sample Location

The Northern Transect crosses the northern Long Range Inlier from east to west, covering a much larger area than either the Central or Southern Transects (Figure 3.8). Five samples were collected at highest plateau levels across the inlier, of which three were datable. Two samples come from amphibolite grade granitic gneiss and the third

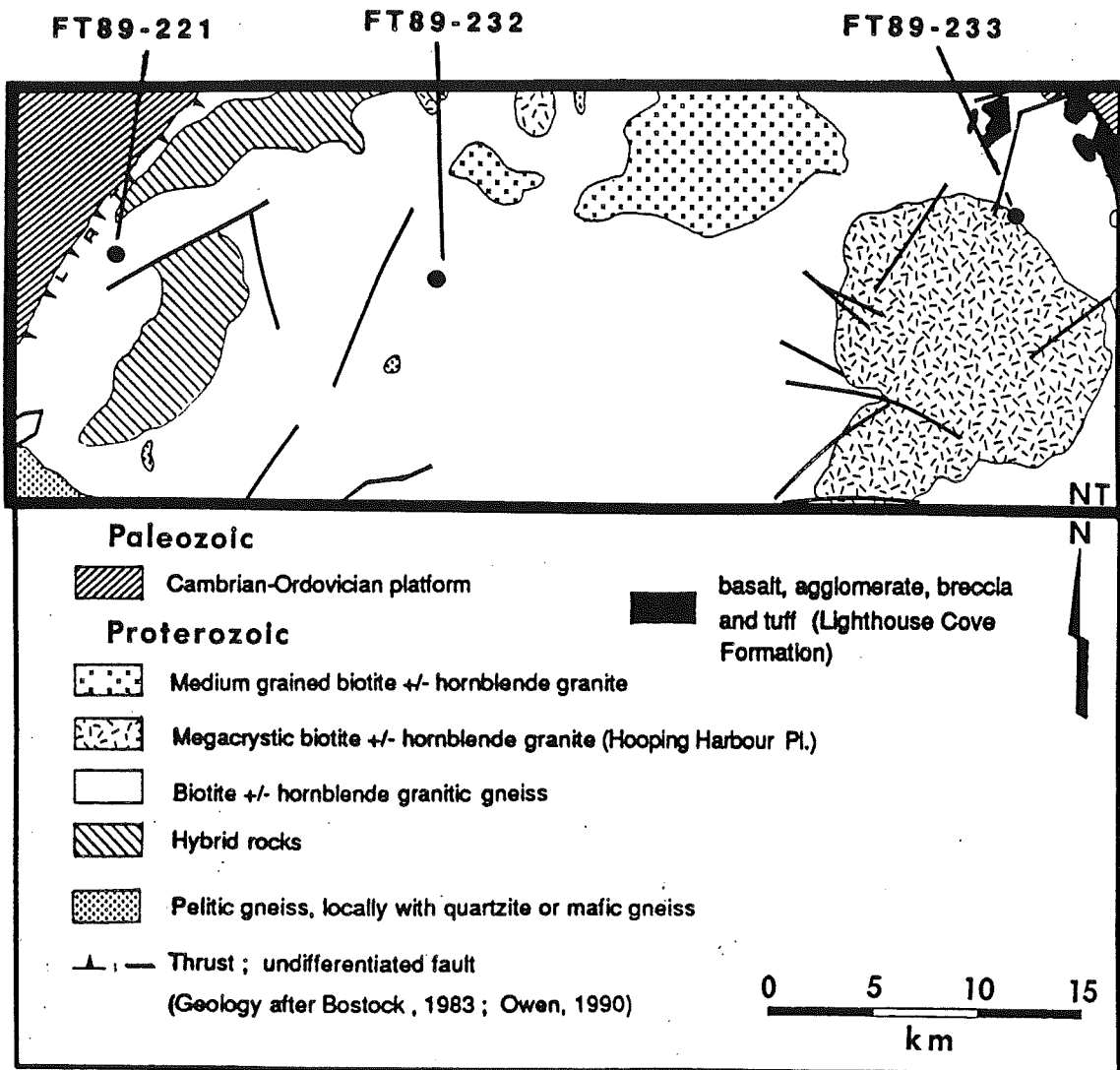


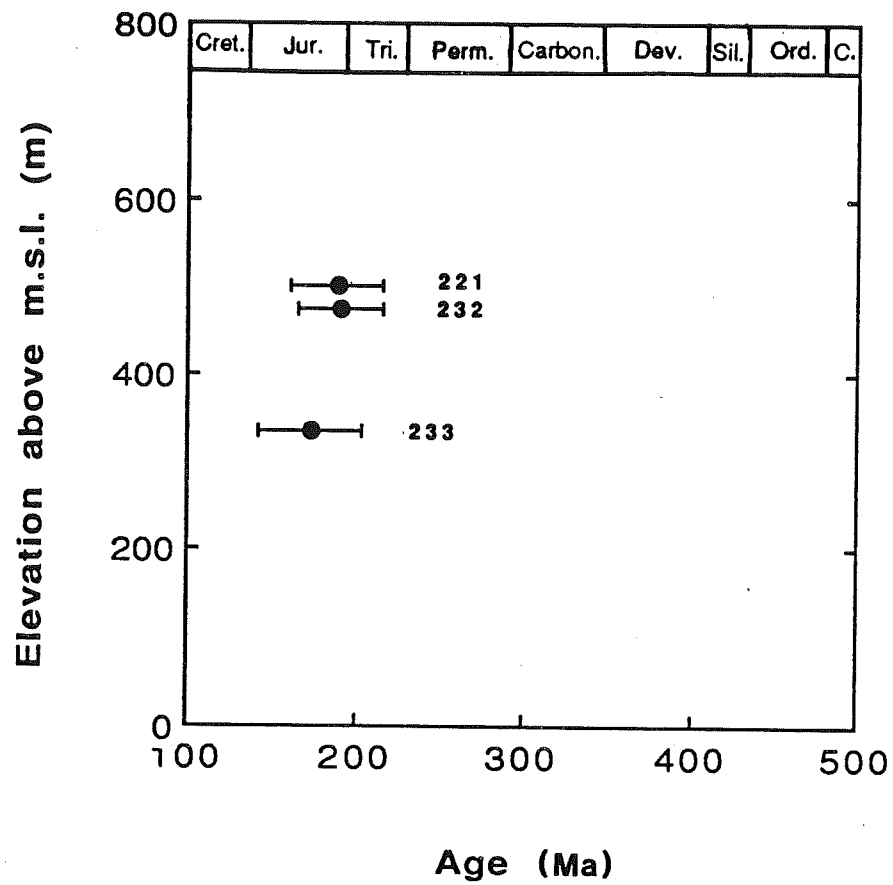
Figure 3.8
Northern Transect sample location map. Transect location shown of Figure 1.3.

from the eastern edge of the Grenvillian Hooping Harbour megacrystic granite (Figure 3.8, Table 3.1). Sample elevations range from 335 to 500 meters above sea level and cover a lateral distance of about 45 km. The Hooping Harbour Pluton sample was collected within several meters of one of the Long Range Swarm dykes which intrude Precambrian rock units in the Northern Transect map area. High angle faults cut the Precambrian pluton and several other rock units including the Cambro-Ordovician rocks that unconformably overlie the northeastern part of the Northern Transect (Figure 3.8). The Long Range Thrust brings the Long Range Inlier above Cambro-Ordovician rocks along the western part of the transect.

3.4.2 Fission Track Age Analysis

Twenty or more apatite grains were counted for each Northern Transect sample. The grains were less fractured and easier to count than those in the Southern and Central Transects. Detector contact was good. CN-1 glass dosimeter densities are based on a CN-1 vs. CN-2 density correlation factor (see section 2.2). Except for a FT89-221 second analysis (separate slides), which failed the Chi-squared test and gave a 223 ± 60.8 Ma (Early Triassic) age, apparent apatite fission track ages in the Northern Transect range from 190 ± 25.0 to 173 ± 30.6 Ma (Jurassic; 2σ error) and are therefore younger than fission track ages in the southern Long Range (Table 3.4). A failure of the Chi-squared test indicates that FT89-221 has an appreciable scatter in its single grain ages and cannot be treated as a single Poissonian distributed population. Since both FT89-221 samples were analyzed with the same zeta, a pooled Early Jurassic age based on 39 grains is used in all calculations (Table 3.4, footnote e). Northern Transect samples are anywhere from 60 to 90 Ma younger than similar elevation samples from the southern Long Range. At 1σ , similar elevation ages in the Southern and Central Transects are distinct from all Northern Transect ages. At 2σ , similar elevation ages FT89-196 and -201 from the Southern Transect overlap with Northern Transect ages FT89-221 and -232. Other ages from the southern Long Range are distinct from similar

Northern Transect

**Figure 3.9**

Apatite apparent fission track age vs. Elevation (meters above mean sea level) for the Northern Transect. Errors are given as $\pm 2\sigma$. Sample number given with each age.

elevation Northern Transect ages within 2σ .

Northern Transect samples are plotted as age vs. elevation in Figure 3.9. Note that the large lateral extent of age data and lack of sufficient elevation precludes the Northern Transect data as a vertical section, therefore data is only used for comparison with other transects.

3.4.3 Fission Track Length Distribution Analysis

Northern Transect track length distributions are presented in Figures 3.4 v-x. All three samples had ninety-five or more confined lengths. Mean etched lengths range from 12.70 to 13.34 μm and standard deviations from 1.73 to 2.11 μm which are inversely proportional to mean etched length. Unlike the apatite fission track ages, Northern Transect length distributions are similar to those found in the southern Long Range and seem to reflect similar low temperature (less than ~ 120 °C) thermal histories. Both mean etched lengths and standard deviations fall within the range of values set by the rest of the Long Range Inlier samples. Northern Transect distributions all contain a component of short tracks and are negatively skewed. A smooth track frequency vs. track length transition between short (less than 8 μm) and long tracks suggests relatively slow, continuous cooling of the samples after their final cooling below apatite fission track annealing temperatures.

3.5 Deer Lake Basin and Greater Northwestern Newfoundland

3.5.1 Sample Location

Five samples were analyzed from various locations around the Long Range Inlier and one from a pluton in the southeastern part of the inlier (Figure 3.10, Table 3.1). Sample FT89-213 consists of several 8-13 cm thick sandstone lenses interspersed between

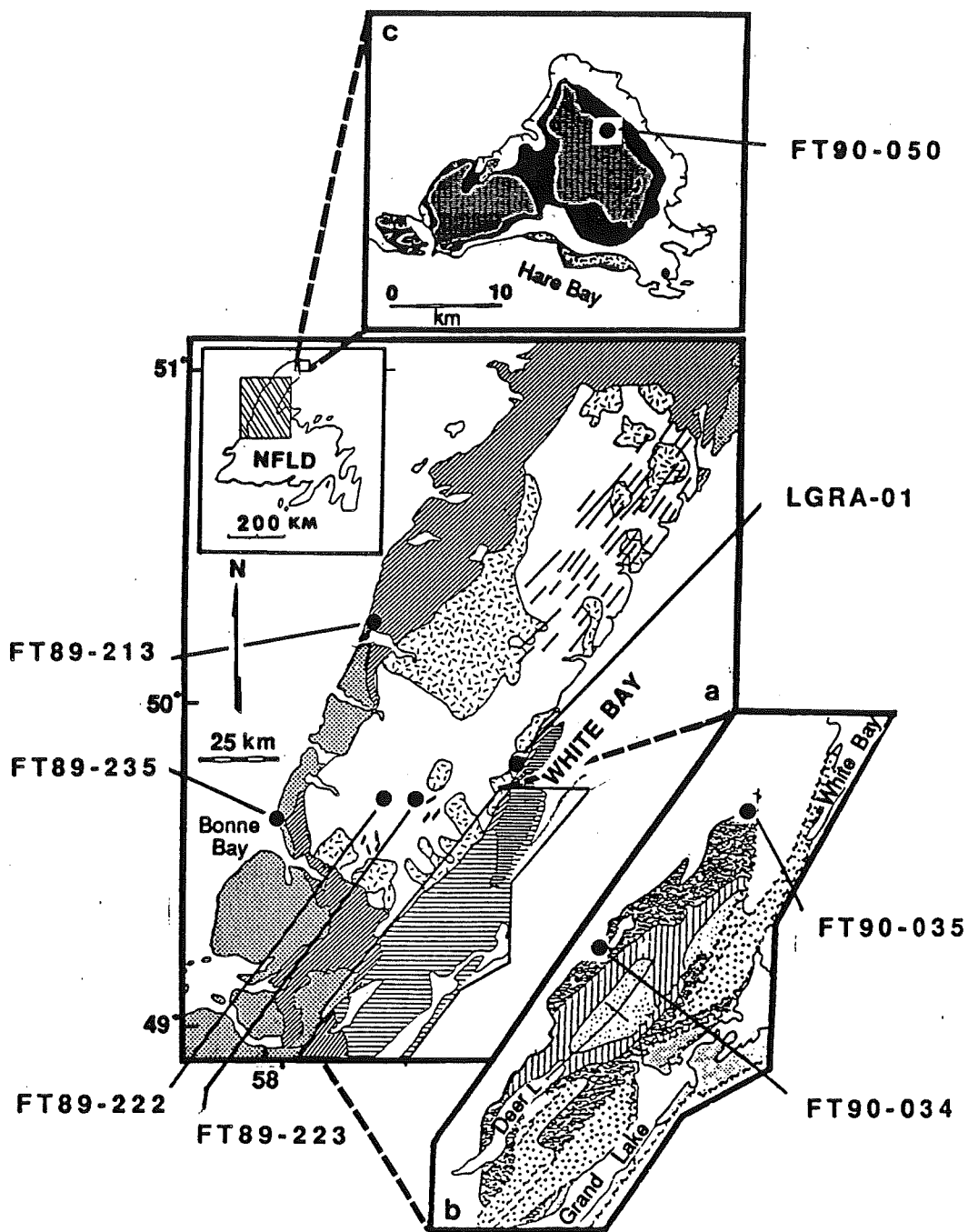


Figure 3.10

Sample location map for a.) the Great Northern Peninsula (Geology after Williams et al., 1978; Owen et al., 1987, 1988), b.) the Deer Lake Basin (from Hyde et al. 1988) and c.) the St. Anthony Complex of the Hare Bay Allochthon (adapted from Jamieson and Talkington, 1980) See similar figures 1.3, 1.6 and 1.11 for geological legend.

siltstone over a drill core interval of about 20 meters. The sample comes from Middle Ordovician autochthonous rocks at Daniel's Harbour, west of the inlier (Figure 3.10a). The core interval was described in the log as the Humber Arm Clastics is correlative with the Norris Point Formation (Goose Tickle Group). Two samples were collected from Taconian allochthonous rocks north and south of the Long Range. FT89-235 comes from the Humber Arm Allochthon (Middle Ordovician Lower Head Formation), a few miles north of Lobster Cove Head along the western Newfoundland coast (Figure 3.10a). FT90-050 comes from a jacupirangite-syenite assemblage in the White Hills Peridotite of the Hare Bay Allochthon north of the Long Range (Jamieson and Talkington, 1980; Figure 3.10b). The final two non-Long Range samples come from the Visean (Early Carboniferous) North Brook Formation fanglomerates of the Deer Lake Basin, along the southeastern perimeter of the inlier (Figure 3.10c). FT90-034 was collected from Deadwater Brook 1 km southwest of Adies Pond and FT90-035 from a gravel quarry along highway 420 in the northern Deer Lake Basin. The final sample comes from the Devil's Room Pluton (LGRA-01, Figure 3.10a). Two Long Range Inlier samples collected east of ST1 are included in Figure 3.10a (FT89-222 and FT89-223). Due to their proximity to ST1 their apatite fission track ages and length distributions are discussed under the Southern Transect.

3.5.2 Fission Track Age Analysis

Samples analyzed from around the Long Range Inlier and the Devil's Room Pluton sample were less fractured and more readily countable than Long Range Inlier samples, although fewer grains were available for analysis. Detector contact was good for all samples. All ages passed the Chi-squared test. Several samples were analyzed using the CN-1 vs. CN-2 dosimeter density correlation factor and one sample (Devil's Room Pluton) using dosimeter glass SRM614.

Apatite fission track ages for the non-Long Range samples range from 262 +/-

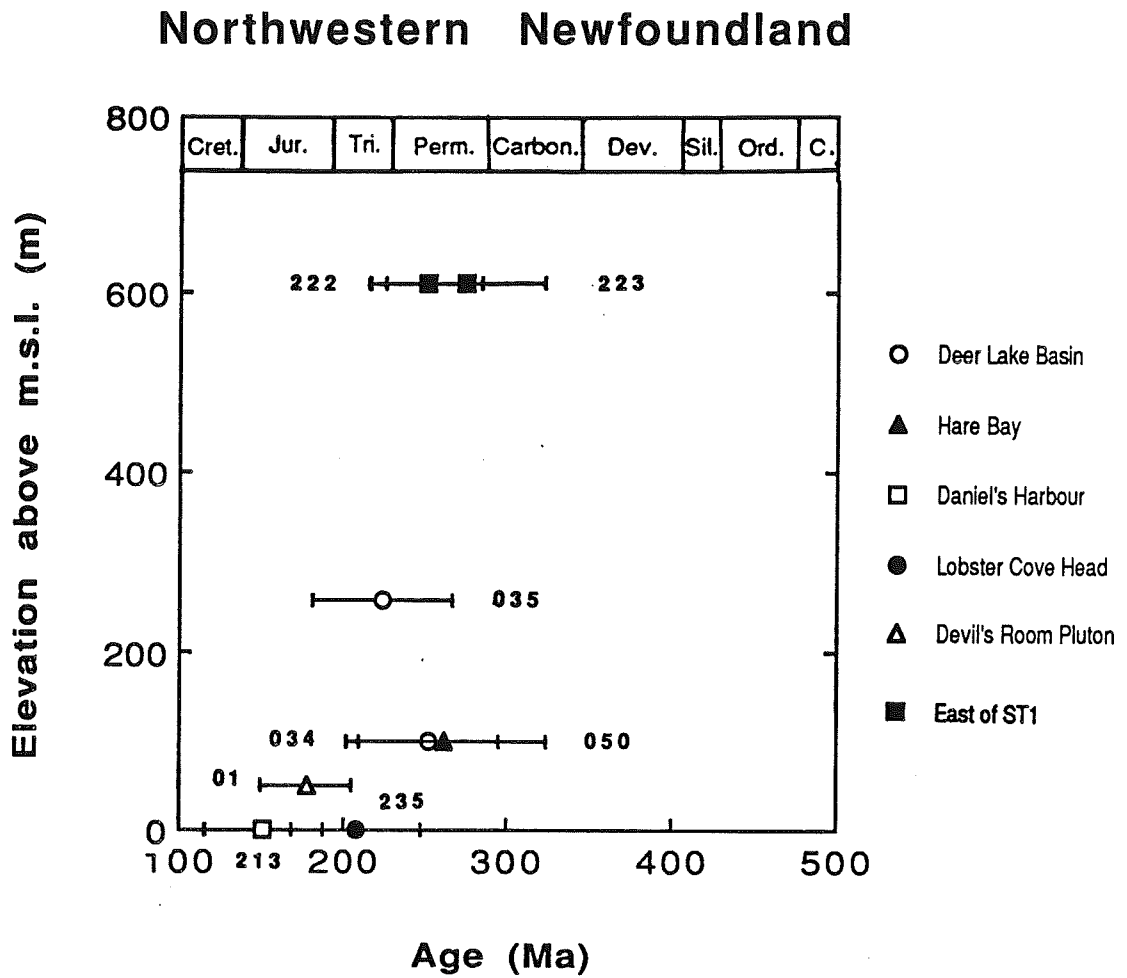


Figure 3.11
 Apatite apparent fission track age vs. Elevation (meters above sea level) for the greater northwestern Newfoundland area. Errors are given as $\pm 2\sigma$. Sample number given with each age.

61.6 to 134 \pm 27.4 Ma (Mid Permian to Late Jurassic) (Table 3.4). A second analysis of FT89-213 (separate slides) gives ages reproducible at 2σ . The average 151 \pm 35.4 Ma (Late Jurassic) age of FT89-213 is considerably younger than any other sample dated in this study. Because of its clastic lithology and 20 m collection interval, there may be some compositional differences in the apatite grains both within the sample and relative to other samples which have had some bearing on its annealing properties, thereby affecting the age. Except for this sample, the non-Long Range samples give ages that generally agree with similar elevation ages in the inlier. FT89-235 gives an age that falls between the ages for similar elevation samples in the Southern Transect (FT89-198 and FT89-194) and is nearly identical to the similar elevation sample FT89-208 in the Central Transect. A 262 \pm 61.6 Ma (Mid-Permian) age from the Hare Bay Allochthon agrees with similar elevation samples in the southern Long Range; however, it is notably older than higher elevation samples in the nearer Northern Transect. The Deer Lake Basin samples also give 252 \pm 42.6 and 224 \pm 43.2 Ma (Permian-Triassic) ages that agree closely with ages from the Southern and Central Transects but are older than ages from the Northern Transect. The Devil's Room Pluton age of 187 \pm 28.8 Ma overlaps a similar elevation Central Transect age (FT89-208) within 1σ . A second analysis of the Devil's Room Pluton sample by J. Mooers gave a corresponding 166 \pm 19.4 Ma (Jurassic) age and an average Early Jurassic age (177 \pm 24.2 Ma) is used in all calculations (Table 3.4, footnote d). All non-Long Range samples as well as samples east of ST1 are plotted as age vs. elevation in Figure 3.11.

3.5.3 Fission Track Length Distribution Analysis

One hundred or more track lengths were measured for the Deer Lake Basin, Devil's Room Pluton and the Hare Bay Allochthon samples (Figure 3.4 y-cc). Mean etched lengths range from 12.80 to 13.14 μm and standard deviations 1.16 to 2.13 μm . The mean etched length values fall within the range given by Long Range Inlier samples. Low standard deviation values from the western platform samples FT89-213 and FT89-

235 may not be realistic because of the small number of confined lengths for each of these samples (26 and 31 tracks respectively, Figure 3.4 bb,cc).

The Deer Lake Basin sample distributions are nearly identical in mean length and standard deviation and both are significantly negatively skewed. Their distributions do not represent anything different from Long Range samples and hence these samples apparently experienced similar slow, continuous cooling styles after their final cooling below 125 °C. The Hare Bay Allochthon sample displays a wide distribution and also the longest mean etched length of all analyzed samples. Its distribution is generally comparable to most other samples with a smooth increase in track frequency with track length, but it also contains a greater component of long tracks not seen in other samples.

If the FT89-235 and -213 narrow distributions are complete, they, along with the Devil's Room Pluton distribution, suggest a different style of cooling from the most other Long Range samples. The Devil's Room Pluton sample contains no tracks shorter than 9 μm and displays a much more peaked distribution than other analyzed samples. Other than the western platform samples it is also the only sample that does not have a significantly negative skewed distribution. The narrowness and peakedness of the distribution is suggestive of a volcanic-type length distribution indicating rapid cooling below annealing temperatures (Gleadow et al., 1983). However, its mean length (13.27 \pm 0.28 μm) is considerably shorter than a volcanic distribution mean length (greater than 14 μm) and indicates temperatures somewhat higher than ambient surface temperatures for a substantial portion of its low temperature history.

3.6 Inferred Thermal History from Analysis of Track Length vs. Age and Track Length Standard Deviation

Many of the Great Northern Peninsula samples have track lengths in the 4-6 μm range which means that they have spent some time at the higher temperatures of the

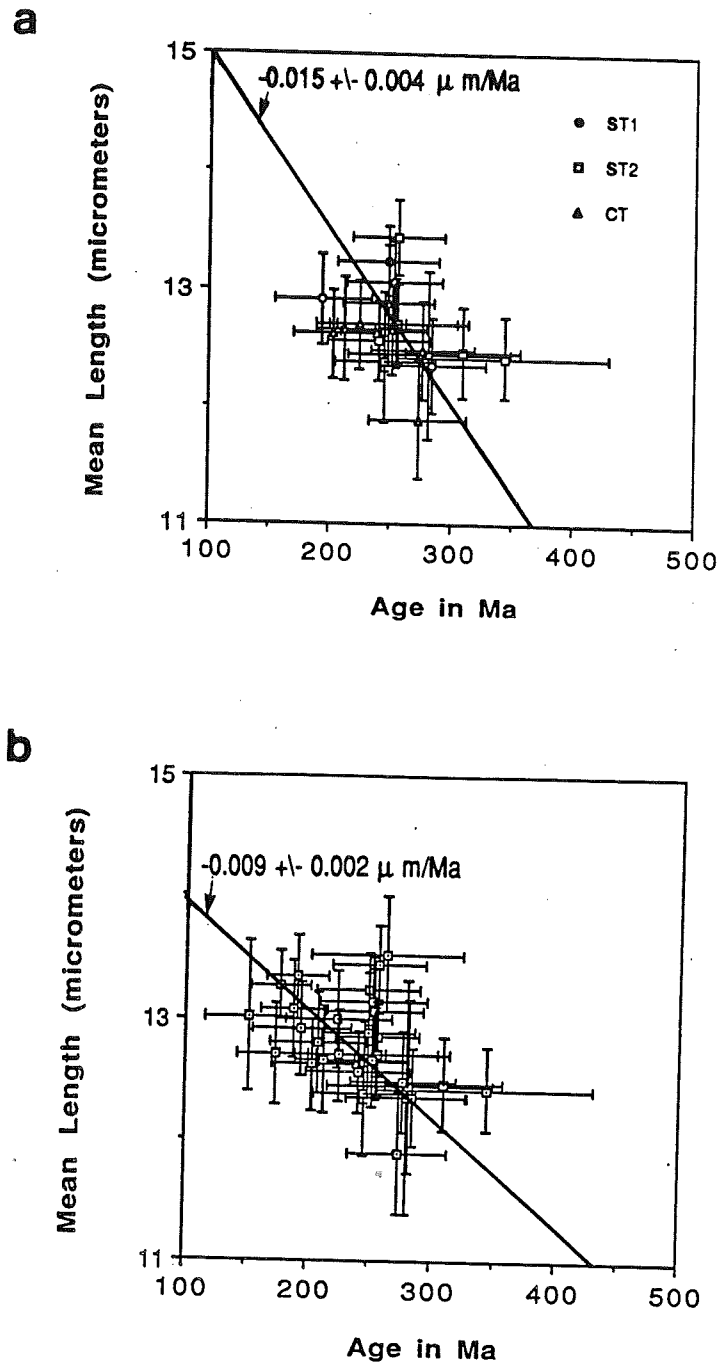
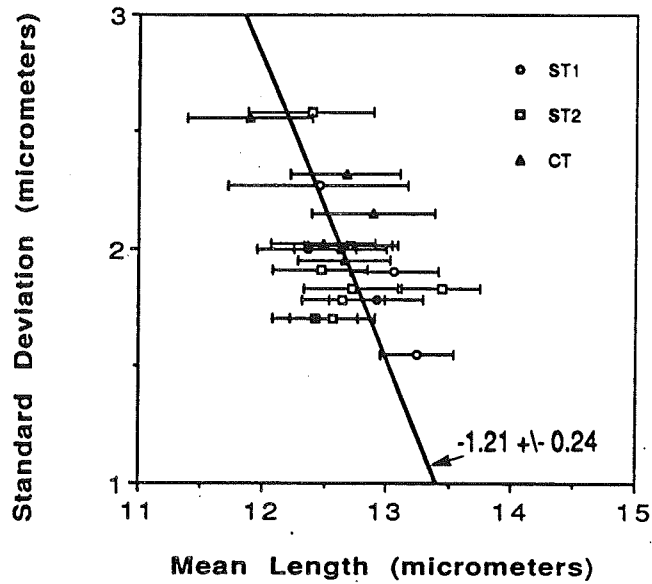


Figure 3.12
 Mean Track Length vs. Apatite fission track age for a.) the Southern and Central Transects and b.) the Great Northern Peninsula. Note inverse relationships: a.) slope of best fit line = $-0.015 \pm 0.004 \mu \text{ m/Ma}$ (sum $s=9.3$, $N=20$) b.) slope of best fit line = $-0.009 \pm 0.002 \mu \text{ m/Ma}$ (sum $s=15.9$, $N=31$).

a



b

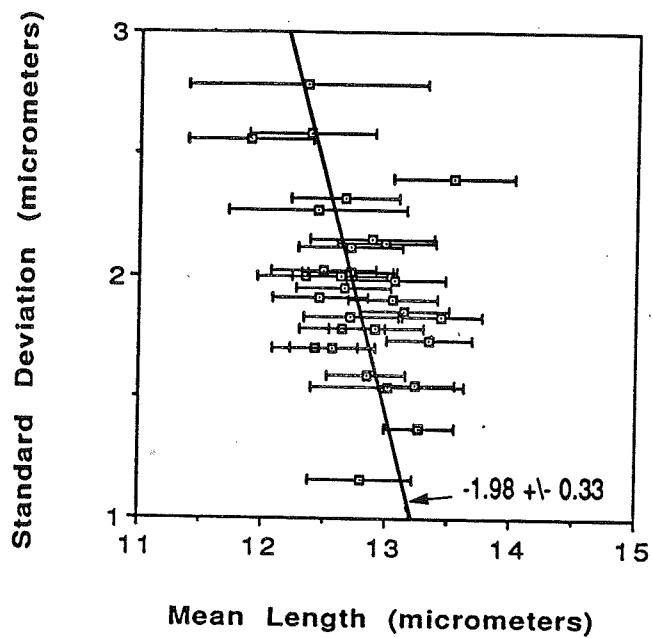


Figure 3.13

Track length distribution standard deviation vs. Mean track length for a.) the Southern and Central Transects. and b.) the Great Northern Peninsula. Note inverse relationship: a.) slope of best fit line = -1.21 ± 0.24 (sum $s=12.73$, $N=20$) b.) slope of best fit line = -1.98 ± 0.33 (sum $s=21.9$, $N=31$).

annealing zone ($> \sim 90$ °C) (Gleadow et al., 1986). In order for these tracks to survive they must have cooled more rapidly to minimal annealing temperatures below 70-80 °C after their residency at higher temperatures.

Samples experiencing similar thermal histories (passed through similar annealing zone temperatures at a similar rate) display longer mean track lengths with age since older samples have had more time to accumulate long tracks at low temperatures. A plot of mean track length versus apatite fission track age for the Southern Transect (ST1 and ST2) and Central Transect samples suggests that older samples do not correlate with longer mean track lengths (Figure 3.12a). A least squares linear regression of the data using Yorkfit (see Chapter 3 for explanation of Yorkfit) indicates that the best fit line through the data has a negative slope (slope = -0.015 ± 0.0038 $\mu\text{m}/\text{Ma}$, sum $s=9.3$, $N=20$). Thus, track length seems generally to decrease with increasing age. A similar regression of all the data suggests that this same relationship may be true over all elevations and ages in the Great Northern Peninsula (slope = -0.008 ± 0.0017 $\mu\text{m}/\text{Ma}$, sum $s=15.9$, $N=31$; Figure 3.12b).

An inverse relationship between mean track length and track length standard deviation (Figure 3.13a) in Southern and Central Transect samples (slope = -1.21 ± 0.24 , sum $s=12.73$, $N=20$) indicates a broadening of the track length distribution with decreasing mean track length. This relationship is also true for the track length data taken as a whole from all of the samples (slope = -1.98 ± 0.33 , sum $s=21.9$, $N=31$; Figure 3.13b). Taken together with the above relationship this suggests that the decreasing mean lengths reflect a progressive preservation of short tracks with age. Short track preservation does not seem uniform in the Great Northern Peninsula samples, further suggesting that the samples experienced somewhat different thermal histories.

Similar plots have been used by Green (1986) to separate 'original', partially reset(mixed), and completely reset ages in Northern England. The suggestion here is that some of the apatite fission track ages in the Great Northern Peninsula may represent

partially reset (mixed) ages. Some of Green's (1986) mixed age track length distributions are clearly bimodal in character whereas Great Northern Peninsula samples are not. However, distinctive bimodal distributions are only expected in samples which have seen high annealing temperatures of relatively short duration (Gleadow et al., 1986).

If the inverse relationship between mean track length and apatite age is real it may indicate that samples were exposed to different maximum reheating temperatures after final cooling below ~ 120 °C and/or spent unequal time periods in the annealing zone. The trend in Figure 3.13 suggests that the younger samples either came through the annealing zone quickly, and therefore did not record many short tracks, or experienced reheating temperatures great enough to anneal completely, or nearly so, all pre-existing tracks (eg. FT89-197, -198, -235). Older samples preserve a greater component of short tracks from this period of high temperatures (eg. FT89-212, -191) suggesting that they either came through the annealing zone more slowly or were exposed to lower temperatures than the younger samples during this time. The last possible time for cooling from this period of high temperatures in the Great Northern Peninsula is about 150 Ma (Late Jurassic), given by the age of the youngest sample (FT89-213).

If the samples came through the annealing zone at different rates this may reflect a change in cooling (and possibly exhumation) rate between younger and older samples. The apatite fission track age vs. elevation plot in ST2 could be recording a change in exhumation rate such that oldest and highest elevation samples FT89-225 and -226 may exhibit a lower rate of exhumation (shallower age vs. elevation slope) relative to the younger and lower elevation samples (steeper age vs. elevation slope). However, other old samples at high elevations (with shortened mean lengths) in both Southern (eg. FT89-227) and Central Transects (eg. FT89-212) do not show this change in exhumation rate in their age vs. elevation plots.

A general observation from the age vs. elevation plots, particularly in the

Mean Length vs. Elevation Great Northern Peninsula

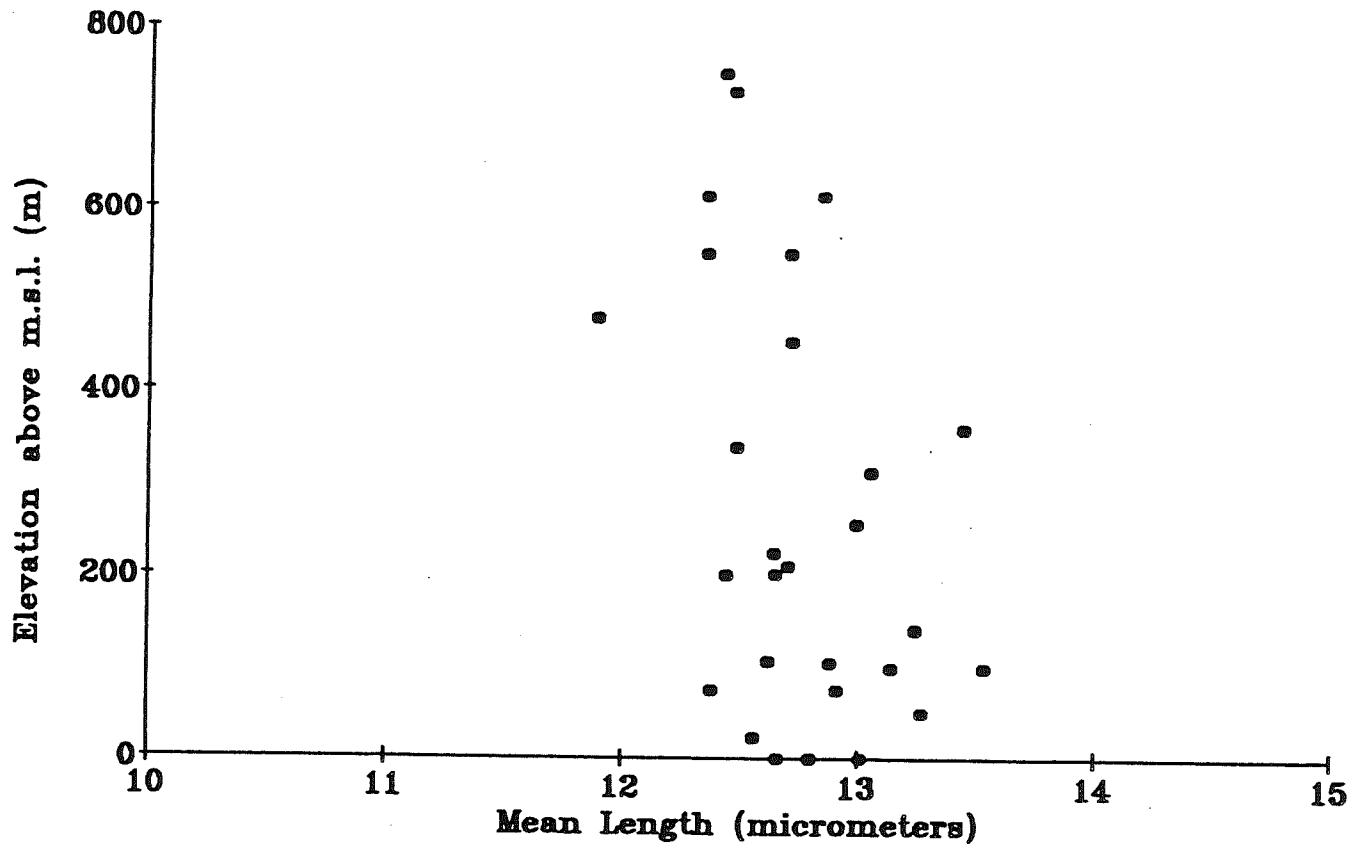


Figure 3.14
Mean track length vs. Elevation for Great Northern Peninsula samples.

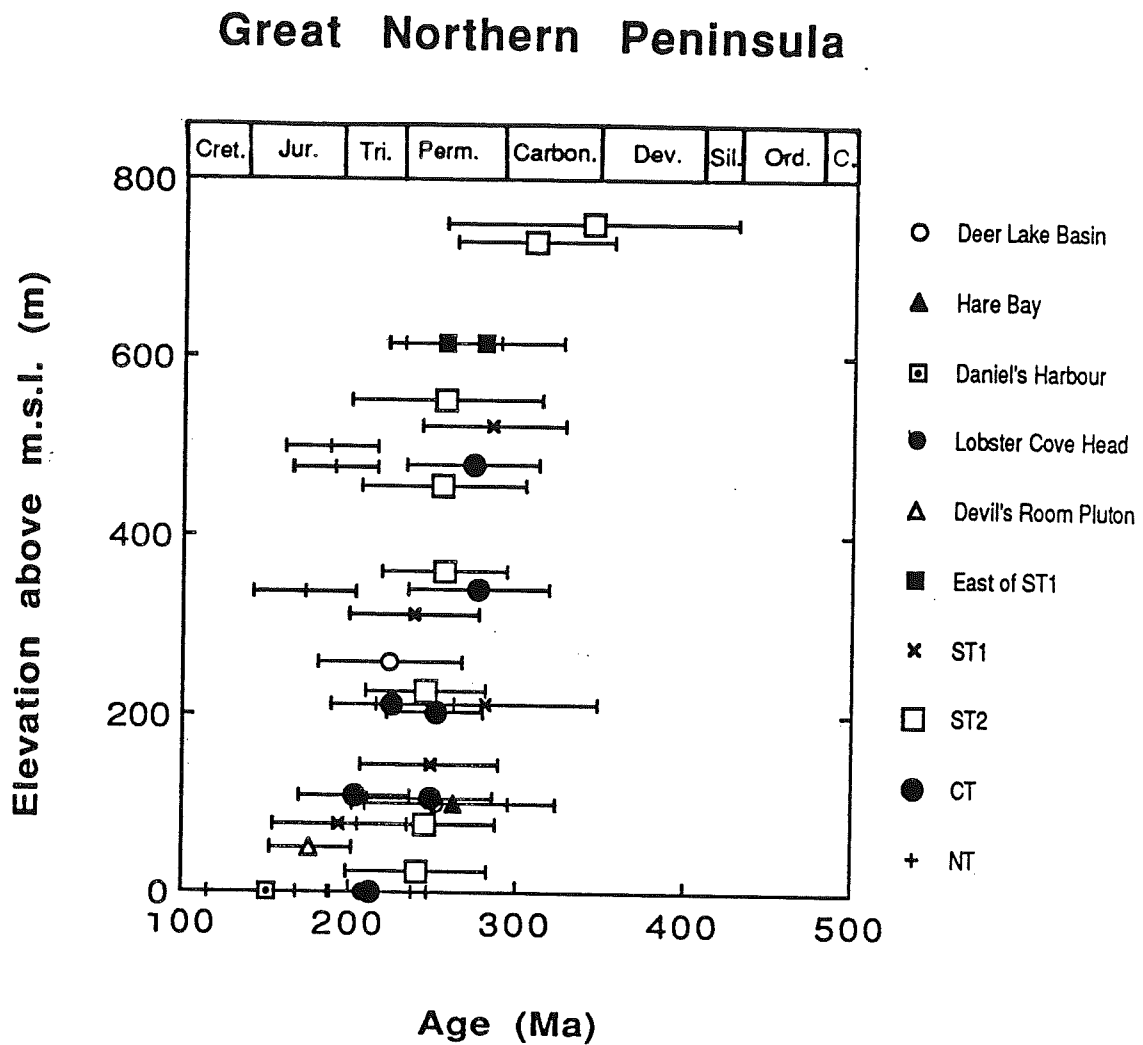


Figure 3.15
Apatite apparent fission track age vs. Elevation (meters above mean sea level) for the Great Northern Peninsula. Note young ages of the Northern Transect samples relative to similar elevation samples elsewhere in the Great Northern Peninsula.

Southern and Central Transects (Figure 3.2, 3.3, and 3.7), is that older age samples are found at higher elevations. Thus, shorter mean track lengths should also generally be found at higher elevations (Figure 3.14). This could mean that higher elevation samples were subjected to lower resetting temperatures therefore preserving a short track length component not found in low elevation samples. In this case the trend in fission track ages and track length distributions would be interpreted to be a result of variable resetting and not only of progressive cooling/exhumation of the sampled rock column.

3.7 Discussion of Experimental Results

Apatite fission track apparent ages in samples from the Great Northern Peninsula range from the Late Paleozoic to Mid Mesozoic, the majority falling within Permian-Triassic time (Figure 3.15). This suggests that samples presently exposed at the surface have not experienced temperatures in excess of approximately 100 °C since Mid Mesozoic time.

Ages for similar elevations in the southern Long Range Inlier (Southern and Central Transects) generally correspond well. All but the highest and lowest elevation sample ages in the Central Transect overlap within 2σ and are equivalent to similar elevation sample ages in the Southern Transect. Southern Long Range Inlier track length distributions contain a component of short tracks (less than 8 μm) and are generally compatible with slow cooling thermal history distributions as described by Gleadow et al. (1983, Figure 2.3b). The only sample which departs from a smooth transition between relatively short and long tracks is FT89-225 which lacks a greater component of tracks in the 8-10 μm range (see Figure 3.4f for comparison). There is some indication that in the Southern Transect standard deviations are on average slightly lower and mean etched lengths slightly greater than in the Central Transect. The Southern Transect has three samples with mean etched lengths greater than 13 μm but none less than 12 μm whereas CT has no mean lengths greater than 12.88 μm and one mean length

less than 12 μm . This pattern may suggest slightly slower cooling rates of Central relative to Southern Transect samples, a conclusion which is compatible with the lower CT age vs. elevation slope.

Northern Long Range Inlier ages (Northern Transect) are consistently and significantly 60-90 Ma younger than similar elevation samples in the southern Long Range. Track length distributions are like those in the southern Long Range, compatible with similar relatively slow cooling thermal histories after final cooling below ~ 120 °C. Ages from the Deer Lake Basin, Hare Bay Allochthon and Humber Arm Allochthon (FT89-235) are all compatible with similar elevation ages in the southern Long Range Inlier. Permian-Triassic ages from the Deer Lake Basin are younger than the Early Carboniferous stratigraphic age of the samples and meaning that the samples have experienced temperatures great enough (in excess of 100 °C) to completely reset their apatite fission track clocks sometime during the Early Carboniferous-Middle Triassic. Track length distributions from these samples do not represent anything different from the inlier samples. The western platform samples (FT89-213, -235) and the Devil's Room Pluton sample have markedly narrower distributions than other Great Northern Peninsula samples. If western platform track length distributions are complete, their low standard deviations and lack of short tracks would indicate that these samples, along with the Devil's Room Pluton sample, spent relatively less time at high annealing temperatures (70-125 °C) than most of the Long Range Inlier samples. FT89-213 also produced the youngest age of the samples analyzed in this study.

Together, the apatite ages and track length distributions suggest that most of the Great Northern Peninsula experienced fairly slow, continuous cooling for much of its post-Paleozoic thermal history. Yet, a closer look at the data reveals that the differences in the apatite fission track ages in the Great Northern Peninsula may be the result of slightly varying thermal histories experienced by the samples. Mean track lengths not only decrease with age in spatially constrained transects (Southern and Central Transects) but also for the Great Northern Peninsula as a whole. Track length standard deviations

decrease with mean length on both a transect and regional scale. These trends may indicate that shorter tracks are progressively preserved with age, suggesting the samples did not all experience similar low temperature thermal histories and that some have mixed ages. This, along with the fact that all the mean lengths reflect substantial annealing of the samples, means that the ages must not be interpreted as dating any specific event of relatively short duration.

Since age generally increases with elevation in the Great Northern Peninsula the data may indicate the existence of a 'mixed age gradient' over the elevation interval. Younger samples, at lower elevations, have longer mean lengths and preserve fewer short tracks which suggests that they either came through high annealing temperatures more quickly or experienced higher resetting temperatures than older samples at higher elevations. The latest possible time for high resetting temperatures (greater than ~ 100 °C) corresponds to the youngest age, about 150 Ma or Late Jurassic time.

Chapter 4. Apatite Fission Track Apparent Age and Track Length Modelling: Temperature-Time Histories

4.1 Introduction

Recent advancements in understanding apatite fission track annealing kinetics can be interpreted in terms of empirical models which can be used to predict track length annealing. The model used in this study can also be run in an inverse sense to predict T-t paths from apatite fission track age and track length distribution data. In this context, apatite annealing temperatures cover the range 120-20 °C since it has been shown that over these temperatures apatite fission track fading is the norm rather than an exception (Green et al., 1985, 1986; 1989; Donelick, pers. comm. 1990).

The modelling of apatite fission track data is essentially a three-fold process. First, data must be obtained which isolate the relationships between a.) temperature, time and track length reduction (see Laslett et al., 1987) and b.) between track density and track length reduction (Green, 1988). Second, empirical interpretations of the data must be made in order to construct a kinetic model of track annealing (Laslett et al., 1987). Third, forward and inverse models can then be developed which give the cumulative effect of time and temperature on the fission track age and track length distribution. The forward and inverse computer model used in this study was developed at Dalhousie University by Sean Willett and has been used in a number of studies involving the Western Canada Basin and the Peace River Arch (Issler et. al., 1990). Apatite fission track T-t modelling (Donelick, 1988) had previously been limited to "cooling only" temperature histories and could not be applied to a situation which involved any reheating of samples after their final cooling below ~ 120 °C. Reheating as well as cooling of samples during their annealing history is allowed using the current model.

4.2 Specifics of the Model

4.2.1 Forward Modelling (track length distribution as $f(T,t)$)

In a natural system temperature varies continuously with time, and fission tracks are produced at an approximately constant rate. This process is discretized in the forward model.

A temperature history varying linearly with time is divided into (m) intervals (where m = number of timesteps in the model) each of a specific time length (t). The temperature history is then described completely by a set of ($m+1$) temperatures. At the start of each interval a component of tracks with a normal distribution around a mean of $16.5 \mu\text{m}$ is introduced and allowed to anneal over the temperature path. The amount of annealing experienced by this component of tracks over one interval (timestep) is obtained by integrating the annealing equation (27) of Laslett et. al. (1987) over a number of sub-time steps each with a different constant temperature. The complete annealing history of this component is given by allowing it to anneal over the time subsequent to the component's formation. The full distribution of tracks is then obtained by taking the component means and convolving them with the appropriate Gaussian function and then summing these distributions. Based on line segment theory, Laslett et al. (1982) argue that short track/long track ratio is not the true ratio since short tracks, by virtue of their length, are inherently more difficult to find. Therefore, a correction for observational bias (Laslett et al., 1982) is included in the algorithm. The final probability density function may be given either as a histogram or as a cumulative density function.

Track length distributions take on a variety of shapes depending on the temperature history experienced by a sample. Three end-member cooling histories are modelled in a forward sense to characterize end-member 'cooling only' track length distributions (Figure 4.1). A sample experiencing a 'convex up' (logarithmic) cooling

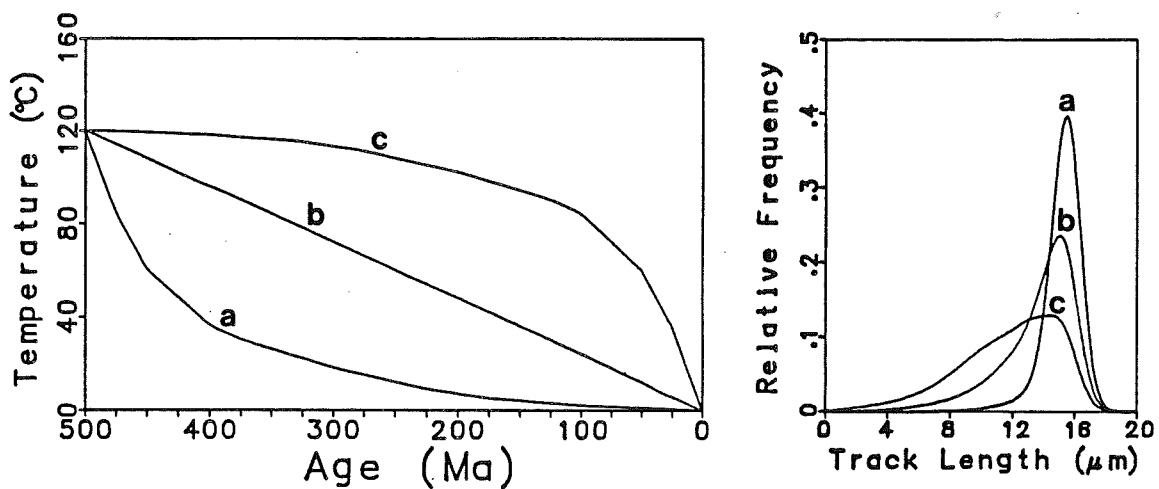


Figure 4.1

Given an apatite sample at 120 °C at 500 Ma, forward modelling of apatite fission track data shows the difference between: a.) a 'convex up' cooling history where a sample resides a relatively short time at high partial annealing temperatures, b.) a linear cooling history and c.) a 'convex down' cooling history where a sample resides a relatively long time at high partial annealing temperatures. Predicted track length distributions are shown for each model. A 'convex up' history produces a unimodal, narrow and nearly normally distributed track length histogram with a relatively long mean length and old apparent model apatite fission track age. A linear history produces a unimodal, negatively skewed, broad track length histogram with a mean length and apparent age that falls between the mean lengths and apparent model ages of 'convex up' and 'convex down' histories. A 'convex down' history produces a unimodal, highly negatively skewed, very broad track length histogram with a relatively short mean length and a young apparent model age.

history (Figure 4.1a) resides only briefly at high partial annealing temperatures spending most of its time below the partial annealing zone (less than 70 °C). A sample cooling linearly spends the same amount of time at all annealing temperatures (Figure 4.1b). A sample experiencing 'convex down' (exponential) cooling spends most of its time at high partial annealing temperatures and relatively little time below the partial annealing zone (Figure 4.1c). The predicted track length distributions are all unimodal and peak at approximately the same length (14-15 μm). Although not shown, a significant reheating event (of short duration relative to the full history) will produce a bimodal distribution such that a shorter peak of tracks represents track shortening caused by the reheating event and a longer peak of tracks those that formed after the reheating event. A very broad, highly negatively skewed track length histogram characterizes the 'convex up' history while the 'convex down' history is represented by a narrow, nearly normally distributed track length histogram. The linear cooling history is characterized by a broad, negatively skewed track length histogram.

4.2.2 Inverse Modelling (T-t history estimation from apatite age and track length distribution fitting)

The forward model gives the cumulative density function (track length distribution) as a non-linear function of $(m+1)$ temperatures through time given a temperature history. The inverse model produces an estimate of this temperature history by a prediction of apatite age and track length distribution.

The algorithm proceeds by randomly generating a set of temperature histories within the T-t space set by the worker. For each temperature history a prediction of the fission track age and length distribution is made and compared with the data through a measure of fit. A new history is then generated by a combination of the set of histories and similar predictions are made for the new history. If the fit to the data of the new history is better than any other history in the set the worst history is replaced by the new

history. This process is continued until all the histories in the set predict the data within the expected measurement error. The expected measurement error is dependent on the number of data points and is given at various confidence levels. The mean of the set of histories is the preferred temperature history and the bounds are given by the loci of the maximum and minimum temperature allowed by the data at any time during the history. The bounds themselves are not acceptable histories but constrain the temperature to fall within their perimeter throughout the temperature history.

The measurement of fit between the track length data and predicted track length distribution is the Kolmogorov-Smirnov statistic (Press et al., 1986) which uses the maximum difference between the measured and predicted cumulative density function, not between the binned (histogram) representation of the track length data. The histograms in this study are only used as a means of presenting the results and are neither predicted nor used statistically in the model.

4.2.3 Modelling Parameters and Assumptions

Temperature histories may be generated completely randomly or constrained to preset maximum and minimum allowable temperatures and rates of cooling or heating. This allows the modeller to address known geological conditions (eg. heating events, depositional events) during any part of the temperature history. The effect of the cooling (or heating) rate parameter may be enhanced or decreased and the resolution of the data controlled by varying the time step length over which a track length component is introduced. For example, if the time step length is increased the resolution of the data is decreased and the maximum allowable cooling or heating rate is effectively increased.

A number of assumptions are made during the modelling: 1. Temperature varies continuously through time and linearly over each time step. 2. Tracks are produced at a constant rate throughout the temperature history. 3. A correction for geometric bias in observing short tracks is proportional to track length and this correction can be applied

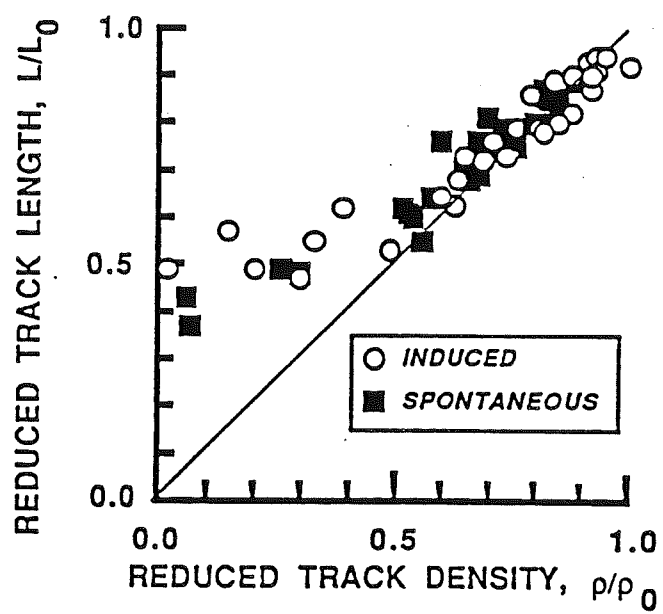


Figure 4.2

The relationship between age (reduced track density) and track length (reduced track length) reduction for both induced and spontaneous apatite fission tracks. Note the divergence from a 1:1 relationship at ~ 0.65 reduced track length. (from Green, 1988)

as a constant to each Gaussian component. 4. Activation energies for track annealing are not greatly dependent upon orientation of tracks to the *c* crystallographic-axis of an apatite crystal. 5. At any point during a sample's temperature history the amount of annealing depends only on the ambient temperature and the current length of the tracks, and is independent of the shape of the T-t path which brought it to this point. 6. The annealing equation (27) of Laslett et. al. (1987) sufficiently describes the annealing kinetics of fission tracks in the Durango apatite. 7. The track length-age reduction model used by Green (1988) to predict model-corrected ages (age of the oldest track population to survive a model T-t history) is accurate.

Investigation into the validity of (4) suggests that activation energies for track annealing vary only slightly with track orientation (Donelick pers. comm., 1989). The current model uses an annealing-dependent activation energy which produces slightly fanning annealing curves on the Arrhenius plot (see Chapter 2, Figure 2.4b). Although other models are available, the slightly fanning annealing model fits the experimental data better than any other proposed model (Laslett et al., 1987). Laboratory experiments confirm that track annealing is independent of the shape of the time-temperature path experienced by the tracks (Donelick pers. comm., 1989). The track length-age reduction model of Green (1988, Figure 4.3) shows a 1:1 relationship between mean track length and age reduction above ~ 0.65 reduced track length. Below this value the 1:1 relationship diverges so that at zero age a distribution of tracks with a considerable mean length (~ 0.5 reduced track length) may still be measured. This is understood in terms of anisotropy of annealing and the bias against measuring short tracks (Green, 1988). More rigorous apatite fission track length-age reduction data calibration suggests that the Laslett et al. (1987) equation may not fully describe annealing kinetics especially for highly annealed (less than $.65$ reduced track length) tracks (Donelick pers. comm., 1990). Because model-corrected ages are dependent on the age-track length reduction relationship, the older the model-corrected age the more dependent it is on the age-track length reduction relationship (Issler et al., 1990). As a result, the meaning of the model-corrected apatite fission track age is not entirely clear and another, zeta parameter

Sample	Model Corrected Age (Ma,Period)
--------	---------------------------------

Southern Transect

FT89-226	470 (Ordovician)
FT89-225	458 (Ordovician)
FT89-201	351 (Carboniferous)
FT89-196	383 (Devonian)
FT89-203	302 (Carboniferous)
FT89-205	382 (Devonian)
FT89-224	374 (Devonian)
FT89-194	372 (Devonian)
FT89-227	454 (Ordovician)
FT89-193	302 (Carboniferous)
FT89-191	343 (Carboniferous)
FT89-197	314 (Carboniferous)
FT89-198	252 (Permian)

Central Transect

FT89-212	374 (Devonian)
FT89-211	374 (Devonian)
FT89-210	296 (Carboniferous)
FT89-207	369 (Devonian)
FT89-209	277 (Permian)
FT89-206	317 (Carboniferous)
FT89-208	280 (Permian)

Northern Transect

FT89-221	270 (Permian)
FT89-232	264 (Permian)
FT89-233	264 (Permian)

Deer Lake Basin and Miscellaneous GNP

LGRA-01	209 (Jurassic)
FT90-050	278 (Permian)
FT90-034	309 (Carboniferous)
FT90-035	284 (Permian)
FT89-235	275 (Permian)
FT89-213	203 (Jurassic)
FT89-222	326 (Carboniferous)
FT89-223	444 (Ordovician)

Table 4.1

Predicted model-corrected apatite fission track ages (age of the oldest fission track) for Great Northern Peninsula samples using T-t inverse models.

dependent, length-corrected age has also been calculated which places less emphasis on highly annealed tracks. The length-corrected method is outlined in Appendix 3. Model-corrected ages are given in Table 4.1.

The length-corrected age estimates are included to provide a qualitative confidence measurement for the predicted T-t paths. T-t information to the left of the length-corrected ages (between solid and dashed lines in Figures 4.4a-ee) must be viewed with relatively less confidence than that to the right, since this information is obtained from fitting the shortest tracks in the distribution. The inverse models were not constrained to be above ~ 120 °C before the time of their length-corrected ages, hence these ages do not represent the age of the oldest fission track component of their corresponding T-t paths (ie. length-corrected ages are not consistent with respective T-t paths). To be consistent with their length-corrected ages (dashed lines in Figures 4.4a-ee), T-t paths would have to be constrained to ~ 120 °C at the time of the length-corrected age.

The model-corrected age in all the T-t models represents the age of the oldest fission track population in the sample and is a unique value for a given T-t path. This age is clearly model dependent, particularly on the track length-age reduction model of Green (1988), and is only significant if the model is accurate.

4.3 Modelling Results

4.3.1 Southern Transect

All the modelling results are presented with similar modelling parameters except where known geological conditions dictate further parameter constraint. These parameters were chosen so that they consistently led to solution convergence and gave the most meaningful geological results. The parameters used represent the result of a range of possible test values. Each modelled sample displays the preferred T-t history (the mean of the set of histories at the 0.50 confidence level) with 0.95 confidence level

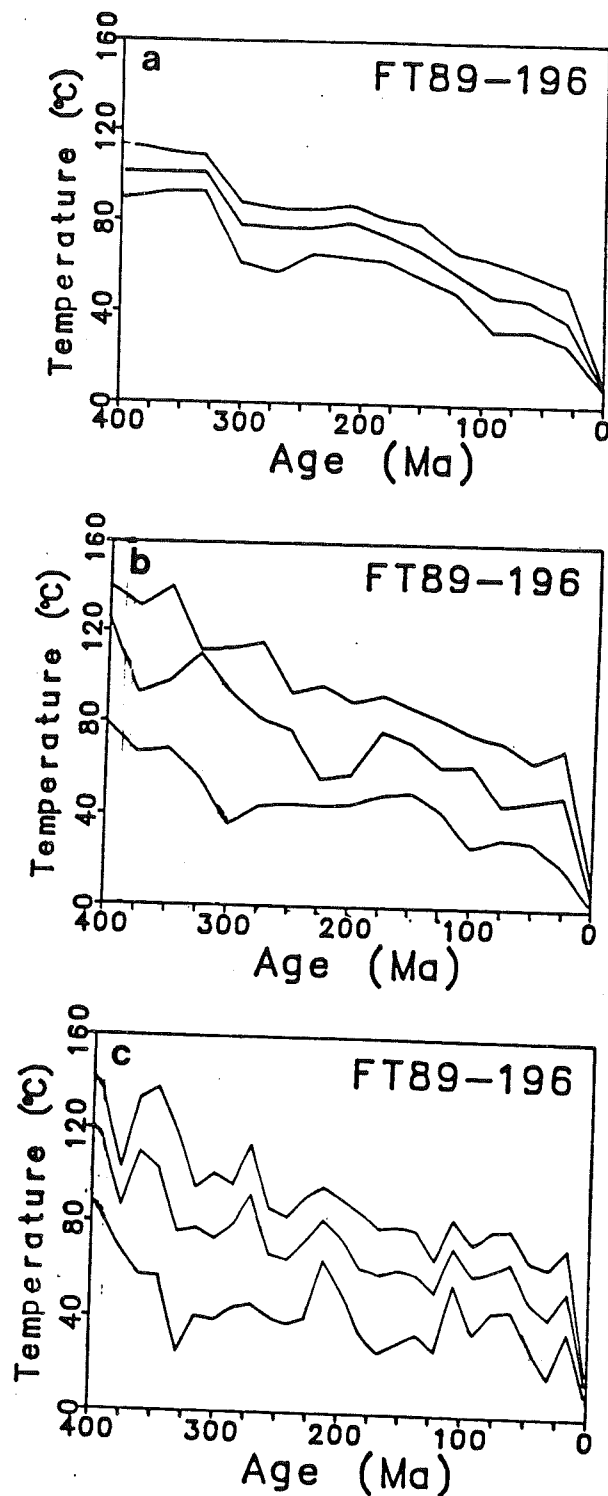
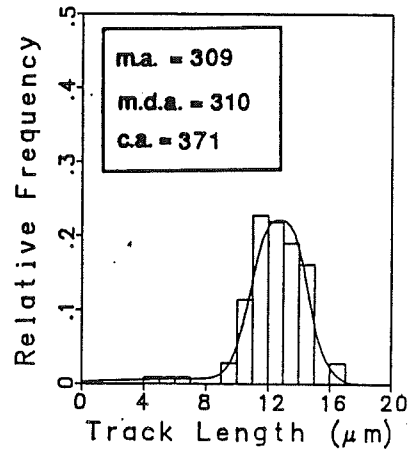
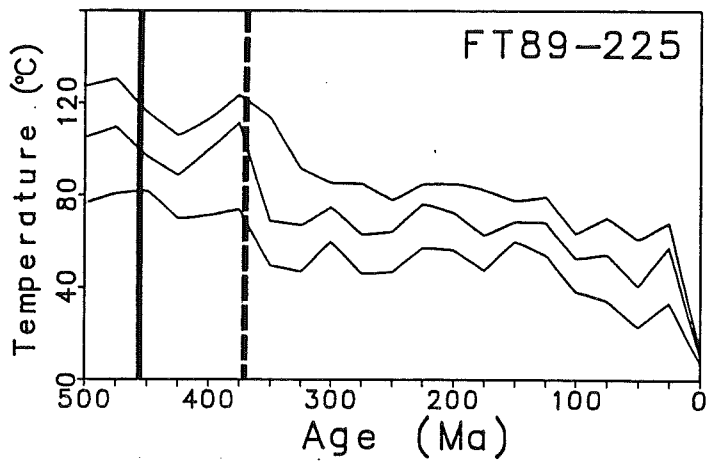


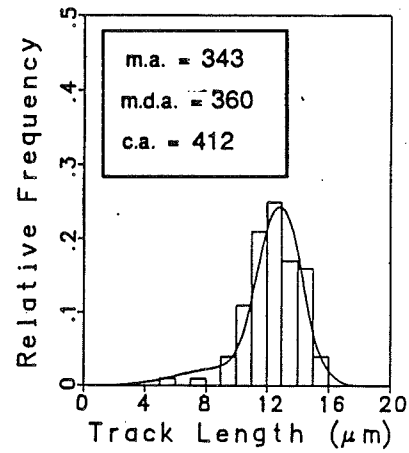
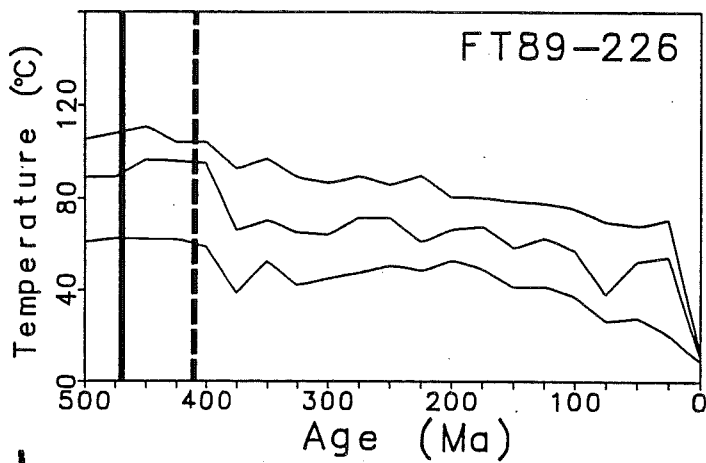
Figure 4.3
 Predicted T-t paths (0.50 preferred histories and 0.95 bounds) for sample FT89-196 showing the effects of changing modelling parameters on the shape of the T-t path. a.) Maximum cooling and heating rate = 10 °C/timestep, maximum and minimum temperatures = 140-20 °C, timestep size = 30 Ma. b.) Parameters used in Figures 4.4 a-ee; maximum cooling and heating rate = 30 °C/timestep, maximum and minimum temperatures = 140-20 °C, timestep size = 25 Ma. c.) Maximum cooling and heating rate = 50 °C/timestep, maximum and minimum temperatures = 140-20 °C, timestep size = 15 Ma.

Figure 4.4 a-ee

Modelling results show predicted T-t paths and track length distributions for samples in the Great Northern Peninsula. Each figure includes the apatite fission track measured age (m.a.), model age (m.d.a.) and length-corrected age (c.a.). Model corrected ages are found in Table 4.1. Only T-t paths to the right of the solid line (model-corrected age) are considered in the study. Note the dramatic increase in cooling rate for all samples at 25 Ma. This is likely an artefact of the calibration equation (Laslett et al., 1987) used to model the annealing kinetics of apatite fission tracks and along with most second order frequencies on the main T-t path are considered to be geologically meaningless. Geological considerations constrain the T-t paths to temperatures below the base of the annealing zone in the Central Transect and Hare Bay Allochthon during the Acadian Orogeny (400-375 Ma), and between 40-20 °C in the Deer Lake Basin during sample deposition (350 Ma). The T-t history shows three T-t paths. The top and bottom T-t paths represent the upper and lower temperature bounds at any time in the T-t history at the 0.95 confidence level. The middle T-t path represents the mean T-t path of the 0.50 confidence level set of T-t histories. The solid and dashed lines on the T-t histories represent the model- and length-corrected ages of the sample respectively. The 0.50 confidence level predicted track length histogram (solid line on top of histogram) is superimposed upon the data histogram.



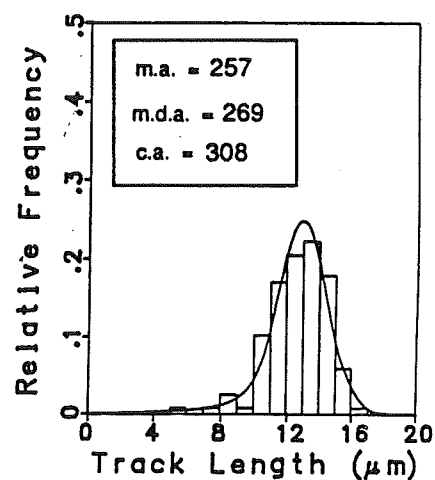
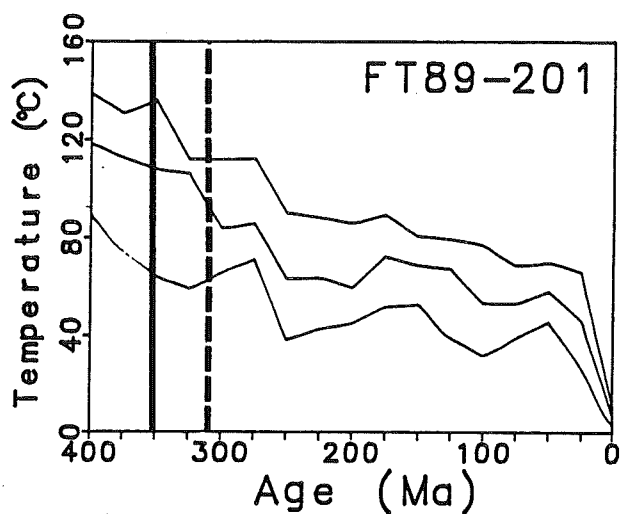
a



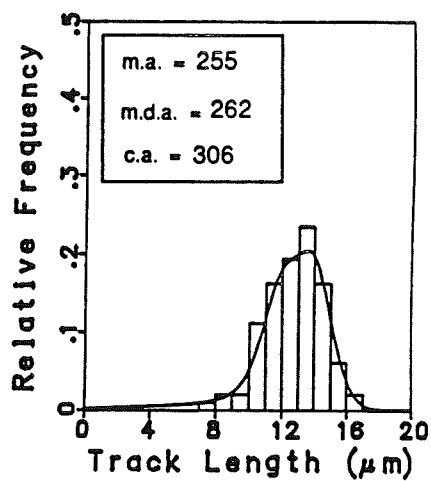
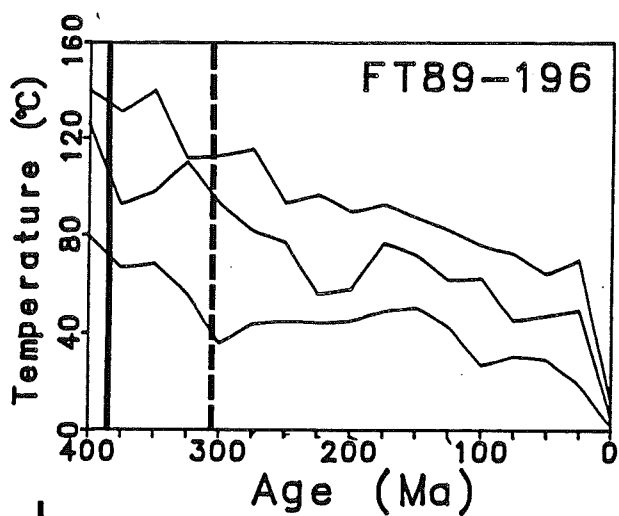
b

Figure 4.4 a,b

Southern Transect 2 modelled T-t paths and track length distributions for a.) FT89-225 and b.) FT89-226. Note cooling trends since the Late Ordovician for FT89-225 and the Middle Ordovician for FT89-226.



c



d

Figure 4.4 c,d

- Southern Transect 2 modelled T-t paths and track length distributions for c.) FT89-201 and d.) FT89-196. Note cooling trends since the Middle Devonian for FT89-196 and the Early Carboniferous for FT89-201. Possible minor reheating at 200 Ma (Early Jurassic).

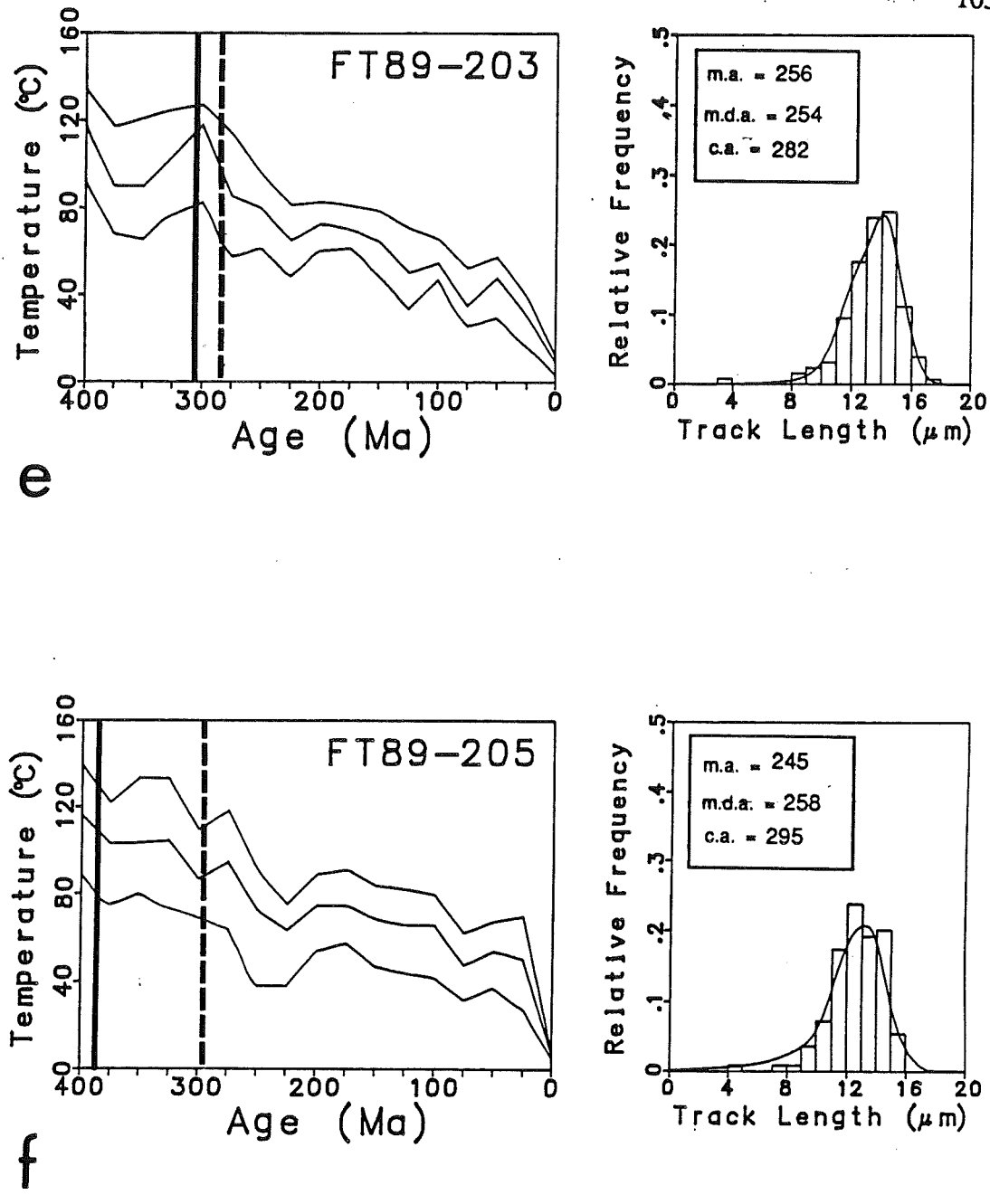
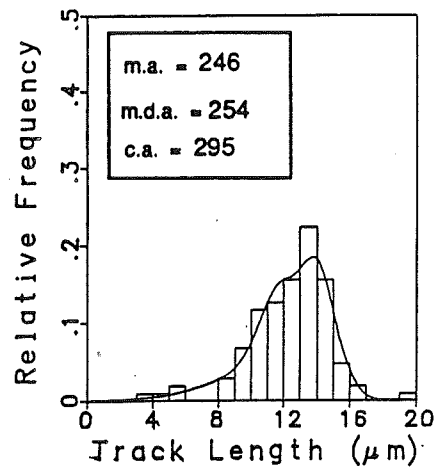
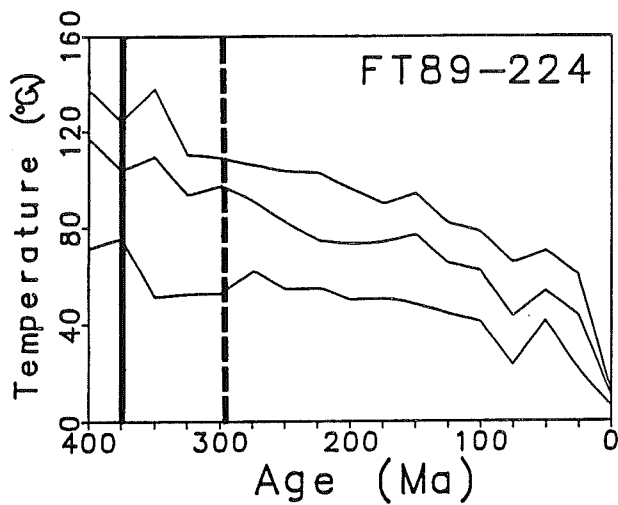
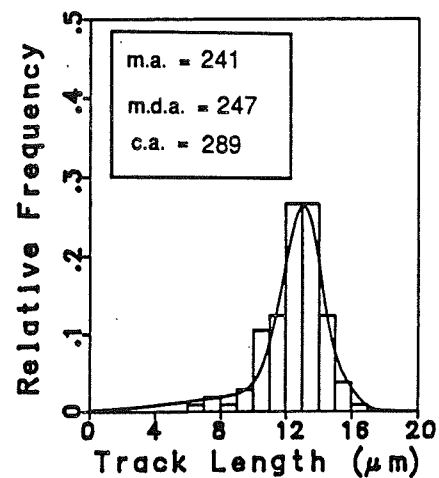
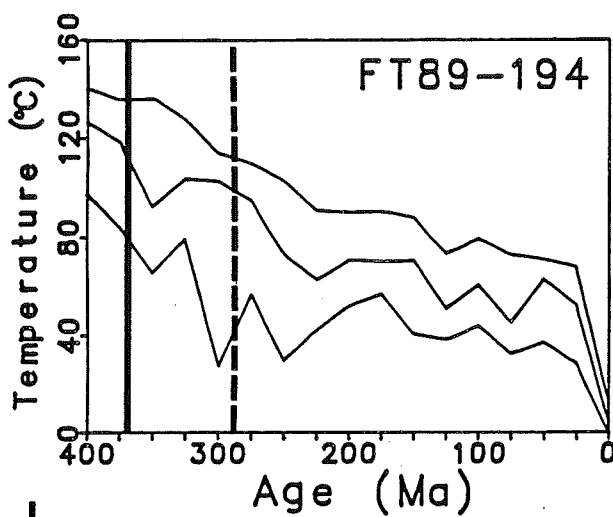


Figure 4.4 e,f
Southern Transect 2 modelled T-t paths and track length distributions for e.) FT89-203 and f.) FT89-205.
Note cooling trends since the Late Carboniferous for FT89-203 and the Middle Devonian for FT89-205.



g



h

Figure 4.4 g,h

Southern Transect 2 modelled T-t paths and track length distributions for g.) FT89-224 and h.) FT89-194. Note cooling trends since the Late Devonian.

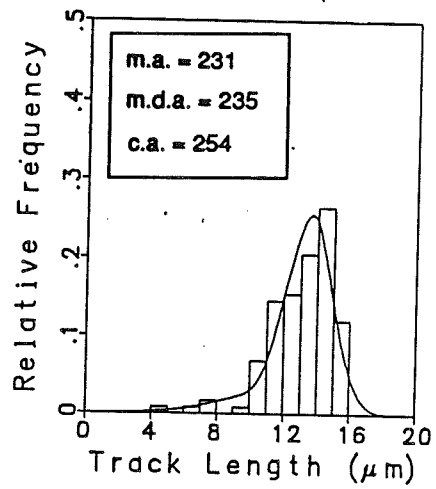
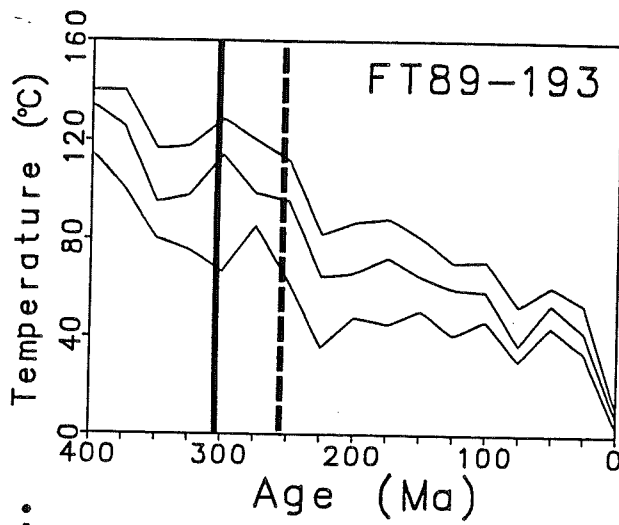
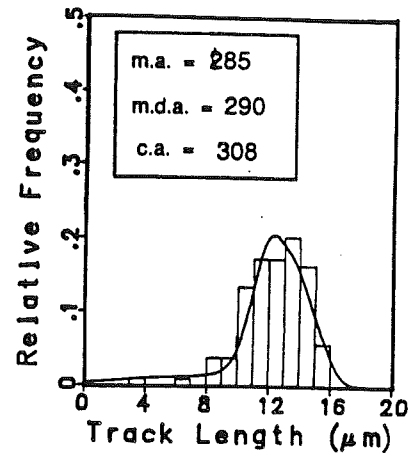
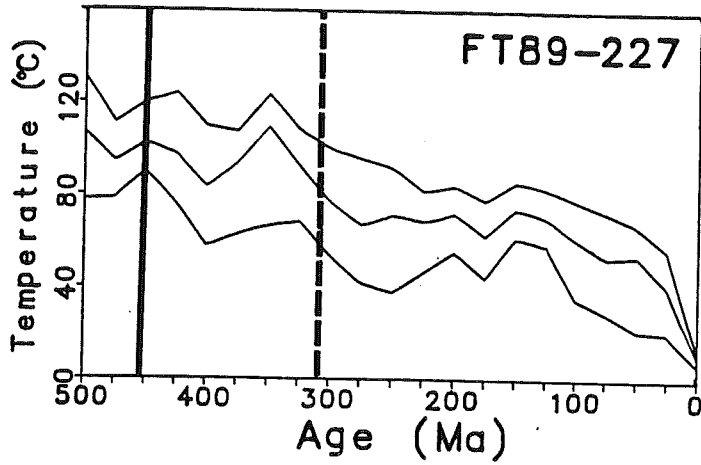


Figure 4.4 i,j

Southern Transect 1 modelled T-t paths and track length distributions for i.) FT89-227 and j.) FT89-193. Note cooling trends since the Late Ordovician for FT89-227 and the Late Carboniferous for FT89-193.

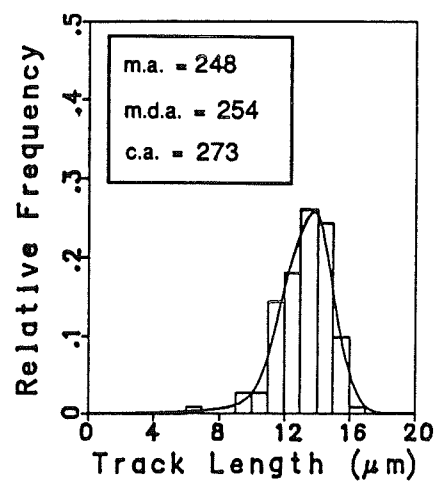
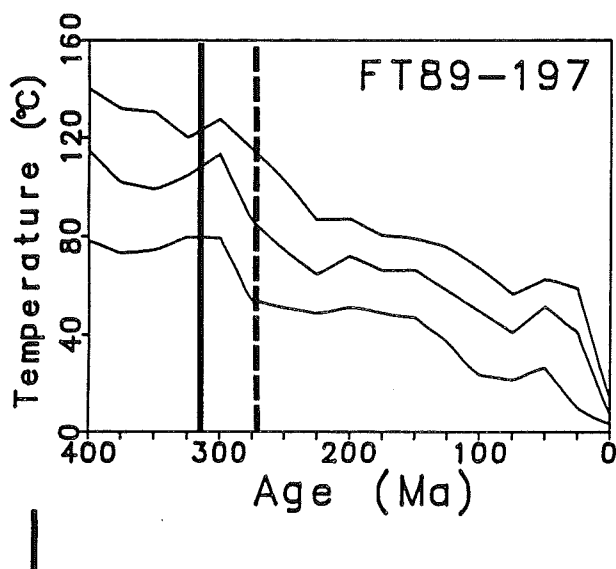
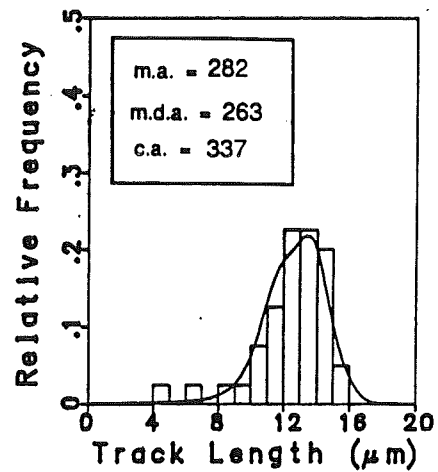
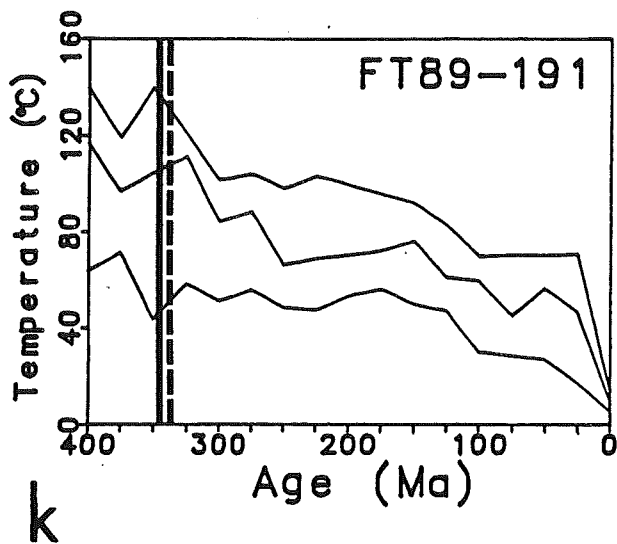
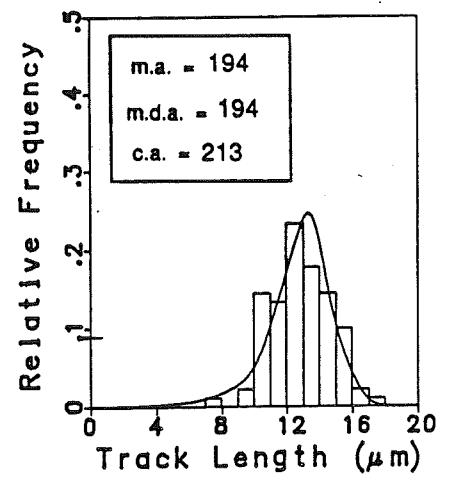
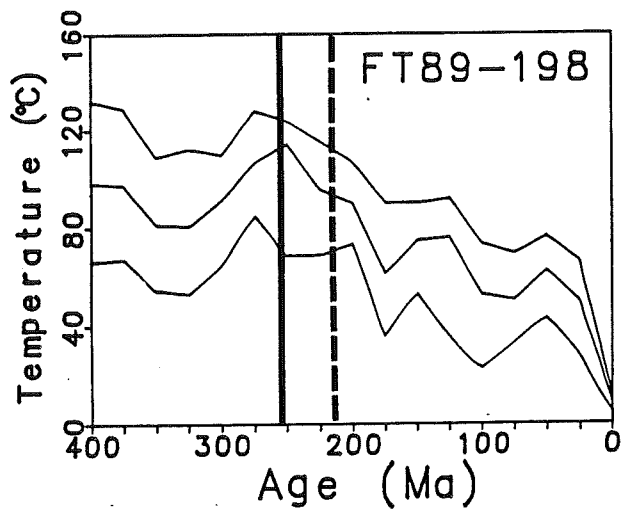


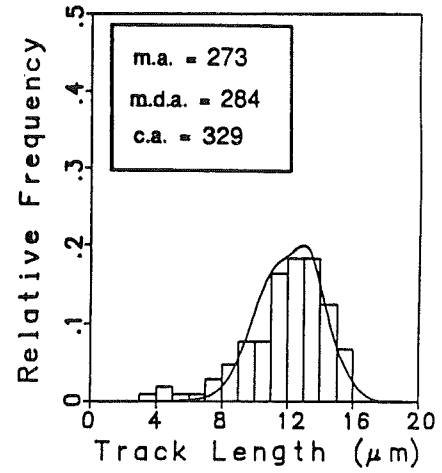
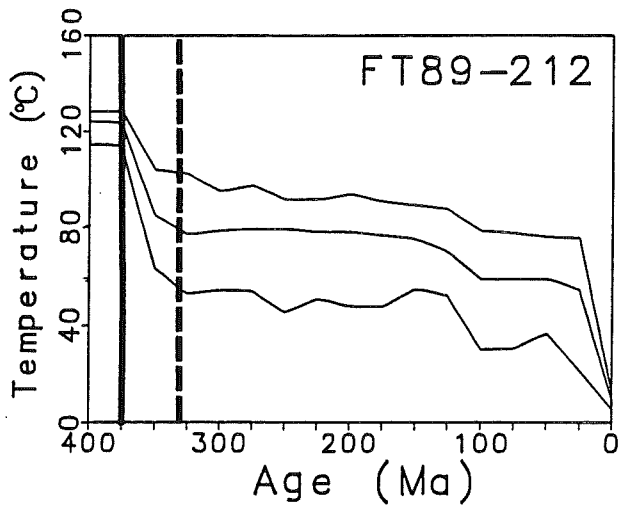
Figure 4.4 k,l

Southern Transect 1 modelled T-t paths and track length distributions for k.) FT89-191 and l.) FT89-197. Note cooling trends since the Early Carboniferous for FT89-191 and the Middle Carboniferous for FT89-197.

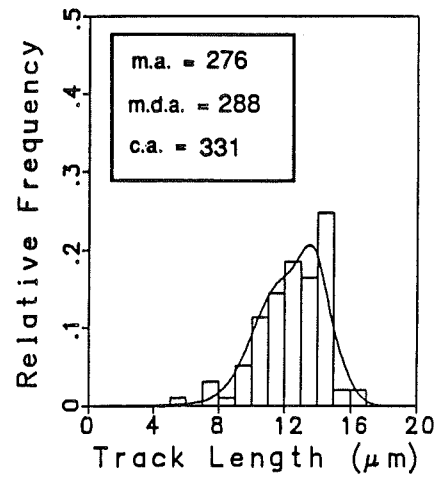
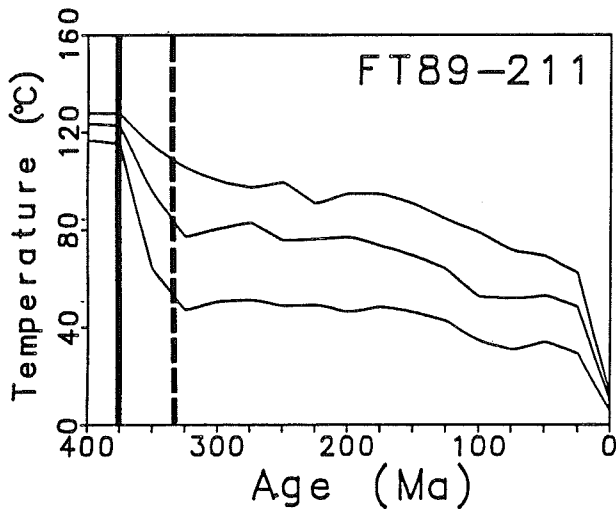


m

Figure 4.4 m
Southern Transect 1 modelled T-t path for m.) FT89-198. Note cooling trend since the Late Permian with possible minor reheating starting at 175 Ma (Middle Jurassic).



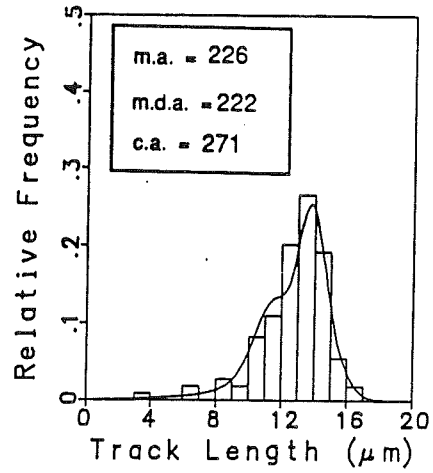
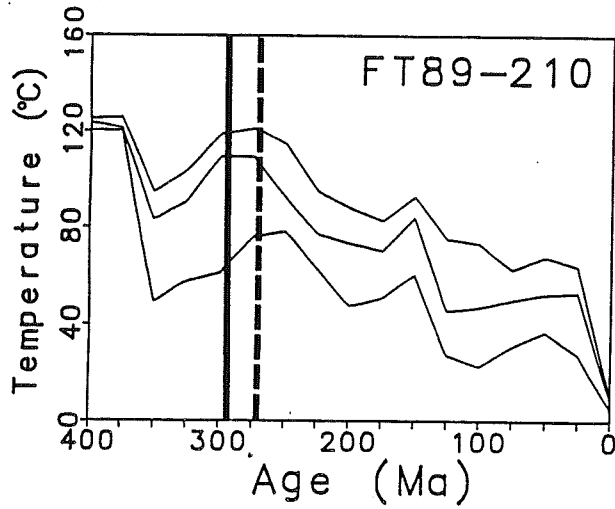
n



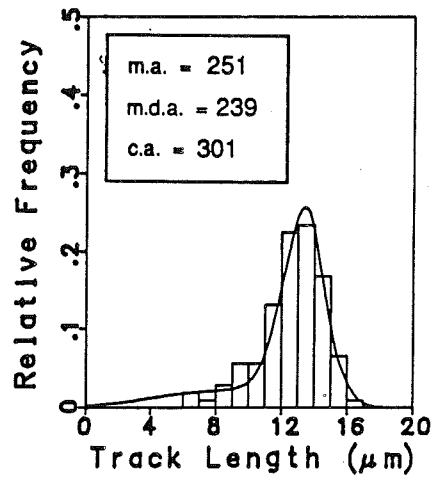
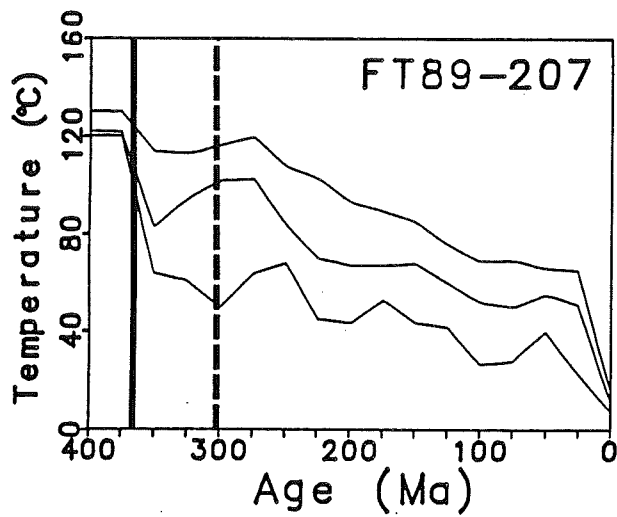
o

Figure 4.4 n,o

Central Transect modelled T-t paths and track length distributions for n.) FT89-212 and o.) FT89-211. Note cooling trends since the Late Devonian.

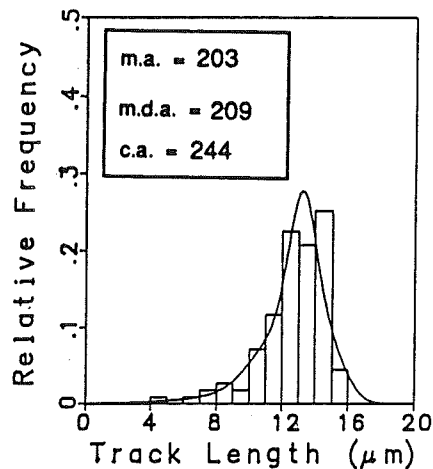
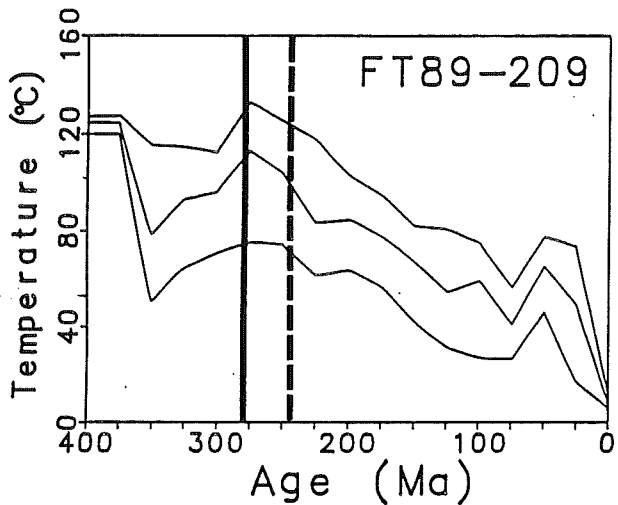


p

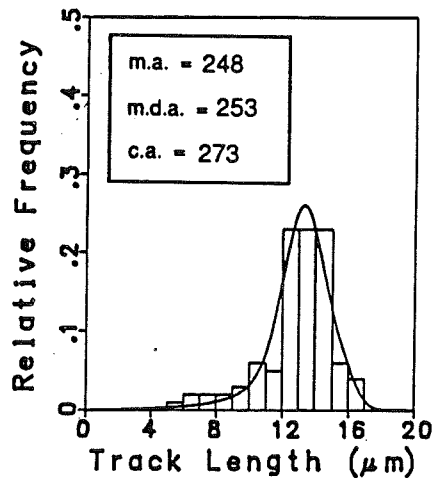
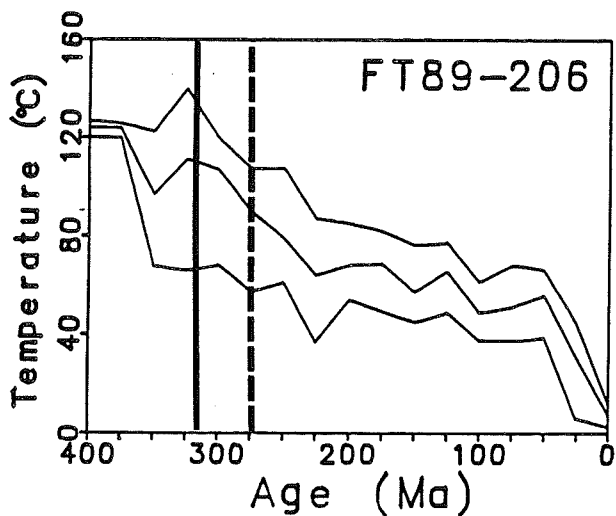


q

Figure 4.4 p,q
Central Transect modelled T-t paths and track length distributions for p.) FT89-210 and q.) FT89-207. Note cooling trends since the Late Carboniferous for FT89-210 with possible minor reheating at 175 Ma (Middle Jurassic) and the Late Devonian for FT89-207.



r



s

Figure 4.4 r,s
Central Transect modelled T-t paths and track length distributions for r.) FT89-209 and s.) FT89-206. Note cooling trends since the Late Permian for FT89-209 and Middle Carboniferous for FT89-206.

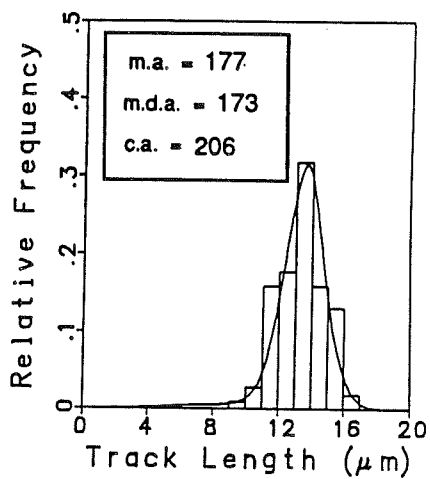
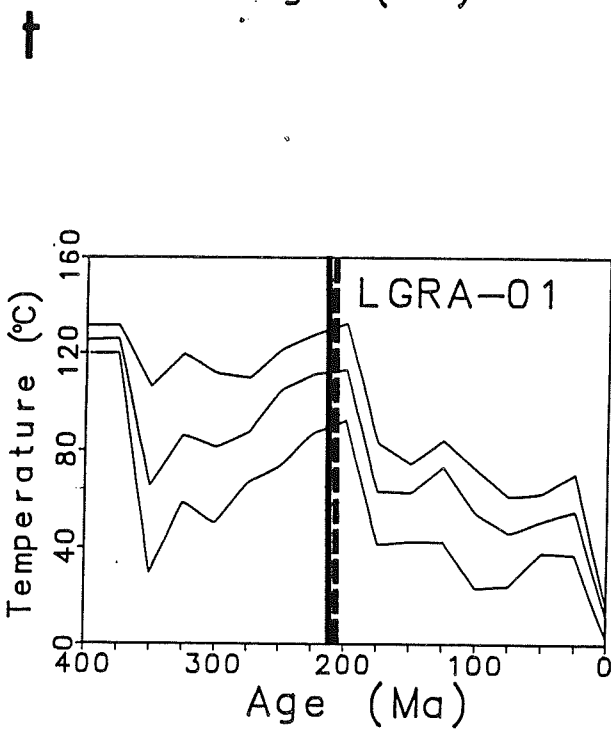
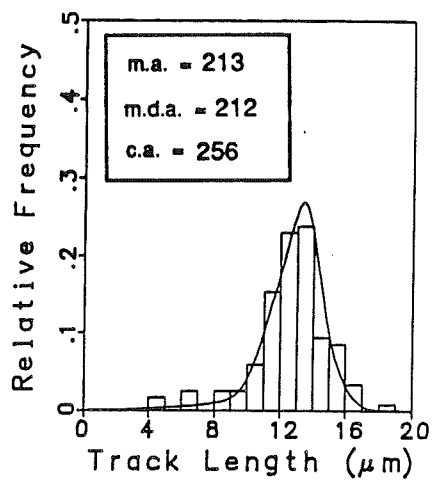
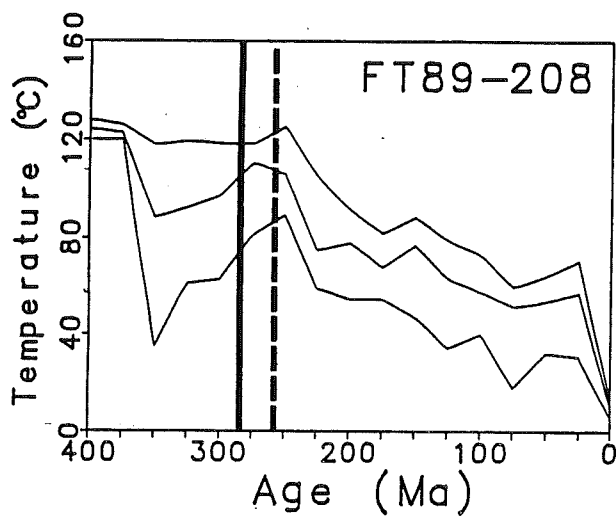
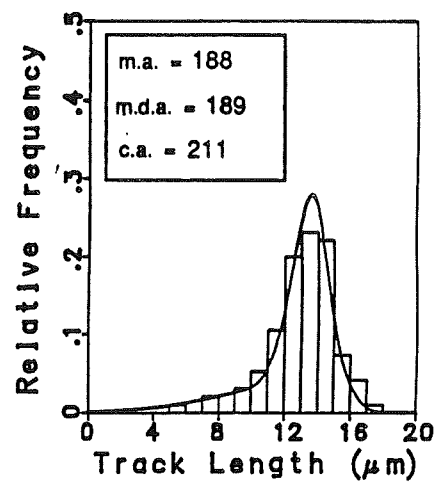
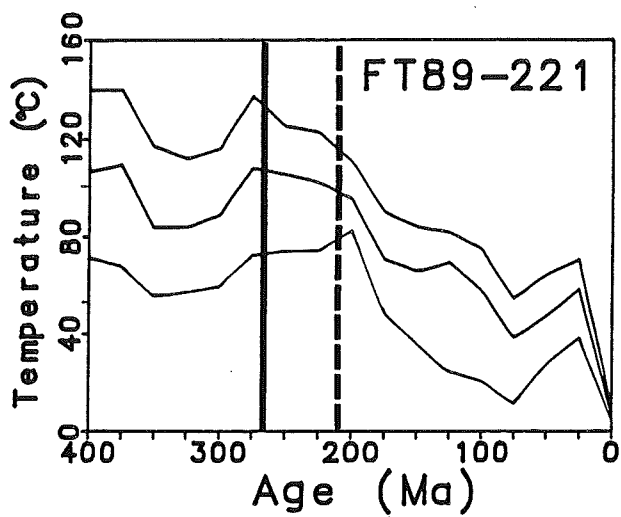
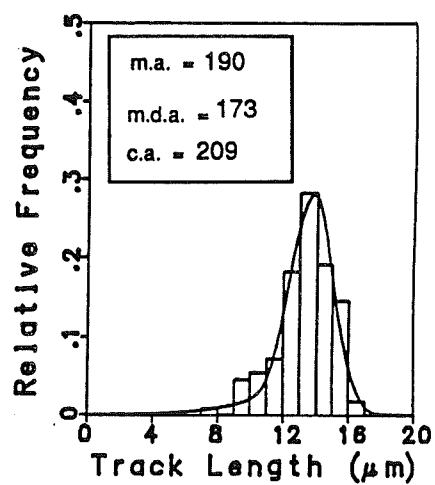
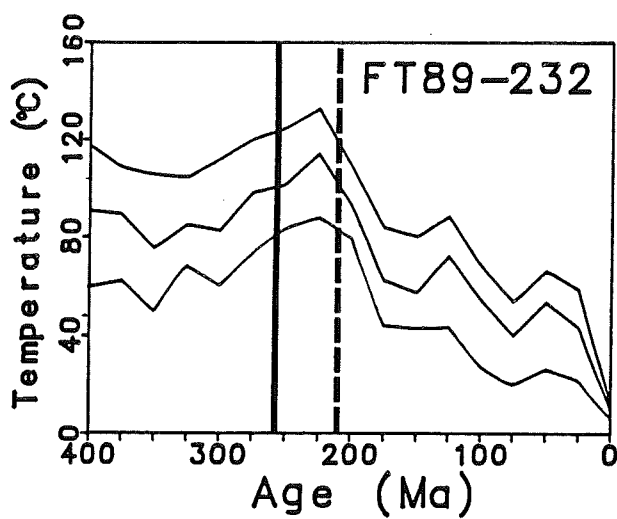


Figure 4.4 t,u

Modelled T-t paths and track length distributions for t.) Central Transect sample FT89-208 and u.) Devil's Room Pluton sample LGRA-01. Note cooling trends since the Early Permian for FT89-208 and the Early Jurassic for LGRA-01. LGRA-01 displays much faster cooling through high partial annealing temperatures (120-75 °C) than other Great Northern Peninsula samples.



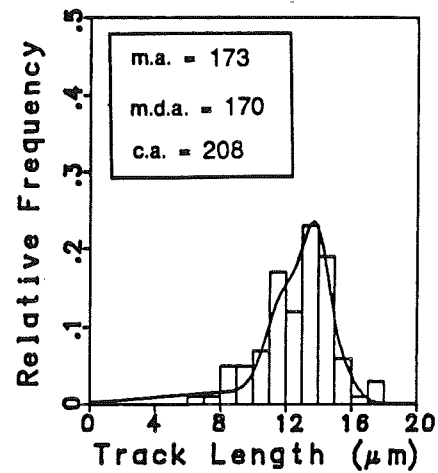
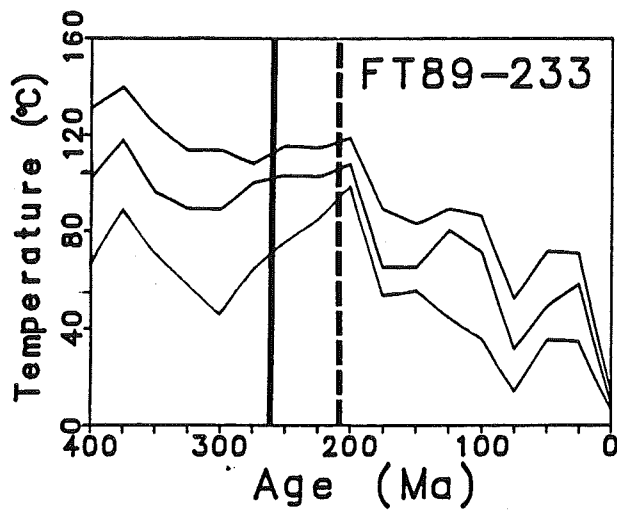
v



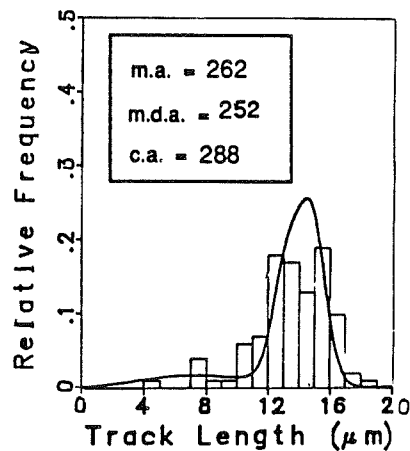
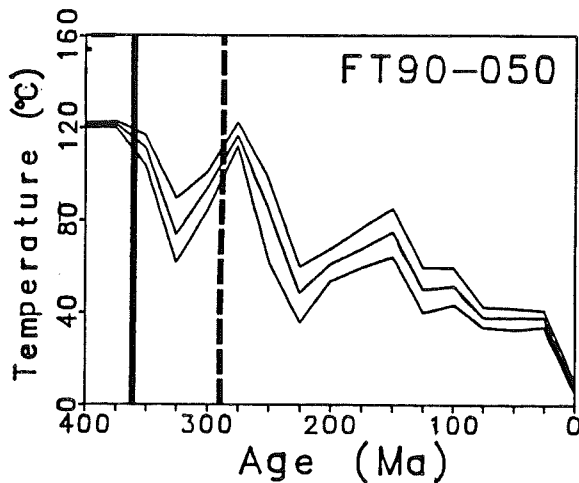
w

Figure 4.4 v,w

Northern Transect modelled T-t paths and track length distributions for v.) FT89-221 and w.) FT89-232. Note cooling trends since the Late Permian. FT89-232 displays possible reheating at 150 Ma (Late Jurassic).



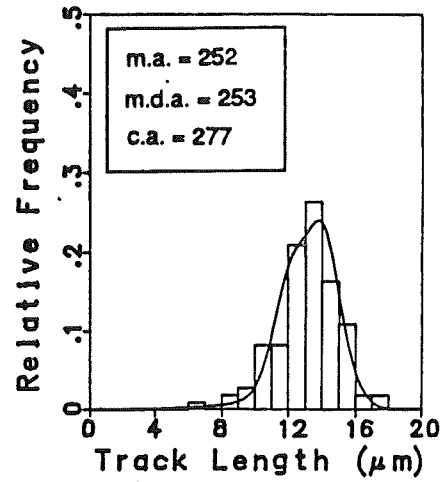
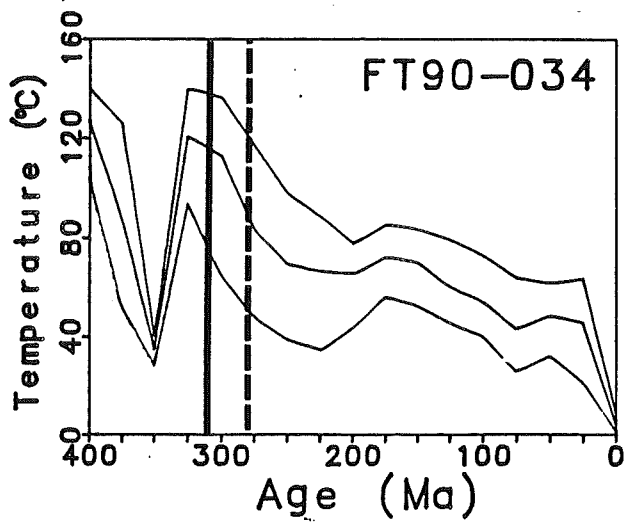
X



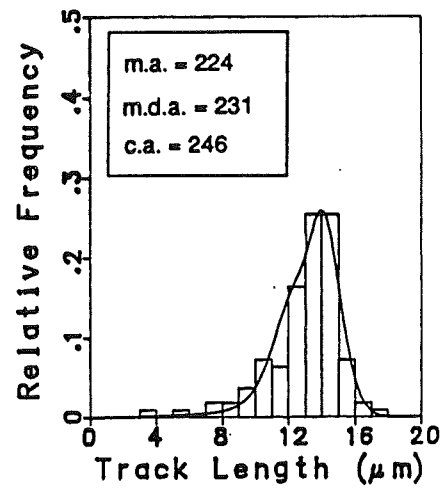
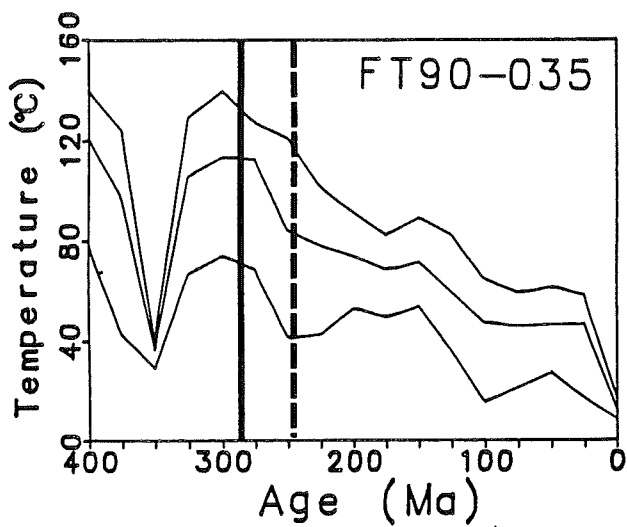
Y

Figure 4.4 x,y

Modelled T-t paths and track length distributions for x.) Northern Transect sample FT89-233 and y.) Hare Bay Allochthon sample FT90-050. Note cooling trends since the Late Permian for FT89-233 and the Late Devonian for FT90-050. The FT90-050 preferred solution did not converge to the 0.50 confidence level so the 0.95 confidence level preferred solution is plotted. FT90-050 shows reheating to ~120 °C during the Late Carboniferous-Early Permian and a second minor reheating to ~80 °C during the Jurassic. Possible reheating is shown at 150 Ma (Late Jurassic) in FT89-233.



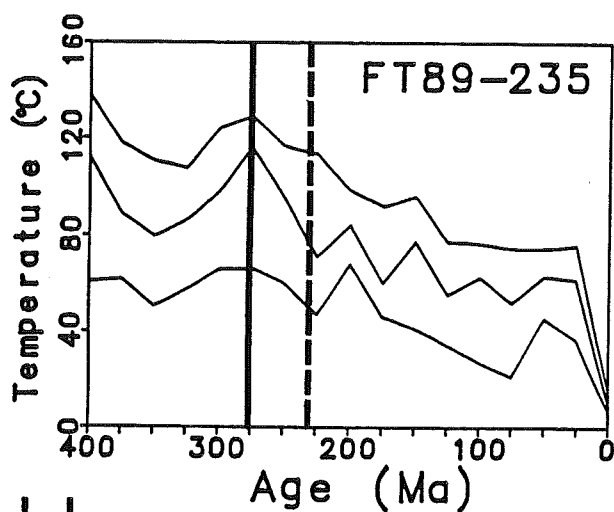
z



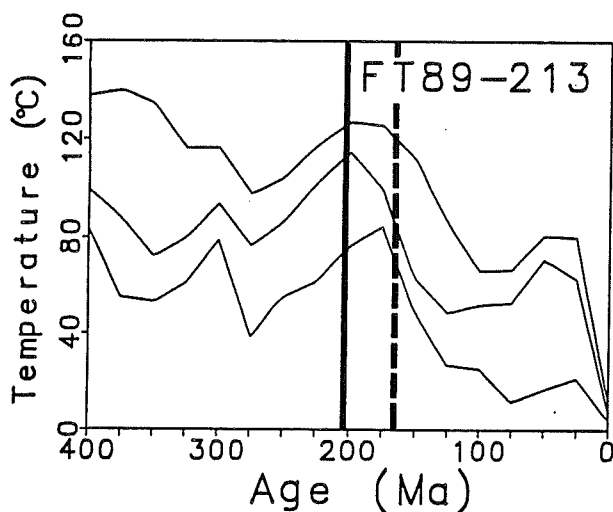
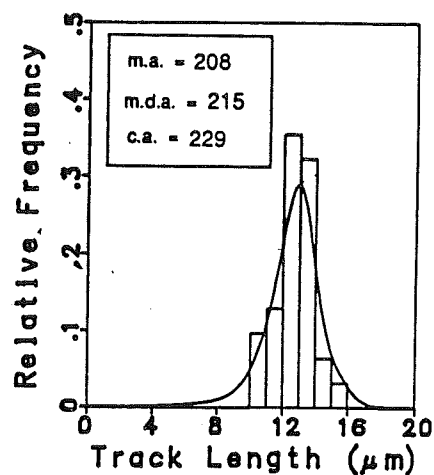
aa

Figure 4.4 z,aa

Deer Lake Basin modelled T-t paths and track length distributions for z.) FT90-034 and aa.) FT90-035. Note cooling trends since the Late Carboniferous for FT90-034 and the Early Permian for FT90-035.



bb



cc

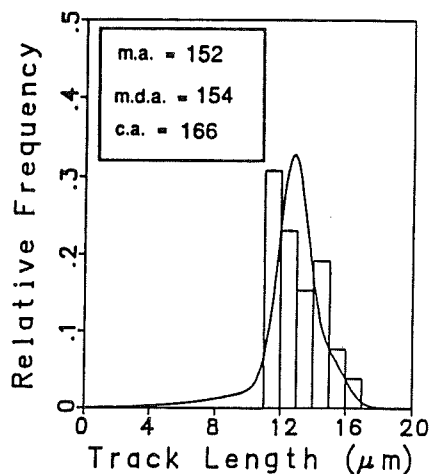
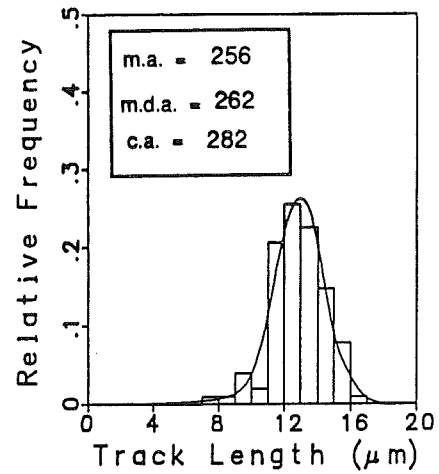
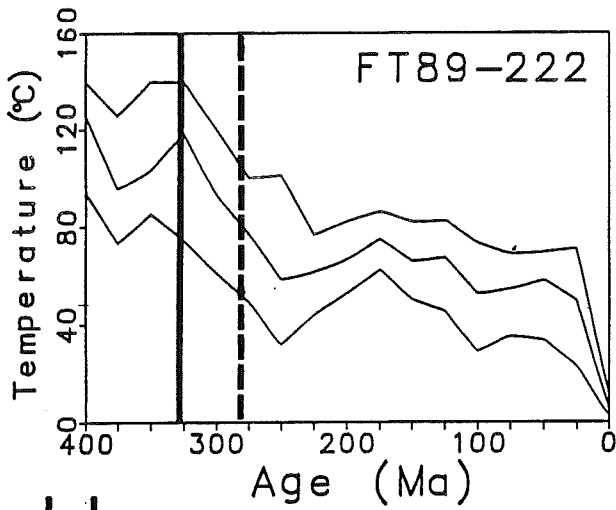
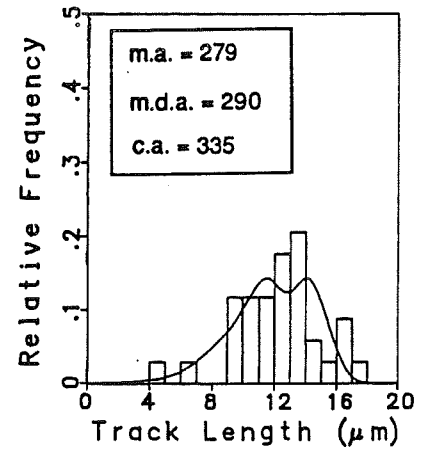
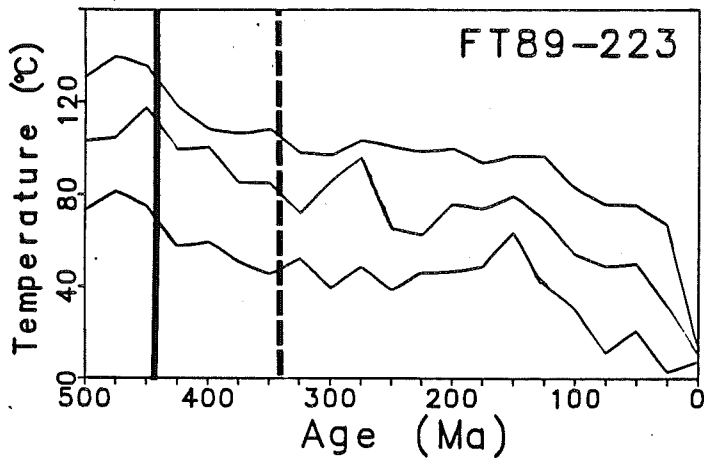


Figure 4.4 bb,cc

Modelled T-t paths and track length distributions for bb.) Humber Arm Allochthon sample FT89-235 and cc.) Daniel's Harbour sample FT89-213. Note cooling trend for FT89-235 since the Late Permian. FT89-213 displays a saddle shaped cooling path with cooling starting during the Early Jurassic followed by reheating at 75 Ma (Late Cretaceous). Track length distributions are based on 35 and 29 track lengths respectively.



dd



ee

Figure 4.4 dd,ee

Modelled T-t paths and track length distributions for samples east of Southern Transect 1. dd.) FT89-222 and ee.) FT89-223. Note cooling trends since the Middle Carboniferous for FT89-222 and the Late Ordovician for FT89-223.

maximum and minimum temperature bounds. The track length data and the predicted track length distributions from the 0.50 confidence level model are presented in histogram form with each temperature history (Figures 4.4 a-ee). Each history also includes the measured, the model (0.50 confidence level), and the corrected apatite fission track ages of the sample. The dashed vertical line on each of the T-t histories represents the length-corrected apatite fission track age of the sample. Model-corrected (solid vertical lines) ages are usually several tens of millions of years older than the length-corrected ages since they are based on a calculation involving the shortest (oldest) track population in the predicted track length distribution and not the mean length as in the length-corrected method. In distributions containing no tracks less than 9 μm (eg. Figure 4.4u) the model- and length-corrected ages are almost equal since the mean length of the sample is not much longer than its shortest track. The parameters used to model each sample are given in Appendix 4.

The modelling results for the Southern Transect are presented in Figures 4.4 a-m. The main observation common to all the T-t histories is their general cooling trend. To first order the preferred histories generally show cooling paths from model-corrected age to the present. A sharp increase in cooling rate at 25 Ma characterizes all T-t histories. In all likelihood this is not a meaningful tectonic event but rather an artefact of the annealing calibration used by the model (Donelick, 1990, pers.com.). There is no independent geological evidence for a significant increase in cooling/exhumation in western Newfoundland at this time. The increase in cooling rate usually occurs between 40-50 °C after which the temperature history is forced to cool to surface temperatures by the present (below 20 °C). The implication is that the present model cannot distinguish between the longest tracks in the distribution which are formed late in T-t history of an apatite sample (say tracks greater than about 14 μm). This suggests that the present algorithm for predicting T-t histories is not well constrained below about 50 °C (Willet pers. comm., 1991). With this in mind, the conclusions from the modelling should be interpreted only together with other independent evidence, before any 'true' conclusion can be made. At present, if modelling results suggest major geological

phenomena for which there is no other evidence it is disregarded in this study.

Average Southern Transect cooling rates range from about 0.08-0.25 °C/Ma. Predicted track length distributions and model ages fit the data fairly well. All predicted track length distributions are negatively skewed as demanded by the data and the predicted ages fall within the 1σ error of the measured age. The majority of the model-corrected ages are Middle Devonian-Carboniferous, although highest elevation samples (Figures 4.4a,b,i,ee) have Middle-Late Ordovician corrected ages and low elevation sample FT89-198 (Figure 4.4m) has a Late Permian corrected age. Based on these observations, highest areas of the Southern Transect cooled through the base of the partial annealing zone during the Middle Ordovician but the majority of the lower elevation samples did not pass through this same temperature until the Middle Devonian-Late Carboniferous. A more conservative time estimate of sample passage through the base of the annealing zone is represented Late Silurian-Early Triassic range of length-corrected ages. All samples show continuous cooling with little sign of reheating since their passage through the base of the annealing zone.

Most second order changes in cooling and heating rates observed in the preferred solutions are a function of the timestep size and the heating and cooling rates set by the modeller. By choosing a larger timestep size (from 25 Ma to 30 Ma) and decreasing the allowable rates of heating and cooling (from 30 °C/timestep to 10 °C/timestep) these effects may be completely eliminated to produce smoothed cooling only paths (Figure 4.2a; compare with Figures 4.2b,c). If second order features are still discernible in the T-t path of the samples after this smoothing they features are singled out as possible reheating events. Alternatively, the second order frequencies may be enhanced by decreasing the timestep size and increasing the allowable rates of heating and cooling (Figure 4.2c; compare with Figures 4.2a,b). One noteworthy second order feature is the sharp increase in cooling during the Devonian observed in the highest elevation samples (Figure 4.4a,b). Other samples do not seem to require this rapid cooling to fit the data. Several T-t histories show a reheating period during the Devonian-Carboniferous (400-

350 Ma, Figure 4.4i), Carboniferous-Permian (325-275, Figure 4.4ee) and Jurassic (200-150 Ma, Figures 4.4d,m) that were attenuated but not eliminated by changing parameters and may represent a geological event (Figures 4.4d,m).

4.3.2 Central Transect

Central Transect T-t history models are shown in Figures 4.4n-t. Model-corrected ages are found in Table 4.1. Geological evidence for Acadian orogenic effects constrains the formation of the first apatite fission track in the Central Transect to be post-Middle Devonian. Acadian deformation is characterized by westward thrusting and local mylonite zones accompanied by granitic intrusions (Devil's Room Pluton and Gull Lake Intrusive Suite) and a pervasive greenschist overprint of the eastern Long Range Inlier (Owen and Erdmer, 1986; Tuach, 1987a). Temperature-time histories are therefore constrained to be above 120 °C until 375 Ma (given the 25 Ma inverse model timestep this is the closest I can get to the end of the Acadian orogeny) represented by flattened T-t paths from 400-375 Ma in the Central Transect figures. There were no observable differences between geologically constrained and non-constrained models.

Central Transect T-t histories display cooling patterns ranging from about 0.15-0.24 °C/Ma. All T-t paths show dramatic increases in cooling rate over the last timestep but for reasons mentioned above these rate increases are not considered geologically meaningful. Most second order departures from Central Transect average cooling trends are also considered geologically meaningless for reasons given above. Model-corrected ages range from Late Devonian to Early Permian, therefore samples came through the base of the partial annealing zone over this time period. Length-corrected ages range from Middle Carboniferous to Late Permian and provide a more conservative estimate of passage through the base of the partial annealing zone. Predicted track length distributions and model ages fit the data fairly well. The typical highly negative skewness observed in the track length data is also predicted by the model fit. Model

ages fall within 1σ error of the measured age of the samples. Sample FT89-210 (Figure 4.4p) shows a reheating event over 175-150 Ma (Mid-Late Jurassic) that is not completely eliminated by changing model parameters; this may represent a geological event.

4.3.3 Northern Transect

Northern Transect T-t histories are shown in Figures 4.4v-x. Model-corrected ages are found in Table 4.1. Geological constraints over the time range represented by the Northern Transect apatite fission track T-t histories are not known so that models were run without any geological constraint.

Apatite fission track T-t paths in the Northern Transect have average cooling rates of 0.22-0.25 °C/Ma. Model ages predict the measured ages within the 1σ measured age error. At various intensities all three samples seem to show a reheating event over 150-125 Ma (Late Jurassic-Early Cretaceous) and at 50-25 Ma (Eocene-Miocene). A few other samples throughout the Great Northern Peninsula also display the latter reheating feature (Figures 4.4f,j,l,m,r,t,u,cc). The significance of the latter reheating feature is unknown. Since this is a late feature, the effect is caused by fitting the youngest track populations in the distribution and, if real, suggests that a component of long tracks in these samples is not as long as expected had there been no recent reheating.

The 270-264 Ma model-corrected age range means that these samples passed through the bottom of the partial annealing zone during the Middle Permian, somewhat later than similar elevation samples elsewhere in the Long Range Inlier. A younger estimate of passage through the base of the partial annealing zone is provided by the length-corrected ages (Late Triassic-Early Jurassic).

4.3.4 Deer Lake Basin and Miscellaneous Great Northern Peninsula

Remaining Great Northern Peninsula apatite fission track temperature histories are found in Figures 4.4u and 4.4y-ee. Where geological events are known they are used to constrain individual sample models.

Deer Lake Basin apatite fission track T-t histories (Figures 4.4z,aa) are constrained by the time of deposition of the analyzed samples. Both FT90-034 and -035 are fanglomerates shed from surrounding highlands into the Deer Lake Basin during Visean time (350-335 Ma)(Hyde, 1984). The dated pebbles and cobbles of FT90-034 are of Long Range Inlier affinity but the provenance of the FT90-035 fine-grained granite is not known. It may be related to Devonian intrusions in the White Bay region. Not much is known about the T-t history of the samples prior to their deposition except that they must have passed through ambient surface temperatures during their erosion and deposition. During the Early Carboniferous, the Deer Lake Basin lay near equatorial latitudes (Irving and Strong, 1984) under arid to semi-arid conditions (Hyde, 1984). Accordingly, Deer Lake Basin T-t histories are constrained to pass through the 40-20 °C temperature range during the Visean but are then allowed to heat up to temperatures greater than the base of the partial annealing zone ($> 120^{\circ}\text{C}$). Resulting T-t histories display cooling paths since the Late Carboniferous-Early Permian model-corrected ages. Therefore, any fission track temperature history recorded prior to deposition seems to have been completely wiped out by subsequent basin temperatures which reached their maximum sometime between the samples' Early Carboniferous stratigraphic age and their respective model-corrected ages. Average cooling rates range from 0.23-0.28 °C/Ma. Both predicted histogram fits are negatively skewed like the track length data, and the model ages predict the measured ages within the 1σ measured age error.

Temperature-time parameters, history styles and cooling rates for Long Range Inlier samples FT89-222 and -223 (Figures 4.4dd,ee) are similar to Southern Transect samples.

Humber Arm Allochthon sample FT89-235 (Figure 4.4bb) and Daniel's Harbour sample FT89-213 (Figure 4.4cc) from the western coastal platform have T-t histories based on 35 and 29 track lengths respectively. Both histories display the same increase in cooling rate at 25 Ma seen in other Great Northern Peninsula sample histories. To first order the FT89-235 T-t history agrees with similar elevation samples from the Long Range Inlier. A 275 Ma model corrected-age means it passed through the base of the annealing zone during the Middle Permian. FT89-213 shows a reheating maximum over 50-25 Ma; the accuracy of this history is in question, however, because of the lack of measured track lengths.

The Hare Bay Allochthon sample T-t history did not converge to a 0.50 confidence level solution (Figure 4.4y). Therefore, the preferred T-t path is the mean of the 0.95 set of histories. The predicted age is still within the 1σ error of the measured age. To first order its T-t path shows cooling since the Early Permian at a rate of about $0.23\text{ }^{\circ}\text{C}/\text{Ma}$. However, two reheating periods seem to be resolvable in the data. Reheating intervals to temperatures of $110\text{-}120\text{ }^{\circ}\text{C}$ during the Late Carboniferous-Early Permian (325-275 Ma) and ca. $90\text{ }^{\circ}\text{C}$ during the Late Triassic-Jurassic (225-150 Ma), follow periods of relatively quick cooling and are similar in timing to reheating in a number of other samples described above.

LGRA-01 from the Devil's Room Pluton has a distinct cooling history from all other analyzed samples (Figure 4.4u). The cooling rate over 209-175 Ma (Early-Mid Jurassic) is around $1.5\text{ }^{\circ}\text{C}/\text{Ma}$ but slows dramatically to an average rate of $0.08\text{ }^{\circ}\text{C}/\text{Ma}$ from 175-25 Ma (Mid Jurassic-Late Tertiary).

4.4 Discussion of Modelling Results

First order results from T-t inverse modelling of apatite fission track data from the Great Northern Peninsula show the dominance of a cooling trend in the T-t paths.

Average cooling rates range from 0.08 - 1.5 °C/Ma. This trend starts at different times in different transects. In the Southern Transect the highest elevation samples start their apatite fission track recorded slow cooling paths (below the base of the partial annealing zone) during the Middle Ordovician. However, the majority of lower elevation Southern Transect samples pass through the base of the partial annealing zone during the Middle Devonian-Late Carboniferous. Cooling rates range from 0.08-0.25 °C/Ma in the Southern Transect. Central Transect cooling below 120 °C begins during the Middle Devonian and all samples have passed through the base of the partial annealing zone by the Early Permian. Cooling rates are slightly lower ranging from 0.15-0.24 °C/Ma. Northern Transect samples do not record apatite fission track cooling until the Middle Permian. Cooling rates are higher ranging from 0.22-0.25 °C/Ma. Deer Lake Basin and Hare Bay Allochthon samples begin their cooling during the Late Carboniferous-Early Permian. Late Carboniferous-Early Permian model-corrected ages for the Deer Lake Basin are younger than sample stratigraphic age and therefore samples experienced temperatures in excess of 120 °C at sometime after the Early Carboniferous but before their respective model-corrected ages. Cooling rates are very similar to the Southern and Central Transect (0.23-0.28 °C) and the Hare Bay Allochthon has a cooling rate similar to the Northern Transect (0.23 °C/Ma). Humber Arm Allochthon (Lobster Cove) and western platform (Daniel's Harbour) samples begin their cooling during the Middle Permian and Early Jurassic respectively. The cooling rate in the Humber Arm Allochthon is similar to the Southern and Central Transects. The Daniel's Harbour sample has an average cooling rate (0.26 °C/Ma) that is compatible with cooling rates in the Southern and Central Transects. A distinct T-t history is recorded by the Devil's Room Pluton. The sample cooled quickly (1.5 °C/Ma) through high annealing temperatures (120-70 °C) during the Early Jurassic so short tracks which are a part of every other track length distribution in the Great Northern Peninsula, except lowest elevation western platform samples, were not formed in LGRA-01 (Figure 4.4u).

Most second order changes in cooling and heating rates superimposed on the main cooling trend are considered geologically inconclusive. Some histories show second

order effects which may be meaningful since the same effect is evident in a number of samples and/or is not completely eliminated by changing the model parameters. A number of samples in the Great Northern Peninsula show reheating during the Carboniferous-Permian (Figure 4.4i,q,y,ee). Figures 4.4c,d,m,p,u,w,x show T-t histories that contain a reheating feature, in varying intensities, during the Jurassic. This may be a fortuitous result from the fitting of track length data since not all the samples show this same feature, which could be expected if it were a regional characteristic. Highest elevation samples (Figures 4.4a,b) show a period of rapid cooling during the Devonian not seen in other samples. These same samples, along with other high elevation samples (Figures 4.4i,ee) also possess much older (Ordovician) model-corrected ages than other Great Northern Peninsula samples.

Chapter 5. Discussion of Results

5.1 Introduction

To first order, apatite fission track age and track length data as well as T-t cooling models can be interpreted in terms of an event of regional significance which affected much of the Great Northern Peninsula. There is no observable evidence for regional thermal perturbations (eg. mineralization, volcanism, plutonism, and metamorphism) that might have reset the apatites, at least at the time recorded by the apatite apparent ages in the study. This is supported by the data since track length distributions record a substantial degree of annealing in all samples and therefore could not be interpreted to reflect solely a thermal event of relatively short duration. Several alternatives remain, all of which involve erosion. Two end members are proposed as working hypotheses to explain the fission track data for the Great Northern Peninsula (Figure 5.1). Except for Models 2.A and B (Partial resetting, Table 5.1), models assume continuous cooling of the samples since their passage through the base of the annealing zone.

5.2 End-Member Hypotheses for Great Northern Peninsula Apatite Fission Track Data

5.2.1 Exhumation and Erosion of the Long Range Inlier

One explanation for the data from the Long Range Inlier is erosional unroofing of igneous and metamorphic rocks from the Long Range Inlier. This implies that the present Long Range Inlier surface was overlain entirely by igneous and metamorphic crystalline rocks. Depending on the paleo-geothermal gradient, 3-5 km of crystalline rocks could have been lost to erosion so that Long Range Inlier fission track ages date a crystalline surface exhumed since the Carboniferous (Figure 5.2a).



Figure 5.1

End-member cooling/exhumation models to explain apatite fission track data from the Great Northern Peninsula: 1. Long Range Basement Exhumation and Erosion: Exhumation and erosion of igneous and metamorphic crystalline basement from the Long Range Inlier 2. Burial, Exhumation and Erosion of Appalachian cover rocks: Taconian, Acadian and/or Alleghanian burial and subsequent erosional exhumation

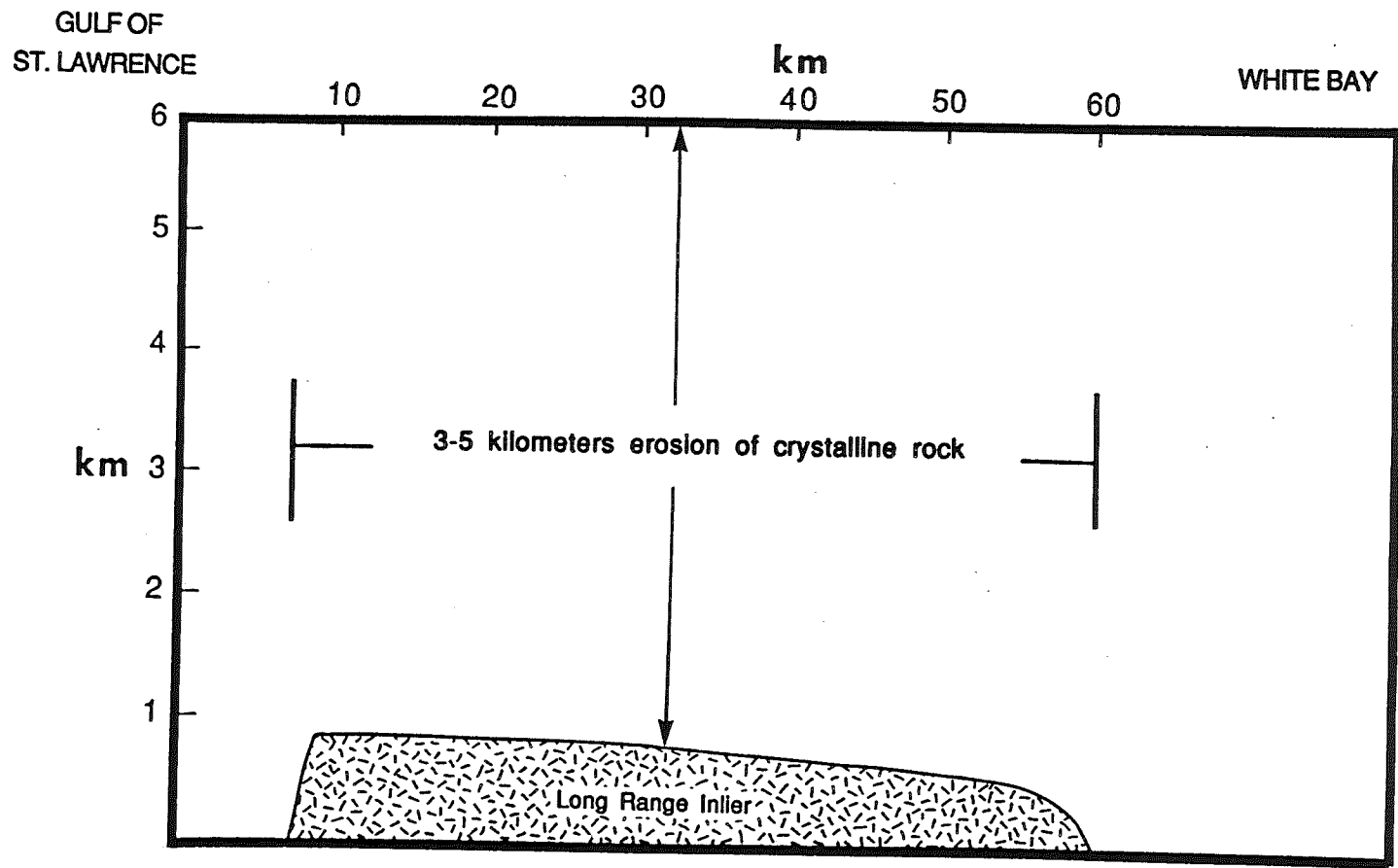


Figure 5.2a
 Cartoon schematic of the Long Range Inlier Basement Erosion model. Exhumation and erosion of 3-5 kilometers of crystalline Long Range Inlier can only explain samples that come from the Long Range Inlier

Unroofing of the Long Range Inlier would produce increasing ages with elevation as higher elevation samples pass through high annealing temperatures and effectively 'close' before lower elevation samples (Table 5.1a, model 1). Track length distributions would be negatively skewed and mean track lengths should be nearly constant or increase with age and standard deviation, depending on the exhumation rate (Table 5.1b, model 1). A large difference in ages ($\sim 10^8$ Ma), implying relatively slow exhumation, would show an increase in mean track length with age since older samples have had much more time to accumulate long tracks at low temperatures. In this case, standard deviations should also increase with mean length with the progressive addition of more long tracks with age. Inverse T-t models would show fairly constant cooling rates since the time the samples experienced temperatures of ~ 120 °C (Table 5.1c, model 1)

5.2.2 Burial, Exhumation and Erosion of Cover Rock

Another interpretation of the data involves emplacement and erosion of cover rocks over the Great Northern Peninsula at various stages during Appalachian orogenesis (Figure 5.2b). Taconian burial of a considerable portion of western Newfoundland is documented by the thin-skinned obduction of sediments and ophiolites of the Humber Arm, Southern White Bay and Hare Bay Allochthons. Acadian deformation is characterized by deeper basement thrusting and reworking of the Taconian Allochthons. If significant burial of western Newfoundland accompanied Acadian orogenesis it seems to be limited to the easternmost margin of the Great Northern Peninsula based on the difference in Appalachian metamorphism between the eastern and western part of the inlier. Carboniferous (Hercynian, Alleghanian) deformation and sedimentation in western Newfoundland is traditionally regarded to be limited to a narrow zone (< 50 km wide; Deer Lake and St. George Basins) associated with the Cabot Fault zone (Betz, 1943 Hyde, 1984). However, offshore zones of Carboniferous sediments widen considerably to the east and southwest of the Great Northern Peninsula.

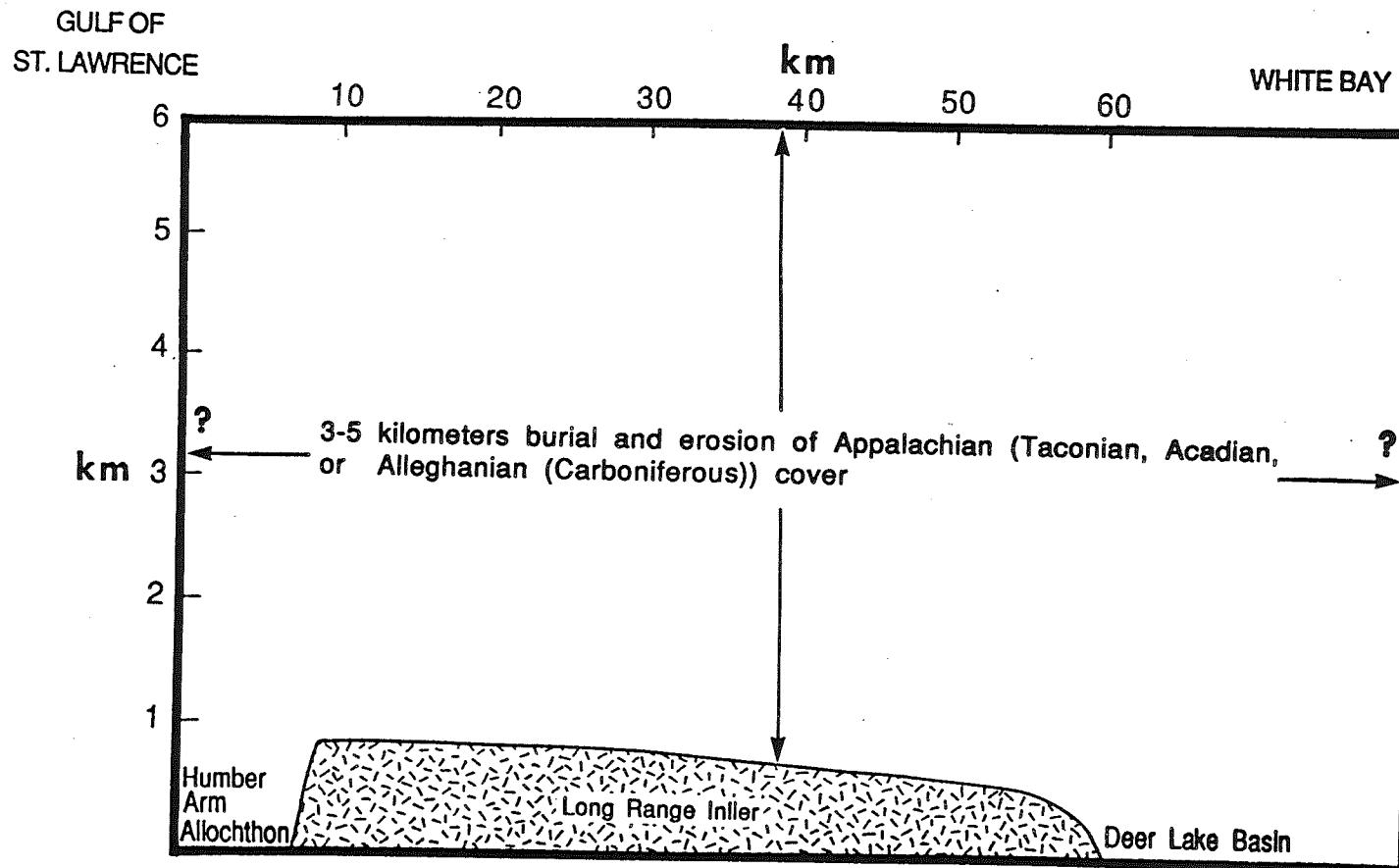


Figure 5.2b

Cartoon schematic of the Appalachian Burial, Exhumation and Erosion model. Great Northern Peninsula apatite fission track data could be explained by burial and subsequent denudation of 3-5 kilometers of Appalachian cover rock. Taconian Humber Arm Allochthon cover rocks immediately west of the Long Range and the Alleghanian (Carboniferous) Deer Lake Basin to the east indicate past burial of parts of the Great Northern Peninsula. Question marks denote unknown lateral extent of possible cover.

Table 5.1

Predicted data trends and characteristics in apatite fission track age vs. elevation, track length distribution shape, mean track length vs. apatite fission track age, standard deviation vs. mean track length and T-t inverse models for the proposed end-member models. Apatite fission track data from the Southern and Central Transects and the Great Northern Peninsula is shown for comparison.

<u>Model</u>	<u>Age vs. Elevation</u>	<u>Distribution Shape</u>
1. Exhumation and Erosion of Long Range Inlier Basement		
A. Relatively rapid exhumation	Age \propto Elevation	slight negative skewness
B. Relatively slow exhumation	Age \propto Elevation	negative skewness
2. Burial, Exhumation and Erosion of Appalachian Cover		
Complete Resetting	Age \propto Elevation	negative skewness
Partial Resetting		
A. Samples in lower half of 'partial annealing zone'	Age \propto Elevation	negative skewness: higher elevation samples more skewed; bimodal (?)
B. Samples in upper half of 'partial annealing zone'	Age \propto Elevation	negative skewness: lower elevation samples more skewed; bimodal (?)
3. Data		
Southern and Central Transects	Age \propto Elevation	negative skewness: low elevation -197,-198 and high elevation -225 less skewed
Great Northern Peninsula	Age \propto Elevation	general negative skewness low elevation -213, -235, LGRA-01 no skewness

Table 5.1a

Age vs. elevation and track length distribution shape for end-member models and apatite fission track data.

<u>Model</u>	<u>Age vs. Mn.Lgth.</u>	<u>Mn.Lgth. vs. Std.Dev.</u>
1. Exhumation and Erosion of Long Range Inlier Basement		
A. Relatively rapid exhumation	Mn.Lgth. = constant	Std.Dev. = constant
B. Relatively slow exhumation	Mn.Lgth. \propto Age	Std.Dev. \propto Mn.Lgth.
2. Burial, Exhumation and Erosion of Appalachian Cover		
Complete Resetting	Mn.Lgth. \propto Age	Std.Dev. \propto Mn.Lgth.
Partial Resetting		
A. Samples in lower half of 'partial annealing zone'	Mn.Lgth. \propto 1/Age	Std.Dev. \propto 1/Mn.Lgth.
B. Samples in upper half of 'partial annealing zone'	Mn.Lgth. \propto Age	Std.Dev. \propto 1/Mn.Lgth.
3. Data		
Southern and Central Transects	Mn.Lgth. \propto 1/Age	Std.Dev. \propto 1/Mn.Lgth.
Great Northern Peninsula	Mn.Lgth. \propto 1/Age	Std.Dev. \propto 1/Mn.Lgth.

Table 5.1b

Mean track length vs apatite fission track age and standard deviation vs. mean track length for end-member models and apatite fission track data.

<u>Model</u>	<u>T-t inverse models</u>
1. Exhumation and Erosion of Long Range Inlier Basement	
A. Relatively rapid exhumation	continuous, relatively rapid cooling since 120 C
B. Relatively slow exhumation	continuous, relatively slow cooling since 120 C
2. Burial, Exhumation and Erosion of Appalachian Cover	
Complete Resetting	continuous, relatively rapid or slow (depending on exhumation rate) cooling rates since 120 C
Partial Resetting	
A. Samples in lower half of 'partial annealing zone'	lower elevation samples continuous cooling; higher elevation samples may show period of reheating during burial; pre-burial ages may be preserved in model-corrected ages of high elevation samples
B. Samples in upper half of 'partial annealing zone'	lower elevation samples may show period of reheating during burial; model-corrected ages for all samples may preserve a pre-burial age, particularly highest elevations
3. Data	
Southern and Central Transects	first order continuous, slow cooling; highest elevation samples have much older model-corrected ages and show evidence of rapid cooling during the Devonian; second order evidence for Jurassic reheating to 70-90 C
Great Northern Peninsula	first order continuous, slow cooling in most samples; periods of rapid cooling in Northern Transect, Hare Bay, and Devil's Room Pluton; second order evidence for Jurassic reheating

Table 5.1c

T-t inverse model characteristics for end-member models and apatite fission track data.

Fission track data could take on two basic patterns depending on the depth of burial. If samples are buried deeply enough to completely reset the apatites then the resulting ages and track length distributions would mimic the simple crystalline basement unroofing scenario (Table 5.1a,b,c; model 2 Complete Resetting).

The thermal difference between burial and erosion of cover and basement unroofing hypotheses is the possibility of partial apatite resetting by burial. If burial is not deep enough to completely reset all the apatites, the fission track data would display a 'resetting gradient' over the sampled elevation interval such that lowest elevation samples, by virtue of their position, are more 'reset' than higher elevation samples. Ages would be expected to increase with elevation, not only because of their earlier closure, but also because higher elevation samples would preserve a greater component of their original age prior to partial resetting (Table 5.1a, model 2.A,B). The relationship between mean track length and fission track age would then be a function of the relative number of fission tracks in the resulting two track-length components (Figure 5.3). Most of the track length distributions would show a significant component of short tracks in their track length distributions (negatively skewed) but, depending on the depth of burial, mean track length could either increase or decrease with age. If burial was enough to completely reset, or nearly so, lowest elevation samples (Table 5.1b, model 2.A) then mean track length should generally decrease with age and elevation as more shortened tracks are preserved at lower temperatures in the lower 'partial annealing zone' (see Figure 5.3). If burial only partially reset the lowest elevation ages (say, halfway into the partial annealing zone, Table 5.1, model 2.B) then mean length might be expected to increase with age and elevation since in this case higher elevations would contain less shortened tracks (see upper 'partial annealing zone', Figure 5.3). Track length standard deviations would decrease with mean length in both cases, since the increase in mean length is the result of the preservation of progressively fewer short tracks. Similar arguments have been put forward by Green (1986). In model 2.B, T-t paths could be expected to show a greater portion of the original age in highest elevation samples and reheating of lower elevation samples during burial (Table 5.1c,

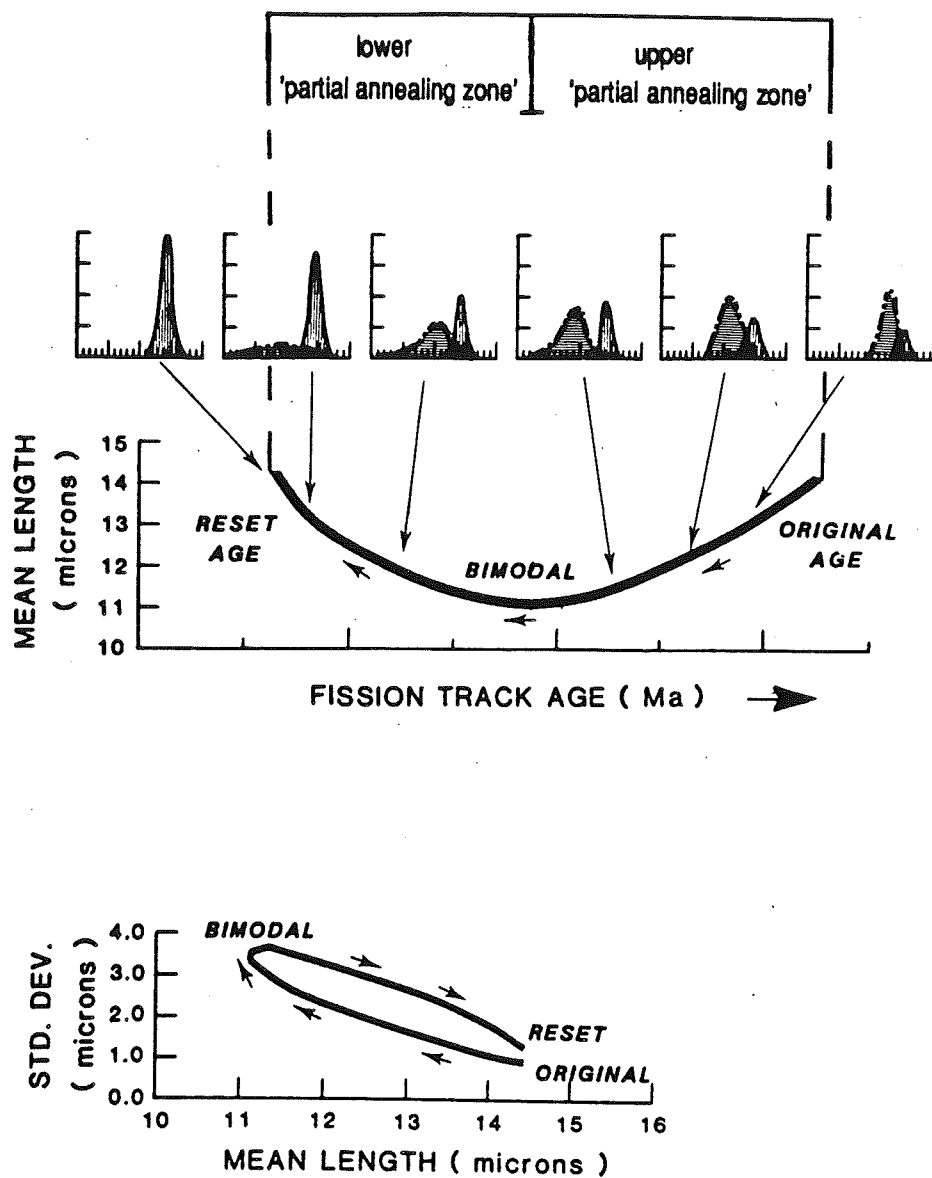


Figure 5.3

Expected trends between mean track length, apatite fission track age, and standard deviation for mixed ages where the data are characterized by two generations or components of fission tracks. The shorter track length distribution corresponds to tracks formed prior to reheating, which were shortened by elevated temperatures while the longer track length distribution reflects tracks produced after reheating. Note the difference in trend for mean track length with age depending on whether samples are reheated to lower temperatures (upper 'partial annealing zone') or higher temperatures (lower 'partial annealing zone'). The terms upper and lower 'partial annealing zone' are simply qualitative nomenclature used for gross distinction of patterns in this study. (from Green, 1986)

model 2.B). In model 2.A, T-t paths should show continuous cooling in the lowest elevation samples but a period of reheating and possibly original age preservation in higher elevation samples (Table 5.1c, model 2.B). Under restricted conditions partial resetting may cause track length distributions to be bimodal (Gleadow et al., 1986), particularly for resetting temperatures of short duration relative to the overall low temperature cooling history. The above hypotheses represent end-member cases, therefore any combination of them is also a potentially valid interpretation of the data. The discussion that follows seeks to limit the possible options and will be argued on data and geological grounds.

5.3 Hypothesis Constraints from Apatite Fission Track Data and Great Northern Peninsula Geology

5.3.1 Hypothesis Constraints from Apatite Fission Track Data: Comparison of Apatite Fission Track Data with Model Predictions

Apatite fission track data are grouped into two categories for simplified comparison with the data trends predicted by the hypothetical models. Combined data from the Southern and Central Transects represent areally restricted vertical sections and come from similar rock types and are, therefore, best suited for comparison with predicted results. The data will also be compared at a regional level for all of the Great Northern Peninsula.

All above hypotheses predict an increase in apatite apparent fission track age with elevation (Table 5.1a). In a uniform rock type a decrease in age with elevation is only possible if higher elevation samples were more 'reset' than lower elevation samples. Ages from the Southern and Central Transects increase with elevation (Figures 3.2, 3.3, 3.7) and together form a relatively low 8.3 ± 1.2 m/Ma slope, the apparent uplift rate for the southern Long Range Inlier. Apparent uplift rates have been interpreted as true

uplift rates assuming that (Parrish, 1983): 1. the critical isotherm ($\sim 100\text{ }^{\circ}\text{C}$) remained horizontal and uninfluenced by surface topography, or variable thermal conductivity. 2. the same isotherm remained at a constant depth with respect to the surface regardless of uplift rate. 3. uplift equalled erosion. Note that only in the crystalline basement unroofing (Model 1, table 5.1) and complete resetting burial (Model 2, Complete Resetting, table 5.1) scenarios could these assumptions be met. Only in these cases could the apparent uplift rate represent the true uplift rate over Middle Carboniferous-Early Jurassic time. On a regional scale, ages also generally increase with elevation (Figure 3.12), therefore consideration of age and elevation data does not discriminate between the hypotheses.

Since all of the proposed models include a significant component of erosion, track length distributions are expected to show shortened mean lengths and broader distributions relative to a volcanic-type distribution (mean length = 14-15 μm , standard deviation = 1-1.5 μm). Distributions should all display (more or less) negative skewness (Table 5.1). Southern and Central Transect distributions are all negatively skewed and considerably shortened and widened (mean lengths = 11.89-13.44, standard deviation = 1.55-2.58 μm) relative to volcanic-type distributions. Lowest elevation samples (< 100 m) tend to be less skewed than higher elevation samples (100-500 m a.s.l.) in these transects. FT89-198 (75 m a.s.l.) is normally distributed. Highest elevation samples (500-750 m a.s.l.) are also somewhat less skewed. Regionally, the samples are also generally negatively skewed, although low elevation western platform samples and the Devil's Room Pluton are either normally distributed (FT89-235, LGRA-01) or positively skewed (FT89-213). Since none of the distributions are clearly different (eg. bimodal vs. unimodal) except for the western platform and Devil's Room Pluton distributions, distinguishing between the different hypotheses is difficult to determine based solely on the shape of the track length distributions. Although most samples are negatively skewed, lowest elevation samples may be less negatively skewed or almost normally distributed suggesting support for the burial, exhumation and erosion model (Table 5.1a, model 2.A).

Hypothetical models predict either a constant, increasing or decreasing mean length with age (Table 5.1b) and therefore the relationship between mean length and age should clearly support or refute certain models. Both the lumped Southern and Central Transects data set and the data set as a whole show that mean length decreases with age (Figures 3.12). Slopes of the respective data sets are $-0.15 \pm 0.004 \mu\text{m}/\text{Ma}$ and $-0.009 \pm 0.002 \mu\text{m}/\text{Ma}$. The data clearly do not convey an increasing mean length with increasing age and therefore supports neither the rapid basement unroofing or complete resetting burial model. Only case A of the partial resetting burial hypothesis (Table 5.1b, model 2.A), where lowest elevation samples are completely reset, or nearly so, is supported by the data.

The hypothetical models also predict a variety of relationships between track length standard deviation and mean track length. The data from the Southern and Central Transects as well as from all of the Great Northern Peninsula show that track length standard deviation decreases with mean length (Figure 3.13). Slopes of the best fit line through the data are -1.21 ± 0.24 and -0.13 ± 0.009 respectively. The inverse relationship between mean length and standard deviation clearly does not support either the basement unroofing model or the complete resetting burial model (Table 5.1b, models 1, 2: Complete Resetting). Only the partial resetting burial (Table 5.1b, model 2.A) model is supported by the data.

All T-t models are expected to broadly agree with slow, continuous cooling since they all involve erosion of a significant thickness of rock. However, T-t paths could show a number of second order characteristics depending upon the hypothetical model. Although the significance of many of the second order characteristics of the inversely modelled T-t histories are not known, for the purpose of this discussion, second order features that occur in more than one sample will be considered to have some geological relevance. Another point of contention concerns corrected apatite fission track ages. Since the inverse models were not originally constrained by length-corrected ages, the model-corrected and not the length-corrected age (c.a.) will be considered to represent

the age of the oldest fission track population (solid line in Figures 4.1 a-ee). It must be stressed however, that T-t information obtained to the left of the length-corrected age (stippled line in Figures 4.1 a-ee) is based on the shortest tracks in the track length distribution which may not be well constrained in the model.

Temperature-time models from the Southern and Central Transects generally display slow, fairly continuous cooling compatible with exhumation and erosion of a considerable thickness of rock. Second order departures from continuous cooling are evident in a number of samples. Highest elevation samples FT89-225 and -226 show a period of relatively fast cooling during the Middle Devonian. Other T-t paths that go back to the Devonian do not show this same characteristic. The rapid cooling may be evidence for increased exhumation of this part of the Long Range Inlier. These same samples, along with other high elevation samples (-227, -223), have much older model-corrected ages (Ordovician) than lower elevation samples (Devonian-Triassic). They may be preserving an older, pre-burial or original age that the lower elevation samples are not, or only partially, preserving. Patterns of significant reheating are not evident in any of the samples. This may be expected since none of the samples have clearly bimodal distributions.

Regional T-t histories are not greatly different from the Southern and Central Transects. All are broadly compatible with relatively slow, continuous cooling except for the Daniel's Harbour (Figure 4.1 cc) and Devil's Room Pluton (Figure 4.1 u) samples. Some T-t histories, most notably the Devil's Room Pluton, show relatively rapid cooling at the beginning of their apatite recorded cooling. In the Devil's Room sample this rapid cooling through high annealing temperatures is required to give the distribution a narrow shape with almost no short tracks. In other cases (eg. FT89-233) rapid cooling through high temperatures is required to preserve a component of short tracks which have been shortened prior to rapid cooling. The mechanism for this fast cooling in the Devil's Room Pluton is difficult to ascertain; it may be cooling from original crystallization or perhaps fault movement resulting in more rapid

exhumation/erosion rates. A number of samples display a reheating period during the Middle Jurassic-Early Cretaceous (175-125 Ma) to temperatures of ~70-90 °C (FT89-201,-196,-198,-210, LGRA-01,-233,-232, FT90-050). Since samples are already at 60-70 °C at the time of reheating, the increased temperature could reflect a maximum burial of about 1 km, or an increase in the geothermal gradient, perhaps from Jurassic rifting further east. No observable evidence (eg. plutons, volcanism) exists for Jurassic rifting in the Great Northern Peninsula, nor is there evidence for lithospheric thinning beneath the region, although this has occurred under offshore basins (Haworth and Keen, 1979; Marillier, et al., 1989).

An important T-t feature concerns the stratigraphically youngest samples from the Deer Lake Basin. Model-corrected ages for both samples are several tens of Ma younger than their Early Carboniferous depositional age, therefore these samples apparently experienced complete resetting of their apatites soon after their deposition. The nature of their cooling paths (slow, continuous cooling) means that a substantial portion of the resetting must have been provided by burial of these samples.

First order inverse computer modelling results are broadly compatible with erosion of a significant thickness of rocks in the Great Northern Peninsula since the Late Paleozoic/Early Mesozoic. Thus, none of the hypotheses can be discounted on the basis of the inverse T-t modelling. Given the uncertainty in the relevance of the second order features it seems that the inverse modelling of individual samples may not be able to resolve subtle regional trends that the data alone may be able to detect.

5.3.2 Hypothesis Constraints from Geological Relationships in the Great Northern Peninsula

5.3.2.1 Southern and Central Transects

The youngest intrusive event in the Southern Transect is the Long Range Dyke Swarm that intrudes the cliffs on both sides of Western Brook Pond. Although not dated at this locality, the dykes are believed to be too old to have had any thermal effect on the apatite fission tracks in the rocks. Samples nearest the dykes have apatite fission track ages, track lengths, and T-t cooling paths comparable to other samples in the Southern Transect. The similarity suggests a regional signature which, based on the shape of the track length distributions and their relatively slow and continuous cooling models, indicates that erosional exhumation played a significant role in the cooling of these samples.

There is no geological constraint to discount the crystalline basement unroofing hypothesis as a model to explain Southern Transect data. However, western platform sample FT89-235, from about ten kilometers southeast of the Southern Transect, gives a similar age (FT89-235) to low elevation Southern Transect samples and can only be explained by the burial and erosion model (or perhaps some unknown hydrothermal event).

The presence of the Humber Arm Allochthon immediately to the west could mean that the Long Range was covered by Taconian thrust sheets, although they would not have been as thick in the northern Humber Arm Allochthon as further south (James and Stevens, 1986). The data from the Southern and Central Transects may represent denudation of the Taconian allochthons but it would mean that the area was still covered by 3-5 km (depending on the geothermal gradient) of Taconian allochthon after a lag time of more than 200 Ma since emplacement of the thin skinned thrust sheets. The highest presently observable Taconian ophiolite thrust slices reside in the Bay of Islands several

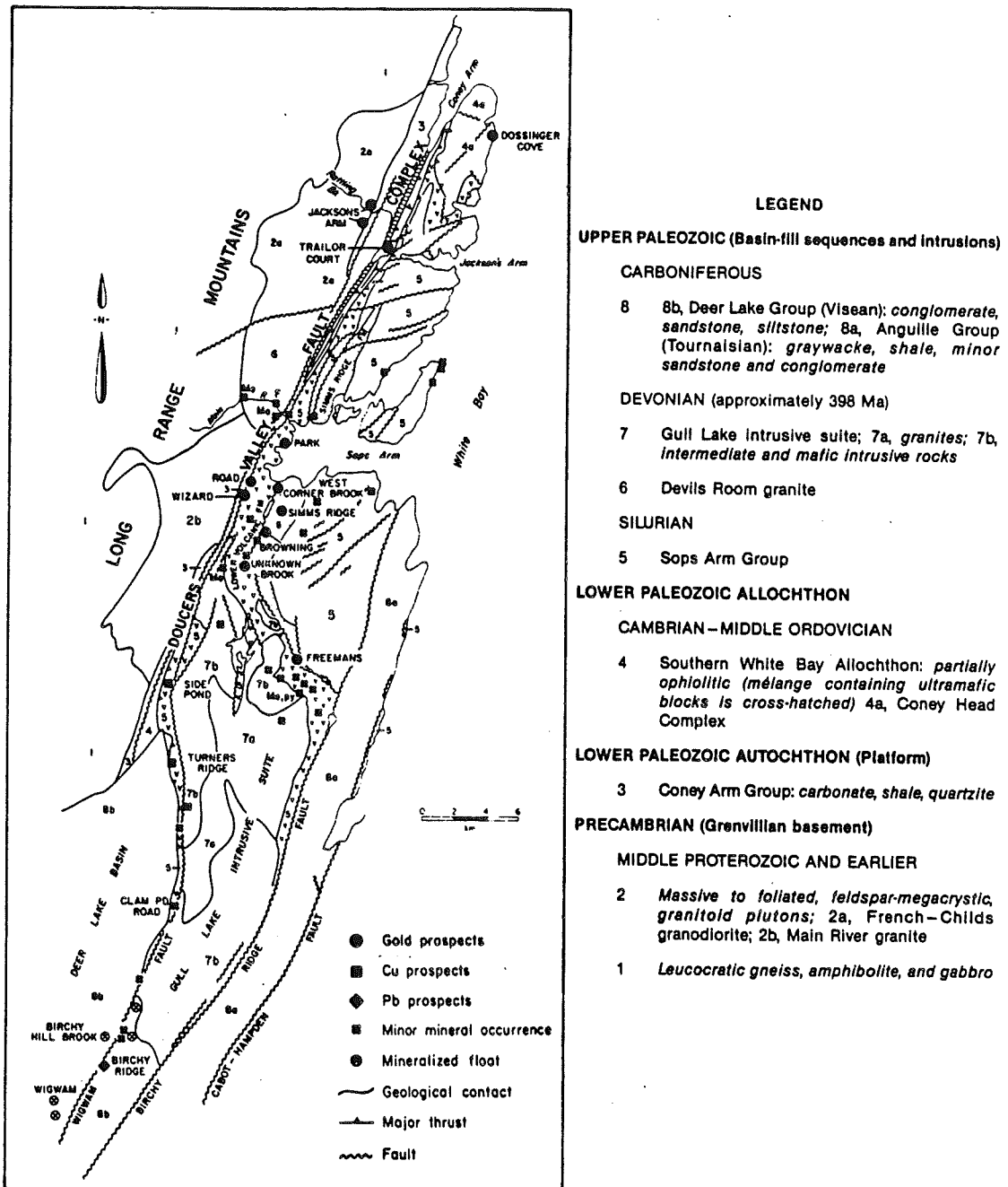


Figure 5.4
 General geology and mineral occurrences of the southeastern Great Northern Peninsula from the Deer Lake Basin to the Central Transect; from Smyth and Schillereff (1981, 1982), Erdmer (1986a,b) and Hyde (1982). (from Tuach, 1987)

tens of kilometers south of the Southern Transect, seemingly incompatible with the idea that a several kilometer thick section of Taconian rock has been removed by erosion. However, the Bay of Islands ophiolite slices are separated from the Southern Transect by a zone in which the top surface of the Grenville rocks dips abruptly SW to an unknown depth, and overlying cover successions all show southwest-plunging structures (Williams et al., 1984). Therefore, the Bay of Islands ophiolite slices are preserved in a structural depression in central west Newfoundland. Although the age of this structure is unknown, it may be an Acadian feature, in which case it would have controlled differential erosion of Taconian thrust sheets south and north of the structure (Waldron pers. comm., 1991). Removal of most, if not all, of the Taconian allochthon that may have covered the southern inlier was completed by Early Carboniferous time since the igneous clasts of the Early Carboniferous Deer Lake Basin indicate exposure of the Long Range to the west. It is, therefore, difficult to appeal to Taconian cover as an interpretation of the data from the southern part of the inlier.

Acadian (Devonian) or Alleghanian (Carboniferous) thermal effects on Southern Transect rocks are unknown, although any Acadian effects must have been significantly less than in the eastern Great Northern Peninsula because of the metamorphic overprint in the east (Owen and Erdmer, 1988). The Southern Transect data are, however, compatible with Acadian or Alleghanian burial and exhumation.

The Long Range Thrust last moved as a thrust during the Acadian Orogeny (410-360 Ma)(Cawood, 1989). Younger movement on the Long Range Fault has not been documented. Significant vertical movement has not taken place since ~200 Ma because similar elevation samples across the fault, FT89-198 and FT89-235, have approximately the same apatite fission track age.

The southeastern Long Range Inlier has been the site of extensive tectonism and associated thermal activity throughout the Paleozoic. The rocks were deformed during the Taconian orogeny and reheated during the Acadian orogeny to greenschist grade, and

during the Carboniferous they were variably subjected to mineralization, brecciation, and intrusion (Owen and Erdmer 1988, 1989; Tuach, 1987a,b). The Central Transect is north of the limit of Carboniferous mineralization but the Carboniferous Cabot Fault runs along its White Bay shoreline (Figure 1.3). The area was also involved in both the Taconian and Acadian orogenies. Central Transect apatite fission tracks were certainly reset during Taconian greenschist metamorphism and probably also during Acadian plutonism and/or burial. Thus, the first apatite fission track could not have been recorded in the Central Transect until after the Acadian orogeny (Mid to Late Devonian). The Central Transect post-Devonian apatite apparent and corrected ages are compatible with this geological constraint.

An unconformable contact between the Precambrian Long Range basement and Cambrian-Ordovician marine sediments in the southeastern Central Transect (Figure 3.6) means that the present basement surface in the Central Transect was near sea level and probably already partially developed during the Late Precambrian-Early Cambrian. It follows that unless there was a substantial elevation difference (3-5 km) between the Precambrian-Cambrian contact and the Long Range (where the samples are from) it is difficult to appeal to the basement erosion model as the sole explanation of the data.

Taconian thrust sheets, remnants of which now reside south and east of the Central Transect map area (Southern White Bay Allochthon, Figure 5.4), probably buried at least part of the Central Transect. Given the lag time of ~ 200 Ma for exhumation and erosion it is possible, but unlikely, that the data represent slow cooling since the Taconian Orogeny. This conclusion corresponds to the one for the Southern Transect.

Acadian thrusting and burial (?) occurred along parts of the eastern margin of the Long Range Inlier (Tuach, 1987b). The fission track data are compatible with slow cooling since the Late Devonian from an Acadian intrusive (Devil's Room Pluton ?) and/or burial overprint. The difference between Acadian orogenic effects in the Central and Southern Transects might be expected to manifest itself in the data. This is not the

case however, which suggests the data may be recording another event, perhaps in addition to early Appalachian burial or intrusion. Although there are no Late Paleozoic sediments in the area of the Central Transect the data do not rule out burial by Carboniferous cover, sediments or thrust sheets. Evidence for low-angle Carboniferous (?) thrusting may exist just south of the Central Transect map area (Owen, 1988).

5.3.4.2 Northern Transect

The Northern Transect data are generally consistent with relatively slow, continuous cooling/exhumation, but the ages suggest that cooling below apatite fission track 'closure' started tens of millions of years later than elsewhere in the Long Range Inlier.

Basaltic flows of the Lighthouse Cove Formation locally cap the northern Long Range Inlier and, in some cases unconformably overlie the Cambrian Bradore Formation which in turn unconformably overlies much of the northern inlier (Strong and Williams, 1972; Bostock, 1983). Dykes of the Long Range Swarm locally serve as feeders for the flows. One such dyke is located only meters away from sample FT89-221. The concordance of this sample's apatite fission track age with other Northern Transect samples shows that these dykes had no effect on the current apatite fission tracks. Younger intrusions have not been documented so that the relatively young ages cannot be explained by thermal reheating as a result of intrusion.

The Long Range basement erosion hypothesis is precluded, since Precambrian flows could not have had older Long Range crystalline basement covering them. The unconformable contact between Cambrian-Ordovician sediments and Precambrian basement at high elevations in the northern and western part of the Northern Transect supports this conclusion.

The flows introduce a possible corollary to the burial hypothesis, namely that the Northern Transect and perhaps other Long Range data could be explained by burial, exhumation and erosion of a thick pile of Precambrian volcanic flows. The similarity of the fission track data from stratigraphically younger rocks in other parts of the Great Northern Peninsula seems to preclude this possibility because the older flows could not possibly have covered samples from the Cambrian-Ordovician sediments nor the Deer Lake Basin.

The White Hills Peridotite (Hare Bay Allochthon) sample comes from the highest structural slice of the Taconian thrust sheets. The emplacement age of the alkaline rocks from this same locality is ~508 Ma (U-Pb zircon, Dunning pers. comm.). The rocks experienced granulite facies metamorphism at ~495 Ma (U-Pb zircon, Dunning pers. comm.) and cooled through $^{40}\text{Ar}/^{39}\text{Ar}$ hornblende closure temperatures between ~495-490 Ma (Reynolds, 1990 pers. comm.). Its Permian apatite fission track age (262 Ma) agrees with apatite ages in the southern Long Range Inlier (CT and ST) and if this is the original top of the allochthon it precludes Taconian cover as a viable erosional option. In fact, an unknown amount of thickness has been removed from the Hare Bay Allochthon by erosion. The present peridotite klippe may be a remnant of an original ocean floor section of five kilometers or more (based on analogy with the Bay of Islands and other ophiolites)(Waldron pers. comm., 1991). By extension, it is possible that the younger ages in the Northern Transect are the result of erosion of Taconian thrust sheets. Other possible interpretations include Acadian or younger cover rocks as erosional candidates.

5.3.2.3 Western Platform and Devil's Room Pluton

Western platform and Devil's Room Pluton samples come from the lowest elevations in the study. Their fission track ages are relatively young (Jurassic) and track length distributions are narrow, containing no tracks less than 8 μm , although one

distribution is probably incomplete (FT89-213). All that can be confidently deduced from FT89-213 is that it last experienced temperatures in excess of ca. 100 °C during the Jurassic. The young age may reflect: 1. A yet unknown and/or undated mineralization event in the Daniel's Harbour area (the timing of Pb-Zn mineralization in the area is not well constrained; Swinden et al., 1988; Lane, 1990). 2. A greater thickness and/or longer period of cover than other areas of the Great Northern Peninsula. 3. A chemical difference in the apatites relative to other samples studied allowing this sample to anneal differently. Although the FT89-235 distribution is based on only 31 tracks, its shape would suggest a more complete distribution than -213. Its continuous, slow T-t cooling path is not compatible with a sudden resetting event which would be expected from mineralizing fluids, and therefore suggests a pattern of burial and exhumation.

LGRA-01 has a reliable track length distribution which, except for FT89-235, is narrower than any other Great Northern Peninsula sample. The narrowness of the distribution (standard deviation = 1.37) indicates that this sample passed relatively quickly through the 'partial annealing zone' (70-125 °C) which is predicted by its T-t model. Such a cooling pattern is unlikely to be caused by slow exhumation, although its mean length (13.2 μm) suggests that it spent some time at the lower temperatures of the 'partial annealing zone'. Several interpretations could lead to the observed track length distribution and associated cooling pattern.

The fission track data may record cooling from the original crystallization of the pluton (390+27,-7 Ma, U/Pb zircon (closure \sim 750 °C), Erdmer, 1986). Cooling from original crystallization could produce the fast initial cooling in the sample and then the observed decrease in the cooling rate the sample reaches the equilibrium geothermal gradient temperatures of the surrounding country rock. Given the fast initial cooling of the pluton recorded by other dating methods (384 Ma biotite $^{40}\text{Ar}/^{39}\text{Ar}$ (closure \sim 300 °C), Reynolds, et al., 1988) it would mean that the first six million years (390-384 Ma) record approximately as much cooling (\sim 200-250 °C) as the subsequent 200 Ma (384-

177 Ma). One way to test this hypothesis is to obtain some ages from intermediate closure minerals to see if the apatite age does indeed reflect cooling from original crystallization of the Devil's Room Pluton.

A period of rapid exhumation may give rise to a narrow track length histogram and the observed fast initial cooling pattern in the Devil's Room Pluton. The fission track age would then indicate a time of rapid exhumation. Apatite fission track cooling histories in Great Northern Peninsula samples generally do not show a noticeable increase in cooling during this same time period (some show reheating over this time period) suggesting that if an increase in exhumation rate caused the fast cooling it must have been very localized. Sedimentologic evidence (eg. Jurassic conglomerates) for such an event does not exist (at least not anymore) since there are no known Jurassic rocks preserved anywhere in western Newfoundland.

Perhaps a more reasonable explanation of the data is that it records a mineralization event not yet recognized in the area or an event that has been recognized but not yet dated. In this case the Devil's Room pluton fission track age records the timing of this event. Mineralization is ubiquitous in the rocks flanking the southeastern Long Range Inlier (Figure 5.4). None of the constrained mineralization has the right age to explain the apatite age from the Devil's Room Pluton. The Devil's Room granite is generally fresh although fluorite, chlorite, and manganese commonly occur as coatings on joint surfaces. Locally fluorite is found with fine grained silica as the matrix in a 1 m wide tuffisite vein, and molybdenite occurs in several quartz veins that all intrude the pluton. The style of fluorite and molybdenite mineralization is indicative of high temperature devolatilization from progressive cooling of the associated magma (Tuach, 1987a). Traces of chalcopyrite and malachite may be also be found locally on joint surfaces (Tuach, 1987a). Jointing and tectonic brecciation increase eastward, presumably in response to Carboniferous (?) movement on the Doucers Valley fault that puts the granite in fault contact with marble of the Ordovician Coney Arm Group (Tuach, 1987a). Occurrences of gold, copper, and other base metals are found in rocks as young as Early

Carboniferous along the southeastern Long Range Inlier, and are abundant in a variety of host rocks from north of Deer Lake Basin to Great Coney Arm along the Doucers Valley Fault zone (Figure 5.4). The mineralization is generally attributed to activation of the fault zone and associated hydrothermal activity during the Appalachian orogenies. Timing of mineralization of ultramafic rocks and associated shear zones just north of the Devil's Room Pluton in the Doucers Valley Fault zone is not known but it may be related to Taconian ophiolite obduction (Tuach, 1987a). It is possible that a younger age for some of the mineralization has not yet been recognized in the Devil's Room Pluton area. Tournaisian rocks in the Deer Lake Basin south of the Devil's Room Pluton host copper (Hyde, 1982), therefore hydrothermal systems responsible for this mineralization must be Late Paleozoic or younger. Uranium mineralization in the Deer Lake Basin is thought to be Permian based on U/Pb ratios (Steed, 1979).

The above hypotheses for the Devil's Room Pluton sample do not exclude the possibility of burial and erosion by Acadian or younger cover, although its track length distribution requires either more rapid exhumation through the 'partial annealing zone' than other Great Northern Peninsula samples or a thermal resetting at 1-2 kilometers depth during the Jurassic.

5.3.2.4 Deer Lake Basin

Apatite fission track ages, track length distributions, and T-t cooling models from the Deer Lake Basin suggest slow, continuous cooling of the samples since Permian time, compatible with erosional exhumation. The ages are younger than the stratigraphic age of the samples therefore their fission track clocks were completely reset. The samples must have experienced temperatures in excess of 100 °C after their initial deposition, but prior to their apatite fission track age. The Deer Lake Basin reset ages cannot be explained by removal of Long Range crystalline basement since the Deer Lake Basin overlies it.

That the Deer Lake Basin experienced elevated temperatures since the Early Carboniferous is supported by vitrinite reflectance and other diagenetic data from various localities around the basin. Late Carboniferous (Westphalian A) Howley Formation surface coals in the eastern Deer Lake Basin have reported %R₀ (% vitrinite reflectance) values of .77-.79 (Hacquebard and Donaldson, 1970). Deer Lake Group R_{0max} (maximum vitrinite reflectance) values (Gall and Hiscott, 1986; Hyde et al., 1988) are similar, ranging from 0.58-1.07, suggesting reheating and burial of up to several kilometers in the Deer Lake Basin. Diagenetic clay mineral assemblages (Gall and Hiscott, 1986, Hyde et al., 1988) suggest reheating of the basin in post-Late Carboniferous time to at least 100 °C. The shape of the track length distributions and resulting cooling histories indicate that the resetting of the samples was not related to a heating pulse (eg. hot fluids), at least not exclusively, but rather a process that allows for heating and then slow cooling such as burial followed by exhumation. Maximum heating would have occurred prior to the model-corrected ages (Late Carboniferous-Early Permian) of the Deer Lake Basin samples. Depending on the paleogeothermal gradient, up to several kilometers of material may have been removed from at least the western part of the Deer Lake Basin.

The dated pebbles and cobbles (FT90-034) from the North Brook Formation are of Long Range Inlier affinity implying that the Long Range was shedding detritus from the west during the Early Carboniferous, perhaps in response to movement on the Long Range Fault or faults within the Deer Lake Basin. Any Taconian or Acadian thrust sheets that may have covered the area immediately west of the Deer Lake Basin must therefore have been completely eroded before the Carboniferous. Carboniferous or younger burial with or without other heat sources must have reset the ages prior to or around the time recorded by the apatite fission track ages (Late Permian-Early Triassic). One possibility is that Upper Carboniferous or younger sediments were deposited over and beyond (?) the present basin surface. Presently, there are no Upper(most) Carboniferous rocks (Westphalian B-Stephanian) in the Deer Lake Basin. Cover may also have been structurally emplaced. Carboniferous sediments in Newfoundland are

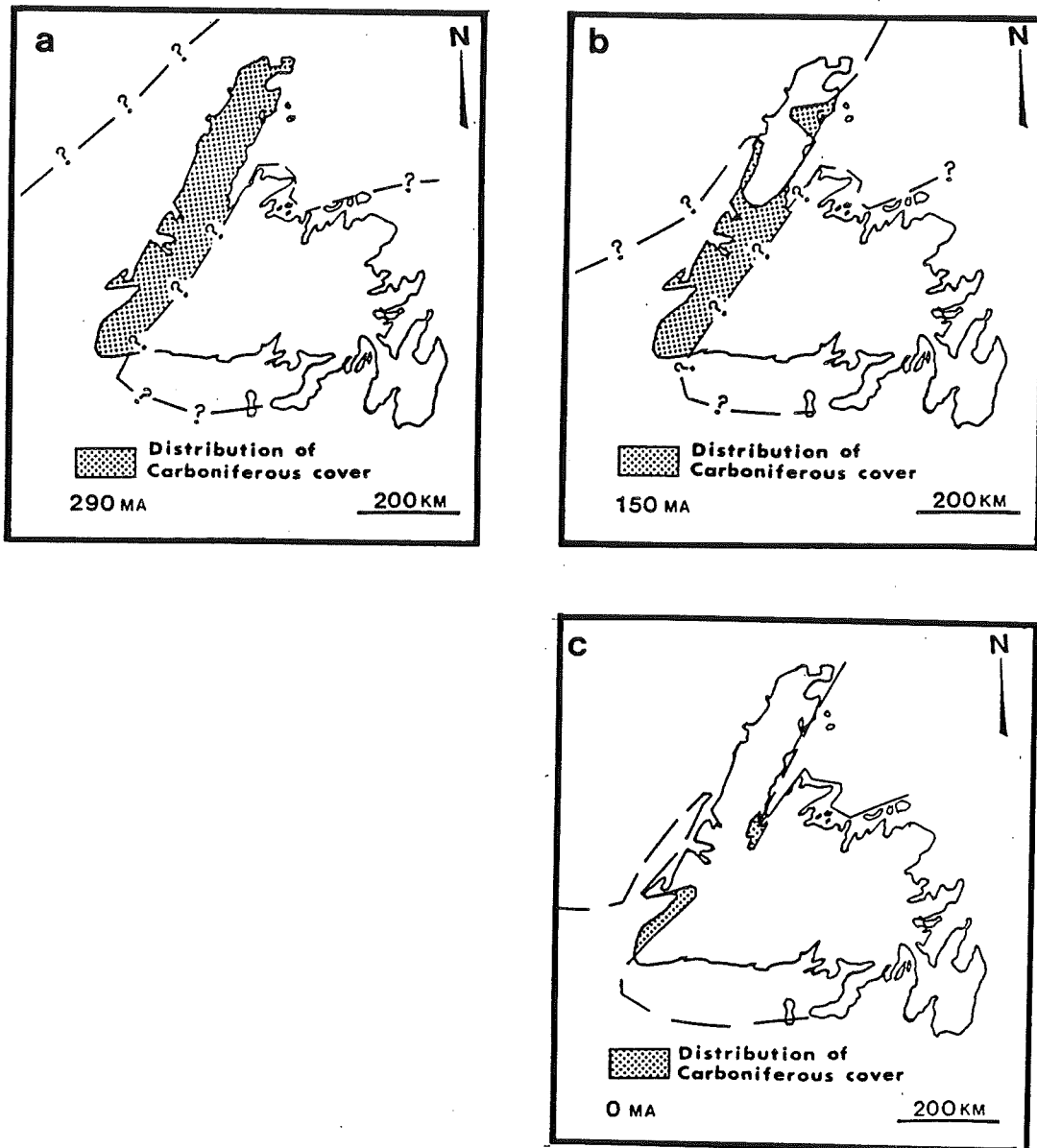


Figure 5.5

Cartoon schematic displaying possible distribution of Carboniferous cover at various times during the post-Appalachian history of the Great Northern Peninsula at a.) the end of the Carboniferous b.) the end of the Jurassic and c.) present. The interpretation is based on the Alleghenian (Carboniferous) cover erosion hypothesis for the apatite fission track data.

displaced by both high-angle and strike-slip faults, although most major movement on them is pre-Late Carboniferous (Knight, 1983; Hyde, 1988). In the southeastern Central Transect, low-angle west-directed Carboniferous (?) thrusts cut a mafic dyke that is comparable in trend to other dykes in the eastern Humber zone (Tuach, 1987b). Locally, Silurian limestone is thrust westward over Early Carboniferous conglomerate in the Deer Lake Basin (Dimmell, 1979), perhaps related to Late Carboniferous tectonics. Depending on the geothermal gradient, anywhere from 3-5 km of overburden may have buried and subsequently been eroded from the Deer Lake Basin. Comparable thicknesses may also have covered the Long Range Inlier and the samples from the Taconian allochthons.

The Deer Lake Basin data do not rule out a Mesozoic or Cenozoic reheating of the basin, by either burial or other heat sources, but this could not have reset the apatite fission track ages because the samples have Late Permian-Triassic ages.

5.4 Conclusion

Two end-member hypotheses have been proposed to explain the apatite fission track data from the Great Northern Peninsula. A comparison of the hypothesis-predicted data trends and the data supports a partial resetting burial, exhumation and erosion model. Inverse relationships between mean track length and age of a sample as well as track length distribution, standard deviation and mean track length support the partial burial model (Table 5.1, model 2.A), where samples are partially reset by temperatures in the lower part of the annealing zone. Except for highest elevation samples (FT89-226,-225), higher samples are somewhat more negatively skewed than lower elevation samples, suggesting further support for this model.

T-t paths generally display slow, continuous cooling since samples came through complete annealing temperatures, evidence for substantial erosion above the sampling

surface. Model-corrected ages for highest elevation samples (-225,-226,-227,-223) are much older than lower elevation samples and may preserve an original pre-burial age, compatible with a partial burial model. A number of T-t paths also indicate periods of rapid cooling/exhumation (-225,-226, Devil's Room Pluton). Some T-t paths show reheating to temperatures of 70-90 °C during the Jurassic. These effects are, however, secondary components of the model predictions and are not certain.

Geological relationships in the Great Northern Peninsula provide the best constraints with which to interpret the results. Detrital apatites from the Deer Lake Basin require complete resetting after Early Carboniferous deposition. Based on the track length histograms and T-t cooling histories these samples must have been buried by several kilometers of post-Early Carboniferous rocks prior to the end of the Permian period. Independent data support a significant amount of post-Early Carboniferous heating of the Deer Lake Basin. Given the regional similarity of the data, the simplest and perhaps most logical explanation of all the data is Late Paleozoic burial and subsequent cover erosion in the Great Northern Peninsula (Figure 5.5 a-c). Recent apatite fission track dating from other parts of the Appalachians also attest to considerable Carboniferous burial and ensuing exhumation in the offshore Maritimes Basin (Ryan, 1990), central Nova Scotia (Arne et al., 1990) and south-central New York state (Appalachian Basin, Johnson, 1985, 1986). In western Newfoundland, the apatite fission track results over an ~800 m vertical section may place constraints on the thickness of burial here since the data seem to be preserving a partial resetting of the apatite fission tracks. One possible interpretation is that higher elevation, older samples were less deeply buried and younger ages may represent deeper burial and/or later exhumation (Figure 5.5b). An important implication of this interpretation is that the positive age vs. elevation slopes are not true uplift rates but at least partially the result of a progressively decreased resetting of the samples with age and elevation. Although bimodal track length distributions might be expected in some of the samples in this case, it is not a necessary feature. From a purely qualitative point of view, some of the samples do contain enough short tracks to at least suggest a 'mixed' population of track

lengths rather than a single population formed from slow, continuous cooling.

With the possible exception of the Southern Transect data, the Long Range crystalline basement unroofing model is precluded for the Long Range data by the preservation of Precambrian-Cambrian unconformities around the inlier and Precambrian basalt flows in the northern part of the Long Range. Taconian burial and subsequent cover erosion is one possible interpretation of the data. The preservation of the highest presently observable structural slices of the allochthons both south and north of the Long Range are not valid arguments against this interpretation given the possibility of significant erosion of both of these allochthons. One argument against this interpretation, though clearly not definitive, is the similarity of the Permian apatite age from the Taconian Hare Bay Allochthon and other apatite ages from the Great Northern Peninsula, particularly the Deer Lake Basin. Slow exhumation of the present erosional surface from beneath Acadian cover could explain all the data except those from the Deer Lake Basin, and therefore remains a possibility. The Long Range provenance of the Deer Lake Basin clasts is important since it indicates that any pre-Carboniferous cover must have been completely removed from the southern inlier by the Early Carboniferous and therefore such cover could not explain the data from this area. In conclusion, the preferred explanation of the fission track data is that they represent burial by Carboniferous cover rocks and subsequent, fairly continuous cooling to the present. This is in accord with independent geological evidence.

Chapter 6. Concluding Remarks

The aim of this study was to use the low closure temperature method of apatite fission track thermochronology and recently developed inverse modelling techniques to establish low temperature thermal histories (less than 120 °C) for a number of specific areas within the Great Northern Peninsula of Newfoundland. This knowledge, together with geological relationships in the Great Northern Peninsula, was used to address several key questions regarding the geological development of the Great Northern Peninsula to limit the possible answers to the following questions. 1. To what extent and for how long was the Great Northern Peninsula buried beneath cover related to the main pulses (Taconian and Acadian) of the Appalachian Orogeny? 2. To what extent did the Alleghanian (Carboniferous and Permian) Appalachian Orogeny affect the rocks presently at the surface in the Great Northern Peninsula? 3. What role has erosion played in the post-Appalachian geological history of the Great Northern Peninsula? 4. When and for how long has the Long Range Inlier been exposed? 5. Have there been any low temperature thermal events (less than 120 °C) in the Great Northern Peninsula since Appalachian orogenesis?

Apatite fission track samples from the Great Northern Peninsula represent a variety of different tectonic and stratigraphic settings. Their apatite fission track ages rule out any temperatures in excess of ca. 100 °C since the Jurassic and therefore no low temperature thermal events are recorded in the samples since at least the Middle Mesozoic. Some of the apatite fission track ages were undoubtedly reset at various times during Appalachian orogenesis. Deer Lake Basin apatite fission track ages, which could not possibly have been reset during Taconian or Acadian tectonics, show a regional concordance with other apatite fission track ages and suggest that the data are the result of post-Acadian cooling. Lack of evidence for regional hydrothermal alteration or mineralization, intrusion or volcanism further indicates that the majority of the data represent exhumation of the Great Northern Peninsula since the Late Paleozoic-Early Mesozoic.

One interpretation is that the data reflect removal of Long Range Inlier basement since the Early Carboniferous. Although this may be a viable option locally (Southern Transect), preservation of the unconformable Long Range Inlier metamorphic basement/Cambrian-Ordovician sedimentary cover relationship at various places around the Long Range Inlier makes this unlikely, unless basement elevations over sampled Long Range Inlier areas were much greater than at the exposed contact with the sedimentary cover. Furthermore, unless there was substantial differential erosion lengthwise (north-south) along the inlier it is difficult to appeal to basement erosion as an option because Precambrian basalt flows still cap the inlier at its northern extent. Regional similarity of other non-Long Range Inlier apatite fission track data support this conclusion because basement could not possibly have covered these areas.

Another explanation of the data appeals to overburden other than crystalline basement which may have been stripped from the Great Northern Peninsula. The data may be reflecting exhumation of the samples from under Taconian and/or Acadian thrust cover. Denudation of Taconian cover could explain the data from the Long Range Inlier (Central and Northern Transects), but given the inlier provenance of the Carboniferous Deer Lake Basin clasts, any Taconian cover, at least in southern Long Range Inlier, must have been completely removed by the Early Carboniferous. Since all of the southern inlier fission track ages are younger than the Early Carboniferous it is difficult to appeal to Taconian cover as an interpretation of the southern inlier data. Assuming that the similarity of the data from the whole of the Great Northern Peninsula is not fortuitous but has regional implications, synthesis of fission track data from the Hare Bay Allochthon and geological relationships from other areas of the Great Northern Peninsula with this explanation is not possible.

The data are generally compatible with denudation of Acadian cover. However, the major thermal effects of the Acadian Orogeny are limited to the eastern margin of the Great Northern Peninsula. If these thermal effects resulted from burial beneath Acadian cover then there must have been a substantial difference in burial across the

width of the inlier and in the resetting and subsequent cooling of their respective apatite fission tracks. The similarity of the data between the Central and Southern Transects and across the east-west width of the Northern Transect makes erosion of Acadian cover as an interpretation of all the data an unlikely option although it can not be excluded as a possibility.

Permian/Triassic ages and track length distributions from the Carboniferous Deer Lake Basin can only be explained by cover, with or without other heat sources, that is younger than the stratigraphic age of the sampled formation.

Late Devonian sedimentary rocks (Kennels Brook Formation) may have covered large areas of Cambrian-Ordovician platform rocks in southwestern Newfoundland. Given the offshore extent of Newfoundland Carboniferous rocks, Early Carboniferous rocks originally seem to have been part of a much larger Carboniferous basin than the Early Carboniferous remnants that are now exposed. Apatite fission track ages from Middle-Upper Carboniferous sediments throughout the Maritimes Basin suggest a regional thermal signature that might be related to basin wide erosion of several kilometers of cover rocks since the Late Carboniferous/Early Permian (Ryan, 1990). Such a thickness of cover would almost certainly have buried substantial areas of Newfoundland if there has been no subsequent relative vertical adjustment.

Apatite fission track data from the whole of the Great Northern Peninsula are also compatible with erosion of several kilometers of Late Carboniferous-Early Permian rock from above the present surface. Preservation of Precambrian basalt flows in the Northern Transect, of contact relationships between Precambrian basement and Cambrian-Ordovician sediments around the Long Range Inlier (some at high elevations) and of highest structural slices of the Taconian Humber Arm and Hare Bay Allochthons in the Great Northern Peninsula support such a conclusion. Although highest elevation samples from the Long Range Inlier seem to have been below temperatures of ca. 120 °C since perhaps as early as the Ordovician, their higher elevation may have allowed

them to escape resetting during burial and therefore preserve an older, pre-burial age. Partial resetting burial of the Long Range is the most likely model based relationships between apatite fission track age, mean track length, and track length standard deviation. Following from this interpretation, the younger Northern Transect and Daniel's Harbour ages may reflect later exhumation of these parts of the Great Northern Peninsula from beneath Late Paleozoic cover.

Apatite fission track data from Daniel's Harbour and Devil's Room Pluton are different from the rest of the data although they are compatible with the burial and cover erosion interpretation. Without a complete track length distribution from the Daniel's Harbour sample, interpretation of its young age is highly dubious. The Devil's Room Pluton sample may have experienced resetting during the Jurassic that had only a minor effect on, or was not felt at all by other Great Northern Peninsula samples. Minor reheating during the Jurassic is shown in some of the T-t paths of the other samples and may be a related (?) feature. Given the abundance of mineralization along the southeastern flank of the Long Range Inlier another possible cause of this young age and unique cooling pattern is a mineralization event which has not yet been recognized or has been recognized but not yet dated.

A generalized geological development history of the Great Northern Peninsula based on the preferred interpretation of the data follows. Since the Long Range Inlier surface has unconformable contacts with Cambrian-Ordovician sediments and is locally overlain by Latest Precambrian basalt flows, this surface was at least partially developed by the Early Paleozoic. Subsequent Taconian orogenesis resulted in burial of much of western Newfoundland, although the extent and thickness of this burial cannot be determined from the present study. If Ordovician model-corrected ages in the southern Long Range are accurate they suggest that Acadian burial and thermal effects, at least in the western Long Range, were relatively minor (less than ~ 120 °C). If this is the case, then much of the erosional development of the present Long Range Inlier surface may have happened prior to and during the Carboniferous. The apatite fission track data

suggest that much of the Great Northern Peninsula was then again buried beneath cover, but this time of Carboniferous-Permian age. Burial may have been enough to completely reset lowest elevation samples but higher elevation samples seem to have escaped with only partial resetting. Subsequent exhumation and erosion uncovered the Long Range Inlier surface before the surrounding lowlands, perhaps during the Mesozoic. Based on the model T-t histories of some samples an episode of reheating may have affected parts of the Great Northern Peninsula during the Jurassic.

Appendix 1: Data for Zeta Determinations

SAMPLE LOCATION (OR STD)...RENFREW, STANDARD
 DATE OF ANALYSIS.....12/8/89
 LAB IDENTIFICATION CODE....RN
 IRRADIATION CODE.....MM034-9
 DISKSD(ALIGN/CALCS/DIST)...A:/A:/A:
 DATAFILE.....RNO9M034.A1Z
 MINERAL ANALYZED.....APATITE
 ANALYSIS BY/NOTES PAGE #...MH/

INDIVIDUAL GRAIN DATA

CRYSTAL	NS	NI	QUADS	RATIO	RHO S	RHO I	EUI ppm	AGE (Ma)
1	49	48	9	1.021	3.48E+06	3.41E+06	36	214.2 q 44.8
2	46	39	9	1.179	3.27E+06	2.77E+06	29	246.8 q 55.2
3	52	56	9	0.929	3.70E+06	3.98E+06	42	195.1 q 38.9
4	38	53	9	0.717	2.70E+06	3.77E+06	39	151.2 q 33.0
5	55	60	9	0.917	3.91E+06	4.27E+06	45	122.6 q 37.3
6	35	47	9	0.745	2.49E+06	3.34E+06	35	156.9 q 35.9
7	50	41	9	1.042	3.55E+06	3.41E+06	36	218.5 q 45.5
8	45	41	9	1.098	3.20E+06	2.91E+06	30	230.0 q 51.0
9	25	31	9	0.806	1.78E+06	2.20E+06	33	169.8 q 46.4
10	47	45	9	1.044	3.34E+06	3.20E+06	33	219.0 q 47.0
11	48	49	9	0.980	3.41E+06	3.48E+06	37	205.6 q 43.1
12	34	52	9	0.654	2.42E+06	3.70E+06	36	138.0 q 31.2
13	41	38	9	1.079	2.91E+06	2.70E+06	39	226.1 q 52.2
14	49	45	9	1.089	3.48E+06	4.20E+06	28	228.2 q 48.5
15	47	33	9	1.424	3.34E+06	4.5E+06	33	296.9 q 69.1
16	34	45	9	0.756	2.42E+06	4.5E+06	24	159.2 q 37.1
17	50	48	9	1.042	3.55E+06	3.41E+06	33	218.5 q 45.5
18	45	51	9	0.882	3.20E+06	3.63E+06	36	185.5 q 39.1
19	45	50	9	0.900	3.20E+06	3.55E+06	38	189.2 q 40.0
20	45	52	9	0.865	3.20E+06	3.70E+06	37	182.0 q 38.2
21	48	55	9	0.873	3.41E+06	3.91E+06	39	183.5 q 37.4
22	39	52	9	0.750	2.77E+06	3.70E+06	39	158.0 q 34.4
23	48	51	9	0.941	3.41E+06	3.63E+06	39	197.7 q 41.0
24	44	52	9	0.846	3.13E+06	3.70E+06	38	178.0 q 37.6
	1059	1141			3.14E+06	3.38E+06	35	

SUMMARY OF STATISTICS

~ Variance of Square root of NS = 0.2997
 ~ Variance of Square root of NI = 0.2799
 ~ Correlation coefficient (R for NS vs. NI) = 0.4114
 ~ Chi² = 15.37725 with 23 degrees of freedom. TEST PASS
 ~ Probability of greater value = .880605

AGE CALCULATION

~ Zeta factor used = 142.4 q 6.7 POOLED AGE =
 ~ Glass dosimeter = CN1
 ~ ND counted = 2599 195 q 13.0 Ma
 ~ RHOD D for glass = 2.995E+06 q 0.587E+05
 ~ Area of 1 QUAD = 1.563E-06
 ~ Pooled NS/NI = 0.928 q 0.040 MEAN AGE =
 ~ Mean NS/NI = 0.941 q 0.036 198 q 12.6 Ma

SAMPLE LOCATION (OR STD)...DURANGO, STANDARD
 DATE OF ANALYSIS.....12/07/89
 LAB IDENTIFICATION CODE....DR
 IRRADIATION CODE.....MMO34-18
 DISKSD(ALIGN/CALCS/DIST)...A/A/A
 DATAFILE.....DR18MO34.A1Z
 MINERAL ANALYZED.....APATITE
 ANALYSIS BY/NOTES PAGE #...MH/

INDIVIDUAL GRAIN DATA

CRYSTAL	NS	NI	QUADS	RATIO	RHO S	RHO I	[U] ppm	AGE (Ma)
1	8	30	25	0.267	2.05E+05	7.68E+05	8	37.7 q 15.4
2	8	42	25	0.190	2.05E+05	1.07E+06	11	26.9 q 10.7
3	8	34	25	0.235	2.05E+05	8.70E+05	9	33.3 q 13.4
4	6	39	25	0.154	1.54E+05	9.98E+05	10	21.8 q 9.8
5	6	37	25	0.182	1.54E+05	9.47E+05	10	22.9 q 10.3
6	4	42	25	0.095	1.02E+05	1.07E+06	11	13.5 q 7.2
7	11	45	25	0.244	2.82E+05	1.15E+06	12	34.6 q 12.1
8	8	28	25	0.286	2.05E+05	7.17E+05	7	40.4 q 16.6
9	8	37	25	0.216	2.05E+05	9.47E+05	10	30.6 q 12.3
10	14	46	25	0.304	3.58E+05	1.18E+06	12	43.0 q 13.7
11	8	31	25	0.258	2.05E+05	7.93E+05	8	36.5 q 14.9
12	6	25	25	0.240	1.54E+05	6.40E+05	7	33.9 q 15.7
13	11	43	25	0.256	2.82E+05	1.10E+06	11	36.2 q 12.7
14	7	30	25	0.233	1.79E+05	7.68E+05	8	33.0 q 14.2
15	7	39	25	0.179	1.79E+05	9.98E+05	10	25.4 q 10.7
16	14	56	25	0.250	3.58E+05	1.43E+06	15	35.3 q 11.1
17	7	37	25	0.189	1.79E+05	9.47E+05	10	26.8 q 11.3
18	8	28	25	0.286	2.05E+05	7.17E+05	7	40.4 q 16.6
19	8	38	25	0.211	2.05E+05	9.72E+05	10	29.8 q 11.9
	157	707			2.11E+05	9.52E+05	10	

SUMMARY OF STATISTICS

~ Variance of Square root of NS = 0.1865
 ~ Variance of Square root of NI = 0.3848
 ~ Correlation coefficient (R for NS vs. NI) = 0.6038
 ~ Chi² = 7.309125 with 18 degrees of freedom. TEST PASS
 ~ Probability of greater value = .9872502

AGE CALCULATION

~ Zeta factor used = 94.7 q 8.6 POOLED AGE =
 ~ Glass dosimeter = CN1
 ~ ND counted = 2599 31.4 q 4.0 Ma
 ~ RHOD D for glass = 2.995E+06 q 0.587E+05
 ~ Area of 1 QUAD = 1.563E-06
 ~ Pooled NS/NI = 0.222 q 0.020 MEAN AGE =
 ~ Mean NS/NI = 0.224 q 0.012 31.7 q 3.4 Ma

SAMPLE LOCATION (OR STD)...FISH CANYON TUFF, STANDARD
 DATE OF ANALYSIS.....11/12/89
 LAB IDENTIFICATION CODE....MM033-12
 IRRADIATION CODE.....MM033-12
 DISKSD(ALIGN/CALCS/DIST)...A:/A:/A:
 DATAFILE.....FC12M033.A1Z
 MINERAL ANALYZED.....AFATITE
 ANALYSIS BY/NOTES PAGE #...MH/A:

INDIVIDUAL GRAIN DATA

CRYSTAL	NS	NI	QUADS	RATIO	RHO S	RHO I	[U] ppm	AGE (Ma)
1	3	38	25	0.079	7.68E+04	9.72E+05	10	12.7 q 7.7
2	8	48	25	0.167	2.05E+05	1.23E+06	13	26.7 q 10.5
3	9	53	25	0.170	2.30E+05	1.36E+06	14	27.2 q 10.1
4	7	17	9	0.412	4.98E+05	1.21E+06	13	65.6 q 30.1
5	4	18	9	0.222	2.84E+05	1.28E+06	13	35.6 q 19.9
6	7	43	25	0.163	1.79E+05	1.10E+06	12	26.1 q 10.9
7	6	39	25	0.154	1.54E+05	9.98E+05	10	24.7 q 11.0
8	6	45	25	0.133	1.54E+05	1.15E+06	12	21.4 q 9.5
9	6	42	25	0.143	1.54E+05	1.07E+06	11	22.9 q 10.2
10	8	46	25	0.174	2.05E+05	1.18E+06	12	27.9 q 11.0
11	8	34	25	0.235	2.05E+05	8.70E+05	9	37.7 q 15.2
12	6	38	25	0.158	1.54E+05	9.72E+05	10	25.3 q 11.3
13	9	49	25	0.184	2.30E+05	1.25E+06	13	29.4 q 11.0
14	5	45	25	0.111	1.28E+05	1.15E+06	12	17.8 q 8.5
15	9	45	25	0.200	2.30E+05	1.43E+06	12	32.0 q 12.0
16	13	56	25	0.232	2.33E+05	1.43E+06	15	37.2 q 11.9
17	8	38	25	0.211	2.05E+05	9.72E+05	10	33.7 q 13.5
18	5	26	25	0.192	1.28E+05	6.65E+05	7	30.8 q 15.3
19	7	31	25	0.226	1.79E+05	7.93E+05	8	36.2 q 15.5
20	5	50	25	0.100	1.28E+05	1.28E+06	13	16.0 q 7.7
21	7	44	25	0.159	1.79E+05	1.13E+06	12	25.5 q 10.6
22	8	26	25	0.308	2.05E+05	6.65E+05	7	49.2 q 20.4
23	7	34	25	0.206	1.79E+05	8.70E+05	9	33.0 q 14.0
24	5	52	25	0.096	1.28E+05	1.33E+06	14	15.4 q 7.3
	166	957			1.87E+05	1.08E+06	11	

SUMMARY OF STATISTICS

- ~ Variance of Square root of NS = 0.1520
- ~ Variance of Square root of NI = 0.8022
- ~ Correlation coefficient (R for NS vs. NI) = 0.3738
- ~ Chi² = 15.30096 with 23 degrees of freedom. TEST PASS
- ~ Probability of greater value = .8835235

AGE CALCULATION

- ~ Zeta factor used = 107.6 q 9.3
 - ~ Glass dosimeter = CN1
 - ~ ND counted = 2900
 - ~ RHOD D for glass = 2.985E+06 q 0.554E+05
 - ~ Area of 1 QUAD = 1.563E-06
 - ~ Pooled NS/NI = 0.173 q 0.015
 - ~ Mean NS/NI = 0.185 q 0.015
- POOLED AGE =**
 27.8 q 3.4 Ma
MEAN AGE =
 29.6 q 3.5 Ma

SAMPLE LOCATION (OR STD)...DURANGO, STANDARD
 DATE OF ANALYSIS.....11/07/89
 LAB IDENTIFICATION CODE...MM033-16
 IRRADIATION CODE.....MM033-16
 DISKSD(ALIGN/CALCS/DIST)...A:/A:/A:
 DATAFILE.....DR16M033.A1Z
 MINERAL ANALYZED.....APATITE
 ANALYSIS BY/NOTES PAGE #...MH/

INDIVIDUAL GRAIN DATA

CRYSTAL	NS	NI	QUADS	RATIO	RHO S	RHO I	[U] ppm	AGE (Ma)	
1	6	33	25	0.182	1.54E+05	8.45E+05	9	30.1 q 13.6	
2	7	31	25	0.226	1.79E+05	7.93E+05	8	37.1 q 16.0	
3	7	38	25	0.184	1.79E+05	9.72E+05	10	30.5 q 12.8	
4	8	28	25	0.286	2.05E+05	7.17E+05	8	47.2 q 19.4	
5	8	39	25	0.231	2.30E+05	9.98E+05	10	38.2 q 14.5	
6	4	35	25	0.114	1.02E+05	8.96E+05	9	18.9 q 10.1	
7	7	36	25	0.194	1.79E+05	9.21E+05	10	32.2 q 13.6	
8	8	42	25	0.190	2.05E+05	1.07E+06	11	31.5 q 12.5	
9	5	30	25	0.167	1.28E+05	7.68E+05	8	27.6 q 13.6	
10	7	43	25	0.163	1.79E+05	1.10E+06	12	26.9 q 11.3	
11	10	45	25	0.222	2.56E+05	1.15E+06	12	36.8 q 13.3	
12	9	51	25	0.176	2.30E+05	1.31E+06	14	29.2 q 10.9	
13	8	45	25	0.178	2.05E+05	1.15E+06	12	29.4 q 11.6	
14	9	59	25	0.153	2.30E+05	1.51E+06	16	25.3 q 9.3	
15	5	26	25	0.192	1.28E+05	6.65E+05	7	31.8 q 15.8	
16	10	37	25	0.270	2.56E+05	9.47E+05	10	44.7 q 16.4	
17	4	33	25	0.121	1.02E+05	8.45E+05	9	20.1 q 10.8	
18	5	31	25	0.161	1.28E+05	7.93E+05	8	26.7 q 13.1	
19	7	37	25	0.189	1.79E+05	9.47E+05	10	31.3 q 13.2	
20	8	36	25	0.222	2.05E+05	9.21E+05	10	36.8 q 14.8	
21	9	46	25	0.196	2.30E+05	1.18E+06	12	32.4 q 12.2	
				152	801	1.85E+05	9.76E+05	10	

SUMMARY OF STATISTICS

~ Variance of Square root of NS = 0.1267
 ~ Variance of Square root of NI = 0.4022
 ~ Correlation coefficient (R for NS vs. NI) = 0.6268
 ~ Chi² = 5.34216 with 20 degrees of freedom. TEST PASS
 ~ Probability of greater value = .9995381

AGE CALCULATION

~ Zeta factor used = 111.1 q 10.0 POOLED AGE =
 ~ Glass dosimeter = CN1
 ~ ND counted = 2900 31.4 q 4.0 Ma
 ~ RHOD D for glass = 2.985E+06 q 0.554E+05
 ~ Area of 1 QUAD = 1.563E-06
 ~ Pooled NS/NI = 0.190 q 0.017 MEAN AGE =
 ~ Mean NS/NI = 0.191 q 0.009 31.7 q 3.3 Ma

SAMPLE LOCATION (OR STD)...FISH CANYON TUFF, STANDARD
 DATE OF ANALYSIS.....11/11/89
 LAB IDENTIFICATION CODE....FC
 IRRADIATION CODE.....MM034-2
 DISKSD(ALIGN/CALCS/DIST)...A/A/A
 DATAFILE.....FC02M034.A1Z
 MINERAL ANALYZED.....APATITE
 ANALYSIS BY/NOTES PAGE #...MH/

INDIVIDUAL GRAIN DATA

CRYSTAL	NS	NI	QUADS	RATIO	RHO S	RHO I	[U] ppm	AGE (Ma)	
1	11	40	25	0.275	2.82E+05	1.02E+06	11	35.2 q 12.4	
2	9	53	25	0.170	2.30E+05	1.36E+06	14	21.7 q 8.1	
3	13	46	25	0.283	3.33E+05	1.18E+06	12	36.1 q 11.8	
4	5	55	25	0.091	1.28E+05	1.41E+06	15	11.6 q 5.5	
5	4	14	9	0.286	2.84E+05	9.95E+05	10	36.5 q 21.0	
6	3	11	9	0.273	2.13E+05	7.82E+05	8	34.9 q 22.9	
7	4	15	9	0.267	2.84E+05	1.07E+06	11	34.1 q 19.4	
8	4	10	9	0.400	2.84E+05	7.11E+05	7	51.1 q 30.6	
9	12	70	25	0.171	3.07E+05	1.79E+06	19	21.9 q 7.1	
10	11	47	25	0.234	2.82E+05	1.20E+06	13	29.9 q 10.4	
11	8	45	25	0.178	2.05E+05	1.15E+06	12	22.8 q 9.0	
12	10	37	10	0.270	2.56E+05	9.47E+05	10	34.6 q 12.7	
13	8	49	25	0.163	2.05E+05	1.25E+06	13	20.9 q 8.2	
14	3	12	9	0.250	2.13E+05	8.53E+05	9	32.0 q 20.8	
15	9	34	25	0.245	2.30E+05	8.70E+05	9	33.9 q 13.0	
16	5	17	9	0.294	4.55E+05	1.21E+06	13	37.6 q 19.4	
17	17	67	25	0.254	4.35E+05	1.71E+06	18	32.5 q 9.3	
18	13	50	25	0.260	3.33E+05	1.28E+06	13	33.3 q 10.8	
19	9	50	25	0.180	2.30E+05	1.28E+06	13	23.0 q 8.6	
20	7	36	25	0.194	1.79E+05	9.21E+05	10	24.9 q 10.5	
21	4	20	9	0.200	2.84E+05	1.42E+06	15	25.6 q 14.2	
				169	778	2.62E+05	1.21E+06	12	

SUMMARY OF STATISTICS

~ Variance of Square root of NS = 0.4866
 ~ Variance of Square root of NI = 2.8037
 ~ Correlation coefficient (R for NS vs. NI) = 0.8151
 ~ Chi² = 10.50285 with 20 degrees of freedom. TEST PASS
 ~ Probability of greater value = .9581112

AGE CALCULATION

~ Zeta factor used = 113.0 q 10.0 POOLED AGE =
 ~ Glass dosimeter = CN1
 ~ ND counted = 2599 27.8 q 3.4 Ma
 ~ RHOD D for glass = 2.995E+06 q 0.587E+05
 ~ Area of 1 QUAD = 1.563E-06
 ~ Pooled NS/NI = 0.217 q 0.018 MEAN AGE =
 ~ Mean NS/NI = 0.236 q 0.015 30.2 q 3.3 Ma

SAMPLE LOCATION (OR STD)...DURANGO, STANDARD
 DATE OF ANALYSIS.....11/15/89
 LAB IDENTIFICATION CODE....MMO33-7
 IRRADIATION CODE.....MMO33-7
 DISKSD(ALIGN/CALCS/DIST)...A:/A:/A:
 DATAFILE.....DR07MO33.A1Z
 MINERAL ANALYZED.....APATITE
 ANALYSIS BY/NOTES PAGE #...MH/

INDIVIDUAL GRAIN DATA

CRYSTAL	NS	NI	QUADS	RATIO	RHO S	RHO I	[U] ppm	AGE (Ma)
1	6	31	25	0.194	1.54E+05	7.93E+05	8	31.9 q 14.5
2	7	40	25	0.175	1.79E+05	1.02E+06	11	28.8 q 12.1
3	7	37	25	0.189	1.79E+05	9.47E+05	10	31.2 q 13.2
4	8	43	25	0.186	2.05E+05	1.10E+06	12	30.6 q 12.1
5	8	49	25	0.184	2.30E+05	1.25E+06	13	30.3 q 11.3
6	8	39	25	0.205	2.05E+05	9.98E+05	10	33.8 q 13.5
7	6	24	25	0.250	1.54E+05	6.14E+05	6	41.1 q 19.2
8	7	44	25	0.159	1.79E+05	1.13E+06	12	26.2 q 10.9
9	7	23	25	0.130	7.68E+04	5.89E+05	6	21.5 q 13.3
10	10	46	25	0.217	2.56E+05	1.18E+06	12	35.8 q 12.9
11	7	39	25	0.179	1.79E+05	9.98E+05	10	29.6 q 12.4
12	7	39	25	0.179	1.79E+05	9.98E+05	10	29.6 q 12.4
13	4	28	25	0.143	1.02E+05	7.17E+05	8	23.5 q 12.8
14	6	39	25	0.154	1.54E+05	9.98E+05	10	25.3 q 11.4
15	8	23	25	0.348	2.05E+05	5.89E+05	6	57.2 q 24.1
16	7	38	25	0.184	1.79E+05	9.72E+05	10	30.3 q 12.8
17	4	25	25	0.160	1.02E+05	6.40E+05	7	26.4 q 14.4
18	8	44	25	0.182	2.05E+05	1.13E+06	12	29.9 q 11.8
19	8	30	25	0.267	2.05E+05	7.68E+05	8	43.9 q 17.9
20	5	32	25	0.156	1.28E+05	8.19E+05	9	25.7 q 12.6
21	9	42	25	0.214	2.30E+05	1.07E+06	11	35.3 q 13.4
22	7	37	25	0.189	1.79E+05	9.47E+05	10	31.2 q 13.2
	151	792			1.76E+05	9.21E+05	10	

SUMMARY OF STATISTICS

~ Variance of Square root of NS = 0.1231
 ~ Variance of Square root of NI = 0.4526
 ~ Correlation coefficient (R for NS vs. NI) = 0.6984
 ~ Chi² = 5.08487 with 21 degrees of freedom. TEST PASS
 ~ Probability of greater value = .9998482

AGE CALCULATION

~ Zeta factor used = 110.6 q 10.0 POOLED AGE =
 ~ Glass dosimeter = CN1
 ~ ND counted = 2900 31.4 q 4.0 Ma
 ~ RHOD D for glass = 2.985E+06 q 0.554E+05
 ~ Area of 1 QUAD = 1.563E-06
 ~ Pooled NS/NI = 0.191 q 0.017 MEAN AGE =
 ~ Mean NS/NI = 0.193 q 0.010 31.8 q 3.4 Ma

SAMPLE LOCATION (OR STD)...DURANGO, STANDARD
 DATE OF ANALYSIS.....OCT/13/1988
 LAB IDENTIFICATION CODE....DU13
 IRRADIATION CODE.....MM018-15
 DISKSD(ALIGN/CALCS/DIST)...A:/A:/A:
 DATAFILE.....DR15M018.A1Z
 MINERAL ANALYZED.....APATITE
 ANALYSIS BY/NOTES PAGE #...MH/

CRYSTAL	NS	NI	QUADS	RATIO	RHO S	RHO I	[U] DPM	AGE (Ma)
1	6	42	25	0.143	1.54E+05	1.07E+06	16	19.1 q 8.5
2	6	30	25	0.200	1.54E+05	7.68E+05	12	26.7 q 12.2
3	7	25	25	0.280	1.79E+05	6.40E+05	12	37.4 q 16.4
4	6	29	25	0.207	1.54E+05	7.42E+05	10	37.6 q 16.4
5	12	27	25	0.444	3.07E+05	6.91E+05	11	59.2 q 22.7
6	10	23	25	0.435	2.56E+05	5.89E+05	10	59.2 q 22.7
7	10	24	25	0.294	2.56E+05	8.70E+05	9	59.2 q 22.7
8	8	43	25	0.333	2.05E+05	6.14E+05	13	39.2 q 14.6
9	7	25	25	0.163	1.79E+05	1.10E+06	9	44.5 q 18.7
10	7	25	25	0.280	1.79E+05	6.40E+05	17	21.7 q 9.1
11	10	25	25	0.400	2.56E+05	6.40E+05	10	37.4 q 16.4
12	6	36	25	0.167	1.54E+05	6.40E+05	14	53.3 q 20.6
13	6	39	25	0.154	1.54E+05	9.21E+05	10	22.3 q 10.1
14	13	47	25	0.277	3.33E+05	9.98E+05	15	20.6 q 9.2
15	6	41	25	0.146	1.54E+05	1.20E+06	18	36.9 q 12.1
16	6	38	25	0.182	1.54E+05	1.05E+06	16	19.6 q 8.8
17	6	25	25	0.240	1.54E+05	6.40E+05	13	24.3 q 11.0
18	7	34	25	0.206	1.79E+05	6.40E+05	10	32.0 q 14.9
19	7	27	25	0.148	1.02E+05	8.70E+05	13	27.5 q 11.7
20	8	33	25	0.242	2.05E+05	6.91E+05	10	19.8 q 10.8
						8.45E+05	13	32.4 q 13.1
	151	642			1.93E+05	8.21E+05	12	

SUMMARY OF STATISTICS

~ Variance of Square root of NS = 0.1618
 ~ Variance of Square root of NI = 0.3991
 ~ Correlation coefficient (R for NS vs. NI) = 0.0342
 ~ Chi² = 16.32791 with 19 degrees of freedom. TEST PASS
 ~ Probability of greater value = .6352999

AGE CALCULATION

~ Zeta factor used = 12351.4 q 346.4 POOLED AGE ==
 ~ Glass dosimeter = SRM614
 ~ ND counted = 1400
 ~ RHOD D for glass = 2.200E+04 q 0.588E+03 31.4 q 4.2 Ma
 ~ Area of 1 QUAD = 1.563E-06
 ~ Pooled NS/NI = 0.235 q 0.021 MEAN AGE ==
 ~ Mean NS/NI = 0.247 q 0.022 33.0 q 4.4 Ma

SAMPLE LOCATION (OR STD)...DURANGO, STANDARD
 DATE OF ANALYSIS.....OCT/13/1988
 LAB IDENTIFICATION CODE....DU13
 IRRADIATION CODE.....MMO18-15
 DISKSD (ALIGN/CALCS/DIST)...A:/A:/A:
 DATAFILE.....DR15MO18.A1Z
 MINERAL ANALYZED.....APATITE
 ANALYSIS BY/NOTES PAGE #...MH/

INDIVIDUAL GRAIN DATA

CRYSTAL	NS	NI	QUADS	RATIO	RHD S	RHD I	[U] ppa	AGE (Ma)
1	6	42	25	0.143	1.54E+05	1.07E+06	16	18.3 q 8.1
2	6	30	25	0.200	1.54E+05	7.68E+05	12	25.7 q 11.6
3	7	25	25	0.280	1.79E+05	6.40E+05	10	35.9 q 15.6
4	6	26	25	0.207	1.54E+05	7.42E+05	11	26.6 q 12.1
5	12	27	25	0.444	3.07E+05	6.91E+05	10	56.9 q 20.2
6	10	23	25	0.435	2.56E+05	5.89E+05	9	55.7 q 21.5
7	10	34	25	0.294	2.56E+05	8.70E+05	13	37.7 q 13.8
8	8	24	25	0.333	2.05E+05	6.14E+05	9	42.7 q 17.7
9	7	43	25	0.163	1.79E+05	1.10E+06	17	20.9 q 8.7
10	7	25	25	0.280	1.79E+05	6.40E+05	10	35.9 q 15.6
11	10	25	25	0.400	2.56E+05	6.40E+05	10	51.2 q 19.5
12	6	36	25	0.167	1.54E+05	9.21E+05	14	21.4 q 9.6
13	6	39	25	0.154	1.54E+05	9.98E+05	15	19.8 q 8.8
14	13	47	25	0.277	3.33E+05	1.20E+06	18	35.5 q 11.4
15	6	41	25	0.146	1.54E+05	1.05E+06	16	18.8 q 8.3
16	6	33	25	0.182	1.54E+05	8.45E+05	13	23.3 q 10.5
17	6	25	25	0.240	1.54E+05	6.40E+05	10	30.8 q 14.2
18	7	34	25	0.206	1.79E+05	8.70E+05	13	26.4 q 11.1
19	4	27	25	0.148	1.02E+05	6.91E+05	10	19.0 q 10.3
20	8	33	25	0.242	2.05E+05	8.45E+05	13	31.1 q 12.5
	151	642			1.93E+05	8.21E+05	12	

SUMMARY OF STATISTICS

~ Variance of Square root of NS = 0.1618
 ~ Variance of Square root of NI = 0.3991
 ~ Correlation coefficient (R for NS vs. NI) = 0.0342
 ~ Chi² = 16.32791 with 19 degrees of freedom. TEST PASS
 ~ Probability of greater value = .6352999

AGE CALCULATION

~ Zeta factor used = 11774.2 q 678.1 POOLED AGE =
 ~ Glass dosimeter = SRM614
 ~ ND counted = 1400 30.2 q 3.5 Ma
 ~ RHD D for glass = 2.200E+04 q 0.588E+03
 ~ Area of 1 QUAD = 1.563E-06
 ~ Pooled NS/NI = 0.235 q 0.021 MEAN AGE =
 ~ Mean NS/NI = 0.247 q 0.022 31.7 q 3.6 Ma

SAMPLE LOCATION (OR STD)...FISH CANYON TUFF, STANDARD
 DATE OF ANALYSIS.....05/02/90
 LAB IDENTIFICATION CODE....FC
 IRRADIATION CODE.....MM041-10
 DISKSD(ALIGN/CALCS/DIST)...//
 DATAFILE.....FC10M041.A1Z
 MINERAL ANALYZED.....APATITE
 ANALYSIS BY/NOTES PAGE #...MH/

INDIVIDUAL GRAIN DATA

CRYSTAL	NS	NI	QUADS	RATIO	RHO S	RHO I	[U] ppm	AGE (Ma)
1	6	28	9	0.214	4.27E+05	1.99E+06	17	32.9 q 15.2
2	4	14	9	0.286	2.84E+05	9.95E+05	8	43.8 q 25.3
3	5	27	9	0.185	3.55E+05	1.92E+06	16	28.4 q 14.2
4	4	20	9	0.200	2.84E+05	1.42E+06	12	30.7 q 17.2
5	2	20	9	0.100	1.42E+05	1.42E+06	12	15.4 q 11.5
6	2	21	9	0.143	2.13E+05	1.49E+06	13	21.9 q 13.8
7	2	20	9	0.100	1.42E+05	1.42E+06	12	15.4 q 11.5
8	6	59	25	0.153	2.30E+05	1.51E+06	13	23.4 q 8.8
9	11	49	25	0.224	2.82E+05	1.25E+06	11	34.4 q 12.1
10	6	54	25	0.111	1.54E+05	1.38E+06	12	17.1 q 7.6
11	3	19	9	0.158	2.13E+05	1.35E+06	11	24.2 q 15.3
12	14	58	25	0.241	3.58E+05	1.48E+06	13	37.0 q 11.8
13	3	29	25	0.103	7.68E+04	1.42E+05	6	15.9 q 9.8
14	3	28	9	0.107	2.13E+05	1.99E+06	17	16.5 q 10.2
15	14	45	25	0.311	3.58E+05	1.15E+06	10	47.7 q 15.5
16	3	12	9	0.250	2.13E+05	6.53E+05	7	38.3 q 25.1
17	3	13	9	0.231	2.13E+05	9.24E+05	8	35.4 q 23.0
18	3	25	9	0.120	2.13E+05	1.78E+06	15	18.4 q 11.4
	98	541			2.43E+05	1.34E+06	12	

SUMMARY OF STATISTICS

~ Variance of Square root of NS = 0.5652
 ~ Variance of Square root of NI = 1.9019
 ~ Correlation coefficient (R for NS vs. NI) = 0.8132
 ~ Chi² = 10.94562 with 17 degrees of freedom. TEST PASS
 ~ Probability of greater value = .8593768

AGE CALCULATION

~ Zeta factor used = 82.9 q 9.2 POOLED AGE =
 ~ Glass dosimeter = CN1
 ~ ND counted = 4488 27.8 q 4.4 Ma
 ~ RHOD D for glass = 3.710E+06 q 0.554E+05
 ~ Area of 1 QUAD = 1.563E-06
 ~ Pooled NS/NI = 0.181 q 0.020 MEAN AGE =
 ~ Mean NS/NI = 0.180 q 0.016 27.6 q 4.0 Ma

SAMPLE LOCATION (OR STD)...DURANGO, STANDARD
 DATE OF ANALYSIS.....11/22/89
 LAB IDENTIFICATION CODE....DR
 IRRADIATION CODE.....MM034-13
 DISKSD(ALIGN/CALCS/DIST)...A:/A:/A:
 DATAFILE.....DR13M034.A1Z
 MINERAL ANALYZED.....APATITE
 ANALYSIS BY/NOTES PAGE #...MH/

INDIVIDUAL GRAIN DATA

CRYSTAL	NS	NI	QUADS	RATIO	RHO S	RHO I	[U] ppm	AGE (Ma)
1	4	26	25	0.154	1.02E+05	6.65E+05	7	29.4 q 16.0
2	10	57	25	0.175	2.56E+05	1.46E+06	15	33.5 q 11.9
3	6	36	25	0.167	1.54E+05	9.21E+05	10	31.8 q 14.3
4	5	52	25	0.096	1.28E+05	1.33E+06	14	18.4 q 8.8
5	5	33	25	0.152	1.28E+05	8.45E+05	9	28.9 q 14.1
6	6	41	25	0.146	1.54E+05	1.05E+06	11	27.9 q 12.5
7	5	51	25	0.098	1.28E+05	1.31E+06	14	27.7 q 12.5
8	5	30	25	0.300	2.30E+05	7.68E+05	8	18.7 q 8.9
9	5	25	25	0.200	3.55E+05	1.78E+06	19	57.1 q 22.3
10	5	41	25	0.122	1.28E+05	1.05E+06	11	38.1 q 19.0
11	9	45	25	0.200	2.30E+05	1.15E+06	12	23.3 q 11.2
12	8	46	25	0.196	2.30E+05	1.15E+06	12	38.1 q 14.3
13	8	55	25	0.151	2.05E+05	1.18E+06	12	37.3 q 14.0
14	6	28	25	0.214	1.54E+05	1.36E+06	14	28.8 q 11.2
15	6	39	25	0.205	2.05E+05	9.98E+05	7	40.9 q 18.7
16	6	43	25	0.140	1.54E+05	7.17E+05	7	28.8 q 11.2
17	8	39	25	0.205	2.05E+05	9.98E+05	10	40.9 q 18.7
18	7	47	25	0.149	1.79E+05	1.10E+06	11	39.1 q 15.6
19	6	44	25	0.136	1.54E+05	1.13E+06	10	29.4 q 11.8
20	6	40	25	0.150	1.54E+05	1.02E+06	12	28.0 q 11.8
21	10	47	25	0.213	2.56E+05	1.20E+06	13	28.6 q 12.8
22	7	60	25	0.117	1.79E+05	1.54E+06	16	40.6 q 14.6
23	7	31	25	0.226	1.79E+05	7.93E+05	8	22.3 q 9.1
							8	43.0 q 18.4
	157	954			1.80E+05	1.09E+06	12	

SUMMARY OF STATISTICS

~ Variance of Square root of NS = 0.1105
 ~ Variance of Square root of NI = 0.5873
 ~ Correlation coefficient (R for NS vs. NI) = 0.3667
 ~ Chi² = 9.752032 with 22 degrees of freedom. TEST PASS
 ~ Probability of greater value = .988417

AGE CALCULATION

~ Zeta factor used = 127.7 q 11.3 POOLED AGE =
 ~ Glass dosimeter = CN1
 ~ ND counted = 2599 31.4 q 3.9 Ma
 ~ RHOD D for glass = 2.995E+06 q 0.587E+05
 ~ Area of 1 QUAD = 1.563E-06
 ~ Pooled NS/NI = 0.165 q 0.014 MEAN AGE =
 ~ Mean NS/NI = 0.170 q 0.010 32.4 q 3.5 Ma

SAMPLE LOCATION (OR STD)...DURANGO, STANDARD
 DATE OF ANALYSIS.....05/02/90
 LAB IDENTIFICATION CODE....DR
 IRRADIATION CODE.....MM041-17
 DISKSD(ALIGN/CALCS/DIST)...//
 DATAFILE.....DR17M041.A1Z
 MINERAL ANALYZED.....APATITE
 ANALYSIS BY/NOTES PAGE #...MH/

INDIVIDUAL GRAIN DATA

CRYSTAL	NS	NI	QUADS	RATIO	RHO S	RHO I	[U] ppm	AGE (Ma)
1	5	46	25	0.109	1.28E+05	1.18E+06	10	21.2 q 10.2
2	8	30	25	0.267	2.05E+05	7.68E+05	6	51.9 q 21.3
3	6	47	25	0.128	1.54E+05	1.20E+06	10	24.9 q 11.1
4	5	42	25	0.119	1.28E+05	1.07E+06	9	27.2 q 11.2
5	11	57	25	0.193	2.82E+05	1.46E+06	12	37.6 q 12.9
6	7	30	25	0.167	1.28E+05	7.68E+05	6	32.5 q 16.0
7	4	34	25	0.206	1.79E+05	8.70E+05	7	40.1 q 17.1
8	7	27	25	0.148	1.02E+05	6.91E+05	6	28.9 q 15.8
9	5	24	25	0.208	1.28E+05	6.14E+05	5	40.6 q 20.4
10	5	38	25	0.132	1.28E+05	9.72E+05	8	25.7 q 12.5
11	9	59	25	0.153	2.30E+05	1.51E+06	13	29.8 q 11.1
12	8	58	25	0.138	2.05E+05	1.48E+06	13	26.9 q 10.5
13	10	45	25	0.222	2.56E+05	1.15E+06	10	43.3 q 15.7
14	4	39	25	0.103	1.02E+05	9.98E+05	8	20.0 q 10.7
15	7	37	25	0.212	1.79E+05	8.45E+05	7	41.4 q 17.7
16	5	34	25	0.147	1.28E+05	8.70E+05	7	28.7 q 14.0
17	6	53	25	0.113	1.54E+05	1.36E+06	11	22.1 q 9.8
18	0	45	25	0.200	2.30E+05	1.15E+06	10	39.0 q 14.8
19	3	17	25	0.176	7.68E+04	4.35E+05	4	34.4 q 21.8
	122	758			1.64E+05	1.02E+06	9	

SUMMARY OF STATISTICS

~ Variance of Square root of NS = 0.1876
 ~ Variance of Square root of NI = 0.9475
 ~ Correlation coefficient (R for NS vs. NI) = 0.6376
 ~ Chi² = 7.517286 with 18 degrees of freedom. TEST PASS
 ~ Probability of greater value = .9849905

AGE CALCULATION

~ Zeta factor used = 105.4 q 10.4
 ~ Glass dosimeter = CN1
 ~ ND counted = 4488
 ~ RHOD D for glass = 3.710E+06 q 0.554E+05
 ~ Area of 1 QUAD = 1.563E-06
 ~ Pooled NS/NI = 0.161 q 0.016
 ~ Mean NS/NI = 0.165 q 0.011
 POOLED AGE = 31.4 q 4.4 Ma
 MEAN AGE = 32.2 q 3.8 Ma

SAMPLE LOCATION (OR STD)...FISH CANYON TUFF, STANDARD
 DATE OF ANALYSIS.....02/07/90
 LAB IDENTIFICATION CODE....FC
 IRRADIATION CODE.....MMO38-17
 DISKSD (ALIGN/CALCS/DIST)...A:/A:/A:
 DATAFILE.....FC17M038.A1Z
 MINERAL ANALYZED.....APATITE
 ANALYSIS BY/NOTES PAGE #...MH/

INDIVIDUAL GRAIN DATA

CRYSTAL	NS	NI	QUADS	RATIO	RHO S	RHO I	CUI ppm	AGE (Ma)
1	13	51	25	0.255	3.33E+05	1.31E+06	10	48.4 q 15.6
2	7	62	25	0.113	1.79E+05	1.59E+06	12	21.5 q 8.7
3	13	60	25	0.217	3.33E+05	1.54E+06	12	41.2 q 13.0
4	6	64	25	0.094	1.54E+05	1.64E+06	13	17.9 q 7.8
5	9	59	25	0.153	2.30E+05	1.51E+06	12	29.0 q 10.7
6	7	57	25	0.123	1.79E+05	1.46E+06	11	23.4 q 9.6
7	3	21	25	0.143	1.68E+04	5.37E+05	4	27.2 q 16.9
8	11	71	25	0.155	2.82E+05	1.82E+06	14	29.5 q 9.8
9	11	57	25	0.193	2.82E+05	1.46E+06	11	36.7 q 12.4
10	11	78	25	0.141	2.82E+05	2.00E+06	15	26.8 q 8.9
11	11	68	25	0.162	2.82E+05	1.74E+06	13	30.8 q 10.3
12	6	41	25	0.146	1.54E+05	1.05E+06	8	27.9 q 12.4
13	7	50	25	0.140	1.79E+05	1.28E+06	10	26.7 q 11.0
14	11	73	25	0.151	2.82E+05	1.87E+06	14	28.7 q 9.6
15	4	44	25	0.091	1.02E+05	1.13E+06	9	17.3 q 9.2
16	11	73	25	0.151	2.82E+05	1.87E+06	14	28.7 q 9.6
17	7	69	25	0.101	1.79E+05	1.77E+06	14	19.3 q 7.8
18	5	58	25	0.086	1.28E+05	1.48E+06	12	16.4 q 7.8
19	17	76	25	0.218	4.35E+05	2.00E+06	15	41.4 q 11.6
20	9	90	25	0.100	2.30E+05	2.30E+06	18	19.0 q 6.8
21	4	29	25	0.138	1.02E+05	7.42E+05	6	26.3 q 14.2
	183	1253			2.23E+05	1.53E+06	12	

SUMMARY OF STATISTICS

~ Variance of Square root of NS = 0.3820
 ~ Variance of Square root of NI = 1.3539
 ~ Correlation coefficient (R for NS vs. NI) = 0.6375
 ~ Chi² = 14.06245 with 20 degrees of freedom. TEST PASS
 ~ Probability of greater value = .8273156

AGE CALCULATION

~ Zeta factor used = 94.6 q 7.6 POOLED AGE =
 ~ Glass dosimeter = CN1
 ~ ND counted = 7374 27.8 q 3.1 Ma
 ~ RHOD D for glass = 4.034E+06 q 0.470E+05
 ~ Area of 1 QUAD = 1.563E-06
 ~ Pooled NS/NI = 0.146 q 0.012 MEAN AGE =
 ~ Mean NS/NI = 0.146 q 0.010 27.8 q 2.9 Ma

SAMPLE LOCATION (OR STD)...DURANGO, STANDARD
 DATE OF ANALYSIS.....05/02/90
 LAB IDENTIFICATION CODE....DR
 IRRADIATION CODE.....MMO41-4
 DISKSD(ALIGN/CALCS/DIST)...//
 DATAFILE.....DR04M041.A1Z
 MINERAL ANALYZED.....APATITE
 ANALYSIS BY/NOTES PAGE #...MH/

INDIVIDUAL GRAIN DATA

CRYSTAL	NS	NI	QUADS	RATIO	RHO S	RHO I	[U] ppm	AGE (Ma)
1	3	46	25	0.065	7.68E+04	1.19E+06	10	12.8 q 7.7
2	8	45	25	0.178	2.05E+05	1.15E+06	10	34.9 q 13.8
3	10	58	25	0.172	2.56E+05	1.48E+06	13	33.9 q 12.0
4	6	40	25	0.150	1.54E+05	1.02E+06	9	29.5 q 13.2
5	8	64	25	0.125	2.05E+05	1.64E+06	14	24.6 q 9.5
6	6	37	25	0.162	1.54E+05	9.47E+05	8	31.9 q 14.3
7	6	21	9	0.286	4.27E+05	1.49E+06	13	56.0 q 26.5
8	6	46	25	0.130	1.54E+05	1.18E+06	10	25.6 q 11.4
9	11	60	25	0.183	2.82E+05	1.54E+06	13	36.0 q 12.3
10	9	37	25	0.243	2.30E+05	9.47E+05	8	47.7 q 18.3
11	8	50	25	0.160	2.05E+05	1.28E+06	11	31.4 q 12.3
12	8	25	25	0.320	2.05E+05	6.40E+05	5	62.7 q 26.1
13	6	47	25	0.128	1.54E+05	1.20E+06	10	25.1 q 11.1
14	4	25	25	0.160	1.02E+05	6.40E+05	5	31.4 q 17.2
15	5	51	25	0.098	1.28E+05	1.31E+06	11	19.3 q 9.2
16	7	34	25	0.206	1.79E+05	8.70E+05	7	40.4 q 17.2
17	7	39	25	0.179	1.79E+05	9.98E+05	8	35.2 q 14.8
18	8	43	25	0.186	2.05E+05	1.10E+06	9	36.5 q 14.5
19	6	37	25	0.162	1.54E+05	9.47E+05	8	31.9 q 14.3
20	5	52	25	0.096	1.28E+05	1.33E+06	11	18.9 q 9.0
	137	857			1.81E+05	1.13E+06	10	

SUMMARY OF STATISTICS

- ~ Variance of Square root of NS = 0.1456
 ~ Variance of Square root of NI = 0.8348
 ~ Correlation coefficient (R for NS vs. NI) = 0.3512
 ~ Chi² = 12.54091 with 19 degrees of freedom. TEST PASS
 ~ Probability of greater value = .8612222

AGE CALCULATION

- ~ Zeta factor used = 106.1 q 9.9 POOLED AGE =
 ~ Glass dosimeter = CN1
 ~ ND counted = 4488 31.4 q 4.1 Ma
 ~ RHOD D for glass = 3.710E+06 q 0.554E+05
 ~ Area of 1 QUAD = 1.563E-06
 ~ Pooled NS/NI = 0.160 q 0.015 MEAN AGE =
 ~ Mean NS/NI = 0.170 q 0.014 33.3 q 4.2 Ma

SAMPLE LOCATION (OR STD)...DURANGO, STANDARD
 DATE OF ANALYSIS.....02/06/90
 LAB IDENTIFICATION CODE....DR
 IRRADIATION CODE.....MM038-11
 DISKSD(ALIGN/CALCS/DIST)...A:/A:/A:
 DATAFILE.....DR11M038.A1Z
 MINERAL ANALYZED.....APATITE
 ANALYSIS BY/NOTES PAGE #...MH/

INDIVIDUAL GRAIN DATA

<u>CRYSTAL</u>	<u>NS</u>	<u>NI</u>	<u>QUADS</u>	<u>RATIO</u>	<u>RHO S</u>	<u>RHO I</u>	<u>[U] ppm</u>	<u>AGE (Ma)</u>
1	8	41	25	0.195	2.05E+05	1.05E+06	8	38.8 q 15.4
2	6	33	25	0.182	1.54E+05	8.45E+05	7	36.2 q q q 16.4
3	6	43	25	0.140	1.54E+05	1.10E+06	9	27.8 q q q 12.3
4	6	41	25	0.146	1.54E+05	1.05E+06	8	29.1 q q q 13.0
5	12	42	25	0.286	3.07E+05	1.07E+06	8	56.7 q q q 19.2
6	11	26	25	0.423	2.82E+05	6.65E+05	8	83.8 q q q 31.0
7	4	56	25	0.107	1.54E+05	1.43E+06	5	21.3 q q q 9.4
8	4	36	25	0.111	1.02E+05	9.21E+05	7	22.1 q q q 11.8
9	3	51	25	0.059	7.68E+04	1.31E+06	11	11.7 q q q 7.0
10	13	82	25	0.159	3.33E+05	2.10E+06	10	31.5 q q q 9.8
11	8	41	25	0.195	2.05E+05	1.05E+06	8	38.8 q q q 15.4
12	6	37	25	0.162	1.54E+05	9.47E+05	7	32.3 q q q 14.5
13	7	61	25	0.115	1.79E+05	1.56E+06	12	22.9 q q q 9.3
14	9	44	25	0.205	2.30E+05	1.13E+06	9	40.7 q q q 15.3
15	10	50	25	0.200	2.56E+05	1.28E+06	10	39.8 q q q 14.2
16	4	39	25	0.103	1.02E+05	9.98E+05	8	20.4 q q q 10.9
17	9	56	25	0.161	2.30E+05	1.43E+06	11	32.0 q q q 11.8
18	2	38	25	0.053	5.12E+04	9.72E+05	8	10.5 q q q 7.7
19	5	46	25	0.109	1.28E+05	1.18E+06	9	21.6 q q q 10.4
20	10	42	25	0.238	2.56E+05	1.07E+06	8	47.3 q q q 17.2
21	8	47	25	0.170	2.05E+05	1.20E+06	9	33.9 q q q 13.3
22	4	43	25	0.093	1.02E+05	1.10E+06	9	16.5 q q q 9.8
	157	995			1.83E+05	1.16E+06	9	

SUMMARY OF STATISTICS

~ Variance of Square root of NS = 0.3269
 ~ Variance of Square root of NI = 0.6480
 ~ Correlation coefficient (R for NS vs. NI) = 0.3184
 ~ Chi² = 24.55854 with 21 degrees of freedom. TEST PASS
 ~ Probability of greater value = .2667895

AGE CALCULATION

~ Zeta factor used = 98.9 q 8.6 POOLED AGE =
 ~ Glass dosimeter = CN1
 ~ ND counted = 7374 31.4 q 3.8 Ma
 ~ RHOD D for glass = 4.034E+06 q 0.470E+05
 ~ Area of 1 QUAD = 1.563E-06
 ~ Pooled NS/NI = 0.158 q 0.014 MEAN AGE =
 ~ Mean NS/NI = 0.164 q 0.018 32.6 q 4.5 Ma

SAMPLE LOCATION (OR STD)...FISH CANYON TUFF, STANDARD
 DATE OF ANALYSIS.....02/07/90
 LAB IDENTIFICATION CODE....FC
 IRRADIATION CODE.....MM039-15
 DISKSD(ALIGN/CALCS/DIST)...A:/A:/A:
 DATAFILE.....FC15M039.A1Z
 MINERAL ANALYZED.....AFATITE
 ANALYSIS BY/NOTES PAGE #...MH/

INDIVIDUAL GRAIN DATA

CRYSTAL	NS	NI	QUADS	RATIO	RHO S	RHO I	[U] ppn	AGE (Ma)
1	10	74	25	0.135	2.56E+05	1.89E+06	15	27.1 q 9.4
2	11	53	25	0.208	2.82E+05	1.36E+06	11	41.6 q 14.2
3	10	71	25	0.141	2.56E+05	1.82E+06	14	28.3 q 9.8
4	12	63	25	0.190	3.07E+05	1.61E+06	12	38.2 q 12.4
5	10	61	25	0.164	2.56E+05	1.56E+06	12	32.9 q 11.5
6	14	107	25	0.131	3.58E+05	2.74E+06	21	26.3 q 7.7
7	8	55	25	0.145	2.05E+05	1.41E+06	11	29.2 q 11.3
8	5	61	25	0.082	1.28E+05	1.56E+06	12	16.5 q 7.8
9	12	71	25	0.169	3.07E+05	1.82E+06	14	33.9 q 10.9
10	9	96	25	0.136	2.30E+05	1.69E+06	13	27.4 q 10.0
11	9	72	25	0.125	2.30E+05	1.84E+06	14	25.1 q 9.1
12	4	25	25	0.160	1.02E+05	6.40E+05	5	32.1 q 17.5
13	10	59	25	0.169	2.56E+05	1.51E+06	12	34.0 q 11.9
14	9	82	25	0.110	2.30E+05	2.10E+06	16	22.0 q 7.9
15	7	54	25	0.130	1.79E+05	1.38E+06	11	26.0 q 10.7
16	7	40	25	0.175	1.79E+05	1.02E+06	8	35.1 q 14.6
17	12	72	25	0.167	3.07E+05	1.84E+06	14	35.4 q 10.8
18	6	73	25	0.082	1.54E+05	1.87E+06	14	16.5 q 7.1
19	6	56	25	0.107	1.54E+05	1.43E+06	11	21.5 q 9.4
20	4	35	25	0.114	1.02E+05	8.96E+05	7	22.9 q 12.2
21	13	107	25	0.121	3.33E+05	2.74E+06	21	24.4 q 7.4
	188	1357			2.29E+05	1.65E+06	13	

SUMMARY OF STATISTICS

~ Variance of Square root of NS = 0.2594
 ~ Variance of Square root of NI = 1.5713
 ~ Correlation coefficient (R for NS vs. NI) = 0.7353
 ~ Chi² = 8.452194 with 20 degrees of freedom. TEST PASS
 ~ Probability of greater value = .9884279

AGE CALCULATION

~ Zeta factor used = 99.7 q 7.8 POOLED AGE =
 ~ Glass dosimeter = CN1
 ~ ND counted = 7374 27.8 q 3.1 Ma
 ~ RHOD D for glass = 4.034E+06 q 0.470E+05
 ~ Area of 1 QUAD = 1.563E-06
 ~ Pooled NS/NI = 0.139 q 0.011 MEAN AGE =
 ~ Mean NS/NI = 0.141 q 0.007 28.3 q 2.7 Ma

SAMPLE LOCATION (OR STD)...DURANGO, STANDARD
 DATE OF ANALYSIS.....02/08/90
 LAB IDENTIFICATION CODE....DR
 IRRADIATION CODE.....MM039-10
 DISKSD(ALIGN/CALCS/DIST)...A:/A:/A:
 DATAFILE.....DR10M039.A1Z
 MINERAL ANALYZED.....APATITE
 ANALYSIS BY/NOTES PAGE #...MH/

INDIVIDUAL GRAIN DATA

CRYSTAL	NS	NI	QUADS	RATIO	RHO S	RHO I	[U] ppm	AGE (Ma)
1	5	49	25	0.102	1.28E+05	1.25E+06	10	21.8 q 10.4
2	8	61	25	0.131	2.05E+05	1.56E+06	12	28.0 q 10.8
3	5	44	25	0.114	1.28E+05	1.13E+06	9	24.3 q 11.7
4	11	36	25	0.306	2.82E+05	9.21E+05	7	65.1 q 23.1
5	3	34	25	0.088	7.68E+04	8.70E+05	7	18.9 q 11.5
6	7	30	25	0.233	1.79E+05	7.68E+05	6	49.8 q 21.3
7	11	72	25	0.153	2.82E+05	1.84E+06	14	32.7 q 10.9
8	8	70	25	0.114	2.05E+05	1.79E+06	14	24.4 q 9.4
9	10	68	25	0.147	2.56E+05	1.74E+06	13	31.4 q 11.0
10	7	37	25	0.189	1.79E+05	9.47E+05	7	40.4 q 17.0
11	10	63	25	0.159	2.56E+05	1.61E+06	12	33.9 q 11.9
12	7	59	25	0.119	1.79E+05	1.51E+06	12	25.4 q 10.4
13	4	53	25	0.075	1.02E+05	1.36E+06	11	16.2 q 8.5
14	11	64	25	0.172	2.82E+05	1.64E+06	13	26.7 q 12.4
15	5	45	25	0.111	1.28E+05	1.15E+06	9	23.8 q 11.4
16	11	40	25	0.275	2.82E+05	1.02E+06	8	58.7 q 20.6
17	5	47	25	0.106	1.28E+05	1.20E+06	9	22.8 q 10.9
18	8	33	25	0.242	2.05E+05	8.45E+05	7	51.7 q 20.9
19	7	49	25	0.143	1.79E+05	1.25E+06	10	30.5 q 12.6
20	5	34	25	0.147	1.28E+05	8.70E+05	7	31.4 q 15.3
21	7	58	25	0.121	1.79E+05	1.48E+06	12	25.8 q 10.6
22	6	50	25	0.120	1.54E+05	1.28E+06	10	25.7 q 11.3
	161	1096			1.87E+05	1.27E+06	10	

SUMMARY OF STATISTICS

~ Variance of Square root of NS = 0.2169
 ~ Variance of Square root of NI = 0.8693
 ~ Correlation coefficient (R for NS vs. NI) = 0.4022
 ~ Chi² = 17.27111 with 21 degrees of freedom. TEST PASS
 ~ Probability of greater value = .6945467

AGE CALCULATION

~ Zeta factor used = 106.2 q 9.1 POOLED AGE =
 ~ Glass dosimeter = CN1
 ~ ND counted = 7374 31.4 q 3.8 Ma
 ~ RHOD D for glass = 4.034E+06 q 0.470E+05
 ~ Area of 1 QUAD = 1.563E-06
 ~ Pooled NS/NI = 0.147 q 0.012 MEAN AGE =
 ~ Mean NS/NI = 0.153 q 0.013 32.7 q 4.0 Ma

Appendix 2: Track Length Distribution Skewness Values

Sample	Skewness
FT89-206	-1.284
FT89-197	-0.987
FT89-201	-0.865
FT89-196	-0.320
FT89-211	-0.729
FT89-226	-0.906
FT89-194	-0.816
FT89-191	-1.630
FT89-210	-1.523
FT89-209	-1.355
FT89-205	-1.168
FT89-203	-1.352
FT89-207	-0.964
FT89-221	-0.754
FT89-233	-0.328
FT89-227	-1.022
FT89-193	-1.460
FT89-232	-0.769
FT89-208	-0.966
FT89-212	-1.084
FT89-225	-0.928
FT89-213	+0.354
FT89-222	-0.360
FT90-034	-0.568
FT90-035	-1.487
FT90-050	-0.932
FT89-198	0.000
FT89-235	-0.001
FT89-224	-0.459
FT89-223	-0.562
LGRA-01	-0.023

Appendix 3: Length-Corrected Apatite Fission Track Ages

Apparent apatite fission track ages are often corrected for annealing by multiplying the apparent age by the ratio of the original mean etched length of the sample ($m_0 = \sim 16.5$ microns) to the measured mean etched length (m) of the sample. However, because the apparent age is determined from a zeta factor based on age standards which have shortened original lengths, consistency demands that the corrected apparent age (length-corrected age) also be considered in terms of shortened original lengths and, therefore, determined as a function of the zeta parameter. Mean etched lengths of the standard samples (Fish Canyon Tuff (FC) = $14.22 \pm 0.03 \mu\text{m}$ (1627 tracks), Durango (DR) = $15.26 \pm 0.06 \mu\text{m}$ (1426 tracks) and Renfrew (RN) ~ 14.22 ; Donelick, pers. com. 1990) are used to calculate a weighted mean etched length unique to each zeta parameter in the study,

$$m_0(\zeta) = \sum_{STD}^N f_{STD} m_{STD}$$

where

$m_0(\zeta)$ = weighted mean etched length for a determined zeta

m_{STD} = mean etched length of standard sample (FC, DR, RN)

N = number of standards used to determine zeta

f_{STD} = fraction of the standard used to determine zeta

given by

$$f_{STD} = \frac{f_{STD}(\text{relative})}{\sum_{STD}^N f_{STD}(\text{relative})}$$

where

$$f_{STD}(relative) = \frac{1}{(sd/\zeta)^2}$$

sd = standard deviation of zeta

Depending on the zeta used to calculate the apparent apatite age, the appropriate weighted mean etched length ($m_0(\text{zeta})$) is then used in ratio with the measured mean etched length of the sample ($m_0(\text{zeta})/m$) to calculate the length-corrected age of each analyzed sample.

Appendix 4: Parameters for Inverse T-t Models

The parameters used during the inversion of the track length data are given for each sample in this appendix. They are defined as follows:

number of solutions = the number of forward models in the set used for predictions

number of timesteps = the number of timesteps used in during inverse modelling

number of parameters = number of timesteps + 1

number of timesteps for integration = timestep subdivision over which the annealing model of Laslett et al., 1987 is used

number of substeps for track component gen. = timestep subdivision over which track component is generated

timestep length = timestep length in seconds

obj fnct = the objective function is the value that must be minimized (dependent on the predicted data from the inverse modelling) below a theoretical value in order to achieve statistical significance at various confidence levels.

convergence tolerance = confidence level of the fit to the data (0.50 or 0.95)

measured age = measured apatite fission track age

variance of error in measured age = statistical variance in measured age error

number of data = number of track lengths measured

intermediate output = value of objective function every 500 forward models

random generator seed = random generator to determine set of forward models

expansion factor = expansion factor

reposition factor = distance inside explicit bound to be repositioned if generated forward model falls outside of explicit bounds

temperature and rate bounds = explicit temperature bounds (°C) and heating and cooling rate bounds (°C/timestep) set by the modeller over every timestep

max obj function = highest value of objective function in the set of forward models

level 95 max obj function = highest value of objective function when all models are

within the 0.95 confidence level

number of forward models = total number of forward models generated for
convergence on a 0.50 confidence level fit of the data

southern transect sample FT89-226
 modified simplex algorithm
 model 1

inversion control parameters:

```

-----
number of solutions (l) = 150
number of timesteps (m) = 20
number of parameters (m+1) = 21
number of substeps for integration (nstep) = 12
number of substeps for track component gen = 2
timestep length (delt) = 7.8750000000000D+14
obj fnct (2 = chi2; 3 = kol-smirnov) = 3
convergence tolerance (tol95) = 0.136000000000000
convergence tolerance (toler) = 8.3300000000000D-02
measured age = 343.000000000000
variance of error in measured age = 1909.6900874000
number of data (n) = 100
number of tracks measured = 100
intermediate output every 500 forward models
random number generator seed = 3
expansion factor (alpha) = 1.30000000000000
reposition factor for explicit bound (delta) = 1.0000000000000D-01

```

	temperature bounds		rate bounds	
1	0.0000	140.0000	120.0000	30.0000
2	0.0000	140.0000	120.0000	30.0000
3	0.0000	140.0000	120.0000	30.0000
4	0.0000	140.0000	120.0000	30.0000
5	0.0000	140.0000	120.0000	30.0000
6	0.0000	140.0000	120.0000	30.0000
7	0.0000	140.0000	120.0000	30.0000
8	0.0000	140.0000	120.0000	30.0000
9	0.0000	140.0000	120.0000	30.0000
10	0.0000	140.0000	120.0000	30.0000
11	0.0000	140.0000	120.0000	30.0000
12	0.0000	140.0000	120.0000	30.0000
13	0.0000	140.0000	120.0000	30.0000
14	0.0000	140.0000	120.0000	30.0000
15	0.0000	140.0000	120.0000	30.0000
16	0.0000	140.0000	120.0000	30.0000
17	0.0000	140.0000	120.0000	30.0000
18	0.0000	140.0000	120.0000	30.0000
19	0.0000	140.0000	120.0000	30.0000
20	0.0000	140.0000	120.0000	30.0000
21	0.0000	20.0000		

```

max obj function = 0.166903
level 95 max obj function = 0.135852
max obj function = 0.109124
max obj function = 0.083010
number of forward models: 1161

```

southern transect sample FT89-225
 modified simplex algorithm
 model 1

inversion control parameters:

```

-----
number of solutions (l) = 150
number of timesteps (m) = 20
number of parameters (m+1) = 21
number of substeps for integration (nstep) = 12
number of substeps for track component gen = 3
timestep length (delt) = 7.8750000000000D+14
obj fnct (2 = chi2; 3 = kol-smirnov) = 3
convergence tolerance (tol95) = 0.13272240992100
convergence tolerance (toler) = 8.1292476076613D-02
measured age = 309.000000000000
variance of error in measured age = 547.55998128000
number of data (n) = 105
number of tracks measured = 105
intermediate output every 500 forward models
random number generator seed = 3
expansion factor (alpha) = 1.30000000000000
reposition factor for explicit bound (delta) = 1.0000000000000D-01

```

	temperature bounds		rate bounds	
1	0.0000	140.0000	120.0000	30.0000
2	0.0000	140.0000	120.0000	30.0000
3	0.0000	140.0000	120.0000	30.0000
4	0.0000	140.0000	120.0000	30.0000
5	0.0000	140.0000	120.0000	30.0000
6	0.0000	140.0000	120.0000	30.0000
7	0.0000	140.0000	120.0000	30.0000
8	0.0000	140.0000	120.0000	30.0000
9	0.0000	140.0000	120.0000	30.0000
10	0.0000	140.0000	120.0000	30.0000
11	0.0000	140.0000	120.0000	30.0000
12	0.0000	140.0000	120.0000	30.0000
13	0.0000	140.0000	120.0000	30.0000
14	0.0000	140.0000	120.0000	30.0000
15	0.0000	140.0000	120.0000	30.0000
16	0.0000	140.0000	120.0000	30.0000
17	0.0000	140.0000	120.0000	30.0000
18	0.0000	140.0000	120.0000	30.0000
19	0.0000	140.0000	120.0000	30.0000
20	0.0000	140.0000	120.0000	30.0000
21	0.0000	20.0000		

```

max obj function = 0.281741
max obj function = 0.189893
level 95 max obj function = 0.132685
max obj function = 0.106938
max obj function = 0.081224
number of forward models: 1680

```

southern transect sample FT89-201
 modified simplex algorithm
 model 1

inversion control parameters:

```

-----
number of solutions (l) = 150
number of timesteps (m) = 16
number of parameters (m+1) = 17
number of substeps for integration (nstep) = 12
number of substeps for track component gen = 3
timestep length (delt) = 7.8750000000000D+14
obj fnct (2 = chi2; 3 = kol-smirnov) = 3
convergence tolerance (tol95) = 0.12573204447772
convergence tolerance (toler) = 7.7010877242603D-02
measured age = 257.000000000000
variance of error in measured age = 812.250000000000
number of data (n) = 117
number of tracks measured = 117
intermediate output every 500 forward models
random number generator seed = 3
expansion factor (alpha) = 1.30000000000000
reposition factor for explicit bound (delta) = 1.0000000000000D-01

```

	temperature bounds		rate bounds	
1	0.0000	140.0000	120.0000	30.0000
2	0.0000	140.0000	120.0000	30.0000
3	0.0000	140.0000	120.0000	30.0000
4	0.0000	140.0000	120.0000	30.0000
5	0.0000	140.0000	120.0000	30.0000
6	0.0000	140.0000	120.0000	30.0000
7	0.0000	140.0000	120.0000	30.0000
8	0.0000	140.0000	120.0000	30.0000
9	0.0000	140.0000	120.0000	30.0000
10	0.0000	140.0000	120.0000	30.0000
11	0.0000	140.0000	120.0000	30.0000
12	0.0000	140.0000	120.0000	30.0000
13	0.0000	140.0000	120.0000	30.0000
14	0.0000	140.0000	120.0000	30.0000
15	0.0000	140.0000	120.0000	30.0000
16	0.0000	140.0000	120.0000	30.0000
17	0.0000	20.0000		

```

max obj function = 0.214625
max obj function = 0.155181
level 95 max obj function = 0.125613
max obj function = 0.098900
max obj function = 0.076745
number of forward models: 1743

```


southern transect sample FT89-196
 modified simplex algorithm
 model 1

inversion control parameters:

 number of solutions (l) = 150
 number of timesteps (m) = 16
 number of parameters (m+1) = 17
 number of substeps for integration (nstep) = 12
 number of substeps for track component gen = 3
 timestep length (delt) = 7.8750000000000D+14
 obj fnct (2 = chi2; 3 = kol-smirnov) = 3
 convergence tolerance (tol95) = 0.13738074605910
 convergence tolerance (toler) = 8.4145706961199D-02
 measured age = 255.000000000000
 variance of error in measured age = 600.250000000000
 number of data (n) = 98
 number of tracks measured = 98
 intermediate output every 500 forward models
 random number generator seed = 3
 expansion factor (alpha) = 1.30000000000000
 reposition factor for explicit bound (delta) = 1.0000000000000D-01

	temperature bounds		rate bounds	
1	0.0000	140.0000	120.0000	30.0000
2	0.0000	140.0000	120.0000	30.0000
3	0.0000	140.0000	120.0000	30.0000
4	0.0000	140.0000	120.0000	30.0000
5	0.0000	140.0000	120.0000	30.0000
6	0.0000	140.0000	120.0000	30.0000
7	0.0000	140.0000	120.0000	30.0000
8	0.0000	140.0000	120.0000	30.0000
9	0.0000	140.0000	120.0000	30.0000
10	0.0000	140.0000	120.0000	30.0000
11	0.0000	140.0000	120.0000	30.0000
12	0.0000	140.0000	120.0000	30.0000
13	0.0000	140.0000	120.0000	30.0000
14	0.0000	140.0000	120.0000	30.0000
15	0.0000	140.0000	120.0000	30.0000
16	0.0000	140.0000	120.0000	30.0000
17	0.0000	20.0000		

max obj function = 0.227445
 max obj function = 0.152380
 level 95 max obj function = 0.137132
 max obj function = 0.118596
 max obj function = 0.091369
 max obj function = 0.083984
 number of forward models: 2114

southern transect sample FT89-203
 modified simplex algorithm
 model 1

inversion control parameters:

```

-----
number of solutions (l) = 150
number of timesteps (m) = 16
number of parameters (m+1) = 17
number of substeps for integration (nstep) = 12
number of substeps for track component gen = 3
timestep length (delt) = 7.8750000000000D+14
obj fnct (2 = chi2; 3 = kol-smirnov) = 3
convergence tolerance (tol95) = 0.12164209797599
convergence tolerance (toler) = 7.4505785010293D-02
measured age = 256.000000000000
variance of error in measured age = 345.96001116000
number of data (n) = 125
number of tracks measured = 125
intermediate output every 500 forward models
random number generator seed = 3
expansion factor (alpha) = 1.30000000000000
reposition factor for explicit bound (delta) = 1.0000000000000D-01

```

	temperature bounds		rate bounds	
1	0.0000	140.0000	120.0000	30.0000
2	0.0000	140.0000	120.0000	30.0000
3	0.0000	140.0000	120.0000	30.0000
4	0.0000	140.0000	120.0000	30.0000
5	0.0000	140.0000	120.0000	30.0000
6	0.0000	140.0000	120.0000	30.0000
7	0.0000	140.0000	120.0000	30.0000
8	0.0000	140.0000	120.0000	30.0000
9	0.0000	140.0000	120.0000	30.0000
10	0.0000	140.0000	120.0000	30.0000
11	0.0000	140.0000	120.0000	30.0000
12	0.0000	140.0000	120.0000	30.0000
13	0.0000	140.0000	120.0000	30.0000
14	0.0000	140.0000	120.0000	30.0000
15	0.0000	140.0000	120.0000	30.0000
16	0.0000	140.0000	120.0000	30.0000
17	0.0000	20.0000		

```

max obj function = 0.327516
max obj function = 0.236783
max obj function = 0.144844
level 95 max obj function = 0.121503
max obj function = 0.080441
max obj function = 0.074457
number of forward models: 2148

```

southern transect sample FT89-205
 modified simplex algorithm
 model 1

inversion control parameters:

 number of solutions (l) = 150
 number of timesteps (m) = 16
 number of parameters (m+1) = 17
 number of substeps for integration (nstep) = 12
 number of substeps for track component gen = 3
 timestep length (delt) = 7.8750000000000D+14
 obj fnct (2 = chi2; 3 = kol-smirnov) = 3
 convergence tolerance (tol95) = 0.13026437479008
 convergence tolerance (toler) = 7.9786929558922D-02
 measured age = 245.500000000000
 variance of error in measured age = 316.84001068000
 number of data (n) = 109
 number of tracks measured = 109
 intermediate output every 500 forward models
 random number generator seed = 3
 expansion factor (alpha) = 1.30000000000000
 reposition factor for explicit bound (delta) = 1.0000000000000D-01

	temperature bounds		rate bounds	
1	0.0000	140.0000	120.0000	30.0000
2	0.0000	140.0000	120.0000	30.0000
3	0.0000	140.0000	120.0000	30.0000
4	0.0000	140.0000	120.0000	30.0000
5	0.0000	140.0000	120.0000	30.0000
6	0.0000	140.0000	120.0000	30.0000
7	0.0000	140.0000	120.0000	30.0000
8	0.0000	140.0000	120.0000	30.0000
9	0.0000	140.0000	120.0000	30.0000
10	0.0000	140.0000	120.0000	30.0000
11	0.0000	140.0000	120.0000	30.0000
12	0.0000	140.0000	120.0000	30.0000
13	0.0000	140.0000	120.0000	30.0000
14	0.0000	140.0000	120.0000	30.0000
15	0.0000	140.0000	120.0000	30.0000
16	0.0000	140.0000	120.0000	30.0000
17	0.0000	20.0000		

max obj function = 0.285917
 max obj function = 0.223139
 max obj function = 0.149346
 level 95 max obj function = 0.130129

southern transect sample FT89-194
 modified simplex algorithm
 model 1

inversion control parameters:

```

-----
number of solutions (l) = 150
number of timesteps (m) = 16
number of parameters (m+1) = 17
number of substeps for integration (nstep) = 12
number of substeps for track component gen = 3
timestep length (delt) = 7.8750000000000D+14
obj fnct (2 = chi2; 3 = kol-smirnov) = 3
convergence tolerance (tol95) = 0.13272240992100
convergence tolerance (toler) = 8.1292476076613D-02
measured age = 241.000000000000
variance of error in measured age = 449.44003392000
number of data (n) = 105
number of tracks measured = 105
intermediate output every 500 forward models
random number generator seed = 3
expansion factor (alpha) = 1.30000000000000
reposition factor for explicit bound (delta) = 1.0000000000000D-01

```

	temperature bounds		rate bounds	
1	0.0000	140.0000	120.0000	30.0000
2	0.0000	140.0000	120.0000	30.0000
3	0.0000	140.0000	120.0000	30.0000
4	0.0000	140.0000	120.0000	30.0000
5	0.0000	140.0000	120.0000	30.0000
6	0.0000	140.0000	120.0000	30.0000
7	0.0000	140.0000	120.0000	30.0000
8	0.0000	140.0000	120.0000	30.0000
9	0.0000	140.0000	120.0000	30.0000
10	0.0000	140.0000	120.0000	30.0000
11	0.0000	140.0000	120.0000	30.0000
12	0.0000	140.0000	120.0000	30.0000
13	0.0000	140.0000	120.0000	30.0000
14	0.0000	140.0000	120.0000	30.0000
15	0.0000	140.0000	120.0000	30.0000
16	0.0000	140.0000	120.0000	30.0000
17	0.0000	20.0000		

```

max obj function = 0.269746
max obj function = 0.195463
max obj function = 0.136060
level 95 max obj function = 0.132645
max obj function = 0.090533
max obj function = 0.081076
number of forward models: 2153

```

southern transect sample FT89-227
 modified simplex algorithm
 model 1

inversion control parameters:

 number of solutions (l) = 150
 number of timesteps (m) = 16
 number of parameters (m+1) = 17
 number of substeps for integration (nstep) = 12
 number of substeps for track component gen = 3
 timestep length (delt) = 7.8750000000000D+14
 obj fnct (2 = chi2; 3 = kol-smirnov) = 3
 convergence tolerance (tol95) = 0.13335897189397
 convergence tolerance (toler) = 8.1682370285054D-02
 measured age = 285.000000000000
 variance of error in measured age = 462.250000000000
 number of data (n) = 104
 number of tracks measured = 104
 intermediate output every 500 forward models
 random number generator seed = 3
 expansion factor (alpha) = 1.30000000000000
 reposition factor for explicit bound (delta) = 1.0000000000000D-01

	temperature bounds		rate bounds	
1	0.0000	140.0000	120.0000	30.0000
2	0.0000	140.0000	120.0000	30.0000
3	0.0000	140.0000	120.0000	30.0000
4	0.0000	140.0000	120.0000	30.0000
5	0.0000	140.0000	120.0000	30.0000
6	0.0000	140.0000	120.0000	30.0000
7	0.0000	140.0000	120.0000	30.0000
8	0.0000	140.0000	120.0000	30.0000
9	0.0000	140.0000	120.0000	30.0000
10	0.0000	140.0000	120.0000	30.0000
11	0.0000	140.0000	120.0000	30.0000
12	0.0000	140.0000	120.0000	30.0000
13	0.0000	140.0000	120.0000	30.0000
14	0.0000	140.0000	120.0000	30.0000
15	0.0000	140.0000	120.0000	30.0000
16	0.0000	140.0000	120.0000	30.0000
17	0.0000	20.0000		

max obj function = 0.147382
 level 95 max obj function = 0.133139
 max obj function = 0.085512
 max obj function = 0.081614
 number of forward models: 1046

southern transect sample FT89-224
 modified simplex algorithm
 model 1

inversion control parameters:

```

-----
number of solutions (l) = 150
number of timesteps (m) = 16
number of parameters (m+1) = 17
number of substeps for integration (nstep) = 12
number of substeps for track component gen = 3
timestep length (delt) = 7.8750000000000D+14
obj fnct (2 = chi2; 3 = kol-smirnov) = 3
convergence tolerance (tol95) = 0.13400478183034
convergence tolerance (toler) = 8.2077928871086D-02
measured age = 246.000000000000
variance of error in measured age = 436.80998328000
number of data (n) = 103
number of tracks measured = 103
intermediate output every 500 forward models
random number generator seed = 3
expansion factor (alpha) = 1.30000000000000
reposition factor for explicit bound (delta) = 1.0000000000000D-01

```

	temperature bounds		rate bounds	
1	0.0000	140.0000	120.0000	30.0000
2	0.0000	140.0000	120.0000	30.0000
3	0.0000	140.0000	120.0000	30.0000
4	0.0000	140.0000	120.0000	30.0000
5	0.0000	140.0000	120.0000	30.0000
6	0.0000	140.0000	120.0000	30.0000
7	0.0000	140.0000	120.0000	30.0000
8	0.0000	140.0000	120.0000	30.0000
9	0.0000	140.0000	120.0000	30.0000
10	0.0000	140.0000	120.0000	30.0000
11	0.0000	140.0000	120.0000	30.0000
12	0.0000	140.0000	120.0000	30.0000
13	0.0000	140.0000	120.0000	30.0000
14	0.0000	140.0000	120.0000	30.0000
15	0.0000	140.0000	120.0000	30.0000
16	0.0000	140.0000	120.0000	30.0000
17	0.0000	20.0000		

```

max obj function = 0.231842
max obj function = 0.152464
level 95 max obj function = 0.134004
max obj function = 0.107507
max obj function = 0.081989
number of forward models: 1879

```

southern transect sample FT89-193
 modified simplex algorithm
 model 1

inversion control parameters:

```

-----
number of solutions (l) = 150
number of timesteps (m) = 16
number of parameters (m+1) = 17
number of substeps for integration (nstep) = 12
number of substeps for track component gen = 3
timestep length (delt) = 7.8750000000000D+14
obj fnct (2 = chi2; 3 = kol-smirnov) = 3
convergence tolerance (tol95) = 0.12573204447772
convergence tolerance (toler) = 7.7010877242603D-02
measured age = 231.000000000000
variance of error in measured age = 324.00000720000
number of data (n) = 117
number of tracks measured = 117
intermediate output every 500 forward models
random number generator seed = 3
expansion factor (alpha) = 1.30000000000000
reposition factor for explicit bound (delta) = 1.0000000000000D-01

```

	temperature bounds		rate bounds	
1	0.0000	140.0000	120.0000	30.0000
2	0.0000	140.0000	120.0000	30.0000
3	0.0000	140.0000	120.0000	30.0000
4	0.0000	140.0000	120.0000	30.0000
5	0.0000	140.0000	120.0000	30.0000
6	0.0000	140.0000	120.0000	30.0000
7	0.0000	140.0000	120.0000	30.0000
8	0.0000	140.0000	120.0000	30.0000
9	0.0000	140.0000	120.0000	30.0000
10	0.0000	140.0000	120.0000	30.0000
11	0.0000	140.0000	120.0000	30.0000
12	0.0000	140.0000	120.0000	30.0000
13	0.0000	140.0000	120.0000	30.0000
14	0.0000	140.0000	120.0000	30.0000
15	0.0000	140.0000	120.0000	30.0000
16	0.0000	140.0000	120.0000	30.0000
17	0.0000	20.0000		

```

max obj function = 0.355894
max obj function = 0.259422
max obj function = 0.153341
level 95 max obj function = 0.125649
max obj function = 0.095744
max obj function = 0.076993
number of forward models: 2405

```

southern transect sample FT89-191
 modified simplex algorithm
 model 1

inversion control parameters:

```

-----
number of solutions (l) = 150
number of timesteps (m) = 16
number of parameters (m+1) = 17
number of substeps for integration (nstep) = 12
number of substeps for track component gen = 3
timestep length (delt) = 7.8750000000000D+14
obj fnct (2 = chi2; 3 = kol-smirnov) = 3
convergence tolerance (tol95) = 0.21503488089145
convergence tolerance (toler) = 0.13170886454601
measured age = 253.000000000000
variance of error in measured age = 761.76002208000
number of data (n) = 40
number of tracks measured = 40
intermediate output every 500 forward models
random number generator seed = 3
expansion factor (alpha) = 1.30000000000000
reposition factor for explicit bound (delta) = 1.0000000000000D-01

```

	temperature bounds		rate bounds	
1	0.0000	140.0000	120.0000	30.0000
2	0.0000	140.0000	120.0000	30.0000
3	0.0000	140.0000	120.0000	30.0000
4	0.0000	140.0000	120.0000	30.0000
5	0.0000	140.0000	120.0000	30.0000
6	0.0000	140.0000	120.0000	30.0000
7	0.0000	140.0000	120.0000	30.0000
8	0.0000	140.0000	120.0000	30.0000
9	0.0000	140.0000	120.0000	30.0000
10	0.0000	140.0000	120.0000	30.0000
11	0.0000	140.0000	120.0000	30.0000
12	0.0000	140.0000	120.0000	30.0000
13	0.0000	140.0000	120.0000	30.0000
14	0.0000	140.0000	120.0000	30.0000
15	0.0000	140.0000	120.0000	30.0000
16	0.0000	140.0000	120.0000	30.0000
17	0.0000	20.0000		

```

max obj function = 0.268509
level 95 max obj function = 0.214947
max obj function = 0.184665
max obj function = 0.131554
number of forward models: 1242

```


southern transect sample FT89-197
 modified simplex algorithm
 model 1

inversion control parameters:

 number of solutions (l) = 150
 number of timesteps (m) = 16
 number of parameters (m+1) = 17
 number of substeps for integration (nstep) = 12
 number of substeps for track component gen = 3
 timestep length (delt) = 7.8750000000000D+14
 obj fnct (2 = chi2; 3 = kol-smirnov) = 3
 convergence tolerance (tol95) = 0.12908548742234
 convergence tolerance (toler) = 7.9064861046183D-02
 measured age = 248.000000000000
 variance of error in measured age = 420.250000000000
 number of data (n) = 111
 number of tracks measured = 111
 intermediate output every 500 forward models
 random number generator seed = 3
 expansion factor (alpha) = 1.30000000000000
 reposition factor for explicit bound (delta) = 1.0000000000000D-01

	temperature bounds		rate bounds	
1	0.0000	140.0000	120.0000	30.0000
2	0.0000	140.0000	120.0000	30.0000
3	0.0000	140.0000	120.0000	30.0000
4	0.0000	140.0000	120.0000	30.0000
5	0.0000	140.0000	120.0000	30.0000
6	0.0000	140.0000	120.0000	30.0000
7	0.0000	140.0000	120.0000	30.0000
8	0.0000	140.0000	120.0000	30.0000
9	0.0000	140.0000	120.0000	30.0000
10	0.0000	140.0000	120.0000	30.0000
11	0.0000	140.0000	120.0000	30.0000
12	0.0000	140.0000	120.0000	30.0000
13	0.0000	140.0000	120.0000	30.0000
14	0.0000	140.0000	120.0000	30.0000
15	0.0000	140.0000	120.0000	30.0000
16	0.0000	140.0000	120.0000	30.0000
17	0.0000	20.0000		

max obj function = 0.328597
 max obj function = 0.208653
 level 95 max obj function = 0.128849
 max obj function = 0.098192
 max obj function = 0.079055
 number of forward models: 1682

southern transect sample FT89-198
 modified simplex algorithm
 model 1

inversion control parameters:

```

-----
number of solutions (l) = 150
number of timesteps (m) = 16
number of parameters (m+1) = 17
number of substeps for integration (nstep) = 12
number of substeps for track component gen = 3
timestep length (delt) = 7.8750000000000D+14
obj fnct (2 = chi2; 3 = kol-smirnov) = 3
convergence tolerance (tol95) = 0.14335658726097
convergence tolerance (toler) = 8.7805909697342D-02
measured age = 194.000000000000
variance of error in measured age = 396.00998408000
number of data (n) = 90
number of tracks measured = 90
intermediate output every 500 forward models
random number generator seed = 3
expansion factor (alpha) = 1.30000000000000
reposition factor for explicit bound (delta) = 1.0000000000000D-01

```

	temperature bounds		rate bounds	
1	0.0000	140.0000	120.0000	30.0000
2	0.0000	140.0000	120.0000	30.0000
3	0.0000	140.0000	120.0000	30.0000
4	0.0000	140.0000	120.0000	30.0000
5	0.0000	140.0000	120.0000	30.0000
6	0.0000	140.0000	120.0000	30.0000
7	0.0000	140.0000	120.0000	30.0000
8	0.0000	140.0000	120.0000	30.0000
9	0.0000	140.0000	120.0000	30.0000
10	0.0000	140.0000	120.0000	30.0000
11	0.0000	140.0000	120.0000	30.0000
12	0.0000	140.0000	120.0000	30.0000
13	0.0000	140.0000	120.0000	30.0000
14	0.0000	140.0000	120.0000	30.0000
15	0.0000	140.0000	120.0000	30.0000
16	0.0000	140.0000	120.0000	30.0000
17	0.0000	20.0000		

```

max obj function = 0.562221
max obj function = 0.264501
level 95 max obj function = 0.142845
max obj function = 0.135775
max obj function = 0.087521
number of forward models: 1950

```

central transect sample FT89-212
 modified simplex algorithm
 model 1

inversion control parameters:

```

-----
number of solutions (l) = 150
number of timesteps (m) = 16
number of parameters (m+1) = 17
number of substeps for integration (nstep) = 12
number of substeps for track component gen = 3
timestep length (delt) = 7.8750000000000D+14
obj fnct (2 = chi2; 3 = kol-smirnov) = 3
convergence tolerance (tol95) = 0.13335897189397
convergence tolerance (toler) = 8.1682370285054D-02
measured age = 273.000000000000
variance of error in measured age = 404.01000804000
number of data (n) = 104
number of tracks measured = 104
intermediate output every 500 forward models
random number generator seed = 3
expansion factor (alpha) = 1.30000000000000
reposition factor for explicit bound (delta) = 1.0000000000000D-01

```

	temperature bounds		rate bounds	
1	120.0000	140.0000	120.0000	30.0000
2	120.0000	140.0000	120.0000	0.0000
3	0.0000	140.0000	120.0000	30.0000
4	0.0000	140.0000	120.0000	30.0000
5	0.0000	140.0000	120.0000	30.0000
6	0.0000	140.0000	120.0000	30.0000
7	0.0000	140.0000	120.0000	30.0000
8	0.0000	140.0000	120.0000	30.0000
9	0.0000	140.0000	120.0000	30.0000
10	0.0000	140.0000	120.0000	30.0000
11	0.0000	140.0000	120.0000	30.0000
12	0.0000	140.0000	120.0000	30.0000
13	0.0000	140.0000	120.0000	30.0000
14	0.0000	140.0000	120.0000	30.0000
15	0.0000	140.0000	120.0000	30.0000
16	0.0000	140.0000	120.0000	30.0000
17	0.0000	20.0000		

```

level 95 max obj function = 0.132743
max obj function = 0.092636
max obj function = 0.081678
number of forward models: 625

```

central transect sample FT89-211
 modified simplex algorithm
 model 1

inversion control parameters:

 number of solutions (l) = 150
 number of timesteps (m) = 16
 number of parameters (m+1) = 17
 number of substeps for integration (nstep) = 12
 number of substeps for track component gen = 3
 timestep length (delt) = 7.8750000000000D+14
 obj fnct (2 = chi2; 3 = kol-smirnov) = 3
 convergence tolerance (tol95) = 0.13808707845817
 convergence tolerance (toler) = 8.4578335555630D-02
 measured age = 276.000000000000
 variance of error in measured age = 445.21002532000
 number of data (n) = 97
 number of tracks measured = 97
 intermediate output every 500 forward models
 random number generator seed = 3
 expansion factor (alpha) = 1.30000000000000
 reposition factor for explicit bound (delta) = 1.0000000000000D-01

	temperature bounds		rate bounds	
1	120.0000	140.0000	120.0000	30.0000
2	120.0000	140.0000	120.0000	0.0000
3	0.0000	140.0000	120.0000	30.0000
4	0.0000	140.0000	120.0000	30.0000
5	0.0000	140.0000	120.0000	30.0000
6	0.0000	140.0000	120.0000	30.0000
7	0.0000	140.0000	120.0000	30.0000
8	0.0000	140.0000	120.0000	30.0000
9	0.0000	140.0000	120.0000	30.0000
10	0.0000	140.0000	120.0000	30.0000
11	0.0000	140.0000	120.0000	30.0000
12	0.0000	140.0000	120.0000	30.0000
13	0.0000	140.0000	120.0000	30.0000
14	0.0000	140.0000	120.0000	30.0000
15	0.0000	140.0000	120.0000	30.0000
16	0.0000	140.0000	120.0000	30.0000
17	0.0000	20.0000		

level 95 max obj function = 0.137856
 max obj function = 0.127752
 max obj function = 0.084532
 number of forward models: 860

central transect sample FT89-210
 modified simplex algorithm
 model 1

inversion control parameters:

 number of solutions (l) = 150
 number of timesteps (m) = 16
 number of parameters (m+1) = 17
 number of substeps for integration (nstep) = 12
 number of substeps for track component gen = 3
 timestep length (delt) = 7.8750000000000D+14
 obj fnct (2 = chi2; 3 = kol-smirnov) = 3
 convergence tolerance (tol95) = 0.13026437479008
 convergence tolerance (toler) = 7.9786929558922D-02
 measured age = 225.500000000000
 variance of error in measured age = 331.24001456000
 number of data (n) = 109
 number of tracks measured = 109
 intermediate output every 500 forward models
 random number generator seed = 3
 expansion factor (alpha) = 1.30000000000000
 reposition factor for explicit bound (delta) = 1.0000000000000D-01

	temperature bounds		rate bounds	
1	120.0000	140.0000	120.0000	30.0000
2	120.0000	140.0000	120.0000	0.0000
3	0.0000	140.0000	120.0000	30.0000
4	0.0000	140.0000	120.0000	30.0000
5	0.0000	140.0000	120.0000	30.0000
6	0.0000	140.0000	120.0000	30.0000
7	0.0000	140.0000	120.0000	30.0000
8	0.0000	140.0000	120.0000	30.0000
9	0.0000	140.0000	120.0000	30.0000
10	0.0000	140.0000	120.0000	30.0000
11	0.0000	140.0000	120.0000	30.0000
12	0.0000	140.0000	120.0000	30.0000
13	0.0000	140.0000	120.0000	30.0000
14	0.0000	140.0000	120.0000	30.0000
15	0.0000	140.0000	120.0000	30.0000
16	0.0000	140.0000	120.0000	30.0000
17	0.0000	20.0000		

max obj function = 0.285499
 max obj function = 0.184289
 level 95 max obj function = 0.130210
 max obj function = 0.117140
 max obj function = 0.079561
 number of forward models: 1836

central transect sample FT89-207
 modified simplex algorithm
 model 1

inversion control parameters:

 number of solutions (l) = 150
 number of timesteps (m) = 16
 number of parameters (m+1) = 17
 number of substeps for integration (nstep) = 12
 number of substeps for track component gen = 3
 timestep length (delt) = 7.8750000000000D+14
 obj fnc (2 = chi2; 3 = kol-smirnov) = 3
 convergence tolerance (tol95) = 0.13147616251021
 convergence tolerance (toler) = 8.0529149537504D-02
 measured age = 239.000000000000
 variance of error in measured age = 237.15998768000
 number of data (n) = 107
 number of tracks measured = 107
 intermediate output every 500 forward models
 random number generator seed = 3
 expansion factor (alpha) = 1.30000000000000
 reposition factor for explicit bound (delta) = 1.0000000000000D-01

	temperature bounds		rate bounds	
1	120.0000	140.0000	120.0000	30.0000
2	120.0000	140.0000	120.0000	0.0000
3	0.0000	140.0000	120.0000	30.0000
4	0.0000	140.0000	120.0000	30.0000
5	0.0000	140.0000	120.0000	30.0000
6	0.0000	140.0000	120.0000	30.0000
7	0.0000	140.0000	120.0000	30.0000
8	0.0000	140.0000	120.0000	30.0000
9	0.0000	140.0000	120.0000	30.0000
10	0.0000	140.0000	120.0000	30.0000
11	0.0000	140.0000	120.0000	30.0000
12	0.0000	140.0000	120.0000	30.0000
13	0.0000	140.0000	120.0000	30.0000
14	0.0000	140.0000	120.0000	30.0000
15	0.0000	140.0000	120.0000	30.0000
16	0.0000	140.0000	120.0000	30.0000
17	0.0000	20.0000		

max obj function = 0.270207
 max obj function = 0.162698
 level 95 max obj function = 0.131329
 max obj function = 0.104871
 max obj function = 0.080484
 number of forward models: 1866

central transect sample FT89-209
 modified simplex algorithm
 model 1

inversion control parameters:

```

-----
number of solutions (l) = 150
number of timesteps (m) = 16
number of parameters (m+1) = 17
number of substeps for integration (nstep) = 12
number of substeps for track component gen = 3
timestep length (delt) = 7.8750000000000D+14
obj fnct (2 = chi2; 3 = kol-smirnov) = 3
convergence tolerance (tol95) = 0.12908548742234
convergence tolerance (toler) = 7.9064861046183D-02
measured age = 203.000000000000
variance of error in measured age = 278.89002672000
number of data (n) = 111
number of tracks measured = 111
intermediate output every 500 forward models
random number generator seed = 3
expansion factor (alpha) = 1.30000000000000
reposition factor for explicit bound (delta) = 1.0000000000000D-01

```

	temperature bounds		rate bounds	
1	120.0000	140.0000	120.0000	30.0000
2	120.0000	140.0000	120.0000	0.0000
3	0.0000	140.0000	120.0000	30.0000
4	0.0000	140.0000	120.0000	30.0000
5	0.0000	140.0000	120.0000	30.0000
6	0.0000	140.0000	120.0000	30.0000
7	0.0000	140.0000	120.0000	30.0000
8	0.0000	140.0000	120.0000	30.0000
9	0.0000	140.0000	120.0000	30.0000
10	0.0000	140.0000	120.0000	30.0000
11	0.0000	140.0000	120.0000	30.0000
12	0.0000	140.0000	120.0000	30.0000
13	0.0000	140.0000	120.0000	30.0000
14	0.0000	140.0000	120.0000	30.0000
15	0.0000	140.0000	120.0000	30.0000
16	0.0000	140.0000	120.0000	30.0000
17	0.0000	20.0000		

```

max obj function = 0.413724
max obj function = 0.215542
level 95 max obj function = 0.128772
max obj function = 0.126393
max obj function = 0.081329
max obj function = 0.079041
number of forward models: 2047

```

central transect sample FT89-206
 modified simplex algorithm
 model 1

inversion control parameters:

```
-----
number of solutions (l) = 150
number of timesteps (m) = 16
number of parameters (m+1) = 17
number of substeps for integration (nstep) = 12
number of substeps for track component gen = 3
timestep length (delt) = 7.8750000000000D+14
obj fnct (2 = chi2; 3 = kol-smirnov) = 3
convergence tolerance (tol95) = 0.136000000000000
convergence tolerance (toler) = 8.3300000000000D-02
measured age = 248.000000000000
variance of error in measured age = 345.960000000000
number of data (n) = 100
number of tracks measured = 100
intermediate output every 500 forward models
random number generator seed = 3
expansion factor (alpha) = 1.30000000000000
reposition factor for explicit bound (delta) = 1.0000000000000D-01
```

	temperature bounds		rate bounds	
1	120.0000	140.0000	120.0000	30.0000
2	120.0000	140.0000	120.0000	0.0000
3	0.0000	140.0000	120.0000	30.0000
4	0.0000	140.0000	120.0000	30.0000
5	0.0000	140.0000	120.0000	30.0000
6	0.0000	140.0000	120.0000	30.0000
7	0.0000	140.0000	120.0000	30.0000
8	0.0000	140.0000	120.0000	30.0000
9	0.0000	140.0000	120.0000	30.0000
10	0.0000	140.0000	120.0000	30.0000
11	0.0000	140.0000	120.0000	30.0000
12	0.0000	140.0000	120.0000	30.0000
13	0.0000	140.0000	120.0000	30.0000
14	0.0000	140.0000	120.0000	30.0000
15	0.0000	140.0000	120.0000	30.0000
16	0.0000	140.0000	120.0000	30.0000
17	0.0000	20.0000		

```
max obj function = 0.278930
max obj function = 0.210665
max obj function = 0.156599
level 95 max obj function = 0.135934
max obj function = 0.087919
max obj function = 0.082829
number of forward models: 2068
```


central transect sample FT89-208
 modified simplex algorithm
 model 1

inversion control parameters:

 number of solutions (l) = 150
 number of timesteps (m) = 16
 number of parameters (m+1) = 17
 number of substeps for integration (nstep) = 12
 number of substeps for track component gen = 3
 timestep length (delt) = 7.8750000000000D+14
 obj fnct (2 = chi2; 3 = kol-smirnov) = 3
 convergence tolerance (tol95) = 0.12573204447772
 convergence tolerance (toler) = 7.7010877242603D-02
 measured age = 213.000000000000
 variance of error in measured age = 141.61000714000
 number of data (n) = 117
 number of tracks measured = 117
 intermediate output every 500 forward models
 random number generator seed = 3
 expansion factor (alpha) = 1.30000000000000
 reposition factor for explicit bound (delta) = 1.0000000000000D-01

	temperature bounds		rate bounds	
1	120.0000	140.0000	120.0000	30.0000
2	120.0000	140.0000	120.0000	0.0000
3	0.0000	140.0000	120.0000	30.0000
4	0.0000	140.0000	120.0000	30.0000
5	0.0000	140.0000	120.0000	30.0000
6	0.0000	140.0000	120.0000	30.0000
7	0.0000	140.0000	120.0000	30.0000
8	0.0000	140.0000	120.0000	30.0000
9	0.0000	140.0000	120.0000	30.0000
10	0.0000	140.0000	120.0000	30.0000
11	0.0000	140.0000	120.0000	30.0000
12	0.0000	140.0000	120.0000	30.0000
13	0.0000	140.0000	120.0000	30.0000
14	0.0000	140.0000	120.0000	30.0000
15	0.0000	140.0000	120.0000	30.0000
16	0.0000	140.0000	120.0000	30.0000
17	0.0000	20.0000		

max obj function = 0.462354
 max obj function = 0.239486
 level 95 max obj function = 0.125460
 max obj function = 0.119067
 max obj function = 0.079659
 max obj function = 0.076984
 number of forward models: 2052

northern transect sample FT89-221
 modified simplex algorithm
 model 1

inversion control parameters:

```

-----
number of solutions (l) = 150
number of timesteps (m) = 16
number of parameters (m+1) = 17
number of substeps for integration (nstep) = 12
number of substeps for track component gen = 3
timestep length (delt) = 7.8750000000000D+14
obj fnct (2 = chi2; 3 = kol-smirnov) = 3
convergence tolerance (tol95) = 0.13953305588358
convergence tolerance (toler) = 8.5463996728693D-02
measured age = 190.000000000000
variance of error in measured age = 324.000000000000
number of data (n) = 95
number of tracks measured = 95
intermediate output every 500 forward models
random number generator seed = 3
expansion factor (alpha) = 1.30000000000000
reposition factor for explicit bound (delta) = 1.0000000000000D-01

```

	temperature bounds		rate bounds	
1	0.0000	140.0000	120.0000	30.0000
2	0.0000	140.0000	120.0000	30.0000
3	0.0000	140.0000	120.0000	30.0000
4	0.0000	140.0000	120.0000	30.0000
5	0.0000	140.0000	120.0000	30.0000
6	0.0000	140.0000	120.0000	30.0000
7	0.0000	140.0000	120.0000	30.0000
8	0.0000	140.0000	120.0000	30.0000
9	0.0000	140.0000	120.0000	30.0000
10	0.0000	140.0000	120.0000	30.0000
11	0.0000	140.0000	120.0000	30.0000
12	0.0000	140.0000	120.0000	30.0000
13	0.0000	140.0000	120.0000	30.0000
14	0.0000	140.0000	120.0000	30.0000
15	0.0000	140.0000	120.0000	30.0000
16	0.0000	140.0000	120.0000	30.0000
17	0.0000	20.0000		

```

max obj function = 0.624099
max obj function = 0.250158
max obj function = 0.146155
level 95 max obj function = 0.139130
max obj function = 0.100527
max obj function = 0.085385
number of forward models: 2318

```

northern transect sample FT89-232
 modified simplex algorithm
 model 1

inversion control parameters:

```

-----
number of solutions (l) = 150
number of timesteps (m) = 16
number of parameters (m+1) = 17
number of substeps for integration (nstep) = 12
number of substeps for track component gen = 3
timestep length (delt) = 7.8750000000000D+14
obj fnct (2 = chi2; 3 = kol-smirnov) = 3
convergence tolerance (tol95) = 0.12967091213740
convergence tolerance (toler) = 7.9423433684158D-02
measured age = 190.000000000000
variance of error in measured age = 156.250000000000
number of data (n) = 110
number of tracks measured = 110
intermediate output every 500 forward models
random number generator seed = 3
expansion factor (alpha) = 1.30000000000000
reposition factor for explicit bound (delta) = 1.0000000000000D-01

```

	temperature bounds		rate bounds	
1	0.0000	140.0000	120.0000	30.0000
2	0.0000	140.0000	120.0000	30.0000
3	0.0000	140.0000	120.0000	30.0000
4	0.0000	140.0000	120.0000	30.0000
5	0.0000	140.0000	120.0000	30.0000
6	0.0000	140.0000	120.0000	30.0000
7	0.0000	140.0000	120.0000	30.0000
8	0.0000	140.0000	120.0000	30.0000
9	0.0000	140.0000	120.0000	30.0000
10	0.0000	140.0000	120.0000	30.0000
11	0.0000	140.0000	120.0000	30.0000
12	0.0000	140.0000	120.0000	30.0000
13	0.0000	140.0000	120.0000	30.0000
14	0.0000	140.0000	120.0000	30.0000
15	0.0000	140.0000	120.0000	30.0000
16	0.0000	140.0000	120.0000	30.0000
17	0.0000	20.0000		

```

max obj function = 0.808216
max obj function = 0.286181
level 95 max obj function = 0.129496
max obj function = 0.128742
max obj function = 0.079414
number of forward models: 1717

```

northern transect sample FT89-233
 modified simplex algorithm
 model 1

inversion control parameters:

 number of solutions (l) = 150
 number of timesteps (m) = 16
 number of parameters (m+1) = 17
 number of substeps for integration (nstep) = 12
 number of substeps for track component gen = 3
 timestep length (delt) = 7.8750000000000D+14
 obj fnct (2 = chi2; 3 = kol-smirnov) = 3
 convergence tolerance (tol95) = 0.136000000000000
 convergence tolerance (toler) = 8.3300000000000D-02
 measured age = 172.000000000000
 variance of error in measured age = 234.09000612000
 number of data (n) = 100
 number of tracks measured = 100
 intermediate output every 500 forward models
 random number generator seed = 3
 expansion factor (alpha) = 1.30000000000000
 reposition factor for explicit bound (delta) = 1.0000000000000D-01

	temperature bounds		rate bounds	
1	0.0000	140.0000	120.0000	30.0000
2	0.0000	140.0000	120.0000	30.0000
3	0.0000	140.0000	120.0000	30.0000
4	0.0000	140.0000	120.0000	30.0000
5	0.0000	140.0000	120.0000	30.0000
6	0.0000	140.0000	120.0000	30.0000
7	0.0000	140.0000	120.0000	30.0000
8	0.0000	140.0000	120.0000	30.0000
9	0.0000	140.0000	120.0000	30.0000
10	0.0000	140.0000	120.0000	30.0000
11	0.0000	140.0000	120.0000	30.0000
12	0.0000	140.0000	120.0000	30.0000
13	0.0000	140.0000	120.0000	30.0000
14	0.0000	140.0000	120.0000	30.0000
15	0.0000	140.0000	120.0000	30.0000
16	0.0000	140.0000	120.0000	30.0000
17	0.0000	20.0000		

max obj function = 0.871541
 max obj function = 0.284079
 max obj function = 0.170782
 level 95 max obj function = 0.135751
 max obj function = 0.123689
 max obj function = 0.083132
 number of forward models: 2460

deer lake basin FT90-034
 modified simplex algorithm
 model 1

inversion control parameters:

```

-----
number of solutions (l) = 150
number of timesteps (m) = 16
number of parameters (m+1) = 17
number of substeps for integration (nstep) = 12
number of substeps for track component gen = 3
timestep length (delt) = 7.8750000000000D+14
obj fnct (2 = chi2; 3 = kol-smirnov) = 3
convergence tolerance (tol95) = 0.12967091213740
convergence tolerance (toler) = 7.9423433684158D-02
measured age = 252.000000000000
variance of error in measured age = 453.68996592000
number of data (n) = 110
number of tracks measured = 110
intermediate output every 500 forward models
random number generator seed = 3
expansion factor (alpha) = 1.30000000000000
reposition factor for explicit bound (delta) = 1.0000000000000D-01

```

	temperature bounds		rate bounds	
1	0.0000	140.0000	120.0000	30.0000
2	0.0000	140.0000	120.0000	0.0000
3	20.0000	40.0000	120.0000	120.0000
4	0.0000	140.0000	120.0000	30.0000
5	0.0000	140.0000	120.0000	30.0000
6	0.0000	140.0000	120.0000	30.0000
7	0.0000	140.0000	120.0000	30.0000
8	0.0000	140.0000	120.0000	30.0000
9	0.0000	140.0000	120.0000	30.0000
10	0.0000	140.0000	120.0000	30.0000
11	0.0000	140.0000	120.0000	30.0000
12	0.0000	140.0000	120.0000	30.0000
13	0.0000	140.0000	120.0000	30.0000
14	0.0000	140.0000	120.0000	30.0000
15	0.0000	140.0000	120.0000	30.0000
16	0.0000	140.0000	120.0000	30.0000
17	0.0000	20.0000		

```

max obj function = 0.309179
max obj function = 0.214428
level 95 max obj function = 0.129636
max obj function = 0.090641
max obj function = 0.078735
number of forward models: 1569

```

deer lake basin sample FT90-035
 modified simplex algorithm
 model 1

inversion control parameters:

```

-----
number of solutions (l) = 150
number of timesteps (m) = 16
number of parameters (m+1) = 17
number of substeps for integration (nstep) = 12
number of substeps for track component gen = 3
timestep length (delt) = 7.8750000000000D+14
obj fnct (2 = chi2; 3 = kol-smirnov) = 3
convergence tolerance (tol95) = 0.12967091213740
convergence tolerance (toler) = 7.9423433684158D-02
measured age = 224.000000000000
variance of error in measured age = 466.56001728000
number of data (n) = 110
number of tracks measured = 110
intermediate output every 500 forward models
random number generator seed = 3
expansion factor (alpha) = 1.30000000000000
reposition factor for explicit bound (delta) = 1.0000000000000D-01

```

	temperature bounds		rate bounds	
1	0.0000	140.0000	120.0000	30.0000
2	0.0000	140.0000	120.0000	0.0000
3	20.0000	40.0000	120.0000	120.0000
4	0.0000	140.0000	120.0000	30.0000
5	0.0000	140.0000	120.0000	30.0000
6	0.0000	140.0000	120.0000	30.0000
7	0.0000	140.0000	120.0000	30.0000
8	0.0000	140.0000	120.0000	30.0000
9	0.0000	140.0000	120.0000	30.0000
10	0.0000	140.0000	120.0000	30.0000
11	0.0000	140.0000	120.0000	30.0000
12	0.0000	140.0000	120.0000	30.0000
13	0.0000	140.0000	120.0000	30.0000
14	0.0000	140.0000	120.0000	30.0000
15	0.0000	140.0000	120.0000	30.0000
16	0.0000	140.0000	120.0000	30.0000
17	0.0000	20.0000		

```

max obj function = 0.361171
max obj function = 0.234507
max obj function = 0.171751
level 95 max obj function = 0.128428
max obj function = 0.085922
max obj function = 0.079384
number of forward models: 2091

```

hare bay sample FT90-050
 modified simplex algorithm
 model 1

inversion control parameters:

```

-----
number of solutions (l) = 150
number of timesteps (m) = 16
number of parameters (m+1) = 17
number of substeps for integration (nstep) = 12
number of substeps for track component gen = 3
timestep length (delt) = 7.8750000000000D+14
obj fnct (2 = chi2; 3 = kol-smirnov) = 3
convergence tolerance (tol95) = 0.136000000000000
convergence tolerance (toler) = 8.3300000000000D-02
measured age = 262.000000000000
variance of error in measured age = 948.63995072000
number of data (n) = 100
number of tracks measured = 100
intermediate output every 500 forward models
random number generator seed = 3
expansion factor (alpha) = 1.300000000000000
reposition factor for explicit bound (delta) = 1.0000000000000D-01

```

	temperature bounds		rate bounds	
1	120.0000	140.0000	120.0000	30.0000
2	120.0000	140.0000	30.0000	120.0000
3	0.0000	140.0000	120.0000	120.0000
4	0.0000	140.0000	120.0000	30.0000
5	0.0000	140.0000	120.0000	30.0000
6	0.0000	140.0000	120.0000	30.0000
7	0.0000	140.0000	120.0000	30.0000
8	0.0000	140.0000	120.0000	30.0000
9	0.0000	140.0000	120.0000	30.0000
10	0.0000	140.0000	120.0000	30.0000
11	0.0000	140.0000	120.0000	30.0000
12	0.0000	140.0000	120.0000	30.0000
13	0.0000	140.0000	120.0000	30.0000
14	0.0000	140.0000	120.0000	30.0000
15	0.0000	140.0000	120.0000	30.0000
16	0.0000	140.0000	120.0000	30.0000
17	0.0000	20.0000		

```

max obj function = 0.249347 max obj function = 0.116672
max obj function = 0.195326 max obj function = 0.116633
max obj function = 0.172376 max obj function = 0.116608
max obj function = 0.161504 max obj function = 0.116599
max obj function = 0.155190 max obj function = 0.116584
max obj function = 0.136569 max obj function = 0.116563
level 95 max obj function = 0.135991 max obj function = 0.116550
max obj function = 0.130090 max obj function = 0.116526
max obj function = 0.127741 max obj function = 0.116507
max obj function = 0.125405 max obj function = 0.116496
max obj function = 0.123588
max obj function = 0.122287
max obj function = 0.120506
max obj function = 0.119243
max obj function = 0.118693
max obj function = 0.118265
max obj function = 0.117970
max obj function = 0.117743
max obj function = 0.117544
max obj function = 0.117414
max obj function = 0.117320
max obj function = 0.117219
max obj function = 0.117105
max obj function = 0.117003
max obj function = 0.116902
max obj function = 0.116827
max obj function = 0.116757
max obj function = 0.116712

```

western platform sample FT89-213
 modified simplex algorithm
 model 1

inversion control parameters:

```

-----
number of solutions (l) = 150
number of timesteps (m) = 16
number of parameters (m+1) = 17
number of substeps for integration (nstep) = 12
number of substeps for track component gen = 3
timestep length (delt) = 7.8750000000000D+14
obj fnct (2 = chi2; 3 = kol-smirnov) = 3
convergence tolerance (tol95) = 0.26671794378793
convergence tolerance (toler) = 0.16336474057011
measured age = 151.500000000000
variance of error in measured age = 313.29002832000
number of data (n) = 26
number of tracks measured = 26
intermediate output every 500 forward models
random number generator seed = 3
expansion factor (alpha) = 1.30000000000000
reposition factor for explicit bound (delta) = 1.0000000000000D-01

```

	temperature bounds		rate bounds	
1	0.0000	140.0000	120.0000	30.0000
2	0.0000	140.0000	120.0000	30.0000
3	0.0000	140.0000	120.0000	30.0000
4	0.0000	140.0000	120.0000	30.0000
5	0.0000	140.0000	120.0000	30.0000
6	0.0000	140.0000	120.0000	30.0000
7	0.0000	140.0000	120.0000	30.0000
8	0.0000	140.0000	120.0000	30.0000
9	0.0000	140.0000	120.0000	30.0000
10	0.0000	140.0000	120.0000	30.0000
11	0.0000	140.0000	120.0000	30.0000
12	0.0000	140.0000	120.0000	30.0000
13	0.0000	140.0000	120.0000	30.0000
14	0.0000	140.0000	120.0000	30.0000
15	0.0000	140.0000	120.0000	30.0000
16	0.0000	140.0000	120.0000	30.0000
17	0.0000	20.0000		

```

max obj function = 1.713215
max obj function = 0.488486
max obj function = 0.316710
level 95 max obj function = 0.266477
max obj function = 0.263622
max obj function = 0.163294
number of forward models: 2360

```


lobster cove sample FT89-235
 modified simplex algorithm
 model 1

inversion control parameters:

 number of solutions (l) = 150
 number of timesteps (m) = 16
 number of parameters (m+1) = 17
 number of substeps for integration (nstep) = 12
 number of substeps for track component gen = 3
 timestep length (delt) = 7.8750000000000D+14
 obj fct (2 = chi2; 3 = kol-smirnov) = 3
 convergence tolerance (tol95) = 0.24426321075641
 convergence tolerance (toler) = 0.14961121658830
 measured age = 208.000000000000
 variance of error in measured age = 388.09003152000
 number of data (n) = 31
 number of tracks measured = 31
 intermediate output every 500 forward models
 random number generator seed = 3
 expansion factor (alpha) = 1.30000000000000
 reposition factor for explicit bound (delta) = 1.0000000000000D-01

	temperature bounds		rate bounds	
1	120.0000	140.0000	120.0000	30.0000
2	120.0000	140.0000	120.0000	0.0000
3	0.0000	140.0000	120.0000	30.0000
4	0.0000	140.0000	120.0000	30.0000
5	0.0000	140.0000	120.0000	30.0000
6	0.0000	140.0000	120.0000	30.0000
7	0.0000	140.0000	120.0000	30.0000
8	0.0000	140.0000	120.0000	30.0000
9	0.0000	140.0000	120.0000	30.0000
10	0.0000	140.0000	120.0000	30.0000
11	0.0000	140.0000	120.0000	30.0000
12	0.0000	140.0000	120.0000	30.0000
13	0.0000	140.0000	120.0000	30.0000
14	0.0000	140.0000	120.0000	30.0000
15	0.0000	140.0000	120.0000	30.0000
16	0.0000	140.0000	120.0000	30.0000
17	0.0000	20.0000		

max obj function = 0.562970
 max obj function = 0.314382
 level 95 max obj function = 0.244110
 max obj function = 0.232081
 max obj function = 0.149261
 number of forward models: 1839

devils room pluton sample LGRA-01
 modified simplex algorithm
 model 1

inversion control parameters:

 number of solutions (l) = 150
 number of timesteps (m) = 16
 number of parameters (m+1) = 17
 number of substeps for integration (nstep) = 12
 number of substeps for track component gen = 3
 timestep length (delt) = 7.8750000000000D+14
 obj fnct (2 = chi2; 3 = kol-smirnov) = 3
 convergence tolerance (tol95) = 0.13147616251021
 convergence tolerance (toler) = 8.0529149537504D-02
 measured age = 177.000000000000
 variance of error in measured age = 144.000000000000
 number of data (n) = 107
 number of tracks measured = 107
 intermediate output every 500 forward models
 random number generator seed = 3
 expansion factor (alpha) = 1.30000000000000
 reposition factor for explicit bound (delta) = 1.0000000000000D-01

	temperature bounds		rate bounds	
1	120.0000	140.0000	120.0000	30.0000
2	120.0000	140.0000	120.0000	0.0000
3	0.0000	140.0000	120.0000	120.0000
4	0.0000	140.0000	120.0000	30.0000
5	0.0000	140.0000	120.0000	30.0000
6	0.0000	140.0000	120.0000	30.0000
7	0.0000	140.0000	120.0000	30.0000
8	0.0000	140.0000	120.0000	30.0000
9	0.0000	140.0000	120.0000	30.0000
10	0.0000	140.0000	120.0000	30.0000
11	0.0000	140.0000	120.0000	30.0000
12	0.0000	140.0000	120.0000	30.0000
13	0.0000	140.0000	120.0000	30.0000
14	0.0000	140.0000	120.0000	30.0000
15	0.0000	140.0000	120.0000	30.0000
16	0.0000	140.0000	120.0000	30.0000
17	0.0000	20.0000		

max obj function = 0.785310
 max obj function = 0.254314
 level 95 max obj function = 0.131462
 max obj function = 0.090537
 max obj function = 0.080490
 number of forward models: 1638

east of southern transect 1 sample FT89-222
 modified simplex algorithm
 model 1

inversion control parameters:

 number of solutions (l) = 150
 number of timesteps (m) = 16
 number of parameters (m+1) = 17
 number of substeps for integration (nstep) = 12
 number of substeps for track component gen = 3
 timestep length (delt) = 7.8750000000000D+14
 obj fnct (2 = chi2; 3 = kol-smirnov) = 3
 convergence tolerance (tol95) = 0.13466006584483
 convergence tolerance (toler) = 8.2479290329957D-02
 measured age = 256.000000000000
 variance of error in measured age = 285.610000000000
 number of data (n) = 102
 number of tracks measured = 102
 intermediate output every 500 forward models
 random number generator seed = 3
 expansion factor (alpha) = 1.30000000000000
 reposition factor for explicit bound (delta) = 1.0000000000000D-01

	temperature bounds		rate bounds	
1	0.0000	140.0000	120.0000	30.0000
2	0.0000	140.0000	120.0000	30.0000
3	0.0000	140.0000	120.0000	30.0000
4	0.0000	140.0000	120.0000	30.0000
5	0.0000	140.0000	120.0000	30.0000
6	0.0000	140.0000	120.0000	30.0000
7	0.0000	140.0000	120.0000	30.0000
8	0.0000	140.0000	120.0000	30.0000
9	0.0000	140.0000	120.0000	30.0000
10	0.0000	140.0000	120.0000	30.0000
11	0.0000	140.0000	120.0000	30.0000
12	0.0000	140.0000	120.0000	30.0000
13	0.0000	140.0000	120.0000	30.0000
14	0.0000	140.0000	120.0000	30.0000
15	0.0000	140.0000	120.0000	30.0000
16	0.0000	140.0000	120.0000	30.0000
17	0.0000	20.0000		

max obj function = 0.317462
 max obj function = 0.205139
 level 95 max obj function = 0.134517
 max obj function = 0.107996
 max obj function = 0.082471
 number of forward models: 1666

east of st1 sample FT89-223
 modified simplex algorithm
 model 1

inversion control parameters:

 number of solutions (l) = 150
 number of timesteps (m) = 16
 number of parameters (m+1) = 17
 number of substeps for integration (nstep) = 12
 number of substeps for track component gen = 3
 timestep length (delt) = 7.8750000000000D+14
 obj fnct (2 = chi2; 3 = kol-smirnov) = 3
 convergence tolerance (tol95) = 0.23323807579381
 convergence tolerance (toler) = 0.14285832142371
 measured age = 279.000000000000
 variance of error in measured age = 571.20998088000
 number of data (n) = 34
 number of tracks measured = 34
 intermediate output every 500 forward models
 random number generator seed = 3
 expansion factor (alpha) = 1.30000000000000
 reposition factor for explicit bound (delta) = 1.0000000000000D-01

	temperature bounds		rate bounds	
1	0.0000	140.0000	120.0000	30.0000
2	0.0000	140.0000	120.0000	30.0000
3	0.0000	140.0000	120.0000	30.0000
4	0.0000	140.0000	120.0000	30.0000
5	0.0000	140.0000	120.0000	30.0000
6	0.0000	140.0000	120.0000	30.0000
7	0.0000	140.0000	120.0000	30.0000
8	0.0000	140.0000	120.0000	30.0000
9	0.0000	140.0000	120.0000	30.0000
10	0.0000	140.0000	120.0000	30.0000
11	0.0000	140.0000	120.0000	30.0000
12	0.0000	140.0000	120.0000	30.0000
13	0.0000	140.0000	120.0000	30.0000
14	0.0000	140.0000	120.0000	30.0000
15	0.0000	140.0000	120.0000	30.0000
16	0.0000	140.0000	120.0000	30.0000
17	0.0000	20.0000		

level 95 max obj function = 0.232015
 max obj function = 0.177222
 max obj function = 0.142405
 number of forward models: 668

References

- Arne, D.C., Duddy, I.R. and Sangster, D.F. (1989) Thermochronologic constraints on ore formation at the Gays River Pb-Zn deposit, Nova Scotia, Canada, from apatite fission track analysis, *Canadian Journal of Earth Sciences*, 27, 1013-1022.
- Baadsgaard, H., Erdmer, P., and Owen, J.V. (in prep.) U-Pb and Pb-Pb geochronology of the Long Range Inlier, Newfoundland.
- Beales, F.W., Carracedo, J.C, and Strangway, D.W. (1974) Paleomagnetism and the origin of Mississippi Valley-type ore deposits, *Canadian Journal of Earth Sciences*, 11, 211-223.
- Belt, E.S. (1968) Post Acadian rifts and related facies, eastern Canada, In: *Studies of Appalachian Geology-Northern and Maritime*, (Ed. by E. Zen, W.S. White, J.B. Hadley and J.B. Thompson, Jr.), Interscience Publishers, New York, 95-113.
- (1969) Newfoundland Carboniferous Stratigraphy and its relation to the Maritimes and Ireland, In: *North Atlantic Geology and Continental Drift* (Ed. M. Kay), American Association of Petroleum Geologists Memoir 12, 754-786.
- Betz, F. (1943) Late Paleozoic faulting in western Newfoundland, *Geological Society of America Bulletin*, 54, 687-706.
- Bevier, M. and Whalen, J.B. (1990) Tectonic significance of Silurian magmatism in the Canadian Appalachians, *Geology*, 18, 411-414.
- Bostock, H.H. (1983) Precambrian rocks of the Strait of Belle Isle area, In: *Geology of the Strait of Belle Isle Area, Northwestern Insular Newfoundland, Southern Labrador, and Adjacent Quebec*, Geological Survey of Canada Memoir 400, Part 1, 1-73.
- Bostock, H.H., and Cumming, L.M. (1973) Some notes on the Precambrian rocks of Gros Morne National Park, western Newfoundland, In: *Report of Activities, Part B*, Geological Survey of Canada Paper 73-1B, 109-119.
- Bostock, H.S. (1970) Physiographic subdivisions of Canada, In: *Geology and Economic Minerals of Canada* (Ed. by R.J.W. Douglas Geological Survey of Canada Economic Geology Report 1, 11-30.
- Bradley, D.C. (1982) Subsidence in Late Paleozoic basins in the Northern Appalachians, *Tectonics*, 1, 107-123.

- Castano, J.R. and Sparks, D.M. (1974) Interpretation of measurements in sedimentary rocks and determination of burial history using vitrinite reflectance and authigenic minerals, *Geol. Soc. Am., Special Paper*, no. 153, 31-52.
- Cawood, P.A. (1989) Acadian remobilization of a Taconian ophiolite, Hare Bay allochthon, northwestern Newfoundland, *Geology*, v. 17, 257-260.
- Cawood, P.A., and Williams, H. (1986) Northern extremity of the Humber Arm Allochthon in the Portland Creek Area, western Newfoundland, and relationships to nearby groups, In: *Current research, Part A, Geological Survey of Canada Paper 86-1A*, 675-682.
- (1988) Acadian basement thrusting, crustal delamination and structural styles in and around Humber Arm Allochthon, western Newfoundland, *Geology*, 16, 370-373.
- Cawood, P.A., Williams, H., and Grenier, R. (1987) Geology of Portland Creek area (12I/4), western Newfoundland, Geological Survey of Canada, Open File 1435, scale 1:50,000.
- Chandler, F.W., Sullivan, R.W. and Currie, K.L. (1987) The age of the Springdale group, Western Newfoundland and correlative rocks--Evidence for a Llandovery overlap assemblage in the Canadian Appalachians, *Royal Society of Edinburgh Transactions, Earth Sciences*, 79, 71-86.
- Clifford, P.M. (1965) Paleozoic flood basalts in northern Newfoundland and Labrador, *Canadian Journal of Earth Sciences*, 2, 183-187.
- Cumming, L.M. (1983) Lower Paleozoic autochthonous strata of the Strait of Belle Isle Area, In: *Geology of the Strait of Belle Isle Area, Northwestern Insular Newfoundland, Southern Labrador, and adjacent Quebec*, Geological Survey of Canada Memoir 400, Part 1, 1-73.
- Dimmell, P.M. (1979) Noranda-Brinex joint venture, Sops Arm-White Bay Concession, Report, January 10-December 31, 1979), Unpublished report, 59 pp.
- Dodge, F.C.W. and Naeser, C.W. (1968) Ages of apatites from granitic rocks of the Sierra Nevada Batholith, *Trans. Am. Geophys. Union*, 49, 259-274.
- Dodson, M.H. (1973) Closure temperature in cooling geochronological and petrological systems, *Contributions to Mineralogy and Petrology*, 40, 259-274.
- Donelick, R.A. (1987) The conventional fission track age equation: Implications for ages, zeta calibration, ^{238}U fission decay constant, and track length

distribution modelling, Rensselaer Polytechnic Institute, Troy, New York, 12180-3590 U.S.A. (copy available from fission track laboratory, Geology Department, Dalhousie University, Halifax, Nova Scotia).

- (1988) Etchable fission track length reduction in apatite: Experimental observations, theory and geological applications, Unpublished Ph.d thesis, Rensselaer Polytechnic Institute, Troy, New York, 414 pp.
- Duddy, I.R., Green, P.F. and Laslett, G.M. (1988) Thermal Annealing of Fission Tracks in Apatite: 3. Variable temperature behaviour. *Chemical Geology (Isotope Geoscience Section)* 73, 25-38.
- Dunning, G.R., Krogh, T.E., O'Brien, S.J., Colman-Sadd, S.P. and O'Neill, P., (1988) Geochronologic framework for the Central Mobile Belt in southern Newfoundland and the importance of Silurian orogeny, *Geological Association of Canada Program with Abstracts*, 13, p. A34.
- Dunning, G.R., O'Brien, S.J., Colman-Sadd, S.P., Blackwood, R.F. and Dickson, W.L. (1990) Silurian orogeny in the Newfoundland Appalachians, *Journal of Geology*, 98, 895-913.
- Epstein, A.G., Epstein, J.B. and Harris, L.D. (1977) conodont colour alteration - An index to organic metamorphism, *U.S. Geol. Surv., Prof. Pap. No. 995*, 26pp.
- Erdmer, P. (1984) Summary of field work in the northern Long Range Mountains, western Newfoundland, In: *Current Research Part A, Geological Survey of Canada Paper 84-1a*, 521-530.
- (1986) Geology of the Long Range Inlier in the Sandy Lake map area, western Newfoundland, In: *Current Research, Part B, Geological Survey of Canada Paper 86-1B*, 19-27.
- Faure, G. (1986) 15. The Fission-Track Method of Dating, In: *Principles of Isotope Geology*, 2nd ed., J. Wiley and Sons, New York, 267-281.
- Fitzgerald, P.G. and Gleadow, A.J.W. (1988) Fission-track geochronology, tectonics and structure of the Transantarctic Mountains in Northern Victoria Land, Antarctica, *Chemical Geology (Isotope Section)*, v. 73, 169-198.
- Fleischer, R., Price, P.B., and Walker, R.M. (1965) Tracks of charged particles in solids, *Science*, 149, 383-393.
- (1975) *Nuclear Tracks in Solids: Principles and Applications*: Los

Angeles, University of California Press.

- Friedlander, G., Kennedy, J.W., Macias, E.S., and Miller, J.M. (1981) Nuclear and Radiochemistry, John Wiley and Sons, New York.
- Gall, Q., and Hiscott, R.N. (1986) Diagenesis of locally uraniferous sandstones of the Deer Lake Group and sandstones of the Howley Formation, Carboniferous Deer Lake Subbasin, western Newfoundland, Bulletin of Canadian Petroleum Geologists, 34, 17-29.
- Galbraith, R.N. (1982) Statistical analysis of some fission track counts and neutron fluence measurements, Nuclear Tracks, 6, 99-107.
- Gleadow, A.J.W. and Duddy, I.R. (1981) A natural long term annealing experiment for apatite, Nuclear Tracks, 5, 169-174.
- Gleadow, A.J.W. and Fitzgerald, P.G. (1987) Uplift history and structure of the Transantarctic Mountains: new evidence from fission track dating of basement apatites in the Dry Valleys area, southern Victoria Land, Earth and Planetary Science Letters, 82, 1-14.
- Gleadow, A.J.W. and Lovering, J.F. (1975) Fission Track dating methods, A manual of principles and techniques applied in the Particle Track Laboratory, Department of Geology, University of Melbourne, Parkville, Australia 3052, Publication No.3.
- Gleadow, A.J.W., Duddy, I.R., and Lovering, J.F. (1983) Fission track analysis: A new tool for the evaluation of thermal histories and hydrocarbon potential, Australian Petroleum Exploration Association Journal, 23, 93-102.
- Gleadow, A.J.W., Duddy, I.R., Green, P.F., and Lovering, J.F. (1986) Confined fission track lengths in apatite: A diagnostic tool for thermal history analysis, Contrib. Mineral. Petrol., 94, 405-415.
- Grant, D.R. (1970) Quaternary geology, Great Northern Peninsula, Island of Newfoundland, In: Report of Activities, Part A, April to October 1969, Geological Survey of Canada Paper 70-1, Part A, 172-174.
- Green, P.F. (1981) A new look at statistics in fission track dating, Nuclear Tracks, v.5, 77-86.
- (1986) On the thermo-tectonic evolution of Northern England: evidence from fission track analysis, Geological Magazine, 123, 493-506.

- (1988) The relationship between track shortening and and fission track age reduction in apatite: combined influences of inherent instability, annealing anisotropy, length bias and system calibration, *Earth and Planetary Science Letters*, 89, 335-352.
- Green, P.F., Duddy, I.R., Gleadow, A.J.W., Tingate, P.T and Laslett, G.M. (1985) Fission-track annealing in apatite: track length measurements and the form of the Arrhenius plot, *Nuclear Tracks*, 10, 323-328.
- Green, P.F., Duddy, I.R., Gleadow, A.J.W., Tingate, P.T. and Laslett, G.M. (1986) Thermal annealing of fission tracks in apatite: 1 - A qualitative description , *Isotope Geoscience*, 59, 237-253.
- Green, P.F., Duddy, I.R., Laslett, G.M., Hegarty, K.A., Gleadow, A.J.W. and Lovering, J.F. (1989) Thermal annealing of fission tracks in apatite: 4. Quantitative modelling techniques and extension to geological timescales, *Chemical Geology (Isotope Geoscience Section)*, 155-182.
- Green, P.F., Duddy, I.R., Gleadow, A.J.W., and Lovering, J.F. (1989) 11. Apatite Fission-Track Analysis as a Paleotemperature Indicator for Hydrocarbon Exploration, In: *Thermal History of Sedimentary Basins Methods and Case Histories*, eds. N.D. Naeser and T.H. McCulloh, Springer-Verlag, 1989, 181-195.
- Grenier, R., and Cawood, P.A. (1988) Variations in structural style along the Long Range Front, western Newfoundland, In: *Current Research , Part B*, Geological Survey of Canada Paper 88-1B, 127-133.
- Grist, S. (1990) Provenance and thermal history of detrital sandstones of the Scotia Basin, offshore Nova Scotia using apatite and $^{40}\text{Ar}/^{39}\text{Ar}$ methods, unpublished M.sc. thesis, Dalhousie University, Halifax, Nova Scotia, 196 pp.
- Hacquebard, P.A., and Donaldson, J.R. (1970) Coal metamorphism and hydrocarbon potential in the Upper Paleozoic of the Atlantic Provinces, Canada, *Canadian Journal of Earth Sciences*, 7, 1139-1163.
- Hammerschmidt, K., Wagner, G.A. and Wagner, M. (1984) Radiometric dating on research drill core Urach III: a contribution to its geothermal history, *Journal of Geophysical Research*, 54, 97-105.
- Hanmer, S. (1981) Tectonic significance of the northeastern Gander Zone, Newfoundland: An Acadian ductile shear zone, *Canadian Journal of Earth*

Sciences, 18, 120-135.

- Harrison, T.M. and McDougall, I. (1980) Investigations of an intrusive contact, northwest Nelson, New Zealand, In: Thermal, chronological and isotopic constraints, *Geochim. Cosmochim. Acta*, 44, 1985-2003.
- Harrison, T.M., Armstrong, R.L, Naeser, C.W., and Harakal, J.E. (1979) Geochronology and thermal history of the Coast Plutonic complex, near Prince Rupert, B.C., *Canadian Journal of Earth Sciences*, 16, 400-410.
- Haworth, R.T. (1975) The development of Atlantic Canada as a result of continental collision - evidence from offshore gravity and magnetic data, *Canadian Society of Petroleum Geologists Memoir* 4, 59-77.
- Haworth, R.T., and Jacobi, R.D. (1983) Geophysical correlation between the geologic zonation of Newfoundland and the British Isles, *Geological Society of America Memoir* 158, 25-32.
- Haworth, R.T., and Keen, C.E. (1979) The Canadian Atlantic margin: a passive continental margin encompassing an active past, *Tectonophysics*, 59, 83-126.
- Haworth, R.T. and Sanford, B.V. (1976) Paleozoic geology of northwest Gulf of St.Lawrence, *Geological Survey of Canada Paper* 76-1A, 1-6.
- Haworth, R.T., Poole, A.C., Grant, A.C., and Sanford, B.V. (1976) Marine geoscience survey northeast of Newfoundland, *Geological Survey of Canada Paper* 76-1A, 7-15.
- Hendriks, M., Jamieson, R.A., Zentilli, M., Donelick, R.A., Reynolds, P.H., Owen, J.V. (1989) Cooling History of the Long Range Inlier, Newfoundland: Argon/Argon and Fission Track Thermochronometry, Report of Transect Meeting, Lithoprobe East, Memorial University, St.John's, Newfoundland, October 19-20, 1989, 51-56.
- Hibbard, J. (1983) Geology of the Baie Verte Peninsula, Newfoundland, Newfoundland Department of Mines and Energy, Min. Dev. Div. Memoir 2, 279 pp.
- Howie, R.D., and Barss, M.S. (1974) Upper Paleozoic rocks of the Atlantic provinces, Gulf of St.Lawrence, and adjacent continental shelf, In: *Offshore Geology of Eastern Canada*, Geological Survey of Canada Paper 74-30, Vol. 2, 35-50.
- Hurford, A.J. and Green, P.F. (1982) A user's guide to fission track calibration, *Earth and Planetary Science Letters*, 59, 343-354.

- (1983) The zeta calibration of fission track dating, *Isotope Geoscience*, 1, 285-317.
- Hurford, A.J. and Hammerschmidt, K. (1985) $^{40}\text{Ar}/^{39}\text{Ar}$ and K/Ar dating of the Bishop and Fish Canyon tuffs: Calibration ages for fission track dating standards, *Chemical Geology (Isotope Geoscience Section)*, 58, 23-32.
- Hyde, R.S. (1982) Geology of the Carboniferous Deer Lake Basin, Newfoundland Department of Mines and Energy, Mineral Development Division, Map 82-7.
- (1983) Geology of the Carboniferous Deer Lake Basin, west-central Newfoundland, Newfoundland Department of Mines and Energy, Mineral Development Division Map 82-7, scale 1:100,000.
 - (1984) Geologic history of the Carboniferous Deer Lake Basin, west-central Newfoundland, Canada, In: *Atlantic Coast Basins, Paleogeography, Paleotectonics, Sedimentology and Geochemistry*, Vol. 3, (Ed. by H.H.J. Geldsetzer, W.W. Nassichuk, E.S. Belt and R.W. MacQueen), 85-104. Ninth International Congress of Carboniferous Stratigraphy and Geology, Southern Illinois University Press, Carbondale, Illinois.
- Hyde, R.S., Miller, H.C., Hiscott, R.N., and Wright, J.A. (1988) Basin architecture and thermal maturation in the strikeslip Deer Lake Basin, Carboniferous of Newfoundland, In: *Basin Research*, Vol. 1, No. 2, June 1988, 85-105.
- Irving, E. and Strong, D.F. (1984) Palaeomagnetism of the Early Carboniferous Deer Lake Group, western Newfoundland: no evidence for mid-Carboniferous displacement of 'Acadia', *Earth and Planetary Science Letters*, 69, 379-390.
- Issler, D.R., Beaumont, C., Willett, S., Mooers, Donelick, R.A., Grist, A. (1990) Preliminary evidence from apatite fission track data on the thermal history of the Peace River Arch region, Western Canada Sedimentary Basin, *Canadian Society of Petroleum Geologists*, in press.
- James, N.P., and Stevens, R.K. (1986) Stratigraphy and correlation of the Cambro-Ordovician Cow Head Group, western Newfoundland, *Geological Survey of Canada Bulletin* 366, 143 pp.
- Jamieson, R.A. (1981) Metamorphism during Ophiolite Emplacement--the Petrology of the St. Anthony Complex, *Journal of Petrology*, 22, 397-443.
- (1990) Metamorphism of an Early Palaeozoic continental margin, western Baie Verte Peninsula, Newfoundland, *Journal Metamorphic Geology*, 8,

269-288.

- Jamieson, R.A. and Talkington, R.W. (1980) A jacupirangite-syenite assemblage beneath the White Hills Peridotite, north-western Newfoundland, *American Journal of Science*, 280, 459-477.
- Jamieson, R.A., van Brëemen, O., Sullivan, R.W. and Currie, K.L. (1986) The age of igneous and metamorphic events in the western Cape Breton Highlands, Nova Scotia, *Canadian Journal of Earth Sciences*, 23, 1891-1901.
- Jansa, L.F. and Pe-Piper, G. (1985) Early Cretaceous volcanism on the northeastern American margin and implications for plate tectonics, *Geological Society of America Bulletin*, v.96, 83-91.
- Johnsson, M.J. (1985) Late Paleozoic-Middle Mesozoic uplift rate, cooling rate and geothermal gradient of south-central New York State, *Nuclear Tracks*, 10, no.3, 295-301.
- (1986) Distribution of maximum burial temperatures across the northern Appalachian Basin and implications for Carboniferous sedimentation patterns, *Geology*, 14, 384-387.
- Keen, C.E., and Hyndman, R.D. (1979) Geophysical review of the continental margins of eastern and western Canada, *Canadian Journal of Earth Sciences*, 16, 712-747.
- Keen, C.E., Hall, B.R., and Sullivan, K.D. (1977) Mesozoic evolution of the Newfoundland Basin, *Earth and Planetary Science Letters*, 37, 307-320.
- Kent, D.V. (1982) Paleomagnetic evidence for post-Devonian displacement of the Avalon Platform (Newfoundland), *Journal Geophysical Research*, 87, 8709-8716.
- Kent, D.V., and Opdyke, N.D. (1978) Paleomagnetism of Devonian Catskill red beds: evidence for motion of coastal New England-Canadian Maritime region relative to North America, *Journal Geophysical Research* 83, 4441-4450.
- Klappa, C.F., Opalinski, P.R., and James, N.P. (1980) Ordovician Table Head Group of western Newfoundland: a revised stratigraphy, *Canadian Journal of Earth Sciences*, 17, 1007-1019.
- Knight, I. (1983) Geology of the Carboniferous Bay St. George Sub-basin, western Newfoundland, Newfoundland Department of Mines and Energy, Mineral Development Division, Memoir 1, 358 pp.
- Knight, I. and James, N.P. (1987) The stratigraphy of the Lower Ordovician St. George

- Group, western Newfoundland: the interaction of eustasy and tectonics, *Canadian Journal of Earth Sciences*, 24, 1927-1951.
- Lane, T.E. (1984) Preliminary classification of carbonate breccias, Newfoundland Zinc Mines, Daniel's Harbour, Newfoundland, In: *Current Research, Part A*, Geological Survey of Canada Paper 84-1A, 505-512.
- (1990) Dolomitization, brecciation and zinc mineralization and paragenetic stratigraphic and structural relationships in the upper Ordovician St. George Group at Daniel's Harbour, western Newfoundland, unpublished Ph.d thesis, Memorial University, 1990.
- Laslett, G.M., Kendal, W.S., Gleadow, A.J.W., and Duddy, I.R. (1982) Bias in measurement of fission-track length distributions, *Nuclear Tracks*, 6, no. 2/3, 79-85.
- Laslett, G.M., Green, P.F., Duddy, I.R, and Gleadow, A.J.W. (1987) Thermal annealing of fission tracks in apatite: 2. A quantitative analysis, *Chemical Geology (Isotope Geoscience Section)*, 65, 1-13.
- Li, G., Donelick, R.A., Zentilli, M. (1990) Neutron Calibration for fission track dating, *Atlantic Geology*, v.26, #2, p.178.
- Ludman, A. (1981) Significance of transcurrent faulting in eastern Maine and the location of the suture between Avalonia and North America, *American Journal of Earth Sciences*, 281, 463-483.
- Maksaev, V. (1990) Metallogeny, geological evolution, and thermochronology of the Chilean Andes between latitudes 21 °S and 26 °South, and the origin of major porphyry copper deposits, Ph.D. Thesis, Dalhousie University, Halifax, Nova Scotia, 554 pp.
- Maksaev, V. and Zentilli, M., Tertiary uplift and formation of porphyry copper deposits in the Andes of northern Chile: fission track evidence, (Abstract) *Nuclear Tracks*, 17D, 421.
- Marillier, F., Keen, C.E., Stockmal, G.S., Quinlan, G., Williams, H., Colmann-Sadd, S.P., and O'Brien, S.J. (1989) Crustal Structure and surface zonation of the Canadian Appalachians: implications of deep seismic reflection data, *Canadian Journal of Earth Sciences*, 26, 305-321.
- Masson, D.G., and Miles, D.R. (1984) Mesozoic seafloor spreading between Iberia, Europe and North America, *Marine Geology*, 56, 279-287.

- McDowell, F.W. and Keizer, R.P. (1977) Timing of mid-Tertiary volcanism in the Sierra Madre Occidental between Durango City and Mazatlan, Mexico, Geological Society of America Bulletin, 88, 1479-1487.
- Naeser, C.W. (1979) Thermal history of sedimentary basins: fission track dating of subsurface rocks, Society of Economic Paleontologists and Mineralogists Special Publication, 26, 109-112.
- Naeser, C.W. and Cunningham, C.G. (1984) Age and paleothermal anomaly of the Eagle Mine ore body, Gilman district, Colorado, Geological Society of America Abstracts with Programs, 16:607.
- Naeser, C.W. and Faul, H. (1969) Fission track annealing in apatite and sphene, Journal of Geophysical Research, 74, 705-710.
- Naeser, C.W., Bryant, B., Crittenden, M.D., and Sorensen, M.L. (1983) Fission track ages of apatite in the Wasatch Mountains, Utah: An uplift study, Geological Society of America Memoir, 157, 29-36.
- Nowlan, G.S., and Barnes, C.R. (1987) Thermal maturation of Paleozoic strata in Eastern Canada from conodont colour index (CAI) data with implications for burial history, tectonic evolution, hot spot tracks and mineral and hydrocarbon exploration, Geological Survey of Canada Bulletin 367, 29 pp.
- O'Brien, S.J., Dickson, W.L., and Blackwood, R.F. (1986) Geology of the central portion of the Hermitage Flexure area, In: Current Research, Newfoundland Department of Mines and Energy, Report 86-1, 189-208.
- Owen, J.V. (1990) Geology of the Long Range Inlier, Geological Survey of Canada Bulletin, in press.
- Owen, J.V., and Erdmer, P. (1986) Precambrian and Paleozoic metamorphism in the Long Range Inlier, western Newfoundland, In: Current Research, Part B, Geological Survey of Canada Paper 86-1B, 29-38.
- (1988) The Grenvillian Long Range Inlier of the Great Northern Peninsula, Newfoundland, 1988 GAC/MAC/CSPG field trip guidebook, Trip B.7, St. John's, Nfld.
 - (1989) Metamorphic Geology and Regional Geothermobarometry of a Grenvillian Massif: the Long Range Inlier, Newfoundland, Precambrian Research, 43, 79-100.

- Owen, J.V., Campbell, J.E.M., and Dennis, F.A.R. (1987) Geology of the Lake Michel area, Long Range Inlier, western Newfoundland, In: Current Research, Part A, Geological Survey of Canada Paper 87-1A, 643-652.
- Parrish, R.R. (1983) Cenozoic thermal evolution and tectonics of the Coast Mountains of British Columbia 1. fission track dating, apparent uplift rates, and patterns of uplift, *Tectonics*, 2, no.6, 601-631.
- Pe-Piper, G. and Jansa, W. (1987), Geochemistry of late Middle Jurassic-Early Cretaceous igneous rocks on the eastern North American margin, *Geological Society of America Bulletin*, v.99, 803-813.
- Pitman, W.C., and Andrews, J.A. (1985) Subsidence and thermal history of small pull apart basins, In: Strike Slip deformation, Basin Formation, and Sedimentation, (ed. by K.T.Biddle and N.Christie-Blick), *Society of Economic Paleontology and Mineralogy Special Publication*, 37, 45-49.
- Poole, W.H. (1972) Plate tectonic evolution of the Canadian Appalachian region, *Geological Survey of Canada Paper* 76-1B, 113-126.
- Popper, G.H.P. (1970) Palaeobasin analysis and structure of the Anguille Group, west-central Newfoundland, Unpublished Ph.d thesis, Lehigh University, Bethlehem, Pennsylvania, 215 pp.
- Press, W.H., Flannery, B.P., Teukolsky, S.A. and Vetterlig, W.T. (1986) *Numerical Recipes: The Art of Scientific Computing*, Cambridge University Press, Cambridge, 818 pp.
- Price, P.B. and Walker, R.M. (1962) Chemical etching of charged-particle tracks in solids, *Journal of Applied Physics*, 33, 3407-3412.
- (1963) Fossil tracks of charged particles in mica and the age of minerals, *Journal of Geophysical Research*, 68, no.16, 4847-4862.
- Pringle, I.R., Miller, J.A., and Warrell, D.M. (1971) Radiometric age determinations from the Long Range Mountains, Newfoundland, *Canadian Journal of Earth Sciences*, Vol. 8, 1325-1330.
- Rodgers, J. and Neale, E.R.W. (1963) Possible 'Taconic' Klippen in western Newfoundland, *American Journal of Science*, 61, 713-730.
- Ryan, R.J. (1990) The thermal and metallogenic evolution of the Maritimes Basin: evidence from the Cumberland Basin of Nova Scotia, Ph.d thesis proposal, Dalhousie University, Halifax, Nova Scotia, January 1990.

- Schaer, J.P., Reimer, G.M., and Wagner, G.A. (1975) Actual and ancient uplift rate in the Gottard region, Swiss Alps: A comparison between precise levelling and fission-track apatite age, *Tectonophysics*, 29, 293-300.
- Scotese, C.R., VanderVoo, R., Johnson, R.E., and Giles, P.S. (1984) Paleomagnetic results from Carboniferous of Nova Scotia, In: *Plate Reconstruction from Paleozoic Paleomagnetism*, Geodynamics Series, Vol. 12, (Ed. by R. VanderVoo, C.R. Scotese, and N. Bonhommet), Blackwell North America Inc., Blackwood, N.J., U.S.A., 63-81.
- Silk, E.C.H. and Barnes, R.S. (1959) *Phil. Mag.*, 4, p.970.
- Smyth, W.R. and Schillereff, H.S. (1981) 1:25,000 geology field maps of Jackson's Arm northwest (Map 81-109), Jackson's Arm southwest (Map 81-110), Hampden northwest (Map 81-111), and Hampden southwest (Map 81-112), Newfoundland Department of Mines and Energy, Mineral Development Division, Open File maps.
- (1982) The pre-Carboniferous geology of southwest White Bay, In: *Current Research*, Newfoundland Department of Mines and Energy, Mineral Development Division, Report 82-1, 78-98.
- Srivastava, S.P. and Tapscott, C.R. (1988) Plate kinematics of the North Atlantic, In: *The Geology of North America*, vol.M, Geological Society of America, 379-404.
- Steed, G.M. (1979) Investigations of uraniferous samples from Wigwam Creek, Canada, In: unpublished report by J. Tuach, 1980, Westfield Minerals Limited.
- Steiger, R.H. and Jaeger, E. (1977) Subcommittee on geochronology: convention on the use of decay constants in geo- and cosmochronology, *Earth and Planetary Science Letters*, 36, 359-362.
- Stevens, R.K. (1970) Cambro-Ordovician flysch sedimentation and tectonics in west Newfoundland, and their possible bearing on a proto-Atlantic Ocean, In: *Flysch sedimentology in North America*, (Ed. J. LaJoie), Geological Association of Canada, Special Paper 7, 165-177.
- St.Julien, P., Hubert, C., and Williams, H. (1976) The Baie Verte-Brompton Line and its possible tectonic significance in the northern Appalachians, *Geological Society of America, Abstracts with Programs*, 8, 259-260.
- Stockmal, G.S., Colmann-Sadd, S.P., Keen, C.E., O'Brien, S.J., and Quinlan, G. (1987) collision along an irregular plate margin: a regional plate tectonic

- interpretation of the Canadian Appalachians, *Canadian Journal of Earth Sciences*, 24, 1098-1107.
- Strong, D.F. (1974) Plateau lavas and diabase dykes of northwestern Newfoundland, *Geological Magazine*, 3, 501-514.
- Strong, D.F. and Williams, H. (1972) Early Paleozoic flood basalts of northwestern Newfoundland, their petrology and tectonic significance, *Geological Association of Canada*, 24, 43-54.
- Saunders, C.M. and Strong, D.F. (1986) Assessment of Pb-Zn deposits of the western Newfoundland carbonate platform, In: *Current Research, Part A*, Geological Survey of Canada Paper 86-1A, 229-237.
- Stukas, V., and Reynolds, P.H. (1974) $^{40}\text{Ar}/^{39}\text{Ar}$ dating of the Long Range dykes, Newfoundland, *Earth and Planetary Science Letters*, 22, 256-266.
- Swinden, H.S., Lane, T.E., Thorpe, R.I. (1988) Lead isotope composition of galena in carbonate-hosted deposits of western Newfoundland: evidence for diverse lead sources, *Canadian Journal of Earth Sciences*, 25, 593-602.
- Tankard, A.J., and Welsink, H.G. (1988) Extensional tectonics and stratigraphy of the Mesozoic Grand Banks of Newfoundland, In: *Triassic-Jurassic rifting and opening of the Atlantic*, ed. W. Marspeizer, American Association of Petroleum Geologists Memoir.
- Todd, B.J., Reid, I. and Keen, C.E. (1988) Crustal structure across the southwest Newfoundland Transform Margin, *Canadian Journal of Earth Sciences*, 25, 744-759.
- Tuach, J. (1987a) Mineralized environment, metallogenesis, and the Doucers Valley Fault complex, western White Bay: a philosophy for gold exploration in Newfoundland, In: *Current Research, Newfoundland Department of Mines and Energy*, Mineral Development Division, Report 87-1, 129-144.
- (1987b) Stratigraphy, structure, and mineralization, western White Bay, Road log and field guide, Geological Association of Canada, Newfoundland Branch, October 10-11, 1987, 19 pp.
- Twenhofel, W.H., and McClintock, P. (1940) Surface of Newfoundland, *Geological Society of America Bulletin*, 51, pt.2, 1665-1728.
- Wagner, G.A. (1972) The geological interpretation of fission track apatite ages, *Trans. Am. Nucl. Soc.*, 15, p.117.

- Wagner, G.A. and Reimer, G.M. (1972) Fission track tectonics: The tectonic interpretation of fission track apatite ages, *Earth and Planetary Science Letters*, 14, 263-268.
- Wagner, G.A., Reimer, G.M., and Jaeger, E. (1977) Cooling ages derived by apatite fission-track, mica Rb-Sr and K-Ar dating: the uplift and cooling history of the Central Alps, Padova: Societa Cooperativa Tipografica, 1-27.
- Waldron, J.W.F and Stockmal, G.S. (1989) Structure of the Acadian Deformation Front, Port Au Port Peninsula, Report of Transect Meeting, Lithoprobe East, Memorial University, St.John's, Newfoundland, October 19-20, 1989, 80-82.
- Wanless, R.K., Stevens, R.D., Lachance, G.R. and Rimsaite, J.Y.H. (1965) Age determinations and geological studies, K-Ar isotopic ages, report 5, Geological Survey of Canada Paper 64-17, pt.1.
- Wanless, R.K., Stevens, R.D., Lachance, G.R., and Edmonds, C.M. (1968) Age determinations and geological studies, K-Ar isotopic ages, Report 8, Geological Survey of Canada Paper 67-2, Part A.
- Wanless, R.K., Stevens, R.D., Lachance, G.R., and Delabio, R.N. (1973) Age determinations and geological studies, K-Ar isotopic ages, Report 11, Geological Survey of Canada Paper 73-2.
- Wanless, R.K., Steven, R.D., Lachance, G.R. and Delabio, R.N. (1974) Age determinations and geological studies, K-Ar isotopic ages, report 12, Geological Survey of Canada Paper 74-2.
- Waples, D.W. (1980) Time and temperature in petroleum formation: Application of Lopatin's method to petroleum exploration, *American Association of Petroleum Geologists Bulletin*, 64, 916-926.
- Webb, G.W. (1969) Paleozoic wrench faults in Canadian Appalachians, In: *North Atlantic Geology and Continental Drift*, (ed.by M.Kay), American Association of Petroleum Geologists Memoir 12, 754-786.
- Whalen, J.B. (1989) Topsails igneous suite, western Newfoundland: a Silurian subduction related magmatic suite?, *Canadian Journal of Earth Sciences*, 26, 2421-2434.
- Willet, S., Beaumont, C., Issler, D., Ravenhurst, C., Donelick, R.A., and Mooers, J. (1990) Paleo-fluid flow in the Alberta Basin inferred from apatite fission track annealing data, submitted to *Canadian Journal of Earth Sciences*.

- Williams, H. (1969) 3. Pre-Carboniferous development of Newfoundland Appalachians, Geological Survey of Canada, In: North Atlantic Geology and Continental Drift, ed. M. Kay, American Association of Petroleum Geologists Memoir 12, 32-58.
- (1975) Structural succession, nomenclature and interpretation of transported rocks in western Newfoundland, Canadian Journal of Earth Sciences, 12, 1874-1894.
 - (compiler) (1978) Tectonic Lithofacies Map of the Appalachian Orogen, Map no. 1, Memorial University, scale 1:1,000,000.
 - (1979) Appalachian Orogen in Canada, Canadian Journal of Earth Sciences, 16, 792-807.
- Williams, H., and Hatcher, R.D. jr (1983) Appalachian suspect terranes, In: contributions to tectonics and geophysics of mountain chains, (Ed. R.D. Hatcher Jr, H. Williams, and I. Zietz), Geological Society of America Memoir 158, 33-53.
- Williams, H., and Smyth, W.R. (1983) Geology of the Hare Bay Allochthon, In: Geology of the Strait of Belle Isle Area, Northwestern Insular Newfoundland, Southern Labrador, and adjacent Quebec, Geological Survey of Canada Memoir 400, pt.3, 109-141.
- Williams, H., and Stevens, R.K. (1974) The ancient continental margin of eastern North America, In: The geology of continental margins (Ed. C.A. Burke and C.L. Drake), Springer-Verlag, New York, N.Y., 781-796.
- Williams, H., and St-Julien, P. (1982) the Baie Verte-Brompton Line: Early Paleozoic continent-ocean interface in the Canadian Appalachian, In: (Ed. P. St-Julien, and J. Beland), Major structural zones and faults of the northern Appalachians, Geological Association of America Special Paper 24, 177-207.
- Williams, H., Quinn, L., Nyman, M. and Reusch, D.N. (1984) Geology, Lomond, Newfoundland, Map and Notes, Geological Survey of Canada, Open File 1012, 1:50,000.
- Williams, H., James, N.P., and Stevens, R.K. (1985) Humber Arm Allochthon and nearby Groups between Bonne Bay and Portland Creek, western Newfoundland, In: Current Research, Part A, Geological Survey of Canada Paper 85-1A, 399-406.
- Wilton, D.H.C. (1983) The geology and structural history of the Cape Ray Fault Zone in southwestern Newfoundland, Canadian Journal of Earth Sciences, 20, 1119-

1133.

- Wright, J.A., Jessop, A.M., Judge, A.S. and Lewis, T.J. (1980) Geothermal measurements in Newfoundland, Canadian Journal of Earth Sciences, 17, 1370-1376.
- York, D. (1969) Least squares fitting of a straight line with correlated errors, Earth and Planetary Science Letters, 5, 320-324.
- Zentilli, M. and Makshev, V. (1989) Genesis of porphyry copper deposits in the Andes of northern Chile in relation to Tertiary magmatism and tectonic uplift: fission track evidence, Abstracts Volume, 28th International Geological Congress, v.3, 429-430.

083500045